Novel modification of Human Myeloma proteasomes and development of non-active site directed inhibitors.

By

David S. Pitcher

A thesis submitted for the degree of Doctor of Philosophy

October 2016

Centre of Haematology

Imperial College London

COPYRIGHT

The copyright of this thesis rests with the author and is made available under a Creative Commons Attribution Non-Commercial No Derivatives licence. Researchers are free to copy, distribute or transmit the thesis on the condition that they attribute it, that they do not use it for commercial purposes and that they do not alter, transform or build upon it. For any reuse or redistribution, researchers must make clear to others the licence terms of this work.

Figures 1.2, 1.3, 1.4 and 1.5 are from the sources stated in the legends of each figure and permission has been obtained for reproduction and republishing in an online open access format by the licences stated below:

Figure 1.2 is licenced by ‘American Society of Hematology’ number #3973070918521
Figure 1.3 is licenced by ‘Nature Publishing Group’ number #3960180094287
Figures 1.4 & 1.5 are licenced by ‘Nature Publishing Group’ #3960180835983

DECLARATION

All the experiments described in this thesis were designed and performed by myself unless otherwise stated. Contributions from other people are acknowledged in the appropriate sections. I performed the experiments, analysed the data, produced the graphs and figures, and wrote the text; all with the guidance of my supervisor, Dr Maurits Kleijnen.

David Pitcher

October 2016

ABSTRACT

Multiple Myeloma (MM) is a plasma cell malignancy that is characterised by bone lesions and production of excessive amounts of monoclonal protein. Treatment involves the use of chemotherapy agents, immunomodulatory agents and proteasome inhibitors (PI). The 26S proteasome is a 2.5 MDa molecular machine that is integral to the viability of all eukaryote cell. Its main function is to hydrolyse proteins that are marked for degradation by a poly-ubiquitin chain. Although MM is treatable, it is as yet incurable with mean survival of ~6 years.

In this thesis, I show that human proteasomes contain a charged polymeric posttranslational modification (PTM), one which has some similarity to poly-ADP-ribose. This modification is not normally resolvable via normal SDS-PAGE electrophoresis, but can be resolved by the lesser used CTAB-PAGE or after separation of the proteasome from other cellular components. This modification appears to be present predominantly in the nucleus of the cell, and may provide a mechanism for how nuclear proteasomes interact with chromatin, DNA and other nuclear components.

The use of proteasome inhibitors as a valid therapy for MM has been hypothesised to be due to a high proteasome load in MM; therefore, a small amount of inhibition would suffice to perturb proteostasis. However, I show that myeloma cells experience severe proteasome inhibition upon treatment with compounds such as Bortezomib, to a degree that far exceeds the levels of inhibition observed with purified proteasomes. This suggests that, when PIs engage with proteasomal active-sites, they trigger a cellular mechanism which exacerbates this inhibition to a far greater degree than would otherwise be achieved. I excluded trivial explanations including additional binding of the inhibitor, caspase mediated proteasome inhibition or cell death initiation. Intriguingly, I found that early changes to CTAB-PAGE detectable PTMs coincided with PIs' ability to achieve an excessive degree of cellular proteasome inhibition.

In addition to this work I continue the development of an allosteric proteasome inhibitor identified by a phage display technique. Through a number of rounds of chemical optimisation, I show the ability of these compounds to inhibit proteasome degradation of an ubiquinated substrate and a lethality in myeloma cells at 25 nM.

ACKNOWLEDGEMENTS

I am greatly indebted to my funding body, Bloodwise (Registered Charity #216032). Without their input to my work over the last four years I would not have been able to fulfil my love of investigative science and hopefully have provided my small input to their overall aims. I also would like to thank all those who have raised money for this hugely great charity. I am so grateful to have been able to contribute to the important work funded by this organisation in the fight against all blood cancers.

I would also like to thank the many other people that as part of the chain that made my PhD possible. It is four years ago that I was invited for an interview at Imperial College London.

I would like to sincerely thank my supervisor Dr Maurits Kleijnen for having the faith in me, and offering me the opportunity to study in his lab. As well as constantly motivating me and pushing me to exceed my own personal expectation, he enabled me to expand my thinking and develop my ability. I am exceedingly grateful for his patience, assistance and most importantly his faith in me enabling me to achieve so many goals and achievements. I also have to thank my second supervisor Prof. Tassos Karadimitris for giving me the additional support as well as conveying his knowledge into my work.

A big thank you goes to my parents who have given me the freedom in my education to develop and pursue my love of science. They have always supported me in my, pathway through life and my love and interest in science, from the very early age of watching 'The Open University' in the early hours on TV whilst they were asleep.

I would also like to acknowledge the efforts, support, training and interest of my previous supervisor Dr Helen Dawe at Exeter University. She gave me the basic experience and taught me the need for strict laboratory skills so necessary for accurate experimentation. I have on many occasions been able to overcome difficulties down to her strict training and advice which I will carry with me forever.

During my time in the lab I have been very privileged to work alongside some great lab members. Katerina, Mai, Kate P, Kate MS and Kostas deserve a special mention

for working alongside and teaching me protocols and sharing reagents as well as the other members of Lab 211 in Exeter, especially Kate McI, Kim, Dan, Natalie. All of these people showed me that science is not just a job and lab members are not just colleagues.

I would also like to thank my housemates Pete and Mo for keeping me sane throughout my four years. They were kind enough to feign excitement upon my discoveries, made to watch scientific documentaries and advise me practicing presentations before Game of Thrones, I sincerely hope they have suffered no lasting damage!!

Lastly my thanks go to Louise and Pete for reading sections of my thesis and giving me invaluable feedback from a laypersons point of view.

CONTENTS

COPYRIGHT I

DECLARATION II

ABSTRACT III

ACKNOWLEDGEMENTS IV

ABBREVIATIONS, UNITS AND PREFIXES 1

LIST OF FIGURES 3

LIST OF TABLES 6

CHAPTER 1 - INTRODUCTION 7

1.1 MULTIPLE MYELOMA (MM) 8
1.2. PROGRESSION OF THE DISEASE 8
1.3. DIAGNOSIS 9
1.3.1. Clinical features 9
1.4. EPIDEMIOLOGY 13
1.5. CYTOGENETIC ABERRATION AND MUTATIONS 14
1.5.1. Common Translocations 14
1.5.2. Copy number variations 16
1.6. CURRENT TREATMENT OF MULTIPLE MYELOMA 18
1.6.1. Prednisone 18
1.6.2. Thalidomide 19
1.6.3. Proteasome Inhibitors 19
1.7. THE UBIQUITIN PROTEASOME PATHWAY (UPP) 20
1.7.1. E1 – Ubiquitin Activating Enzymes 23
1.7.2. E2 – Ubiquitin Conjugating Enzymes 23
1.7.3. E3 – Ubiquitin Ligases 24
1.7.4. The 26S Proteasome. 26
1.8. REGULATION OF THE PROTEASOME 30
1.9. ROLE AND FUNCTION OF THE 26S PROTEASOME 32
1.9.1. Cell cycle control by the 26S proteasome 32
1.9.2. Regulation of pathogenesis by the 26S proteasome 35
1.9.4. Cell differentiation by the 26S proteasome 36
1.10. INTERCELLULAR LOCALISATION OF PROTEASOMES 37
1.10.1. Cytoplasmic proteasomes 37
1.10.2. Nuclear Proteasomes 38
1.11. AIMS OF THIS WORK 40

CHAPTER 2 – MATERIALS & METHODS 41

2.1 MOLECULAR CLONING 42
2.1.1 DNA digestion with restriction enzymes 42
2.1.2 Phosphorylation and Annealing of Oligo DNA 42
2.1.3 Polymerase Chain Reaction (PCR) 42
2.1.4 Agarose gel electrophoresis of DNA 44
2.1.5 Ligation 44
2.1.6 Sequencing 45
2.2. HANDLING *ESCHERICHIA COLI* AND ISOLATION OF PLASMA DNA 45
2.2.1. E. Coli Strains and Genotype 45
2.2.2. Liquid and Solid Media 45
2.2.3. Preparation of Competent Cells 46
2.2.4. Chemical Transformation 46
2.2.5. Isolation of Plasmid DNA 46

2.2.6. Glycerol Stock *47*
2.2.7. Purification of bacterially expressed proteins *47*
2.3. HANDLING OF SACCHAROMYCES CEREVISIAE AND PURIFICATION OF YEAST PROTEASOMES. 48
2.3.1. S. cerevisiae Strains and Genotype *48*
2.3.2. Liquid and Solid Media *49*
2.3.3. Purification of yeast proteasomes *49*
2.3.4. Nuclear and Cytoplasic yeast extracts. *50*
2.4. MAMMALIAN CELL CULTURE, DRUG TREATMENT AND VIRAL TRANSDUCTION 51
2.4.1. Cell Culture of Suspension cells *51*
2.4.2. Cell Culture of adherent cells *52*
2.4.3. Cryo preservation *52*
2.4.4. Drug Treatment *53*
2.4.4. Viral production, concentration and transduction *53*
2.4.5. Small Scale Cell fractionation *54*
2.4.6. Whole cell lysis of Mammalian cells *55*
2.4.7. Isolation of Nuclear Proteasomes from Primary Human leukocytes *55*
2.4.8. FPLC Size exclusion chromatography *56*
2.5. FLOW CYTOMETRIC ANALYSIS AND SORTING 57
2.5.1. Staining *57*
2.5.2. Flow Cytometric Analysis *57*
2.5.3. Fluorescence-Activated Cell Sorting (FACS) *58*
2.5.4. Analysis of flow cytometry data *58*
2.6. DIGESTION OF MODIFICATIONS ON PURIFIED PROTEASOMES 58
2.7. PROTEIN ELECTROPHORESIS 60
2.7.1. Sodium Dodecyl Sulphate Protein Electrophoresis (SDS-PAGE) *60*
2.7.2. Cetyl Trimethylammonium Bromide Protein Electrophoresis (CTAB-PAGE) *60*
2.7.3. Isoelectric Focusing IEF *61*
2.7.4. In Gel Protein Staining *61*
2.7.5. Semi-Dry transfer and Western Blot *62*
2.8. PROTEASOME ASSAYS 63
2.8.1. In Vitro Degradation Assay *63*
2.8.2. Proteasome Activity Assay *65*
2.9. CONSTRUCTS AND CELL LINES CREATED 65
2.9.1 The His^6-2(StrepIITag)-TeV-Rpn11 expression construct *65*
2.9.2 His_6 tagged ADPRHL1 variant 1 & 2 ..... *67*

CHAPTER 3 - POST-TRANSLATIONAL MODIFICATION OF PROTEASOME SUBUNITS, UNRESOLVABLE BY SDS-PAGE **69**

3.1. INTRODUCTION 70
3.2. WORK LEADING UP TO COMMENCEMENT OF PROJECT 72
3.3. MANY PROTEASOME SUBUNITS HAVE MODIFIED SPECIES NOT RESOLVABLE BY SDS-PAGE 76
3.4. MODIFIED PROTEASOMES LIKELY CARRY A CHARGED POLYMER MODIFICATION. 82
3.5. DISCUSSION 92

CHAPTER 4 - POST TRANSLATIONAL MODIFICATION OF PROTEASOME SUBUNITS CHANGE EARLY AFTER BORTEZOMIB CHALLENGE. **97**

4.1. INTRODUCTION 98
4.2.1. MEASUREMENT OF CT-LIKE ACTIVITY UPON BORTEZOMIB TREATMENT. 100
4.2.2. INVESTIGATION INTO WHETHER CASPASE ACTIVITY PLAYS A ROLE IN PROTEASOME ACTIVITY SHUTDOWN. 106
4.2.3. INVESTIGATION INTO ACTIVE-SITE OCCUPATION OVER TIME BY PROTEASOME INHIBITORS. 110
4.2.4. INVESTIGATION INTO WHETHER PROTEASOME MODIFICATIONS PLAY A ROLE IN ITS INHIBITION UPON PI TREATMENT. 112
4.3. DISCUSSION 123
4.3.1. PROPOSED MECHANISM OF PROTEASOME INHIBITION 128
4.4. FUTURE WORK 131

CHAPTER 5 - DEVELOPMENT OF ALLOSTERIC PROTEASOME INHIBITORS. 132

5.1 INTRODUCTION 133
5.2. IDENTIFICATION OF PROTEASOME BINDING PEPTIDES 136
5.3. IDENTIFICATION THE MINIMAL CORE INHIBITORY RESIDUES. 139
5.4. FIRST ROUND OPTIMISATION 141
5.5. SECOND ROUND OPTIMISATION. 143
5.6. THIRD ROUND OPTIMISATION. 145
5.7. FOURTH ROUND OPTIMISATION. 150
5.8. FIFTH ROUND OPTIMISATION. 153
5.9. DISCUSSION. 156
5.10. FUTURE WORK. 159

CHAPTER 6 – DISCUSSION AND CONCLUSION. 160

6.1. DISCUSSION 161
6.1.1. Post-translational modification of proteasome subunits, unresolvable by SDS-PAGE 162
6.1.2. Post-translational modification of proteasome subunits change early after Bortezomib challenge 165
6.1.3. Development of Allosteric proteasome inhibitors 167
6.2. LIMITATIONS OF STUDY 169
6.3. FUTURE WORK 171
6.4. CONCLUSIONS 172

APPENDIX A - CONFIRMATION OF *IN VITRO* DEGRADATION SYSTEM 174

APPENDIX B - PLASMID AND SEQUENCE MAPS FOR ADPRHL1 VARIANT 1 + 2 BACTERIAL OVER EXPRESSION PLASMIDS 178

APPENDIX C - CREATION OF AN OPM2 CELL LINE OVER EXPRESSING A TAGGED RPN11 SUBUNIT 184

APPENDIX D - FLOW CYTOMETRY GATING STRATEGY 188

APPENDIX E - PUBLISHED PAPERS 191

REFERENCES 205

ABBREVIATIONS, UNITS AND PREFIXES

2DE	Two Dimensional Electrophoresis
aa	Amino acid
AAA+	ATPases Associated with diverse cellular Activities
ADP	Adenosine diphosphate
ATP	Adenosine triphosphate
ATPase	Enzyme that hydrolyses ATP to ADP
BMI	Body Mass Index
cDNA	Complementary DNA
CE	Cytosolic Extract
CP	Core Particle
DAPI	4',6-diamidino-2-phenylindole
DMEM	Dulbecco's Modified Eagle Medium
DMSO	Dimethyl sulfoxide
DNA	Deoxyribonucleic acid
E1	Ubiquitin Activating Enzyme
E2	Ubiquitin Conjugating Enzyme
E3	Ubiquitin Ligating Enzyme
EGCG	Epigallocatechin gallate
eGFP	Enhanced green fluorescent protein
ER	Endoplasmic reticulum
ERAD	Endoplasmic-reticulum-associated protein degradation
FBS	Foetal bovine serum
FPLC	Fast Protein Liquid Chromatography
GST	Glutathione S-Transferase
HECT	Homologous to the E6-AP Carboxyl Terminus Domain
HEPES	4-(2-hydroxyethyl)-1-piperazineethanesulfonic acid
HIV	Human immunodeficiency virus
Ig	Immunoglobulin
IL	Interleukin
MGUS	Monoclonal Gammopathy of Undetermined Significance
MM	Multiple Myeloma

M-protein	Monoclonal protein
mRNA	Messenger RNA
NE	Nuclear Extract
OPG	Osteoprotegerin
PAR	Poly-ADP-Ribose
PBS	Phosphate-buffered saline
PC	Plasma Cell
RANKL	Receptor Activator of Nuclear Factor κB Ligand
RBR	RING-between-RING
RING	Really Interesting New Gene domain
RNA	Ribonucleic acid
RP	Regulatory Particle
RPMI-1640	Roswell Park Memorial Institute 1640 medium
SMM	Smouldering Multiple Myeloma
Ub	Ubiquitin
UBL	Ubiquitin-like
UPP	Ubiquitin Proteasome Pathway
VSVG	Vesicular stomatitis virus G Protein

Units

Å	Ångström
bp	Base pair
Da	Dalton
g	Gram
l	Litre
m	Metre
M	Molar = mol/L
psi	Pounds per square inch
u	Units*
x g	Relative centrifugal force

*Defined per enzyme/substrate

Unit Prefixes

M	mega	10^{6}
k	kilo	10^{3}
d	deci	10^{-1}
m	milli	10^{-3}
µ	micro	10^{-6}
n	nano	10^{-9}

LIST OF FIGURES

Figure 1.1. The multiple processes that result in the common symptoms of MM. 12

Figure 1.2. Example karyotyping of a MM patient. 15

Figure 1.3. The complex nature of Ub and UBL post translational modification. 22

Figure 1.4. Structure of the 26S Proteasome. 25

Figure 1.5. The major catalytic subunits of the 19S regulatory particle. 29

Figure 2.1. Schematic showing the products of annealing of the two parts of the His^6-2(StrepIITag)-TeV construct. 66

Figure 3.1. CTAB-PAGE shows increased diffuse signal of proteasome subunits compared to SDS-PAGE. 73

Figure 3.2. High molecular weight smear can be separated from the main resolved band by simple Triton-X100 extraction. 74

Figure 3.3. Majority of proteasome subunits show increased diffuse signal on CTAB-PAGE compared to SDS-PAGE. 75

Figure 3.4. CTAB-PAGE achieves similar resolution of proteins to SDS-PAGE. 77

Figure 3.5. Cytoplasmic and nuclear fractionation of *S. cerevisiae* does not yield proteasome smearing on CTAB-PAGE. 78

Figure 3.6. Double purification of proteasomes by AP and FPLC techniques allows modified proteasomes to resolve on SDS-PAGE. 81

Figure 3.7. Modified species of Rpt2 are found mostly in the nucleus of the cell and can be still visualised after subsequent capture by UBL resin and FPLC purification. 82

Figure 3.8. Two Dimensional electrophoresis of purified proteasomes show a charge and molecular weight shift of nuclear proteasome subunits. 84

Figure 3.9. Enzymatic treatment of proteasome modifications. 87

Figure 3.10. PDE1 has activity against modified Rpt2 subunits. 89

Figure 3.11. PDE1/S1 Nuclease treated proteasomes have no effect on their ability to degrade ubiquitinated proteins. 91

Figure 4.1. CT-Like active site inhibition of various human cell-lines over the first 24 h of Bortezomib treatment. 101

Figure 4.2. Inhibition of the CT-Like active site of intracellular proteasomes over the first 24 h of Bortezomib treatment. 102

Figure 4.3. Inhibition of the CT-Like active site over the first 24 h of Bortezomib treatment. 104

Figure 4.4. Inhibition of the CT-Like active site of purified yeast or human proteasomes over the first 6 h of Bortezomib treatment. 105

Figure 4.5. Inhibition of the CT-Like active site over the first 24 h of Bortezomib treatment. 107

Figure 4.6. Assessing whether caspase inhibition rescues severe CT-Like inhibition in the first 24 h of Bortezomib treatment. 108

Figure 4.7. Cell viability of NCI-H929 cells upon lethal 10 nM Bortezomib challenge over time. 109

Figure 4.8. Inhibition and occupation of the CT-Like active site by a biotinylated vinyl sulfone inhibitor over the first 6 h of treatment. 111

Figure 4.9. Investigation to see if Bortezomib plays a role in proteasome subunit modification changes. 113

Figure 4.10. Changes in modified Rpn12 subunits in the early hours after Proteasome inhibition. 115

Figure 4.11. Bortezomib mediated changes to Rpn12 are prevented by addition of EGCG. 116

Figure 4.12. EGCG has no effect on proteasome inhibitor mediated changes. 118

Figure 4.13. Deciphering the changes to proteasome subunits caused by Bortezomib or intracellular caspase activation. 120

Figure 4.14. Affinity purification of proteasomes using incorporated His^6 tagged RPN11 from cytosolic and nuclear lysate of H929 cells treated with/without 10 nM Bortezomib. 122

Figure 4.15. Proposed mechanism of severe proteasome inhibition upon treatment with PIs. 130

Figure 5.1. Capture of human proteasomes using Peptide 15 identified from Phage display experiment. 138

Figure 5.2. Finding the minimal inhibitory core sequence of peptide 15. 140

Figure 5.3. First round optimisation of the 5-mer core. 142

Figure 5.4. Investigating the potency of 2nd round optimisation. 144

Figure 5.5. Viability as measured by AnnexinV/DAPI staining of NCI-H929 cells treated with 150 µM peptide. 146

Figure 5.6. Effect of media change on BC-MK5 toxicity. 148

Figure 5.7. Titration of BC-MK5 on RPMI-8226 myeloma cells. 149

Figure 5.8. Testing derivatives of BC-MK5 on the ability to kill RPMI-8226 cells. 152

Figure 5.9. Structures or L/D-Proline and L/D-Silaproline. 153

Figure 5.10. Viability of OPM-2 cells after 48h treatment with peptide variants. 154

Figure 5.11. Viability of OPM-2 cells after 48h treatment with peptide variants. 155

Figure 5.12. Overview of Peptide 15 optimisation. 158

Figure A.1. Testing the ubiquitination of a model substrate and its ability to be degraded by proteasomes..... 177

Figure B.1. Plasmid map and confirmed sequence of ADP-ribosylhydrolase like 1 (ADPRHL1) transcript variant 1..... 181

Figure B.2. Plasmid map and confirmed sequence of ADP-ribosylhydrolase like 1 (ADPRHL1) transcript variant 2..... 183

Figure C.1. Plasmid map and confirmed sequence of His^6-2(StrepIITag)-TeV-PSMD14 retroviral expression plasmid 186

Figure C.2. FACS Gating strategy, Purity and stability analysis 187

Figure D.1. Gating strategies for flow cytometric analysis of cells..... 190

LIST OF TABLES

Table 2.1. List of used compounds, Supplier and Solute..... 53

Table 2.2. List of lasers and filters used in flow cytometry..... 58

Table 2.3. List of enzymes used in the digestion of proteasome modifications..... 59

Table 2.4. List of antibodies used in thesis..... 63

Table 2.5. Primer sequences for the creation of the His^6-2(StrepIITag)-TeV-Rpn11 expression construct..... 67

Table 2.6. Primer sequences for the creation of the ARH2 expression constructs..... 68

Table 3.1. List of the proteins used in Figure 3.4..... 77

Table 5.1. List of peptides identified from phage display capture of differently treated human and yeast proteasomes..... 137

CHAPTER 1 - INTRODUCTION

CHAPTER I: INTRODUCTION

1.1 Multiple Myeloma (MM)

Multiple Myeloma (MM) is a clonal B-cell malignancy of terminally differentiated plasma cells (PC). The disease manifests itself with symptoms such as bone lesions, hypercalcaemia, renal insufficiency and immunodeficiency. It makes up 2 % of all new cancer cases in the United Kingdom, being the 17th most common cancer and 2nd most common haematological malignancy. Incidences vary in a number of subpopulations, most significantly with age - with the mean age of diagnosis being between 65-70 years. Incidences are slightly higher in males vs females, with a male: female ratio of around 13:10. The lifetime risk of developing MM is around 1 in 115 for men and around 1 in 155 for women. Ethnicity also proves to be of significance, with those of African origin being twice as likely to develop the malignancy as well as having a significantly lower age of onset, whilst rates are the lowest in Asian populations (Waxman et al., 2010). This may suggest a genetic pre-disposition in developing MM, although these ethnic differences have yet to be explained.

There are various treatment methods for MM, but as of yet MM remains an incurable disease. Five-year survival for MM decreases with increasing age, with net survival ranging from 74 % in 15-49 year-olds to 24 % in 80-99 year-olds. All statistics are from Cancer Research's analysis of the Office for National Statistics publication Cancer Registration Statistics, England: 2015 (Cancer Research UK, 2015)

1.2. Progression of the disease

It is widely accepted that MM progresses from the asymptomatic pre-malignancy named Monoclonal Gammopathy of Undetermined Significance (MGUS). Although this dyscrasia precedes MM, with 1 % of adults over 25 years of age having MGUS, not all those who are diagnosed with MGUS go on to progress, with only around 1 % per year doing so. Just as with MM, there is a greater prevalence and earlier development of MGUS in those of African origin, although progression of the disease

is equivalent (Kyle et al., 2002). MGUS is then thought to develop into an additional asymptomatic pre-malignant state termed Smouldering Multiple Myeloma (SMM). This is another asymptomatic PC dyscrasia with far more severe rates of progression to MM (20-30 %). Although many clinicians will diagnose it as symptomatic MM due to similarities, it does have definite and distinct diagnostic criteria (Van De Donk et al., 2016).

1.3. Diagnosis

The diagnostic criteria for MM are now set internationally by the International Myeloma Working Group (IMWG) with the latest revision in 2014 (Rajkumar et al., 2014). For diagnosis of MM there needs to be ≥10 % clonal PCs in the bone marrow and at least one myeloma defining event. The myeloma defining events are: hypercalcemia, characterised by a serum calcium level >0·25 mM higher than the upper limit of normal; renal insufficiency, characterised by a creatinine clearance <40 mL/min; anaemia, characterised by a haemoglobin value of >20 g/L below the lower limit of normal; serum free light chain ratio of >100, and Bone lesions, characterised by one or more osteolytic lesions on skeletal radiography, CT, or PET-CT.

The MM criteria differ from those for SMM, which is characterised by a 10-60 % clonal plasma cells in the bone marrow but without any myeloma defining events. Diagnostic criteria for MGUS require there to be no evidence of end organ damage, <10 % bone marrow plasma cells and low <3 g/dL presence of monoclonal protein (M-Protein) in the serum (Rajkumar et al., 2014).

1.3.1. Clinical features

Around 20 % of MM patients exhibit no symptoms, with the percentage increasing significantly over the past 25 years due to earlier diagnosis from better screening. When symptoms do present, either at diagnosis or from progression of the disease, they come about due to a number of physiological effects driven by the pathogenesis of myeloma cell as summarised in Figure 1.1.

Bone Pain and Hypercalcemia

Bone pain is one of the main symptoms of MM with around two thirds presenting with it in some form. Fractures are common in MM due to the destruction of bone from hyperactivity of osteoclasts and suppression of osteoblasts. Hypercalcemia occurs in 20-30 % of patients and normally correlates with a higher burden of disease. It is related to osteoclast over-stimulation and bone reabsorption, and manifests as mental changes, lethargy, nausea and vomiting and constipation (Oyajobi, 2007).

Two of the most significant molecules in causing bone destruction are Receptor Activator of Nuclear factor κ-B Ligand (RANKL) and Dick Kopf–related protein 1 (DKK-1). RANKL is secreted by bone marrow stromal cells (BMSC) and osteoblasts, and stimulates osteoclast growth as well as stimulating differentiation and maturation of osteoclast progenitors. Osteoprotegerin (OPG) acts as a decoy receptor for RANKL in myeloma. Heparan sulfates on the cell surface of myeloma cells allow for internalisation and degradation of OPG, leading to excess RANKL activity that induces osteoclast differentiation and proliferation (Standal et al., 2002). DKK-1 secreted by MM cells inhibits osteoblast activity, suppressing new bone formation and further contributing to the bone disease seen in myeloma patients (Tian et al., 2003).

Anaemia

Another highly prevalent symptom, seen in around two thirds of patients, is anaemia, characterised by fatigue and shortness of breath. This is due to a number of reasons relating to MM such as bone marrow infiltration, cytokine release, inadequate erythropoietin production and erythropoietin unresponsiveness (Ludwig, Pohl, & Osterborg, 2004). Cytokines released such as Interleukin-2 (IL-2), Fas Ligand, Tumour Necrosis Factor-β (TNF-β), Macrophage Inflammatory Protein-1α (MIP-1α) and TNF-related apoptosis-inducing ligand (TRAIL) all cause erythroblast apoptosis reducing red blood cell (RBC) count leading to anaemia (Silvestris, Cafforio, Tucci, & Dammacco, 2002).

Renal Insufficiency

Renal insufficiency is a frequent manifestation of MM and one of the more lethal symptoms. Two different processes can be involved in renal insufficiency with M-protein production being the biggest cause. Light-chain tubular cast deposition (normally associated with κ light chains) and amyloidosis (predominantly involving λ light chains) worsen over time without treatment and are associated with nephrotic range proteinuria leading to the development of kidney failure (Hutchison et al., 2012). In those patients that present with hypercalcemia, elevated calcium levels can lead to osmotic diuresis and pre-renal dysfunction, reducing urine volume. Additionally, hypercalcemia can also lead to the deposition of renal calcium further causing renal insufficiency (Hutchison et al., 2012).

Immunodeficiency

Immunodeficiency is also a symptom of concern in MM and is one of the leading causes of death in myeloma patients. Immunodeficiency is caused by several dysfunctions in immune cells. Dendritic cells are shown to be functionally defective in MM as they are unable to upregulate the important T-cell activation co-receptor CD80 (Brown et al., 2000). Inversion of CD4:CD8 T-cell ratio is also a symptom of MM. Reduction of CD4 T-cells disrupts many additional functions such as regulating macrophages and phagocytes as well as B-cell antibody class switching (Koike et al., 2002). In addition, other sub-types of T-cells are also perturbed such as natural killer T-cells (Dhodapkar et al., 2003). As such patients get frequent secondary infections. Apart from the dysfunction of the immune system caused by the disease itself, treatment of patients with medications such as corticosteroids or Bortezomib increase the likelihood of fungal and viral infections such as *Herpes zoster* (Nucci & Anaissie, 2009).

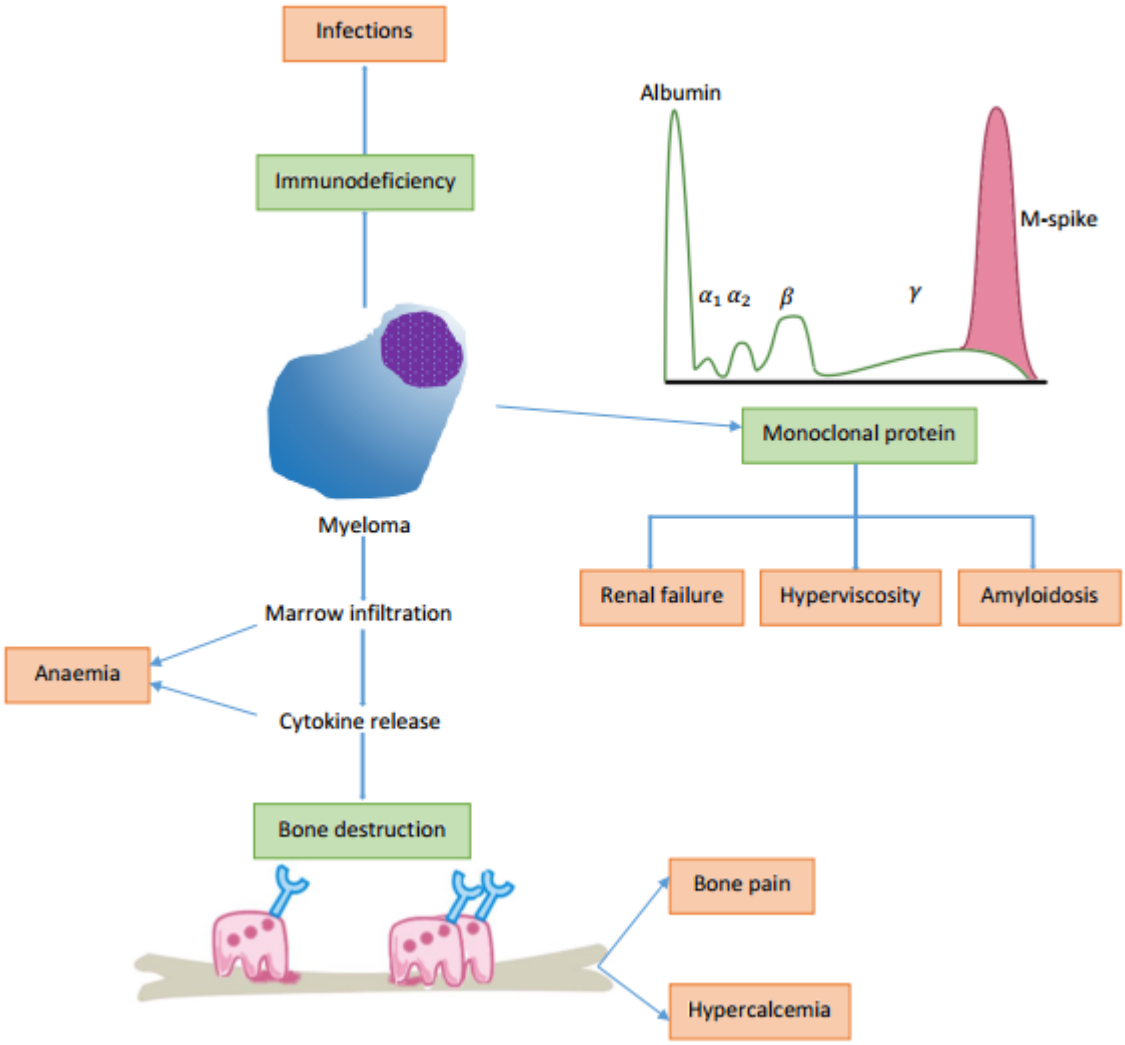


Figure 1.1. The multiple processes that result in the common symptoms of MM.

Synopsis of pathogenesis of Myeloma and the clinical features that the disease presents as shown in orange boxes. Through the proliferation of a clonal plasma cell and suppression of other immune cells and functions leading to immunodeficiency, repetitive infections are common in the later stages of the disease. Expression of monoclonal (M) protein by the myeloma cells cause hyperviscosity of the blood and M protein deposition in vital organs leading to amyloidosis and renal failure. Expansion of myeloma cells in the bone marrow outcompete other stem cells and progenitors leading to reduction in other haematopoiesis such as erythrocyte development leading to anaemia. Cytokine release by myeloma cells lead to osteoclast differentiation and proliferation and an inhibition of osteoblast activity leading to bone destruction and causing bone pain and hypercalcemia.

1.4. Epidemiology

Although genetic alterations are known to be the driving force for myeloma progression, the factors that initiate and drive these alterations are still largely unknown. Common carcinogens such as cigarette smoke and alcohol have been shown to play no role in the incidence of MM (Alexander et al., 2007). However, other lifestyle causes such as a high Body Mass Index (BMI), not associated with elite athletes, have been shown to increase the incidence in both men and women, although there is a higher incidence in women with a high BMI than that in men (Teras et al., 2014). Research has shown that adiponectin levels that are inversely correlated to obesity could explain this increased risk. Levels of adiponectin have been shown to be lower in patients with MM, and increasing adiponectin by pharmacological means has been shown to induce apoptosis in MM and prevent development of bone disease in mice (Wallin & Larsson, 2011).

Many studies have looked at the incidence of different occupations. Farming has been extensively studied and conflicting reports have both shown and disproven correlations between: exposure to grain dusts, wood dust, pesticides and sprays, as well as working in close proximity to poultry and other animals (reviewed in Alexander et al., 2007).

Radiation has also been mostly disproven, with studies on the survivors of the Japanese atomic bomb blasts showing no increased incidence of MM linked to the high exposure caused by the atomic blast (Hsu et al., 2013). This has also been further backed up by workers exposed to ionizing radiation and plutonium in the UK (Alexander et al., 2007) and X-Ray technicians in China (J. X. Wang, Boice Jr., Li, Zhang, & Fraumeni Jr., 1988).

Due to the nature of B-cells to undergo somatic hypermutation (SHM) in response to foreign elements, it has long been thought that overzealous SHM may cause MM by immunoglobulin enhancer elements being translocated in juxtaposition next to an oncogene, driving cancer development. Studies of military veterans have shown that infections such as Human Immunodeficiency Virus (HIV) (Goedert et al., 1998) and Hepatitis C virus (Duberg et al., 2005) do show significantly greater incidences of MM of 4.5 and 2.54 fold respectively.

Genetic predispositions increase incidences of many cancers. It has been shown that first-degree relative with a PC dyscrasia increases the likelihood of developing MM or MGUS (Vachon et al., 2009). Genome wide studies have identified a number of single nucleotide polymorphisms (SNP) including at chromosomes 2p23.3, 3p22.1, 3q26.2, 6p21.33, 7p15.3, 17p11.2, and 22q13.1 corresponding to genes *DNMT3A, ULK4, TERC, PSORS1C1, CDCA7L/DNAH1, TNFRSF13B, and CBX7* (Morgan et al., 2014). Although these SNPs have not been validated as driver genes in MM, they have been independently associated with development of MGUS (Weinhold et al., 2014). One known mutation that causes susceptibility to MM is that of rare low-penetrance mutation caused by the germ-line mutation observed in CDKN2A ($p16^{INK4A}$) (de Ávila et al., 2014).

1.5. Cytogenetic aberration and mutations

Although some cancers can be driven by a single mutation like that of t(9;22)(q34;q11) Philadelphia translocation in the majority of Chronic Myeloid Leukaemia (CML) cases, Myeloma has a far more comple*x g*enetic landscape. Gain, loss and translocations have been seen in both the p and q arms of every chromosome and can be identified by techniques such as fluorescent *in situ* hybridization (FISH) Figure 1.2. Here I will talk about some of the most common genetic aberrations.

1.5.1. Common Translocations

The most common translocations all involve the immunoglobulin heavy chain (IGH) locus on chromosome 14, suggesting that SHM may initiate the first driver mutations in the development of MM.

Translocation t(4; 14) presents in 15 % of MM patients and is associated with an adverse prognosis, resulting in the overexpression of *FGFR3* and *MMSET*. However, 30 % of these mutations also result in loss of *FGFR3* without a reduction in the adverse prognosis of the translocation, suggesting that *FGFR3* plays less of a role than *MMSET* in the pathogenesis of this translocation (Keats et al., 2003). The role of both

these genes on the drive of MM is unknown, however, the t(4; 14) translocation does result in cyclin D2 (CCND2) and in some instances cyclin D1 (CCND1) overexpression through an unknown mechanism (Prideaux, Conway O'Brien, & Chevassut, 2014). Translocations t(6; 14) upregulating cyclin D3 (CCND3) and t(11;14) upregulating cyclin D1 (CCND1) present in 2 % and 17 % of patients respectively (Zhan et al., 2006). Cyclin D isoforms promote the transition of cells in the G1 state to S-Phase, but only when present in an active complex with Cdk4/6 (Alao, 2007). Both these translocations and the t(4; 14) show just how important cyclins are in the proliferation and progression of MM.

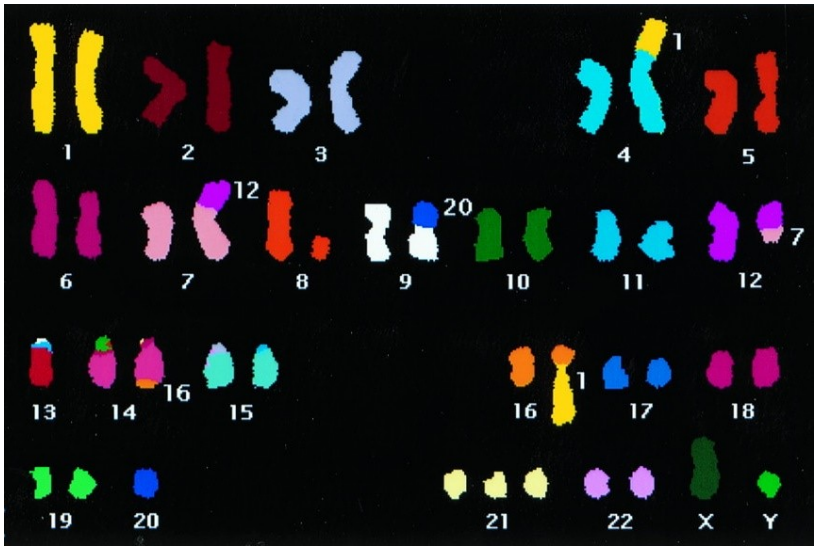


Figure 1.2. Example karyotyping of a MM patient.

Chromosome painting of a multiple myeloma cell by FISH. Each chromosome pair is given a solid unique colour. This patient profile shows loss of chromosomes e.g. 20, 13 and trisomies of chromosome 21. Multiple translocations are also present and shown by multiple colours on single chromosomes e.g. one of the sister chromosomes 16 shows a translocation with chromosome 1. Reprinted by permission from American Society of Hematology: Blood (Sawyer et al., 1998), copyright (1998)

Translocations t(14; 16) and t(14; 20) both result in overexpression of MAF oncogenes. t(14; 16) is especially associated with a poor prognosis, and is seen in 5-10 % of patients and results in overexpression of a c-MAF variant that, amongst other genes, regulate *CCND2*. t(14; 20) is quite rare and presents in 2 % of patients and results in over expression of the MAF gene homologue *MAFB*, which has also been shown to have a similar gene expression profile to c-MAF (Zhan et al., 2006).

Secondary translocations in later disease usually activate MYC and are indicative of an extremely poor prognosis. The most common secondary translocation is t(8; 14), although these secondary events do not always involve the IGH locus with 40 % of cases linking to different partner genes (Dib, Gabrea, Glebov, Bergsagel, & Kuehl, 2008). MYC over expression is seldom observed in MGUS but is seen in 15 % of MM patients rising to 50 % in the advanced later stages; this supports MYC's role as a driver of progression of MM (Avet-Loiseau et al., 2001).

1.5.2. Copy number variations

Hyperdiploidy is one of the most common genetic abnormalities, with close to 50 % of patients presenting with an increased number of chromosomes. Strangely, this usually involves trisomies of the odd numbered chromosomes 3, 5, 7, 9, 11, 15, 19 and 21 (Smadja, et al., 2001). Although hyperploidy is associated with patients with a higher level of bone disease, it is one of the more favourable prognoses. The mechanism by which hyperdiploidy benefits myelomagenesis is poorly understood. However, a number of genes, such as those in the Cyclin D family, have been shown to be overexpressed in patients with hyperdiploidy, as well as a high proportion of protein biosynthesis genes including those of ribosomes. These are thought to be attributable to the overactivation of the MYC, NF-κB MAPK signalling pathways (Chng et al., 2007). In 35-40 % of myeloma cases the gain of chromosome 1q arm is observed and normally correlates with the loss of the 1p arm (Chang et al., 2010). The gain of the 1q arm is also associated with a poor prognosis, even when secondary adverse cytogenetic lesions are not present. The correlation between this gain and a worsening prognosis has not yet been characterised but many oncogenes such as *CKS1B,*

ANP32E, BCL-9, and *PDZK1* may enhance the proliferation and invasiveness of this cytogenetic abnormality (Shaughnessy, 2005).

The loss of the 1p arm is observed in roughly 30 % of myeloma patients. The tumour suppresser gene *FAM46C*'s expression is dramatically reduced from the loss of the 1p arm. Its function is as yet unknown, although its role in suppressing tumours and the incidence of mutation of this gene in myeloma shows it is highly important for the pathogenesis of patients with this loss (Boyd et al., 2011). Two other genes, *FAF1* and *CDKN2C*, are negative regulators of the cell cycle and can enhance apoptosis through the Fas pathway, therefore deletion of these can lead to a more proliferative disease (Leone et al., 2008). Loss of either whole chromosome 13 or 13q arm is observed in 50 % of cases and is frequently observed alongside t(4; 14) translocation; as such the prognostic impact of this loss is hard to establish. However, it has been noted that patients with del(13/13q) do have a poorer prognostic outcome than patients that receive autologous transplantation. Although a number of genes are lost, there is evidence that the RB1 gene is the most important. *RB1* is shown to be significantly under expressed in myeloma with del(13/13q) (Walker et al., 2010). .

Loss of the 17p arm of chromosome 17 is only observed in 10 % of patients, with this frequency increasing in the later stages of the disease (Fonseca et al., 2003). This is one of the most important cytogenetic abnormalities for the prognostication of the disease and strongly correlates with an extreme aggressive disease phenotype, a higher degree of extramedullary disease and shortened survival. This is thought to be mostly due to a reduction in the expression of *TP53* and its role in being a transcriptional regulator of cell cycle, its role in DNA repair and initiation of apoptosis in response to DNA damage. As yet no biological evidence has been obtained to support this interpretation (Tiedemann et al., 2008).

1.6. Current Treatment of Multiple Myeloma

The therapy for MM has changed drastically since the first documented case in 1844 where a simple rhubarb pill and infusion of orange peel was prescribed (Kyle & Rajkumar, 2008). Today newly diagnosed MM patients are placed into two categories: those that are candidates for stem cell transplant (SCT), and those that are not. Unfortunately, due to the fact that the disease afflicts mostly the elderly (>65), the vast majority of patients are not suitable for SCT.

Those that are not candidates for SCT undergo multiple (normally 12) rounds of treatment with a combination of melphalan, prednisone, and thalidomide. After this time, patients are observed and subsequent cycles are given to patients who relapse (Kyle & Rajkumar, 2008).

Those candidates that are suitable for transplant undergo 2-4 cycles with non-alkylator based treatments such as thalidomide-dexamethasone combination therapy. Three methods of stem cell transplantation are open to patients. Autologous stem cell transplant (ASCT) is the most common procedure and although not curative it prolongs overall survival by approximately 12 months (Child et al., 2003). Tandem ASCT is where patients receive a second planned ASCT after recovery from the first procedure. This has been found to significantly reduce relapse and increase overall survival compared to single ASCT (Attal et al., 2003). The third transplantation procedure open to patients is allogeneic transplantation where an HLA-matched sibling donor is used instead of the patient's own treated stem cells. This, however, is not routinely carried out due to the age of patients and high incidences of graft-versus-host disease, which lead to high mortality rates (Bensinger, 2014).

1.6.1. Prednisone

It was not until 1962, when prednisone was trialled under double-blind conditions, that myeloma's first response to a drug was observed with a reduced serum globulin level. However, this had no effect on the survival rate, until it was combined with melphalan where a six-month survival increase was observed (Kyle & Rajkumar, 2008).

1.6.2. Thalidomide

The use of Thalidomide came from a very tainted past. In just over four years, as a treatment for morning sickness, its teratogenic effect had become evident with 10,000 children being affected with foetal malformations. Although it found additional uses, away from expectant mothers, it was not until 1994 that D'Amato described the antiangiogenic properties (D 'Amato, Loughnan, Flynn, & Folkman, 1994). In 1997 awareness of myeloma's increased angiogenesis became evident and Barlogie conducted the first trial enrolling 84 myeloma patients (Singhal et al., 1999). The results of which were very promising, with 32 % of patients responding to thalidomide treatment, making it the first new single agent for myeloma therapy in over three decades. Interestingly Thalidomide has been found to act on the UPS and binds to cereblon (CRBN), a substrate receptor of the cullin-4 Really Interesting New Gene (RING) E3 ligase complex (Liu et al., 2015)

1.6.3. Proteasome Inhibitors

Bortezomib,along with a number of other proteasome inhibitors were developed by Adams et al., 1999 and were found to be the first specific inhibitors of the proteasome. In 2002, a use for Bortezomib as a therapeutic agent was discovered, and led to a phase 1 study against myeloma (Orlowski et al., 2002). Later phase 2 trials, taking on 202 patients with relapsed refractory myeloma, showed one third response rate with an average survival increase of ~1 year (Richardson et al., 2003). This led to the rapid approval of Bortezomib by the FDA in May 2003 for the treatment of MM. Bortezomib works by inhibiting the chymo-trypsin like active site of the proteasome with a IC^{50} of 6 nM calculated from treatment of cell lysate (Demo et al., 2007).

However, Bortezomib was never explicitly designed for multiple myeloma and its use was only found after it was developed. It was thought (prior to this thesis) that Bortezomib inhibits all intracellular proteasomes to a similar degree no matter the cell type, and that the specificity in the treatment of myeloma over non-cancerous cells

was due to increased protein turnover. This increased protein turnover is not just due to the cancerous nature of myeloma cells. Whereas other cancers are highly proliferative, and the strain on protein degradation is down to proteins involved in the regulation of cell cycle and other cell state proteins, myeloma is a very slow proliferating disease. Genetic alterations such as hyperdiploidy increase copy numbers & overexpression of genes, this puts strain on protein degradation through the ubiquitin proteasome pathway, but this is not just a characteristic of myeloma. Other theories for the effectiveness of Bortezomib, such as site specific degradation of substrates and inhibition of proteasomal degradation of IkBα (an NF-κB inhibitor), have also been dismissed (Hideshima et al., 2009). The current consensus is that the highly secretory nature of myeloma cells, with the secretion of large amounts of M-protein, leads to a much higher load on the ubiquitin proteasome pathway (UPP) than other cells, meaning that only a modest inhibition is enough to cause a failure of the UPP and cell death (Bianchi et al., 2009). It is important to note that this model is open to questioning as well, especially in light of some of my observations in this thesis which argue against it. The hypothesis also does not explain why there is not a complete response in all myeloma patients (all of which produce large amounts of M-protein), as well as how resistance to Bortezomib arises.

1.7. The Ubiquitin Proteasome Pathway (UPP)

The proteins that make up the proteome of an organism are in a state of flux, constantly being synthesised and degraded. Proteolysis of proteins is done by the hydrolysis of the amide bond, which releases free amino acids that can be utilised in the synthesis of new proteins. Proteins can be classified into two groups: extracellular or intracellular. Extracellular proteins such as immunoglobulin, albumin or low density lipoprotein are found in the extracellular space around cells and are taken up by pinocytosis or receptor mediated endocytosis. The endosomes that are formed then fuse with lysosomes, where the extracellular proteins are hydrolysed by a multitude of the fifty known lysosomal hydrolases, such as the cathepsin family of lysosomal proteases, and are never exposed to the intracellular environment (Turk et al., 2012).

Intracellular proteins, however, differ in the means by which they are degraded, with inhibition of the lysosome degradation pathway not significantly perturbing intracellular metabolism. The half-life of the intracellular proteins vary greatly, from the tumour supressing protein p53 of a few minutes (Moll & Petrenko, 2003) to the 117 years of collagen in articular cartilage, (Verzijl et al., 2000) suggesting that intracellular proteins undergo a more selective mechanism of degradation. In 1975 Dr Gideon Goldstein discovered a protein that he found ubiquitously expressed in eukaryotic systems; he termed this protein 'ubiquitin' (Goldstein et al., 1975). In 1980, Herschko and Ciechanover showed that the protein APF-1 (subsequently identified as ubiquitin) attached covalently to a lysine residue on a target protein by an ATP dependent reaction (Ciechanover, Heller, Elias, Haas, & Hershko, 1980). Aaron Ciechanover, Avram Hershko and Irwin Rose further characterised the process of ubiquitination and ubiquitinated degradation between 1981-1983 earning them the Nobel Prize in Chemistry in 2004 (The Royal Swedish Academy of Sciences, 2004).

This finally shone light on the mechanism that allowed for the high degree of specificity needed to allow proteins to have wildly different half-lives compared to the aspecific nature of the lysosomal degradation pathway. It was further found that ubiquitin mediated proteolysis by the proteasome is important in the role of many cellular processes such as cell cycle and division, differentiation, response to stress, removal of misfolded proteins, DNA repair and transcriptional regulation, and inflammatory responses. It is also involved in the endoplasmic reticulum associated protein degradation pathway (ERAD).

Degradation of proteins through the UPP occurs in two successive steps, 1) the tagging and elongation of the substrate by ubiquitin monomers, 2) the recognition and degradation of the protein by the 26S proteasome.

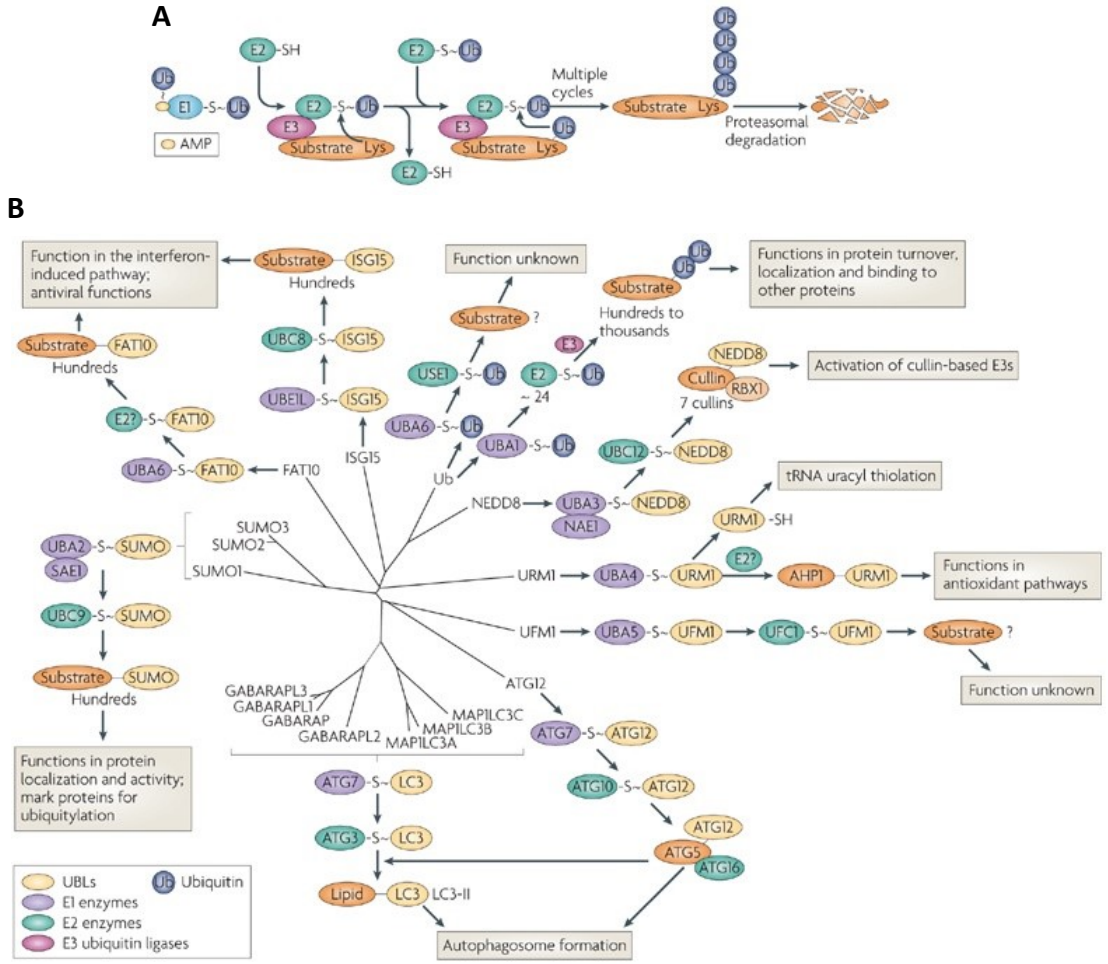


Figure 1.3. The complex nature of Ub and UBL post translational modification.

A) Shows the overall mechanism of ubiquitin conjugation onto a target substrate. Firstly, in an ATP dependant reaction a ubiquitin monomer forms a covalent link with a cysteine residue on a ubiquitin activating enzyme E1. The ubiquitin monomer bound to the E1 enzyme is then transferred to a ubiquitin conjugating enzyme E2. A substrate specific ubiquitin ligase E3 then brings the substrate and the ubiquitin loaded E2 into proximity for transfer of the ubiquitin directly or via an ub~E3 intermediate. B) How E1, E2 and E3 enzymes allow for the transfer of ubiquitin and a multitude of other UBL monomers onto protein substrates. Reprinted by permission from Macmillan Publishers Ltd: Nature Reviews Molecular Cell Biology (Schulman & Wade Harper, 2009), copyright (2009)

1.7.1. E1 – Ubiquitin Activating Enzymes

Ubiquitination of a protein starts with the ubiquitin monomer, a 76 amino acid protein with a molecular mass of about 8.5 kDa. Ubiquitin is highly conserved throughout all eukaryotes, with only 3 aa substitution between human and yeast sequences. The process in which this ubiquitin monomer is conjugated to a protein requiring degradation starts with the ATP dependent conjugation of ubiquitin to the cysteine residue of a ubiquitin activating enzyme (E1). In humans only two E1 enzymes have been discovered to date, encoded by *UBA1* and *UBA6* genes, with the latter also being involved in the addition of ubiquitin-like (UBL) protein modifier FAT10 onto proteins (Groettrup, Pelzer, Schmidtke, & Hofmann, 2008). Inactivation of Uba1, but not Uba6 is lethal to all human cells, showing that Uba1 is the main player in protein ubiquitination (Kulkarni & Smith, 2008; McGrath, Jentsch, & Varshavsky, 1991). Uba1 has two isoforms, Uba1a and Uba1b, with the former having an N-terminus nuclear localisation signal that promotes accumulation within this compartment (Stephen, Trausch-Azar, Handley-Gearhart, Ciechanover, & Schwartz, 1997). After the addition of ubiquitin to one of the E1 enzymes it is transferred to the next class of enzymes termed Ubiquitin Conjugating Enzymes (E2).

1.7.2. E2 – Ubiquitin Conjugating Enzymes

Transfer of the ubiquitin monomer from the E1 enzyme to one of ~35 human Ubiquitin Conjugating Enzymes (E2) is an ATP-independent reaction (van Wijk & Timmers, 2010). E2 enzymes are characterised by a highly conserved 150-200 aa ubiquitin conjugating catalytic fold, with a roughly 35 % conserved sequence between the different family members (Burroughs, Jaffee, Iyer, & Aravind, 2008). This fold provides the binding for both the E1 and E3 enzymes and activated ubiquitin (Burroughs et al., 2008). Within this domain a catalytic cysteine residue accepts activated ubiquitin from an E1 enzyme via a thio-ester bond. Just like the E1 enzyme Uba6 a portion of E2 enzymes also have activity in conjugating UBL proteins, such as Interferon Stimulating Gene 15 (ISG15) (Staub, 2004), autophagy related proteins ATG3, 8, 10, 12 (J. Geng & Klionsky, 2008), FAT10 (Hipp, Kalveram, Raasi, Groettrup, & Schmidtke, 2005) and SUMO (Michelle, Vourc'H, Mignon, & Andres, 2009) to protein substrates Figure 1.3.

1.7.3. E3 – Ubiquitin Ligases

The third group of enzymes in the UPP are termed the E3 ubiquitin ligase class of enzymes. An E3 ligase interacts with both ubiquitinated E2 enzymes and the protein substrate requiring ubiquitination. This is done by transfer of the Ub thioester from E2 cysteine to a lysine residue or N-terminus of the protein substrate either directly or through a Ub~E3 intermediate (Deshaies & Joazeiro, 2009). The E3 class of enzymes act as a molecular match maker bringing together the right substrate with the right E2 enzyme and catalysing the transfer of Ubiquitin from one to the other. Due to their role being specific to certain protein substrates E3 enzymes are by far the most diverse of the UPP with >600 E3 enzymes being predicted in humans (W. Li et al., 2008). E3 ligases fall into three distinct classes: Really Interesting New Gene (RING), Homology to E6AP C Terminus (HECT), and the recently discovered RING-Between-RING (RBR) families (Metzger, Hristova, & Weissman, 2012).

The RING class of E3 ligases do not form a Ub~E3 intermediate and contain no active site, but instead bring together E2 and substrate in close proximity greatly enhancing the rate of transfer of Ubiquitin from one to the other. The RING domain itself is highly conserved and contains two structural Zn^{2+} ions and can be found as either monomeric or dimeric depending on the enzyme. The RING domain binds to the N-terminal helix of the E2 conjugating enzymes (Zheng, Wang, Jeffrey, & Pavletich, 2000). They also contain multiple additional domains that vary and are involved in other functions including recruitment of the substrate for ubiquitination.

HECT E3 ligases catalyse the transfer of Ub to the substrate in two distinct reactions. After binding of the specific substrate and E2 enzyme a first reaction transfers the Ub from cysteine residue on the E2 enzyme to a cysteine residue in the HECT domain. This HECT~Ub undergoes a second reaction to transfer the Ub from the HECT cysteine to the substrate lysine (Huibregtse, Scheffner, Beaudenon, & Howley, 1995). The HECT domain itself is highly conserved and comprises an N-lobe that binds to the E2 enzyme and a C-lobe that contains the active site cysteine. Between these two lobes a flexible linker allows multiple configurations to allow for the HECT E3 activity. A substrate binding domain close to the N-lobe holds the substrate in place for the transfer of donor Ub from the C-lobe to the substrate lysine.

RBR E3 ligases have only recently emerged as a distinct class of E3 ligases sharing features of both HECT and RING E3 enzymes. These enzymes are characterised by two or more RING domains separated by a conserved in-between-RING (IBR) Domain and was first discovered in the Drosophila ariadne-1 enzyme (Aguilera, Oliveros, Martínez-Padrón, Barbas, & Ferrús, 2000). One of the most famous RBR E3 enzymes is Parkin, which is mutated in early onset Parkinson's Disease (Dawson & Dawson, 2010). The RBR class of E3 enzymes contain highly conserved histidine, aspartate and glutamate residues. These residues resemble the catalytic triad found in most deubiquitinating (DUB) enzymes, though here serve the opposite effect in ligating ubiquitin monomers onto the target substrate (Komander, Clague, & Urbé, 2009).

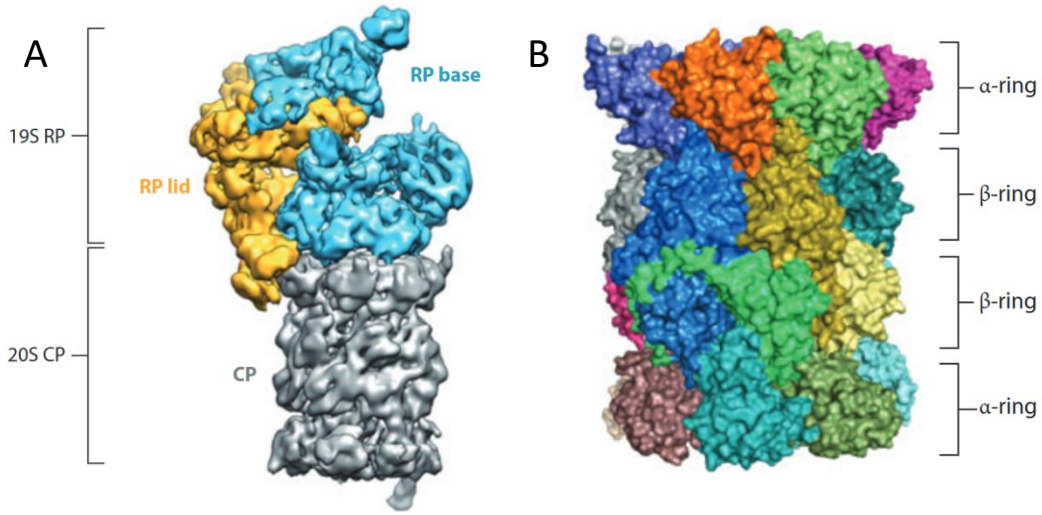


Figure 1.4. Structure of the 26S Proteasome.

A) 3D reconstruction at ~15 Å shows a 19S (coloured) singly capped 20S core particle (grey). The regulatory particle is further compartmentalised into the base (cyan) and the lid (yellow). B) Shows a 3D reconstruction of the 20S core particle with each subunit individually coloured to show the stacking of the seven α and seven β subunits into heptidomeric rings stacked in an αββα arrangement. Reprinted by permission from Macmillan Publishers Ltd: Nature Reviews Molecular Cell Biology (Lander et al., 2012), copyright (2012)

1.7.4. The 26S Proteasome.

The proteasome is a member of the ATPases Associated with diverse cellular Activities (AAA+) being by far the largest and most complex of these at 2.5 MDa in size. The proteasome is made up of two main components, the core particle (CP) and the regulatory particle (RP). The 20S core particle contains the proteolytic activity of the proteasome and is capped by one or more different RP types with the most common being the 19S RP. The CP is evolutionarily conserved in eukaryotes, archaea, and bacteria of the *Actinomycetes* phylum (Gille et al., 2003). Those bacteria that do not express the 20S proteasome expressing a homododecamer of the ClpQ/HslV complex (considered a phylogenetic ancestor of the 20S proteasome) (Bochtler, Ditzel, Groll, Hartmann, & Huber, 1999). However, ubiquitin has only been found in eukaryotes (Gille et al., 2003). This suggests that in prokaryotes a separate modification or chaperone is necessary for degradation by the 20S proteasome.

The 20S core particle

In humans the 20S core particle is made up of four axially stacked heteroheptameric rings comprised of two copies of 14 separate subunits. The outer two rings are comprised of the α1-7 subunits encoded by *PSMA6, 2, 4, 7, 5, 1 & 3* respectively. Whilst the inner two rings are comprised of the β1-7 subunits encoded by *PSMB6, 7, 3, 2, 5, 1 & 4* respectively. The subunit nomenclature for the 20S proteasome used in this thesis is as defined by (Baumeister, Walz, Zühl, & Seemüller, 1998).

There are six proteolytic active sites from the duplicates of three different catalytic subunits. These subunits have distinct specificity for cleavage of the amide bond after certain residues. The β1-subunit cleaves after acidic amino acids and is termed the caspase-like (C-Like) active site. The β2-subunit cleaves after basic amino acids and is termed the trypsin-like (T-Like) active site. The β5-subunit cleaves after hydrophobic amino acids and is termed the chymotrypsin-like (CT-Like) active site, this being the predominate site of Bortezomib inhibition (Harris, Alper, Li, Rechsteiner, & Backes, 2001).

In a subset of human cells there is expression of alternative catalytic subunits. Upon interferon-γ stimulation many immune cells replace their site bearing β-subunits with the immune specific proteolytic active sites β1i, β2i and β5i, encoded by *PSMB9,*

PSMB10 and *PSMB8* genes respectively. These changes are thought to enhance loading of peptides onto the class I major histocompatibility complex for immune presentation to killer T-cells (M Gaczynska, Rock, & Goldberg, 1993).

Within the thymus, the β1, β2 are replaced with β1i, β2i subunits while the β5 is replaced with a thymus specific catalytic subunit β5t encoded by *PSMB11*. This substitution appears to help with positive selection of T-cells during development by increasing the diversity of self-peptides (Murata et al., 2007).

The N-terminus of some of the α subunits of the 20S CP face into the lumen, forming a gate that is in a state of flux between open and closed (but predominately in the closed state) (P. A. Osmulski, Hochstrasser, & Gaczynska, 2009). Proteasomal activators such as the 19S RP house HbYX motif (where Hb is a hydrophobic amino acid, Y is tyrosine, and X is any amino acid) on the C-terminus of some subunits. These form salt bridges with the ε-amine on lysine residues of the α-subunits and induce a conformational change opening the gate (Rabl et al., 2008).

The 19S Regulatory Particle

The regulatory particle, as the name suggests, regulates the proteolytic activity of the CP by restricting access of substrates. It is comprised of at least nineteen subunits and is split into two subcomplexes termed the lid and base. These terms can be a little confusing as, contrary to the base residing between the lid and the alpha subunits of the core particle, it actually straddles the lid and has subunits both closest to and furthest away from the core particle Figure 1.4.

The RP base is comprised of a heterohexamer of AAA+ ATPase's in addition to three non-ATPase subunits. The ATPase ring forms a pore that abuts the pore of the CP lumen, but is offset by ~30Å (Tomko, Funakoshi, Schneider, Wang, & Hochstrasser, 2010). This ring is homologous to the proteasome-activating nucleotidase (PAN) structure found in archaea. Proline residues in these subunits adopt an alternating *cis* or *trans* arrangement allowing the N-terminal helices to pair together. Rpn1 closely associates with the ATPase ring and may help substrate docking to the proteasome, whilst Rpn10 and Rpn13 recognise ubiquitin on the ubiquitinated substrate. They are, however, not always found bound to the proteasome, though studies have shown they

occupy the proteasome more than 50 % of the time (Sakata et al., 2012). Rpn13 binds ubiquitin with a high affinity via β-strands comprising of a Pleckstrin-like receptor for ubiquitin (PRU) domain. Rpn10 on the other hand binds ubiquitin via three Ub-interacting motifs (UIM). Although Rpn10 contains three UIM's, orthologues that contain just a single domain do not enhance its preference of monoUb over polyUb. The ATPase ring binds a maximum of four nucleotides at once with the other two sites remaining empty. The nucleotides in the ring are hydrolysed simultaneously in pairs *para* to one another. This creates mechanical force that is thought to drive the terminus of the protein into the catalytic core of the CP (Lander et al., 2012) (Figure 1.5.).

The RP-lid is comprised of Rpn9, 5, 6, 7, 3, and 12. It is thought that the Rpn5 and 6 subunit stabilise the CP-RP via its N-termini, which extend and interact with both the base and the CP. Rpn11, along with other less tightly associated Deubiquitinases (DUB) such as Ubp6, recognise polyUb chains and cleave them from the distal end of the substrate (Figure 1.5.). Rpn11 is the primary DUB responsible for the removal of polyUb chains. Located in the RP lid with its active site positioned 10 to 20Å over the opening of the ATPase ring (Lander et al., 2012).

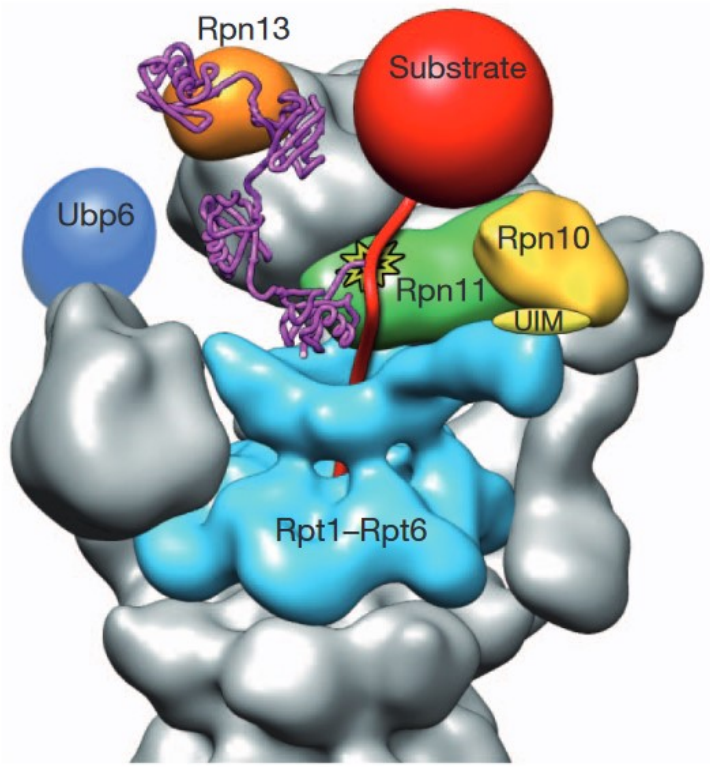


Figure 1.5. The major catalytic subunits of the 19S regulatory particle.

3D reconstruction of the 19S RP bound to the CP, highlighting the key players in the processing of ubiquitinated substrates and translocation into the CP. PolyUb chains of ubiquitinated substrates are recognised and held by Rpn13 and Rpn10 subunits. Next the polyUb chain is cleaved at the substrate lysine by Rpn11 and the substrate is unfolded and mechanically fed into the core particle by Rpt1-6 into the CP. Reprinted by permission from Macmillan Publishers Ltd: Nature Reviews Molecular Cell Biology (Lander et al., 2012), copyright (2012)

1.8. Regulation of the Proteasome

The proteasome, like other cellular enzymes and signalling proteins, are only active or functional when modified or bound to other molecular/protein co-factors. This allows the cell to rapidly regulate pathways without the slow and energy consuming process of protein biosynthesis and degradation.

Posttranslational Modifications

The 20S proteasome is regulated via a multitude of modifications and binding of activating proteins. Studies in yeast have found over 345 unique modifications to the 26S proteasome comprising of 11 different types of modification (Hirano, Kimura, & Kimura, 2016). A major modification in controlling activities of cellular enzymes is phosphorylation. It has been shown that all the subunits of the 26S proteasome have some level of phosphorylation, and protein kinase A (PKA)-treated proteasomes showed increased activity of all three catalytic active sites (Lu et al., 2008). Half of all of the phosphorylation events are found on serine or threonine residues followed by proline, which are sites usually phosphorylated by MAP and CDKs phosphatases. These enzymes are heavily involved in the cell cycle, perhaps indicating a role for some of these phosphorylation events in the regulation of cell cycle by the proteasome (X. Wang et al., 2007). In humans, a number of modifications identified have been shown to play a role in proteasome biology. Upon interferon-γ stimulation phosphorylation of α7 and α3 decreases. This decrease in phosphorylation of α7 reduces proteasome stability contributing to disassembly of the proteasome (Bose, Stratford, Broadfoot, Mason, & Rivett, 2004). PKA phosphorylation, through cyclic AMP signalling, activates Rpt6 on Ser14 (Lokireddy, Kukushkin, & Goldberg, 2015), and dephosphorylation of Rpt6 promotes the disassembly of the RP in porcine cardiac cells (Satoh, Sasajima, Nyoumura, Yokosawa, & Sawada, 2001). Not all phosphorylation is beneficial to the activity of the proteasome, as MAPK treatment of proteasomes or mutation of Thr273 in Rpt2 causes inhibition in the activity of the proteasome (Lee, Park, Yoon, & Yoon, 2010). Other modifications such as monoUb of Rpn10 inhibits the recognition of Ubiquitin substrates by the UIM motif (Isasa et al., 2010). Under cellular stress Rpn13 is poly-ubiquitinated, which leads to the degradation of whole proteasome particles through autophagy (Besche et al., 2014). O-GlcNAc of Rpt2 has also been shown to decrease proteasome activity (Zhang et

al., 2003). Nuclear proteasomes have also been shown to have a Poly-(ADP)-Ribose modification that is thought to activate proteasomes to degrade oxidatively damaged histones (Ullrich et al., 1999) Numerous other modifications have also been shown to reside on human proteasomes, such as sumoylation, 4-hydroxy-2-nonenal modification, oxidation and acetylation although the functions of these still remain elusive, reviewed in (Scruggs et al., 2012).

Regulation by factor binding

The 20S core particle, although able to degrade small peptides, is able to extend its repertoire of proteins that it is capable of degrading by binding to a number of regulatory particles. The most common of these is the 19S RP (described above) and 11S RP. The 11S RP is comprised of three copies of the two major subunits PA28α and PA28β encoded by the genes *PSME1* and *PSME2* respectively forming a heteroheptameric ring. Following interferon-γ treatment, the cells replace these with the six PA28γ subunits encoded by *PSME3* form a homohexameric ring (Rechsteiner & Hill, 2005). This ring harbours a central channel of 20-30 Å in which the substrate translocates down to the proteolytic core of the CP (Knowlton et al., 1997). Whereas the 19S RP has been involved in the hydrolysis of ubiquitinated substrate the 11S requires no Ubiquitin presentation and is thought to be implicated in the production of MHC class I ligands (Groettrup, Kirk, & Basler, 2010). Unlike the 19S this RP does not require ATP to process proteins for degradation. Another smaller activator is PA200 does not utilize ATP and is generally believed to stimulate the hydrolysis of peptides but not proteins. PA200 is another proteasome activator encoded by PSME4 it has been found to play a role in a wide variety of processes including: 20S proteasome assembly (Fehlker, Wendler, Lehmann, & Enenkel, 2003), DNA repair (Ustrell, Hoffman, Pratt, & Rechsteiner, 2002), and spermatogenesis (Khor et al., 2006).

Regulation by allosteric inhibitors

To date a few naturally occurring inhibitors bind to other subunits and cause allosteric inhibition of the proteasome. The peptide PR-39 was discovered in the intestine of pigs and was first identified to have antibacterial properties. Later it was shown to bind to the α7 subunit of the core particle inhibiting the proteolytic activity of the 20S proteasome allosterically as well as disrupting the proper engagement of the core and regulatory particles (Maria Gaczynska, Osmulski, Gao, Post, & Simons, 2003). Another identified allosteric proteasome inhibitor is 5-amino-8-hydroxyquino-line. It was shown by NMR to bind to the inner core in a non-competitive manor again to the α7 subunit (X. Li et al., 2010) Rampamycin has also been shown to inhibit the proteasome, through a mechanism of binding to the *α* face of the proteasome (P. a Osmulski & Gaczynska, 2013). To date no allosteric inhibitors are used to target the proteasome in vitro, although they present an exciting new target that may allow for synergistic inhibition in combination with active site inhibitors of the proteasome such as Bortezomib. Which there method of inhibition being distinct to that of Bortezomib, allosteric inhibitors may also be able to combat the resistance that is seen with traditional PIs.

1.9. Role and function of the 26S proteasome

The majority of intercellular proteins are degraded to some extent by the proteasome. Targeting of proteins, to regulate cellular functions during certain cell states, is carried out by specific E3 ligases that are active during certain cellular processes. The function of the proteasome therefore has major influences on all processes that require timely and selective degradation of proteins. This includes but is not limited to cell cycle control, apoptosis, pathogenesis and cell differentiation.

1.9.1. Cell cycle control by the 26S proteasome

Cell division requires two major processes: firstly genome duplication, where the chromosomal DNA is duplicated; and secondly separation of sister chromosomes and cytokinesis of the cell. During G1/S phase the sister chromatids are separated from each other at the centromere and replication of each sister chromatid occurs. This is

a highly regulated cellular process where progression from the different phases of cell cycle are strictly bound to the completion of each step to prevent genome loss and to reduce mutagenesis. The duplication is regulated by positive regulators such as cyclins, cyclin dependant kinases (CDK), CDK-cyclin complexes, E2F and Cdc6, and negative regulators such as Cip/Kip and IMK4 family CDK inhibitors. The timely regulation of each of these positive and negative regulators is controlled by inactivation and degradation by the proteasome (Renee Yew, 2001). During the G2/M phase of the cell cycle the duplicated chromosomes are orientated along the central plane of the cell where the kinetochore microtubules pull each chromosome to poles of the cell ; the cell is then divided into two via cytokinesis. During these processes there are a number of positive and negative regulators that are known to be degraded at certain checkpoints in order for cell division to progress.

Positive regulators of cell cycle

The majority of positive regulators allow for the transition of the cell cycle from G1 to S phase. Cyclin A is required for mitosis to happen and specifically for S phase progression. It is ubiquitinated by the E3 ligase anaphase-promoting complex/cyclosome (APC/C), a cell cycle regulating multi-subunit ubiquitin ligase, during the M2/G1 phase of the cell cycle (Bastians, Topper, Gorbsky, & Ruderman, 1999). This proteasome degradation is essential for the entry into S phase. The D type family of cyclins are growth factors that bind to Cyclin-Dependant kinase inhibitors (CKIs) such as p21Cip1/Waf1 and p27Kip1 resulting in cyclin-CKI complexes (Cheng et al., 1999). The D type cyclin family are also required for progression into S phase and tightly regulated by proteasome degradation after relocalisation to the cytoplasm of the cell during S phase (Diehl, Zindy, & Sherr, 1997). Abnormal or defective degradation of the cyclin D family by the proteasome leads to a build-up of these proteins and is observed in certain breast cancers and thought to contribute to their neoplastic proliferation (Russell et al., 1999). Cyclin E is required for the initiation of chromosome replication and is found bound to CDK2 during late G1 early S phase. Both CDK 2-bound cyclin E and free cyclin E are targeted for proteasome degradation at the G1 to S phase transition also demonstrating a role of this cyclin in S phase entry (Singer, Gurian-West, Clurman, & Roberts, 1999). The transcription factor E2F1 is also found to be required for G1 to S phase transition and is dissociated with the

retinoblastoma tumour suppressor protein Rb through degradation by the 26S proteasome (Campanero & Flemington, 1997). Another important positive regulator is the cell division cycle 6 protein (Cdc6). Its role is essential in the unwinding of chromosome DNA before replication can occur in S phase after which cdc6 dissociates from the DNA replication complexes and is targeted for proteasome degradation by APC/C (Petersen et al., 2000).

Negative regulators of cell cycle

Negative regulators undergo proteasome degradation allowing for transition into the next phase of the cell cycle. The CKI p21Cip1/Waf1 negatively regulates G1 and early S phase events through binding to CDKs and proliferating cell nuclear antigen (PCNA) (Luo, Hurwitz, & Massagué, 1995). If the DNA in the cell is damaged during replication, levels of p21Cip1/Waf1 are increased by tumour suppressor protein p53 arresting the cell in G1 phase until the cell DNA is repaired or the cell cycle aborted and apoptosis ensues (El-Deiry et al., 1994). Although p21Cip1/Waf1 is shown to be ubiquitinated and degraded by the proteasome, *in vitro* experiments interestingly show that ubiquitination is not strictly necessary for processing by the 26S proteasome (Sheaff et al., 2000). p27Kip1 is highly abundant in G0 and G1 phases. Removal of this cell cycle block is again required for transition of the cell into S phase and this is done via proteasomal degradation and other proteolytic processing (Shirane et al., 1999). Geminin was discovered in fertilised *Xenopus* eggs. It is expressed during S, G2, and M phases of the cell cycle but is ubiquitinated by APC/C and degraded by the 26S proteasome at the metaphase-anaphase transition (McGarry & Kirschner, 1998). p19INK4d is expressed at S, G2/M phases where it binds to cyclin D to form complexes that negatively regulate cell cycle progression. Its removal from the cell has also been shown to be regulated by ubiquitination and degradation of the 26S proteasome (Thullberg, Bartek, & Lukas, 2000).

With a large number of cell cycle regulators requiring degradation of by the proteasome for cell cycle to ensue, the activity of the proteasome is essential for normal mitosis of the cell. Therefore prevention of the processing of the above factors would be lethal to any cell type.

1.9.2. Regulation of pathogenesis by the 26S proteasome

An increasing body of work shows strong evidence that perturbment of the UPS contributes to pathogenesis of several human diseases, most extensively studied is that of cancer and neurological diseases such as Parkinson's and Alzheimer's.

Cancer

Due to its role in the removal and regulation of many cellular factors and proteins disruption of the normal regulation of, especially that of tumour suppressors and oncoproteins are strongly associated with initiation of neoplastic proliferation and tumour progression. Enhanced proteasomal degradation of p27Kip1 in lung carcinomas (Catzavelos et al., 1999), colorectal carcinomas (Loda et al., 1997), breast carcinomas (Catzavelos et al., 1997), gliomas (Piva et al., 1999) and lymphomas (Chiarle et al., 2000) have been reported. Perturbment of the UPS allowing for dedifferentiation or metastasis of cancers by cell specific transcription factors and cell anchoring proteins connexins have also been shown (Korinek et al., 1997).

Neurological diseases

Parkinson's disease, a neurodegenerative movement disorder, is characterised by progressive cell death of the neurons contained within the substantia nigra of the mid brain. α-synuclein normally found at the presynaptic terminals builds up in patients with Parkinson's creating a toxic accumulation of protein, lewy bodies, and cytoplasmic inclusion bodies eventually leading to apoptosis and death of the neuron (Hattori et al., 2000). In the majority of cases the E3 ligase, parkin, is mutated and therefore ubiquitination of α-synuclein does not occur (Shimura et al., 2000).

Alzheimer's disease is the most common form of senile dementia and caused by the progressive loss of cortical and limbic neurons. The role the UPS plays in this is more complex than in Parkinson's disease, amyloid β-peptides and hyperphosphorylated tau proteins are extra cellularly deposited in senile plaques (Fergusson et al., 1996). The 26S proteasome has been found residing in these senile plaques suggesting the perturbment of the proteasome's ability to degrade the proteins of which the plaque is comprised. In some patients a mutant form of ubiquitin has been shown to be

expressed and competes with normal ubiquitin inhibiting proteasome degradation (Hong, Huang, & Jiang, 2014)

1.9.4. Cell differentiation by the 26S proteasome

With all cells in metazoans containing the same DNA regulation of tissue specific proteins is done via precise intrinsic programs [reviewed in 1.28]. This area of research is still in its infancy but a number of proteins degraded by the 26S proteasome or regulated by transcription through 19S sub complex have been shown to promote differentiation of cells in multiple animal systems. The 26S proteasome proteolytic activity has been shown to be absolutely essential for oocyte maturation in *Xenopus* and *Rattus rattus* and is presumably essential for all other metazoans (Reverte, Ahearn, & Hake, 2001). In human oocytes proteasome inhibition has also been shown to inhibit meiosis (Alvarez Sedó et al., 2012).

1.10. Intercellular localisation of proteasomes

Proteasomes are highly abundant and make up approximately 0.6% of total cellular protein (Hendil, 1988). Many studies have been carried out to work out intercellular localisation of proteasomes and how they are organised within the cell. Early studies utilised electron micrographs after immunogold labelling (Rivett et al., 1992). They showed that proteasome composition changes between the different compartments of the cell depending on cell type. The results by Rivett et al., 1992 and others were highly variable due to the different techniques, antibodies and cell types utilised. A major advance in the quantification in the amount and distribution of the proteasomes came with a GFP-LMP2 fusion proteasomal subunit that was able to be actively incorporated into native 20S particles in living cells (Reits et al., 1997). From these fluorescently labelled proteasomes it was possible to see proteasome localisation and abundance changed dramatically through the different stages of the cell cycle, cell differentiation, as well as in cancer.

1.10.1. Cytoplasmic proteasomes

Early studies by Rivett et al., 1992 showed that 83 % of 20S proteasomes resided in the cytoplasm of rat hepatocytes in comparison to 50 % residing in the cytoplasm of L123 cells. Later studies showed that poor growth conditions and high cell density resulted in an increase in cytoplasmic proteasome accumulation (Machiels et al., 1995). The cytoplasmic proteasomes regularly interact and associate with the cytoskeletal network within cells especially with intermediate filaments (Olink-Coux et al., 1994). This is especially pronounced during the G2 phase of the cell cycle (Palmer et al., 1994). With proteasomes playing an important role in ERAD it is not surprising that proteasomes also associate with the ER. The proportion of proteasomes that associate varies greatly, with one study estimating that 14 % of cytoplasmic proteasomes are associated with ER in rat hepatocytes (Amparo Palmer et al., 1996; Rivett et al., 1992), while other studies looking at proteasomes associating with ER in crustacean mussels calculate it to be closer to 1% (Beyette & Mykles, 1992). Subcellular fractionation has shown that proteasomes almost exclusively associate with the smooth, and not the rough, ER and the cis-Golgi (Amparo Palmer et al., 1996). Studies have also shown that the proteasomes that tend to associate with the ER are enriched in immuno-subunits, which, as discussed previously are expressed in

immune cells, especially those of plasma and myeloma cells for the degradation of peptides for MHC antigen presentation (Kloetzel, 2001; Palmer et al., 1996). Interestingly, yeast that do not encode/express immunoproteasomes also show the majority of proteasome localisation to the ER and nuclear envelope suggesting that proteasome localisation to the ER may not be purely due to MHC presentation (Enenkel, Lehmann, & Kloetzel, 1999). Other studies show the 26S proteasome being mostly localised to the nucleus in yeast. These two findings could suggest that the faster growth and cell cycles in yeast require more timely degradation of nuclear transcription factors and nuclear proteins (Russell et al., 1999). Proteasomes have also been found upon starvation of cells to be localised to lysosomes, and is probably due to non selective autophagy of cellular proteins, and are unlikely to survive degradation within the lysosome compartment (Cuervo, Palmer, Rivett, & Knecht, 1995).

1.10.2. Nuclear Proteasomes

The exact mechanism of how proteasomes enter the nucleus remained a mystery for some time. At particular cell stages, especially G2 phase, the majority of proteasomes reside in the nucleus of the cell. It had been known that a number of proteasome subunits carry nuclear localisation signals such as subunits α1-4. Others have shown that tyrosine phosphorylation of some subunits such as α7 and α3 may also play a role in cytoplasmic nuclear transfer of proteasomes (Tanaka et al., 1989; Wang, et al., 1997). Until relatively recently it was not understood how such large complexes or proteasomes could enter the nucleus even with nuclear localisation signals on certain subunits. It was also hard to understand how proteasome assembly could be carried out in the nucleus due to the number of subunits that lack nuclear localisation signals and other assembly chaperones not present in the nucleus. Studies on yeast identified blm-10 protein (human orthologue p200), which binds to proteasomes and is important to proteasome storage granules is plays a role in the transport of core particles into the nucleus [[]]. Further studies in yeast have shown that importins can also transport immature partially assembled proteasome particles such as single α and β rings that can mature and form complete 20S core particles within the nuclei of yeast. A number of regulatory particle subunits also carry nuclear localisation signals such as Rpn2 and

Rpt2. These are imported again by importins α β as a complete regulatory particle into the nucleus.

From GFP tagging of lmp2 it is shown that after nuclear envelope breakdown during mitosis proteasomes diffuse throughout the cell but after telophase and the restoration of the nuclear envelope proteasomes are actively transported slowly back into the nuclear compartment (Reits et al., 1997). In quiescent cells or post mitotic cells such as neurones there is greater localisation of proteasomes in the cytoplasm further suggesting that nuclear localisation of proteasomes is important for cell cycle regulation (Pitzer et al., 1996). Although some studies have shown proteasomes in the nucleoli of cells (Mattsson et al., 2001) this is highly disputed and others that have put forward detailed proteomic analysis of nucleoli do not support this (Andersen et al., 2002).

1.11. Aims of this work

Although the proteasome is subject to extensive PTMs, it is evident from the current literature that the full extent and function of these modifications are as of yet unknown. From understanding these PTMs, manipulation of the processes in which they are regulated maybe possible by pharmacokinetic compounds and could yield better non-activesite proteasome inhibitors. Other compounds have been shown to inhibit the proteasome by binding to other non-catalytic subunits of the proteasome as described above. The aims for this project are therefore threefold:

1) To understand the role an as of yet unknown modification identified in the Kleijnen Lab, and what effect it has on the proteasome and how this may regulate it.
2) To decipher the ability of PIs ability to kill myeloma cells over that of other cell types and cancers.
3) To develop and test the ability of a proteasome binding peptide in its ability to inhibit degradation of ubiquitinated substrates.

CHAPTER 2 – MATERIALS & METHODS

CHAPTER II: MATERIALS AND METHODS

2.1 Molecular cloning

2.1.1 DNA digestion with restriction enzymes

The restriction enzymes used in this project unless otherwise stated were all from ThermoScientific's Fast Digest range. The digestions were all carried out following the products protocol. Reactions were carried out in 25 µl or 50 µl volumes comprising of 1-2 µg of DNA, 1 µl of each restriction enzyme and 1x Fast Digest buffer. Digestions were incubated at the optimum temperature for 30 min - 1 hour.

2.1.2 Phosphorylation and Annealing of Oligo DNA

Oligos synthesised by Sigma were diluted to a 20 µM stock solution. Firstly, the oligo's were phosphorylated and a reaction was set up consisting of 5 µl of the forward oligo, 5 µl reverse oligo, 5 µl 10x Ligase Buffer(NEB) (Source of ATP), 1 µl T4 Polynucleotide Kinase (PNK)(NEB) and 34 µl ddH_2O. The reaction was placed in a thermocycler (2720, Applied Biosciences) and heated to 37 °C for 1 h. The samples immediately proceeded into the annealing cycle where the temperature was raised to 99.5 °C and lowered 0.25 °C every 15 seconds until it reached 20 °C. Annealed oligos were used immediately in ligations or stored long term at -20 °C.

2.1.3 Polymerase Chain Reaction (PCR)

All PCR amplifications were made up on ice in thin walled PCR tubes (FisherScientific) or 96 well plates (FisherScientific) and cycles preformed in a thermocycler (2720, Applied Biosciences). High Fidelity PCR was carried out for any DNA that was amplified for the purpose of cloning. Standard Taq PCR and Taq Colony PCR was used to validate cloning to confirm that inserts had been successfully ligated into the plasmid vector.

High Fidelity PCR was carried out using Q5 Polymerase (NEB). Amplification of target sequence was carried out in 50 µl reactions comprising of 1x Q5 Reaction buffer, 200 µM dNTPs, 0.5 µM Forward Primer, 0.5 µM Reverse Primer, Template DNA (0.5 µg cDNA or 1 ng Plasmid), 2 U Q5 Polymerase (NEB) and ddH_2O up to 50 µl. Amplification was carried out using the below cycling conditions detailed below:

Stage	Step	Temp	Time	Cycles
Denaturation		98 °C	30 Sec	1
Amplification	Denaturation	98 °C	5 Sec	28
	Annealing	50-72* °C	20 Sec	
	Extension	72 °C	30 Sec/kb	
Final Extension		72 °C	2 min	1
	Hold	4 °C	∞	1

*Annealing temperatures varied with primers used

Taq Polymerase PCR were carried out using DreamTaq Green PCR Master Mix (ThermoFisher). Amplification of target sequence was carried out in 50 µl reactions comprising of 25 µl DreamTaq master mix, 0.5 µM Forward Primer, 0.5 µM Reverse Primer, Template DNA (0.5 µg cDNA or 1 ng Plasmid) and ddH_2O up to 50 µl. Amplification was carried out using the below cycling conditions detailed below:

Stage	Step	Temp	Time	Cycles
Denaturation		95 °C	2 min	1
Amplification	Denaturation	95 °C	30 s	30
	Annealing	50-72* °C	30 s	
	Extension	72 °C	1 min/kb	
Final Extension		72 °C	6 min	1
	Hold	4 °C	∞	1

*Annealing temperatures varied with primers used

Colony PCR of bacterial transformants were carried using DreamTaq Green PCR Master Mix (ThermoScientific). Amplification of target sequence was carried out in 50 µl reactions comprising of 25 µl DreamTaq master mix, 0.5 µM Forward Primer, 0.5 µM Reverse Primer, Template DNA (colonies were lightly touched with pipette tip and then reaction mixture pipetted up and down twice, to transfer bacteria) and ddH_2O up to 50 µl. Amplification was carried out using the below cycling conditions detailed below

Stage	Step	Temp	Time	Cycles
Denaturation		95 °C	2 min	1
Amplification	Denaturation	95 °C	30 s	30
	Annealing	50-72* °C	30 s	
	Extension	72 °C	1 min/kb	
Final Extension		72 °C	6 min	1
	Hold	4 °C	∞	1

*Annealing temperatures varied with primers used

2.1.4 Agarose gel electrophoresis of DNA

DNA agarose gels were cast by melting between 1 % (w/v) and 1.2 % (w/v) Molecular grade agarose (Sigma) in 1x TAE (40 mM Tris (pH 7.6), 20 mM acetic acid, 1 mM EDTA). This was allowed to cool to around 50 °C before adding 1x Syber Safe DNA stain (Invitrogen) and cast in an Owl D3-14 Horizontal Electrophoresis System (ThermoScientific).

6x loading buffer (ThermoFisher) was added to DNA samples to a final 1x concentration and then loaded into the cast agarose gel submerged in 1x TAE. Samples were flanked by Generuler 1 kb Plus (ThermoFisher) DNA standard and run at 70-90 V using the Owl D3-14 Horizontal Electrophoresis System (ThermoScientific). Visualisation of DNA bands was carried out by exposing agarose gels to UV light on a transilluminator (BioDoc-It imaging system, UVP).

2.1.5 Ligation

Ligation of DNA fragments was performed using T4 DNA Ligase (NEB) following manufacturer's protocol. Ligation was performed with a 1:3 molar ratio calculated using the calculation detailed below. In the case of three-way ligations a ratio of 1:3:3 was used with each insert. 50 or 100 ng of linear vector was added with 1x ligase buffer and 0.5-1 µl T4 DNA Ligase and ligated at room temperature for 30 min in a variable volume depending on DNA concentration.

$$\text{ng of Insert(s)} = \text{ng of Vector} \times \frac{\text{Length of Insert (bp)}}{\text{Length of Vector (bp)}} \times 3$$

2.1.6 Sequencing

Confirmation of DNA sequence was performed by adding 300-600 ng of plasmid DNA with 3.2 pmoles of sequencing primer and brought to a final volume of 10 µl in ddH_2O and sequenced using the sequencing service at MRC CSC Genomics Laboratory (Hammersmith Hospital, London). Sequencing was performed using big dye terminator technique and read by an automated fluorescent DNA sequencing instrument Applied Biosystems 3730XL. Chromographs and sequencing files were analysed using SnapGene 2.3.2 software.

2.2. Handling *Escherichia coli* and Isolation of Plasma DNA

2.2.1. *E. Coli* Strains and Genotype

Throughout this project the bacterial strain DH5α (NEB 5α) was used for the expansion of plasmid DNA and BL21(DE3) (NEB) was used for bacterial protein expression.

DH5α Genotype: (*fhuA2 Δ(argF-lacZ)U169 phoA glnV44 Φ80 Δ(lacZ)M15 gyrA96 recA1 relA1 endA1 thi-1 hsdR17)*

BL21(DE3) Genotype: (*BfhuA2 [lon] ompT gal (λ DE3) [dcm] ∆hsdS λ DE3 = λ sBamHIo ∆EcoRI-B int::(lacI::PlacUV5::T7 gene1)i21 ∆nin5*)

2.2.2. Liquid and Solid Media

Lysogeny Broth (LB) (Sigma) Liquid Media or LB Agar (Sigma) Solid Media was used to support and grow all bacterial strains throughout this thesis. Media was always autoclaved and left to cool before the addition of antibiotics. LB agar was melted and cooled to around 50 °C before antibiotics were added. 9 cm petri dishes (Corning) were then poured in laminar flow hood with lids left open to dry for 20 min before storage at 4 °C. Selection of transformants was done by the addition of the following antibiotics of 100 µg/ml ampicillin (Sigma) or 25 µg/ml chloramphenicol (Sigma)depending on the transformed plasmid.

2.2.3. Preparation of Competent Cells

Competent bacterial strain DH5α (NEB) were expanded and made chemically competent via the following method. Bacteria were streaked onto LB Agar plate containing no selectable antibiotics and incubated for 16 hours. A single colony was picked from this plate and added to 5 ml of antibiotic free LB Broth for a further 16 hours. The 5 ml culture was then decanted into an Erlenmeyer flask containing 400 ml antibiotic free LB and incubated at 37 °C until an OD_{600} of 0.6 was reached. The flask was placed immediately for 15 min on ice and then centrifuged for 20 min at 3,500 *x g* at 4 °C. The resulting pellet was resuspended in 100 ml of 0.1 M $MgCl_2$. Cells were again centrifuged for 20 min at 3,500 *x g* at 4 °C and the pellets resuspended in 200 ml of 0.1 M $CaCl_2$, and placed on ice for a further 30 min. The cells were again centrifuged for 20 min at 3,500 *x g* and pellet resuspended in 8 ml ice cold 0.1 M $CaCl_2$ 15 % (v/v) glycerol and aliquoted into 100 µl aliquots and snap frozen for 15 min on dry ice. The resulting competent cells were further stored at -80 °C until needed.

2.2.4. Chemical Transformation

Transformation of 'home made' and purchased DH5α cells was carried out as stated in the NEB DH5α instruction manual. Briefly, cells were thawed on ice and 3-5 µl of ligation reaction was added to 50 µl of competent cells and incubated on ice for 20 min. The cells were then heat shocked at 42 °C for 40 s and then immediately quenched on ice for a further 5 min. After this time 500 µl of warm 37 °C LB was added to the cells and the cells were allowed to recover on a shaking thermo-mixer set to 37 °C with aggregation for 1 hour. Cells were then plated on a pre warmed LB Agar plate containing selectable antibiotic and incubated at 37 °C for 14 h.

2.2.5. Isolation of Plasmid DNA

Plasmid DNA from transduced bacteria was isolated by means of kits utilising an alkaline-SDS lysis method. GeneJet Plasmid MiniPrep Kit (ThermoScientific) isolated 2.5 µg to 20 µg from a 5 ml culture as per manufacturers protocol. Larger quantities of plasmid DNA was isolated for long term storage or for use in virus production using GeneJet Endo-free Plasmid MaxiPrep Kit (ThermoScientific). The protocol was carried

out as per manufacturers protocol with the exception of starting from a 300 ml culture. This resulted in 800 µg to 2 mg of plasmid DNA.

2.2.6. Glycerol Stock

For long term storage of transformants 750 µl of overnight culture was added to 250 µl of glycerol in a screw top tube and gently but thoroughly mixed. Tubes were snap frozen on dry ice and stored at -80 °C. To recover bacteria for growth and expansion, the tube was briefly removed from -80 °C and a sterile loop used to scrape some of the frozen bacteria off of the top of the frozen stock. The glycerol stock was immediately returned to -80 °C to prevent thawing and the bacteria streaked onto a warm LB agar plate.

2.2.7. Purification of bacterially expressed proteins

Induction and lysis of BL21(DE3) transformants

Cells were streaked out from glycerol stocks and incubated at 37 °C for 16 h, single colonies were plucked and added to small 5 ml cultures and incubated for a further 16 h at 37 °C with aggregation. The 5 ml culture was then added to 1 L of LB Broth and incubated at 30 °C for 16 h. Induction of expression of bacterial plasmid was induced by the addition of Isopropyl β-D-1-thiogalactopyranoside (IPTG)(SigmaAldrich) to a final concentration of 500 µM and the culture raised to 37 °C for a further 4 h. Cells were then pelleted at 3,500 *x g* for 20 min. The bacterial pellet was then resuspended in 50 ml of PBS and lysed through a pre cooled NanoDeBEE (BEE International) homogeniser at 19,000 psi. The lysate was precleared of cellular debris by centrifugation at 3,500 *x g*.

Isolation of proteins from bacterial lysate

After induction of the bacterial protein and lysis of the cells as stated above the expressed protein was purified using an affinity matrix depending on the fusion tag expressed. Below are the bacterial proteins purified throughout this thesis and the capture and elution protocol.

The C-terminally His^6-tagged ubiquitin-like (UBL) domain of hPLIC2 (construct #4615 (Walters, Kleijnen, Goh, Wagner, & Howley, 2002)), and the C-terminally His^6-tagged I76A A77S H100A mutant ubiquitin-like (UBL) domain of hPLIC2 (construct #4616 (Walters et al., 2002)). Both constructs were captured using 600 µl 50 % His Select HF Nickel Affinity Gel slurry, (Sigma) resin incubated in the lysate at 4 °C for 1 h. Beads were then pelleted at 500 *x g* for 5 min, washed and re-pelleted five times in PBS before being left as a ~50 % (v/v) slurry in PBS for up to 3 weeks at 4 °C.

C-terminal tagged His^6 β-glucanase (*Oerskovia xanthineolytica*) using an *Escherichia coli* strain given to us as a gift by Dr Randy Schekman, UC Berkeley. β-glucanase was captured using 600 µl 50 % His Select HF Nickel Affinity Gel slurry (Sigma), resin incubated in the lysate at 4 °C for 1 h. Beads were then pelleted at 500 *x g* for 5 min, washed and re-pelleted five times in PBS before being eluted in 200 µl 250 mM Imidazole/PBS.

GST-UBL (construct #4602; (M F Kleijnen, Alarcon, & Howley, 2003)) and GST-Uba (construct #4607; (M F Kleijnen et al., 2003)). Each construct was captured using 600 µl 50 % Glutathione Agarose (Peirce), resin incubated in the lysate at 4 °C for 1 h. Beads were then pelleted at 500 *x g* for 5 min, washed and re-pelleted five times in PBS before being left as a ~50 % (v/v) slurry in PBS for up to 3 weeks at 4 °C.

2.3. Handling of Saccharomyces cerevisiae and purification of yeast proteasomes.

2.3.1. *S. cerevisiae* Strains and Genotype

Proteasomes were purified from sMK-50 strain described in (M F Kleijnen et al., 2007) expressing ProteinA tagged Rpn11 proteasome subunit. Genotype *MATα lys2-801 leu2-3, 112 ura3-52 his3Δ200 trpl-l (am) RPN11-TeV-ProA::HIS3*

2.3.2. Liquid and Solid Media

Yeast Extract Peptone Dextrose (YEPD) liquid and solid media was used to support and grow yeast referred to throughout this thesis. YPD media was comprised of 20 g/l Bacto peptone, 10 g/l Yeast extract (with 24 g/l Bacto agar if making solid media for plates) and autoclaved. Liquid media was supplemented with 50 ml of sterile 40 % (w/v) Glucose per litre before use.

Solid media was melted and cooled to around 50 °C before 50 ml of sterile 40 % (w/v) Glucose per litre was added. 9 cm petri dishes (Corning) were then poured in laminar flow hood with lids left open to dry for 20 min before storage at 4 °C.

2.3.3. Purification of yeast proteasomes

Yeast strain sMK50 cells were streaked onto a YEPD agar plate and incubated at 30 °C until colonies had formed. Single colonies were then plucked and added to a multiple 5 ml of YPD and incubated at 30 °C in shaking (150 rpm) cultures for 24 hours. The small 5 ml cultures were then transferred to six Erlenmeyer flasks and expanded in 1L of YEPD until the stationary phase was met (~ 2 days). The cells were then harvested at 3,000 *x g* for 10 min (Beckman) and each litre culture resuspended in 50 ml PBS to wash before being pelleted again at 2,000 *x g* for 10 min.

The pellets were then resuspended in 50 ml of ice-cold Buffer 1 (3.75 mM Tris-HCl [pH 8], 2 µM EDTA, 0.5 µM ADP) and lysed through a pre cooled NanoDeBEE (BEE International) homogeniser at 18,000 psi. Lysate was then cleared by spinning at 4,500 *x g* for 30 min. The supernatant from the six tubes was then combined and 10 ml of IgG beads slurry (Sigma) was added and incubated on a roller for 1 hour at 4 °C.

The beads were then spun down at 500 *x g* for 10 min and supernatant discarded. Beads were then washed three times in 30 ml of Buffer 2 (2.5 mM Tris-HCl [pH 7.5], 2 µM EDTA, 0.5 µM ADP, 2 mM NaCl). Beads were then washed one further time in 30 ml Tobacco Etch Virus (TeV) cleavage buffer (2.5 mM Tris-HCl [pH 7.5], 2 µM EDTA, 0.5 µM ADP, 0.1 µM DTT).

The captured yeast proteasome was then cleaved from the beads by TeV protease. Beads were resuspended in 40 ml of TeV cleavage Buffer and 60 µl acTeV protease (ThermoScientific) added before being incubated at 30 °C for 1.5 h. After this time the beads were pelleted at 500 *x g* and put aside to be restored. The supernatant containing yeast proteasome was cooled on ice and then concentrated by spin concentrators YM-50 Centricon (MerckMillipore) to a final volume of ~3 ml. 10 % (v/v) Glycerol was added to the supernatant and aliquoted in 10 µl aliquots and stored at -80 °C.

2.3.4. Nuclear and Cytoplasic yeast extracts.

We generated β-glucanase (*Oerskovia xanthineolytica*) using an *Escherichia coli* strain given to us as a gift by Dr Randy Schekman, UC Berkeley.

Yeast strain sMK50 was grown as stated in 2.3.2 to the stationary phase before being harvested at 3000 *x g*; 4 °C for 10 min and resuspended in 50 ml PBS. Cells were then spun down at 2000 *x g* for 10 min to remove remaining media. The mass of the cell pellet was then recorded. Cells were then resuspended in 2-4 volumes of ice-cold water and immediately spun down at 2000 *x g* for 5 min. The cells were then resuspended in one volume of β-glucanase buffer (0.1 M sodium phosphate buffer [pH 7.5], 30 mM DTT) and incubated at room temp for 15 min before being spun down at 2000 *x g* for 5 min. Again the cells were resuspended in one volume β-glucanase buffer before being split four ways. To the four samples 0, 20, 50 & 100 µl of β-glucanase purified as stated in 2.2.7 was added and incubated for 40 min at 30 °C with gentle shaking after which the cells were centrifuged for 8 min at 2000 *x g* and the supernatant carefully removed. The protoblast were then washed two times by gently resuspending in two volumes of ice-cold zymolyase buffer centrifuged for 8 min at 2000 *x g*. Cytosolic extraction was carried out by carefully resuspending in 1 volume of Cytosolic Extraction Buffer (25 mM Tris–HCl [pH 7.8], 5 mM $MgCl_2$/EDTA, 1 mM ATP/ADP, 2 mM DTT, 150 mM NaCl, and 0.1 % (v/v) NP40/IGEPAL) and incubating for 15 min. The cytoplasmic extraction was then cleared by spinning down, 2500 rpm for 10 min before being removed and kept. To the remaining pellet a nuclear extraction was carried out by resuspending the pellet in ½ volume of nuclear extract (NE) buffer

(20 mM HEPES [pH 7.4], 420 mM NaCl, 0.5 mM EDTA, 0.5 mM EGTA, 1 mM DTT, and 1 tablet of protease inhibitor cocktail (cOmplete EDTA Free, Roche) per 50 ml) (Bakondi et al., 2011). The nuclear supernatant was then carefully collected and diluted with 1 volume of ddH_2O. Both cytosolic and nuclear extracts from the 4 samples were then run on CTAB-PAGE as stated in 2.7.2

2.4. Mammalian Cell Culture, Drug treatment and viral transduction

All culturing of mammalian cells was performed in Faster BHG2004 biological safety cabinets. Dedicated reagents and equipment, such as pipettes, were used for cell culture and not used for any other organism or experiment.

2.4.1. Cell Culture of Suspension cells

Suspension cells NCI-H929, U266, C1R, RPMI-8226, Jurkat, OPM2, HL60 and KMS12-BM cell lines were obtained from the American Tissue Culture Collection (ATCC). All these cell lines were grown in RPMI-1640 media supplemented with 10 % (v/v) Heat inactivated Foetal Bovine Serum (FBS) (Lot: 08Q9057K Gibco) 1 % (v/v) MEM Non Essential Amino Acids, 1 % (v/v) Sodium Pyruvate, 2 % (v/v) Penicillin/Streptomycin and 2 % (v/v) L-Glutamine.

Cells were either grown statically in cell culture treated 25 cm^3, 75 cm^3 vented flasks (Corning) in 37 °C cell culture incubator (Galaxy 170s, New Brunswick) supplemented with 5 % CO_2, or in aggregated cultures in cell culture treated 25 cm^3, 500 cm^3 or 1000 cm^3 baffled Erlenmeyer flask with vented cap (Corning), shaking at 180 rpm in a cell culture incubator (S41i, New Brunswick) supplemented with 5 % CO_2.

Cells were passaged when they reached $1x10^6$ cells/ml in static cultures or $1.5 x10^6$ cells/ml in aggregated cultures. This was performed by removal of a third of the culture and addition of the same volume of fresh growth media.

2.4.2. Cell Culture of adherent cells

Adherent cells HEK-293T, DG75, SAOS2 and HeLa cells were grown in DMEM media (Sigma) with 10 % (v/v) FBS, and 1 % (v/v) Penicillin/Streptomycin. Cells were propagated in cell culture treated 25 cm^3/75 cm^3 vented flasks laid down in 37 °C cell culture incubator supplemented with 5 % CO_2.

Cells were passaged at 75-85 % confluency, this was done by removal of the media and washing of the mono-layer of cells in room temperature PBS. The PBS was then removed and enough 37 °C Trypsin-EDTA solution (Sigma Aldrich) was added to just cover the cells. At the point where the cells had partially dissociated from the plasicware, ~1 min, 3 volumes of supplemented growth media was added to compete with the extracellular matrix digestion. A 5 ml serological pipette was used to dislodge any cells still adhered to the flask. The cells were then transferred to a sterile 50 ml centrifuge tube and pelleted at 500 *x g* for 5 min. The cells were then resuspended in 10 ml of fresh media by pipetting up and down multiple times with a 5 ml stippettes. For every new flask, 15 ml of media and 1 ml of the resuspended cell solution was added. Flasks were gently swirled to mix the cells and then laid down horizontally in cell culture incubator.

2.4.3. Cryo preservation

For long term storage of mammalian cells, $5x10^6$ cells were pelleted at 500 *x g* for 5 min. The pellet was then resuspended in 1 ml of freezing media (70 % (v/v) RPMI-1640 or DMEM Media containing no supplements, 20 % (v/v) FBS, 10 % (v/v) DMSO) and added to a 2 ml screw top cryo-tube. Tubes were placed in room temperature Mr Frosty (ThermoScientific) passive freezer which in turn was transferred to -80 °C to achieve 1°C/min cooling rate for 24 h. After this time tubes were retrieved and placed in Liquid Nitrogen (Liquid Phase).

2.4.4. Drug Treatment

Throughout this thesis cells were treated with a number of compounds. All treatments were carried out in tissue culture treated 12, 24 or 46 well plates with 200 µl of suspension cells at a concentration of $1x10^6$ ml^{-1}. Drug names, supplier and solute used are listed below. Concentrations for each experiment can be found in the results section.

Name	Supplier	Solute
Bortezomib	Millennium/Takeda	DMSO
Ada-K(Biot)-Ahx3-L3-VS	Enzo Lifesciences	DMSO
Doxorubicin	Sigma-Aldrich	DMSO
Vinblastin	Sigma-Aldrich	DMSO
Cycloheximide	Sigma-Aldrich	DMSO
Epigallocatechin gallate (EGCG)	Sigma-Aldrich	DMSO
Epoxomicin	Enzo Lifesciences	DMSO
Caspase Inhibitor Set III	Enzo Lifesciences	DMSO
Lab derived Peptides		DMSO

Table 2.1. List of used compounds, Supplier and Solute.

Table contains a list of all the compounds used in this thesis, the supplier and what solute the compound was dissolved in. The lab derived peptides were synthesised by our collaborators Prof. Steven Ballet of the Vrije Universiteit Brussel.

2.4.4. Viral production, concentration and transduction

To achieve stable expression of constructs in mammalian cells a retroviral transduction technique was utilised. Around twelve 10 cm cell culture dishes were each seeded with $3x10^6$ HEK-293T cells (with a passage of no more than 12), for each viral construct. The next day, 24 h after seeding the media was replaced with 9 ml fresh media and returned to the incubator. After a further hour a transfection mixture with the following composition per plate; 3 µg VSVG, 12 µg GAG/Pol and 12 µg of plasmid DNA was diluted to a final volume of 450 µl in Low TE (10 mM Tris-HCl, 0.1 mM EDTA, pH 8.0) and 50 µl of 2.5 M $CaCl_2$ added. Finally, 500 µl of 2x HEPES Buffered Saline (274 mM NaCl, 10 mM KCl, 1.4 mM Na_2HPO_4, 15 mM D-Glucose and 42 mM HEPES) (HBS) was added dropwise to the existing mixture whilst vortexing.

N.B. 2xHBS was stored at -20 °C for up to a month and thawed on ice and used immediately. The resulting 1 ml mixture was added dropwise across the 10 cm plate and the plate gently swirled to mix before placing back in the incubator.

14-16 hours after adding the Ca-Pi-precipitated plasmid DNA the media was replaced with 7 ml of fresh media and the transfected cells were then returned to the incubator. 24 h after the media change the media that now contains virus was collected and pooled together and a further 7 ml of fresh media was added carefully to the cells. The media collected was then spun at 500 rpm in a refrigerated centrifuge and then filtered with a 0.45 µm filter to remove any cell debris. The virus containing media was then balanced in volumes of 36 ml and spun at 23,000 *x g* in a Hitachi ultra-centrifuge for 1 hour 40 min. The supernatant was then removed and 200 µl of media, without any supplementation, was added to resuspended the viral pellet for 4 hours at 4 °C with light aggregation. The resulting resuspended virus was either directly added to cells or flash frozen in LN and stored at -80 °C for a maximum of a month. 24 h after the first collection and concentration a second round of collection and concentration was performed and the cells disposed of.

Transduction of the cells was done by resuspending 850,000 cells with a viability of at least 70 % in 1 ml of fresh media before being plated in a 48 well plate and incubated in a cell culture incubator. One hour later addition of 8 mg ml^{-1} of polybrene was added to the cells before the addition 200 µl of concentrated virus. 16 h later the cells were spun down at 500 *x g* and resuspended in 1 ml of fresh media and left to expand in cell culture incubator before use.

2.4.5. Small Scale Cell fractionation

Cytosolic and nuclear proteins were isolated from approximately 2 × 10^6 NCI-H929 or KMS12-BM myeloma cells, harvested by centrifugation at 500 *x g* for 5 min. All following steps were carried out on ice with pre-chilled reagents and equipment. Cell pellets were washed once with 1 ml PBS and harvested by centrifugation at 500 ×*g* for 5 min, at 4 °C. The pellet was then resuspended in 110 µl cytosolic extraction buffer (25 mM Tris–HCl [pH 7.8], 5 mM $MgCl_2$/EDTA, 1 mM ATP/ADP, 2 mM DTT, 150 mM

NaCl, and 0.1 % (v/v) NP40/IGEPAL) by pipetting up and down 20 times before being spun down at 3000 ×*g* for 5 min at 4 °C. 100 µl of the CE supernatant was split and mixed with an equal amount of 2 × SDS and CTAB sample buffers and placed back on ice. The remaining supernatant was discarded and the pellet re-suspended in 110 µl nuclear extract (NE) buffer (Bakondi et al., 2011)(20 mM HEPES [pH 7.4], 420 mM NaCl, 0.5 mM EDTA, 0.5 mM EGTA, 1 mM DTT, and 1 tablet of protease inhibitor cocktail (cOmplete EDTA Free, Roche) per 50 ml) and pipetted up and down 20 times before being left on ice for 20 min. The sample was then briefly vortexed for 10 s, before being spun down hard at 20,500 ×*g* for 20 min at 4 °C. 100 µl of NE supernatant was split and mixed with an equal amount of 2 × SDS and CTAB sample buffers and placed on ice. The remainder of the supernatant was discarded. Next, 100 µl of nuclear extract buffer was added to the pellet remaining after nuclear extraction before again being split and mixed with an equal amount of 2 × SDS and CTAB sample buffers. The three extracts in SDS sample buffer was then run on SDS-PAGE as described in 2.7.1. and the three extracts in CTAB sample buffer run equidistance on CTAB-PAGE as explained in 2.7.2.

2.4.6. Whole cell lysis of Mammalian cells

Whole cell lysate was prepared from, $3x10^9$-$4.5x10^9$ cells harvested from 3 L shaking culture of C1R cells retroviraly transduced with MigRI-(H-SS-Rpn11)-eGFP construct (Cloning strategy 2.9.1.) equivalent to ~5-7cm^3 pellet. Cell were washed in 40 ml PBS+10 % (v/v) Glycerol and snap-frozen in LN before being stored up to 4 months at −80 °C. The frozen pellet was resuspended and combined in 10 volumes of CE buffer and passed through a NanoDeBEE (BEE international) homogeniser at 19,000 PSI. The lysate was cleared by centrifuging at 3400 *x g* for 20 minutes and supernatant collected.

2.4.7. Isolation of Nuclear Proteasomes from Primary Human leukocytes

Human leukocytes from anonymised donor leukophoresis collections (released for research with donor consent) were thawed, washed twice in PBS. The cells were then

pelleted at 500 *x g* at 4 °C before being resuspended in 6 ml of cytosolic extraction (CE) buffer by pipetting up/down ten times. Cells were then spun at 3,000 *x g* for 7 min at 4 °C and supernatant containing cytosolic extract was discarded. The pellet was then resuspended in 5 ml of nuclear extract (NE) buffer by pipetting up and down 20 times before being left on ice for 20 min. The NE was then harvested by centrifugation at 4,500 *x g* and the remaining pellet discarded. The nuclear extract was diluted in two volumes of ddH_2O to reduce salt concentrations.

Proteasomes were then captured from the diluted nuclear extract by adding 600 µl of UBL-His^6-loaded Ni^{++}-NTA resin from 2.2.7. and rotated at 4 °C for 1 h. Beads were then pelleted at 500 *x g* and washed six times in wash buffer (25 mM Tris–HCl [pH 7.6], 1 mM ADP, 2 mM DTT, 100 mM NaCl, 0.1 % (v/v) NP40/IGEPAL, and 1 mM EDTA). Proteasomes, and His^6-UBL were eluted by incubating the beads twice in 750 µl elution buffer (75 % (v/v) wash buffer 25 % (v/v) 1 M imidazole solution) for 10 min each. The resulting 1.5 ml elute was then run on FPLC Sepharose6 column as stated in 2.4.8

2.4.8. FPLC Size exclusion chromatography

FPLC Size exclusion chromatography was done at 4 °C using a Sepharose6 Fast Flow Column attached to Pharmica LLC-500 Plus programmable controller, Pharmica P-500 pump and Pharmica Frac 200 sample collector. The column and tubing was stored in 30 % (v/v) Ethanol and flushed through with three volumes of CE Buffer and left to equilibrate 24 h before use. Up to 2.5 ml of proteasomes eluted from bead capture was injected into the system and 7/8ths of a column volume was run before collection of 100-200 µl fractions.10 µl samples from each fraction were run on SDS-PAGE to analyse the fractions contain proteasomes.

After use the column was flush with 3 volumes of CE buffer and then 2 volumes of 30 % Ethanol.

2.5. Flow cytometric analysis and sorting

2.5.1. Staining

Cell death was measured using AnnexinV-APC, AnnexinV-FITC or AnnexinV-PE (eBiosciences) and DAPI (Sigma). 1-5x10^6 cells/ml were pelleted at 500 *x g* and washed in ice cold PBS. Cells were washed a second time in 1x Binding Buffer (10x Binding buffer diluted in ddH2O) (eBiosciences) before being resuspended in 1 ml ice cold 1x Binding buffer. 2.5 µl of fluorochrome-conjugated AnnexinV was added to the cells and incubated for 45 min. Cells were then pelleted and resuspended in 1 ml ice cold 1x Binding Buffer and transferred to 5 ml flow cytometory tube (Beckton-Dickinson) and left at 4 °C until analysis. Thirty seconds prior to analysis 2 µl of 3.6 µM DAPI was added to the tube and cells vortexed briefly.

Cell cycle staining was done by the use of a cell permeable, non-toxic DNA stain Vybrant DyeCycle Violet Stain (Invitrogen). Staining was carried out as stated in the manufacturer's instructions except the media was changed on the cells to a minimal Media composition (RPMI-1640 + 10 % (v/v) FBS) 1h prior to staining due to incompatibilities of staining in the complete media stated in 2.4.1. In brief, 1 h after the media change the dye was removed from 4 °C storage and allowed to reach room temperature 1 x of the Vybrant DyeCycle Violet Stain 1000x stock was added to reach a final concentration of 5 µM. The plate was then wrapped in tin foil to protect from light and returned to the incubator for 45 minutes. Cells were then resuspended and the cells in the media/stain were added to 5 ml flow cytometry tubes ready for analysis.

2.5.2. Flow Cytometric Analysis

Samples were analysed using a custom configured LSR Fortessa (Beckton-Dickinson, Oxford, UK) with FACSDiva v6.2 acquisition. Although non-overlapping fluorophores where used each experimental technique and cell line, the data was compensated to remove cellular auto-florescence. Fluorophores and fluorescent proteins were excited and detected using the laser and filter combination detailed in Table 2.2. Gating Strategies are shown in Appendix D.

Fluorophore	Excitation Laser	Detection Filter
APC	Red 640 nm	670/30
FITC	Blue 488 nm	530/30
eGFP	Blue 488 nm	530/30
PE	Blue 488 nm	575/26
Pacific Blue	Violet 405 nm	450/50
DAPI	Ultra Violet 355 nm	450/50

Table 2.2. List of lasers and filters used in flow cytometry.

The laser wavelength and detection filter for each fluorophore and fluorescent protein used in this thesis.

2.5.3. Fluorescence-Activated Cell Sorting (FACS)

Samples were sorted on FACSAria (Beckton Dickinson, Oxford, UK) machines utilising an 85 µm nozzle. The eGFP was excited by 488 nm laser and detected using a 525/50 filter. Control of the FACSAria was done with use of BD FACSDiva v8.03.

2.5.4. Analysis of flow cytometry data

Data was analysed on FloJo vX software (Tree Star, Oregon, USA). Gating strategies are as described in the results and Appendix D. In all cases this involved an initial gate on viable cells.

2.6. Digestion of modifications on purified proteasomes

Modification moieties were attempted to be cleaved off the modified proteasome subunits by a number of enzymes. A number of FPLC fractions containing proteasomes were combined and then split and treated with different combinations of enzymes (listed in Table 2.3. and described in each Results section). The fractions numbers and enzymes used are explained per experiment in the results sections. Reactions were carried out for 1 h at 37 °C (except for Micrococcal nuclease where

reactions were incubated at 30 °C). Supplementation ion or buffer and source of enzymes are listed below.

Enzyme	Source	Final Buffer/ion conc.
Micrococcal nuclease	Thermo Scientific	1x Reaction buffer
RNaseA/T1	Thermo Scientific	1x Reaction buffer
RNaseH	Thermo Scientific	1x Reaction buffer
RNAse1	Thermo Scientific	1x Reaction buffer
Phosphodiesterase 1 (PDE1)	Sigma-Aldrich	10 mM Tris-HCl [pH 7.5] 5 mM $CaCl_2$
ADP-ribosylarginine hydrolase 1 (ARH1)	Enzo Life Sciences	10 mM Tris-HCl [pH 7.5] 5 mM $MgCl_2$
ADP-ribosylarginine hydrolase 2 variant 1 (ARH2.1)	Cloned in house (Section 2.9.2)	10 mM Tris-HCl [pH 7.5] 5 mM $MgCl_2$
ADP-ribosylarginine hydrolase 2 variant 2 (ARH2.2)	Cloned in house (Section 2.9.2)	10 mM Tris-HCl [pH 7.5] 5 mM $MgCl_2$
ADP-ribosylarginine hydrolase 3 (ARH3)	Enzo Life Sciences	10 mM Tris-HCl [pH 7.5] 5 mM $MgCl_2$
Poly(ADP-ribose) glycohydrolase (PARG)	Enzo Life Sciences	10 mM Tris-HCl [pH 7.5]

Table 2.3. List of enzymes used in the digestion of proteasome modifications.

A list of the enzymes used, the supplier and the reaction buffer for optimal activity. ADP-ribosylarginine hydrolase 2 variants 1 & 2 were cloned and expressed in house (Method 2.9.2)

2.7. Protein electrophoresis

2.7.1. Sodium Dodecyl Sulphate Protein Electrophoresis (SDS-PAGE)

Cells were grown in culture flasks/plates for the length of the experiment. Adherent cells scrapped off plastic ware using a sterile cell scraper, before being counted and ~250,000 cells washed in ice cold PBS and pelleted. Suspension cells were likewise counted and ~250,000 cells washed in ice cold PBS and pelleted. Cells were resuspended and lysed in 20 µl ice cold RIPA Buffer (10 mM Tris-HCl (pH 8.0), 1 mM EDTA, 0.5 mM EGTA, 1 % Triton X-100, 0.1 % sodium deoxycholate, 0.1 % SDS, 140 mM NaCl and 1 Proteasome cocktail inhibitor tablet/50ml (Roche)). 20 µl 2X SDS sample buffer (100 mM Tris-Cl (pH 6.8) 4 % (w/v) SDS, 0.2 % (w/v) bromophenol blue, 20 % (v/v) glycerol, 200 mM β-Mercapto ethanol) was then added and then denatured at 100 °C for 5 min.

In the case of purified proteins from IP elution, digestion experiments, *in vitro* degradation assay or FPLC size exclusion, an equal volume of 2X SDS sample buffer was added. 10 or 12 % polyacrylamide gels were used to separate proteins by gel electrophoresis. 15 µL of sample-buffer mix per lane was run alongside PageRuler™ Plus Protein standard (ThermoFisher).

N.B. Normalisation was done via the number of cells as experiments inducing cell death skewed BCA protein quantification and did not represent the true effect of the experiment.

2.7.2. Cetyl Trimethylammonium Bromide Protein Electrophoresis (CTAB-PAGE)

CTAB-PAGE was prepared as published (Simpson, 2010). Samples were prepared in a similar manor to SDS-PAGE technique above although the RIPA buffer was modified to comprise of 0.1 % CTAB in place of the SDS. 1:1 volume of 2 × CTAB sample buffer (10 mM Tricine–NaOH [pH 8.8], 1 % (w/v) CTAB, 10 % (v/v) glycerol, 10 µl/ml saturated aqueous solution of crystal violet, and 2 % (v/v) β-mercaptoethanol) was added to the samples and denatured at 100 °C for 5 min

CTAB-PAGE was run on a 6 % resolving gel (2.4 ml 40 % acrylamide, 4 ml 1.5 M Tricine–NaOH [pH 8.0], 9.4 ml water, 160 µl 10 % APS, 16 µl TEMED) was poured

into SE245 gel caster (Hoefer) and levelled with a layer of iso-propanol which was removed after setting. For the stacking gel, 30 mg agarose was mixed with 1.25 ml 0.5 M Tricine–NaOH [pH 10], 3.7 ml water, and 50 µl 10 % (w/v) CTAB solution and poured on top of the resolving gel. The CTAB-PAGE gel was run in 1x CTAB running buffer (25 mM Tricine, 13.75 mM CTAB, 75 mM arginine). A total of 20 µl of sample was loaded in the wells, no protein standard was used as no commercial product is available for CTAB-PAGE. The gel was then run at 100 V, with reversed polarity to SDS. After the Bromophenol blue dye front had left the stacking gel and migrated at least 0.5 cm into the resolving gel the stacking gel was gently removed (due to a tendency to melt and clog resolving gel) and the voltage increased to 150 V till the dye front reached the bottom.

2.7.3. Isoelectric Focusing IEF

Isoelectric focusing was done with the IPG-ZOOM system (Invitrogen) as per the manufacturers protocol. In brief, up to 100 µl of GST-UBL purified proteasomes (2.4.6.) were added to 100 µl rehydration buffer. Linear pH 3–10 (ZM0018) or pH 4–7 (ZM0012) strips were inserted into the cassette and rehydrated for 1 h in the rehydration buffer containing proteasomes and free GST-UBL. The proteins were then focused by applying a stepwise voltage increase (200 V for 20 min, 450 V for 15 min, 750 V for 15 min and finally 2000 V for 30 min). The focused strips were then removed and incubated in 1X NuPAGE® LDS Sample Buffer (Invitrogen) containing 1x NuPAGE® Sample Reducing Agent for 15 min in preparation for second dimension SDS-PAGE. The strips were then laid horizontally at the top of an SDS-PAGE gel and run as stated in 2.7.1.

2.7.4. In Gel Protein Staining

In gel protein staining was carried out by fixing the proteins in gel using fixing solution (40 % (v/v) Methanol, 10 % (v/v) Glacial acetic acid) for 1 h. The proteins were then stained using Coomassie-R250 solution (BioRad) and destained using fixing solution or 30 % ethanol.

2.7.5. Semi-Dry transfer and Western Blot

Semi-dry transfer was used to transfer proteins from the gel onto 0.45 µm methanol activated PVDF membrane using 0.8 mA/cm^2 in transfer buffer (48 mM Tris, 39 mM glycine, 0.037 % (w/v) SDS) for 1 h.

PVDF membrane was incubated in blocking solution (5 % (w/v) non-fat dry milk, 0.5 % (v/v) Tween-20 in PBS) for 1 hour. Primary antibodies were diluted 1:1,000 times in PBS-Tween solution and incubated for 1-16 h. Membrane was washed for five min three times in PBS-Tween before the corresponding HRP conjugated secondary added. ECL reaction mixture (GE Healthcare) was added and chemiluminescence visualised by exposure to X-ray film (Hyperfilm, Amersham). PVDF membranes were re-probed multiple times as described in (Yeung & Stanley, 2009). Briefly the PVDF membrane was incubated in guanidine hydrochloride-based (GnHCl) stripping solution (6M GnHCl, 0.2% Nonidet P-40 (NP-40), 0.1M β-mercaptoethanol, 20mM Tris-HCl, pH7.5) initially for 5 min followed by a 10 min wash. After which the PVDF membrane was washed in PBS-Tween for four 5 minute washes. The membrane was then blocked and probed as before.

Against	Type	Host	Supplier	Product code
α-Rpn10/S5a	mAb	Mouse	Enzo	BML-PW9250
α-Rpn12/S14	pAb	Rabbit	Enzo	BML-PW8815
α-20S α7	mAb	Mouse	Enzo	BML-PW8110
α-20S α6	mAb	Mouse	Enzo	BML-PW8100
α-Rpt1/S7	mAb	Mouse	Enzo	BML-PW8825
α-Rpt2/S4	pAb	Rabbit	Enzo	BML-PW8305
α-Rpt3/S6b	pAb	Rabbit	Enzo	BML-PW8175
α-Rpt4/S10b	mAb	Mouse	Enzo	PW8830
α-Rpt5/S6a	mAb	Mouse	Enzo	PW8770
α-'core' CP subunits	pAb	Rabbit	Enzo	PW8155
α-β5i/LMP7	pAb	Rabbit	Enzo	PW8355
α-ubiquitin FK2	mAb	Mouse	Enzo	PW8810
α-poly(ADP-ribose)	pAb	Rabbit	Enzo	ALX-210-890-R100
α-Rpn1/S2	pAb	Rabbit	Calbiochem	539166
α-Lamin B2	mAb	Mouse	Abcam	ab8983
α-SMARCB1/Ini1	pAb	Rabbit	Santa Cruz	sc-13055
α-Ubiquilin1	mAb	Mouse	Invitrogen	377700
α-PARP	mAb	Rabbit	Cell Signalling	#9532
α-Caspase3	mAb	Mouse	Enzo	ALX-804-242-C100

Table 2.4. List of antibodies used in thesis.

List of antibodies, what they were raised against, in which species, the supplier and the clonicity. mAb = Monoclonal Antibody, pAB = Polyclonal Antibody. Antibodies against yeast proteasome are from Dr Daniel Finley, Harvard Medical School. The α-Dbf11 antibody is from Dr Christian Speck, CSC-MRC London.

2.8. Proteasome Assays

2.8.1. *In Vitro* Degradation Assay

Preparation of ubiquitnated substrate

The *in vitro* proteasome degradation assay was kindly gifted by Dr Andreas Martin and carried out as stated in (Matyskiela, Lander, & Martin, 2013; Saeki, Isono, & Toh-E, 2005). In brief, E1 (His^6-Uba1, *S. cerevisiae*), E2 (Ubc4-His^6, *S. cerevisiae*) and E3 (Rsp5-ΔN-His^6, S*. cerevisiae*) ubiquitation enzymes were used to ubiquitinate a single

lysine residue on a G3P model substrate that contained a PY domain, recognised by Rsp5 E3 ubiquitin ligase, as well as His^6 and StepTags (Matyskiela et al., 2013).

The model substrate, E2 and E3 were individually expressed in BL21(DE3) cells selected with ampicillin and induced and lysed as stated in 2.2.7. purified using Ni-NTA^{++} sepharose and eluted in 200 mM imidizol/PBS.

Uba1 was purified from ΔUba1 yeast transformed with His^6-Uba1 under copper-inducible promotor. Selection was not necessary as loss of Uba1 was lethal and copper-promotor allowed enough expression un-induced to keep the strain viable.

The substrate was ubiquitinated by combining ~150 µM G3P substrate, ~175 nM Rsp5, ~170 nM Uba1, ~5 µM Ubc4, 1 mM ATP 0.1 mM $MgCl_2$ and 1.2 mM ubiquitin and incubated at 30 °C for 1 h. The now ubiquitinated substrate was then purified away from the ubiquiting enzymes and free ubiquitin by capturing with 500 µl strep-tactin superflow® Plus (Qiagen) bead slurry for 1 h. Beads were washed three times in PBS and then eluted in 200 µl PBS + 5 mM Biotin. The elution was carried out a second time and then 44 µl Glycerol was added to the 400 µl elutant before being aliquoted in 10 µl and stored at -80 °C. For proof of successful purification, ubiquitination and ability to be degraded by proteasome please see Appendix A.

Setting up and running of in vitro degradation assay

Yeast and human proteasomes used in this experiment were isolated as stated prior in 2.3.3 and 2.4.6. respectively.

Firstly, a master mix (2 µl ubiquitinated G3P substrate, 2.5 mM ATP, 2.5 mM $MgCl_2$, 2.5 mM DTT, in 10 µl PBS) per reaction was made up with extra for control lanes. 2-3 µl of yeast proteasomes, that are quantified from each purification, were diluted to 8 µl in PBS before 2 µl of varying concentrations of peptides or Bortezomib dissolved in DMSO were added and incubated for 20 minutes on ice. 10 µl of the master mix was then added to each of the treated proteasomes and the reactions incubated at 30 °C for yeast proteasomes or 37 °C for human for 1 h. After this time the reaction was stopped by addition of 20 µl 2 × SDS sample buffer and boiled. Samples were then run on SDS-PAGE (2.7.1.) and probed by Western (2.7.5.) with α-Ubiquitin and α-StepTag antibodies.

2.8.2. Proteasome Activity Assay

To measure each of the three activities of the proteasome a fluorogenic readout was performed based on methods described previously (Kisselev & Goldberg 2005; Vilchez et al 2012). Briefly, a variety of cells were harvested, washed three times in ice-cold PBS and resuspended in proteasome activity assay buffer (50mM Tris-HCl, pH 7.5, 250 mM sucrose, 5 mM $MgCl_2$, 0.5 mM EDTA, 2 mM ATP and 1 mM DTT). Cells were then lysed by passing cells 10 times through a 27-gauge needle, and lysate was clarified by centrifugation at 20,000 *x g* for 10 min at 4 ºC. Total protein concentrations were calculated using the bicinchoninic acid (BCA) assay kit (Sigma). Twenty-five micrograms of total protein were transferred to a 96-well microtiter plate (Greiner) and incubated with active-site specific fluorogenic substrates Suc-LLVY-AMC, Ac-RLR-AMC, Ac-GPLD-AMC (Enzo Life Sciences).

Fluorescence (380 nm excitation, 460 nm emission) was monitored continuously on a FluoStar Omega microplate fluorometer (BMG Labtech) for 1 h at 37 °C. To measure for the presence of free 20S proteasomes, 0.015 % (w/v) SDS was added to the proteasome activity assay buffer. For each well, a second was set up with the addition of 40 mM Bortezomib; any activity in the Bortezomib wells was subtracted from corresponding wells to compensate for unspecific protease activity.

2.9. Constructs and cell lines created

This section lays out the method by which constructs were cloned and cell lines created. The primers listed in this section can be found at the end of each subsection in Tables 2.5 and 2.6.

2.9.1 The His^6-2(StrepIITag)-TeV-Rpn11 expression construct

To capture large amounts of human proteasomes from myeloma cell lines a MigRI retroviral expression plasmid (Pear et al., 1998) was modified to encode a tandem affinity purification (TAP) cassette encoding a Met start site, a His^6 tag, two Strep-II-Tags, a TeV cleavage site, linker sequence and *Not*I restriction site and cloned into the 5’ side of the multiple cloning site.

The generation of the TAP tag was done in two parts. The forward oligo for the first half of the tag (H-SS-T_P1_F) and reverse oligo (H-SS-T_P1_R) were combined, phosphorylated and annealed as stated in 2.1.2. The same was done for the second half of the tag using the oligo's (H-SS-T_P2_F) and (H-SS-T_P2_R). The annealed oligos created two DNA fragments with overhangs on each end to allow for directional cloning into MigRI with the first part of the tag contained a 5' overhang complimentary to *Bgl*II and a 3' overhang complimentary to the second half's 5' overhang, the second tag also contained a 3' overhang complimentary to *Xho*I (Figure 2.1)

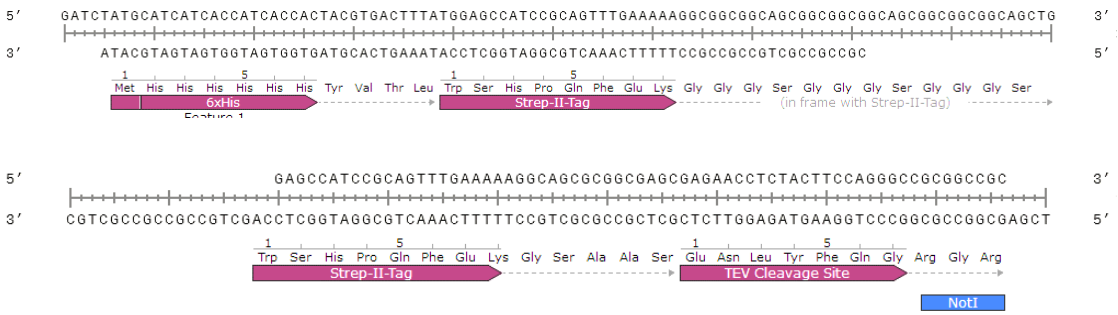


Figure 2.1. Schematic showing the products of annealing of the two parts of the His^{6}-2(StrepIITag)-TeV construct.

Two fragments of dsDNA created after annealing of the four oligos. Tag domains highlighted and amino acid code shown below

Next empty MigRI plasmid was linearized by *Bgl*II:*Xho*I digestion (as described in 2.1.1) and run on a DNA gel (as described in 2.1.4) before being finally gel purified using GeneJET Gel Extraction Kit (Thermo Fisher) as per manufacturer's instructions. Finally, a three-way ligation was set up with 100 ng of linearised vector and 4.6 ng of each of the TAP annealed DNA (as described in 2.1.5) and transformed into DH5α (as described in 2.2.4) purified (as described in 2.2.5) and sequence confirmed (as described in 2.1.6) using MigRI_F_seq primer.

Next the proteasome regulatory particle subunit Rpn11 encoded by *PSMD14* was amplified using the forward primer (PSMD14_F) and reverse primer (PSMD14_R) using Q5 polymerase with an annealing temperature of 58 ºC (as described in 2.1.3). The PCR product and newly created MigRI vector now harbouring the N-terminal His$_6$-2(StrepIITag)-TeV- cassette were both digested using *Not*I *and Eco*RI restriction

nucleases and run on DNA agarose gel (as described in 2.1.4). A band of 933 bp was excised from the digested PCR lane and a 6,631 bp band from the digested vector lane. The DNA concentrations were measured using nanodrop (Thermo Scientific) and ligated as stated in method 2.1.5. The sequence was then confirmed by Sanger Sequencing resulting plasmid map and expressed sequence can be found in Appendix C.

The confirmed MigRI His^6-2(StrepIITag)-TeV-Rpn11 retroviral expression plasmid was packaged into viral particles and OPM2 cells were then transduced as stated in Method 2.4.4. eGFP positive cells were then sorted as stated in Method 2.5.3 as per the gating shown in Appendix C.

H-SS-T_P1_F
GATCTATGCATCATCACCATCACCACTACGTGACTTTATGGAGCCATCCGCAGTTTGAAAAAGGCG GCGGCAGCGGCGGCGGCAGCGGCGGCGGCAGCTG
H-SS-T_P1_R
CGCCGCCGCTGCCGCCGCCTTTTTCAAACTGCGGATGGCTCCATAAAGTCACGTAGTGGTGATGGT GATGATGCATA
H-SS-T_P2_F
GAGCCATCCGCAGTTTGAAAAAGGCAGCGCGGCGAGCGAGAACCTCTACTTCCAGGGCCGCGGC CGC
H-SS-T_P2_R
TCGAGCGGCCGCGGCCCTGGAAGTAGAGGTTCTCGCTCGCCGCGCTGCCTTTTTCAAACTGCGGA TGGCTCCAGCTGCCGCCGCCGCTGC
PSMD14_F
GATCGAATTCCATGGACAGACTTCTTAGACTTGG
PSMD14_R
GCATGAATTCTTATTTAAATACGACAGTATCCAACATAGCTGC
MigRI_F_seq
CCTTTATCCAGCCCTCACTCC

Table 2.5. Primer sequences for the creation of the His^6-2(StrepIITag)-TeV-Rpn11 expression construct.

Oligo's annealed together to create the tag sequence as well as primers used for the amplification of PSMD14.

2.9.2 His_6 tagged ADPRHL1 variant 1 & 2

ADPRHL1 variant 1 was amplified from HeLa cDNA using the forward primer (ADPRHL1v1_F) and reverse primer (ADPRHL1v1_R) using Q5 polymerase with an

annealing temperature of 71 ºC (as described in 2.1.3). The PCR product and pET2a(+) bacterial expression vector were digested using *Not*I *and Nde*I restriction nucleases and run on DNA agarose gel (as described in 2.1.4). A band of 1,065 bp was excised from the digested PCR lane and a 3,590 bp band from the digested vector lane. The DNA concentrations were measured using nanodrop (Thermo Scientific) and ligated as stated in method 2.1.5. The sequence was then confirmed by Sanger Sequencing using pET2a+_Seq primer resulting plasmid map and expressed sequence can be found in Appendix B. The resulting plasmid transformed into BL21 (DE3) *E. coli* cells for bacterial expression.

ADPRHL1 variant 2 was amplified from HeLa cDNA using the forward primer (ADPRHL1v2_F) and reverse primer (ADPRHL1v2_R) using Q5 polymerase with an annealing temperature of 69 ºC (as described in 2.1.3). The PCR product and pET2a(+) bacterial expression vector were digested using *Not*I *and Nde*I restriction nucleases and run on DNA agarose gel (as described in 2.1.4). A band of 819 bp was excised from the digested PCR lane and a 3,590 bp band from the digested vector lane. The DNA concentrations were measured using nanodrop (Thermo Scientific) and ligated as stated in method 2.1.5. The sequence was then confirmed by Sanger Sequencing using pET2a+_Seq primer resulting plasmid map and expressed sequence can be found in Appendix B. The resulting plasmid transformed into BL21 (DE3) *E. coli* cells for bacterial expression.

ADPRHL1v1_F
TACATATGGAGAAATTTAAGGCTGCGATGTTGC
ADPRHL1v1_R
AAGCGGCCGCCTTCTCCTCTGTGGACAGGCGGTAG
ADPRHL1v2_F
TACATATGGTGAGATGCTATGTGGAAATCG
ADPRHL1v2_R
GGGCGGCCGCCTTCTCCTCTGTGGACAGGCGGTAG
pET2a+_Seq
TATAGTTCCTCCTTTCAGC

Table 2.6. Primer sequences for the creation of the ARH2 expression constructs.

Primers used for the amplification of ADPRHL1 variants 1 & 2.

CHAPTER 3 - Post-translational modification of proteasome subunits, unresolvable by SDS-PAGE

Chapter 3: Post-translational modification of proteasome subunits, unresolvable by SDS-PAGE

3.1. Introduction

As described in the introduction chapter of this thesis, proteasomes reside within both the cytoplasm and nucleus of the cell and interact with other organelles such as the endoplasmic reticulum and mitochondria. A lot of research has been done looking at proteasome biology within *S. cervisiae*. In this organism it has been shown that the majority of proteasomes that reside within the cell are nuclear in origin. During mitosis of the cell the breakdown of the nuclear membrane releases nuclear proteasomes into the cytoplasm where they are rapidly reappropriated to the nucleus upon exit of the cell cycle. In humans nuclear and cytoplasmic specific proteasomes have been shown to exist similar to yeast although few studies have been carried out to understand what marks the proteasome for its particular location. Understanding the differences in these two distinct populations of proteasomes may help in understanding why myeloma is so sensitive to proteasome inhibition above that of other cancers and non-cancerous cells and may allude to mechanisms in which the cell can decrease its sensitivity to proteasome inhibition e.g. by changing the cellular composition of proteasomes, the compartment-specific modification of proteasomes - potentially altering their kinetics or binding affinity of bortezomib.

Previous work done by members of this lab have shown the isolation of proteasomes from the nucleus and cytoplasm of myeloma cells are not comparable when run on CTAB-PAGE as oppose to SDS-PAGE. Understanding the reason for this anomaly may open up understanding of the difference between nuclear cytoplasmic proteasomes, their role in cellular biology, and their susceptibility to proteasome inhibition.

Using a number of bio-chemical approaches, outlined in this chapter, I confirm that these apparent differences are not an artefact of CTAB-PAGE itself and are *bona fide* modified proteasome subunits. These CTAB-PAGE resolvable modified proteasomes remain through Affinity Precipitation (AP) and Fast Protein Liquid Chromatography (FPLC) purification techniques and are mostly restricted to the nuclear compartment

of the cell. I then go on to rule out a number of typical nuclear modifications before finding two enzymes (S1 Nuclease, Phospho-diesterase 1) that have partial activity in selectively changing the modified patterns resolvable on CTAB-PAGE. Finally, further testing of proteasomes treated with these enzymes did not show any difference in their ability to degrade ubiquitinated substrates.

Work done in this chapter has been subsequently published (Pitcher et al., 2014, 2015) copies of which can be found at the back of this thesis (Appendix E).

3.2. Work leading up to commencement of project.

Work done just prior to my commencement had shown that there were large discrepancies in the running behaviour of proteasome subunits between the commonly used SDS-PAGE protein electrophoresis technique and the lesser common CTAB-PAGE. Lab member Ms. Ziming Wang split lysate from the myeloma cell line KMS12-BM in two and added either SDS-PAGE sample buffer or CTAB-PAGE sample buffer before running it on the corresponding system. Gels from both PAGE systems were transferred and blotted for Rpn12 and Rpn10 proteasomal subunits as well as Lamin B2

Western blots of a number of proteasome subunits run on CTAB-PAGE showed increased signal that ran as a higher molecular weight ‘smear’ with a number of proteasome subunit antibodies (Figure 3.1). Other blots such as α-Lamin B2 ran as two defined bands on CTAB-PAGE showing that proteins can be successfully resolved on the system. Although no molecular weight marker is commercially available, the gels were run for the same distance and aligned to give rough indication of weight.

Although SDS-PAGE did show multiple species of both Rpn10 and Rpn12 subunits, the extent of the smear observed in the CTAB-PAGE run samples suggested that it was not just a resolving issue but one of extra modified subunits resolving and transferring from the CTAB gel not found in that of the SDS-PAGE gel.

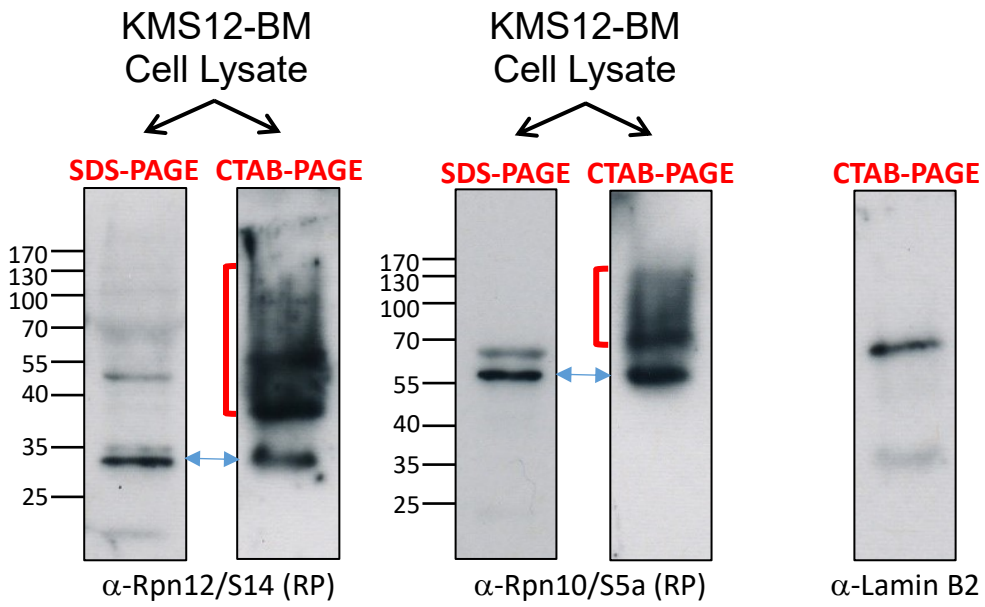


Figure 3.1. CTAB-PAGE shows increased diffuse signal of proteasome subunits compared to SDS-PAGE.

Whole cell lysate from KMS12-BM myeloma cells was split and run on SDS-PAGE and CTAB-PAGE systems, before being blotted for Rpn12 and Rpn10 proteasome regulatory subunits. Red brackets indicate signal unique to CTAB-PAGE. Nuclear membrane protein Lamin B2 was also probed and shown to run a defined species on CTAB-PAGE.

In order to confirm that these were indeed separate species and this was not an artefact of CTAB-PAGE, an attempt was made to separate the smear material from the more defined bands below. A simple Triton-X100 purification was carried out on NCI-H929 cells and the Triton-X100 soluble and insoluble (pellet material) as well as whole cell lysate was run on CTAB-PAGE (Figure 3.2).

The fact that the smear and the lower MW banding could be separated suggested that they were indeed distinct species and that they did not represent an artefact of the system or incomplete loading of detergent. Additionally, it was also shown that the smear material was not confined to just one myeloma cell line, but was found in multiple myeloma cell lines.

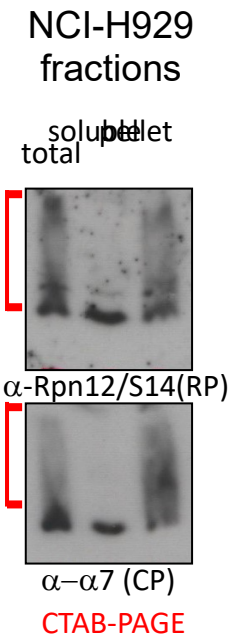


Figure 3.2. High molecular weight smear can be separated from the main resolved band by simple Triton-X100 extraction.

Triton-X100 was used to extract soluble proteins from the myeloma cell line NCI-H929. This along with non-soluble pellet and total cellular protein was run on CTAB-PAGE and probed for Rpn12 and α7 subunits. Red brackets indicate CTAB-PAGE unique signal.

Due to the majority of the smear material residing in the Triton-X100 insoluble fraction Ms Ziming Wang tested to see if the smear material was confined to the nuclear compartment un-lysable by the low Triton-X100 concentration. A simple cell fractionation protocol was implemented again on the NCI-H929 myeloma cell line. A detergent step would release cytosolic proteins whilst subsequent extraction with high salt would release nuclear proteins leaving behind a pellet of non lysed organelles and cellular membranes. The concentration of protein for each fraction was measured and three fractions were normalised by protein concentration then split in two and run on CTAB-PAGE and SDS-PAGE systems before being transferred and probed with a number of proteasome antibodies (Figure 3.3). Antibodies against housekeeping genes were not used as a loading control as each protein tested showed variation between fractions, therefore lanes were normalised to total protein. The membranes were stripped and reprobed each time to remove experimental and pipetting errors.

Out of the subunits probed by Western all had very different signal between the SDS-PAGE and CTAB-PAGE run samples. The signal for each of the subunits tested in the SDS-PAGE samples seemed to be mostly confined to the nuclear extract with very little in either the cytosolic extract or post lysed pellet. CTAB-PAGE run samples again showed that the majority of high molecular weight smear material was confined to the nuclear extract and pellet, and opposed to SDS-PAGE showed signal within all three

extracts. Not all proteasome subunits showed smearing on CTAB-PAGE, Rpt5 and Rpt3 resolved in defined bands throughout all three isolates showing that modification causing this smearing on some subunits was not ubiquitous across all of them. Successful fractionation was also shown by probing the membranes for INI1 found in the nucleoplasm and Lamin B2 found in the nuclear membrane. The nuclear extraction step does not release the genomic DNA, although small fragments of DNA and RNA can be released. The smear still evident in the NE suggest this is not due to DNA, known to aggregate readily in SDS. The appearance of single bands of Rpt3 and defined bands present in the Rpt5 blot also suggest that the subunits had not aggregated and affected the running pattern. Results are representative of n = 2.

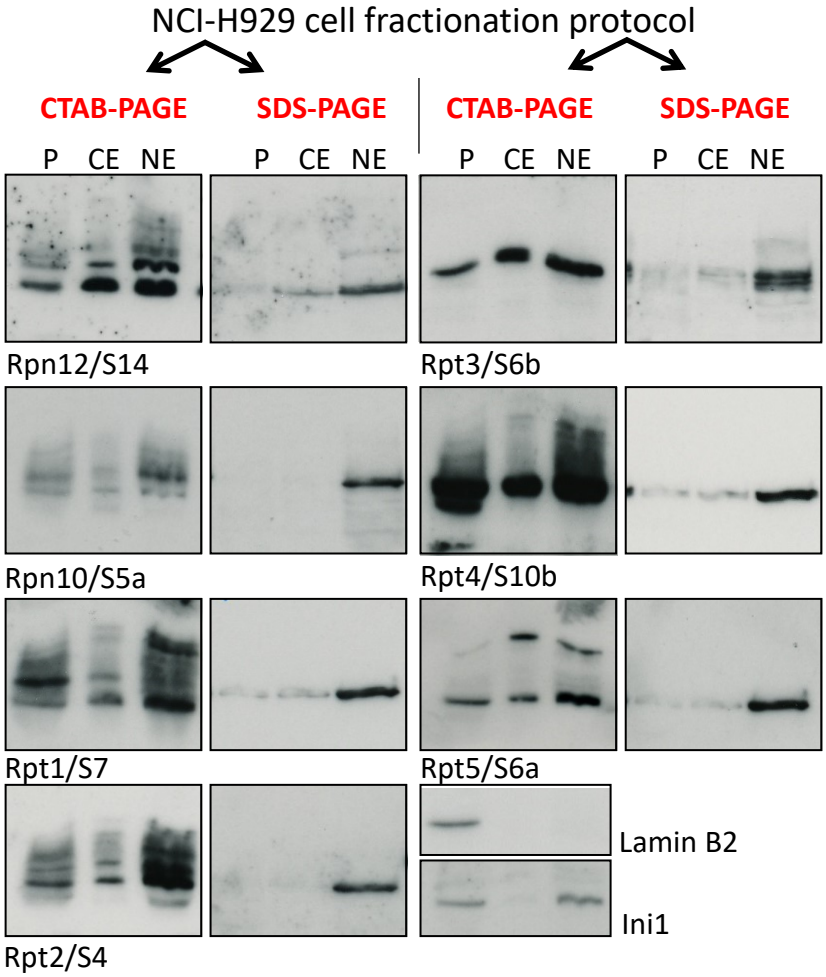


Figure 3.3. Majority of proteasome subunits show increased diffuse signal on CTAB-PAGE compared to SDS-PAGE.

Myeloma cell line NCI-H929 cells were fractionated utilising a detergent cytosolic lysis step and then subjected to a high salt nuclear lysis. The two fractions as well as the leftover pellet were split and subjected to CTAB-PAGE and SDS-PAGE, and analysed by Western blotting against the stated proteasome subunits. P = pellet remaining after nuclear extraction, CE = cytosolic extract, NE = nuclear extract. Note that even though the samples run different systems the samples were from lysate split between them and should in theory be identical, SDS-PAGE does not display all of the species observed in CTAB-PAGE.

3.3. Many Proteasome Subunits have modified species not resolvable by SDS-PAGE

In continuation of Ms Ziming Wang's work I first confirmed that CTAB-PAGE was able to resolve proteins in a manner similar to SDS-PAGE as stated in published literature. To confirm this a number of purified proteins of different molecular weights and quaternary structures (Table 3.1) were dissolved in water, split in two and run on both CTAB and SDS-PAGE electrophoresis systems. In-gel staining was then carried out by fixation and staining with Coomassie-R250 (Figure 3.4). Although no commercial protein standard is available for CTAB-PAGE the relative heights of the proteins to one another and the ability of the sample buffers to dissociate multimetic proteins was similar to SDS-PAGE.

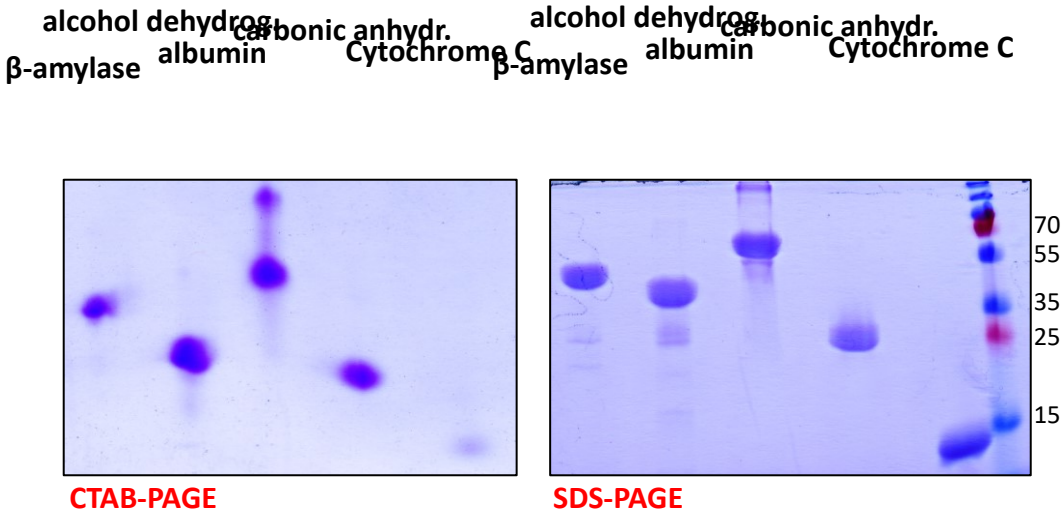


Figure 3.4. CTAB-PAGE achieves similar resolution of proteins to SDS-PAGE.

Individual purified proteins were obtained from Sigma, dissolved and the samples split and run on both SDS and CTAB-PAGE systems. Gels were stained with Coomassie-R250. β-amylase and alcohol dehydrogenase are terameric complexes dissociated into its monomeric form, whilst the others are all monomeric. Note no protein standard is available for CTAB-PAGE

.

Protein	Source	Size
β-amylase	Potato (Sigma A8781)	55.9 kDa (monomer size of tetramer complex)
Alcohol dehydrogenase (ADH)	Yeast *S. cerevisiae* (Sigma A8656)	36.9 kDa (monomer size of tetramer complex)
Albumin	Bovine (Sigma A8531)	66.5 kDa
Carbonic anhydrase	Bovine (Sigma C7025)	29.1 kDa
Cytochrome C	Equine (Sigma C7150)	12.4 kDa

Table 3.1. List of the proteins used in Figure 3.4.

List of purified proteins used in Figure 3.4 as well as their corresponding sources and monomeric sizes.

To ascertain if the cytoplasmic/nuclear enrichment technique was incompatible with CTAB-PAGE, as well as ascertaining if smearing of proteasomal subunits was a general property of proteasomes in all organisms, fractionation of *S. cerevisiae* was carried out on β-glucanase treated yeast cells and lysate fractions run on CTAB-PAGE. β-glucanase was produced in *E. coli* as stated in 2.2.7 and increasing volumes added to yeast cells to ensure complete digestion of the glucans in the fungal cell wall. The cells were then fractionated using the same buffer system as used in Figure 3.3. and run on CTAB-PAGE. The gel was transferred and probed with antibodies against Rpt5, Rpn8, Rpn10, Rpn12, Rpt6 and α7 (Figure 3.5). All six proteasome subunits

tested showed no diffuse smear material and resolved into defined bands suggesting both that the fractionation method is compatible with CTAB-PAGE and that *S. cerevisiae* doesn't contain proteasomes with the same modification as that on human myeloma cells.

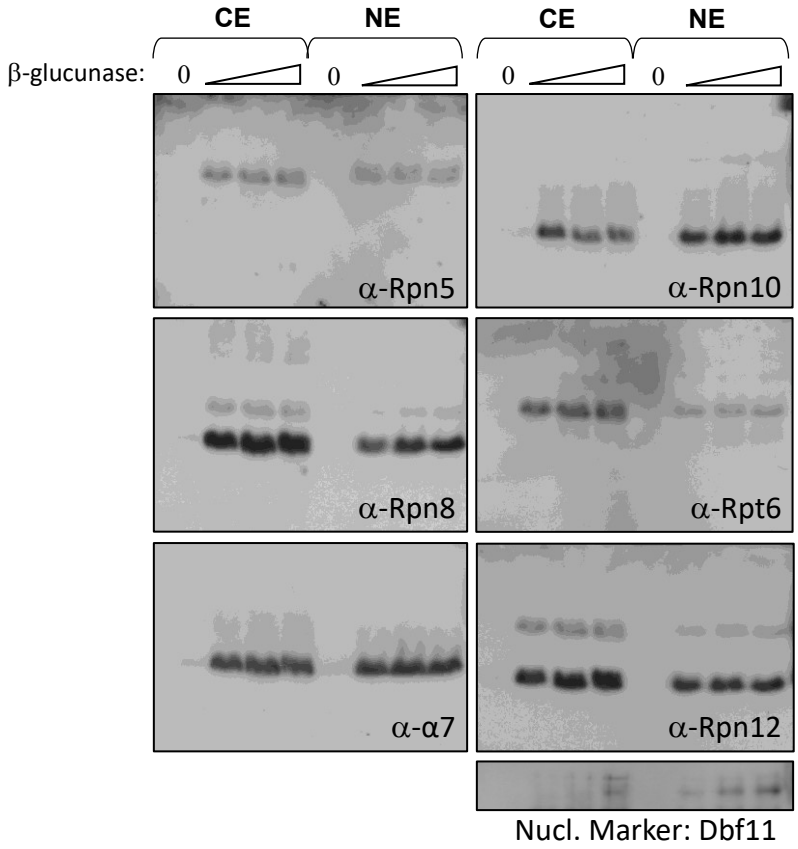


Figure 3.5. Cytoplasmic and nuclear fractionation of *S. cerevisiae* does not yield proteasome smearing on CTAB-PAGE.

Yeast cells were treated with β-glucanase (from *O. xanthineolytica*) to digest away their cell wall, after which cytoplasmic and then nuclear extracts were made. Extracts were subjected to CTAB-PAGE, and probed with antibodies against yeast proteasome subunits. An antibody against nuclear marker Dbf11 served as control for successful nuclear extraction.

In order to further purify the proteasomes away from any other nuclear proteins/components that may be interfering in the running behaviour in CTAB-PAGE I performed a cell fractionation from primary patient leukocytes released to research

from frozen patients leukapheresis, containing in the order of 1-3 x 10^{11} cells. Then using a resin immobilised UBL domain from hPLIC2/Ubiquilin2 I captured proteasomes by affinity purification (AP) from the nuclear fraction. Proteasomes were eluted by competition with Glutathione S-transferase (GST) tagged yeast s5a subunit which binds to the UBL domain. Excess s5a was then removed from the eluted proteasomes by capturing with glutathione immobilised beads. Eluted proteasomes from the UBL capture was run on SDS-PAGE and stained with coomassie-r250 to visualise all proteins. The lower bands visualised correspond to mostly Core Particle (CP) subunits and the higher molecular weight bands correspond to Regulatory Particle (RP) subunits. Another SDS-PAGE gel was run longer to better resolve RP subunits and labelled with likely band products (Figure 3.6 A). The majority of proteasome elutant was subjected to FPLC size exclusion chromatography using Superose6 column. Each fraction was pooled with its neighbouring fraction and then split and run on both SDS-PAGE and CTAB-PAGE electrophoresis systems (Figure 3.6.B).

Coomassie stains SDS_PAGE gels show the distinct pattern of resolved proteasome subunits with the lower portion of bands mostly corresponding to CP subunits and the higher resolved band comprising of RP subunits. With CP subunits resolved from 20 to 40 kDa and RP resolving from 45 to 120 kDa. The second gel shows better resolution of the RP subunits annotated with the most likely subunits. A high molecular weight smear was observed both on CTAB-PAGE and for the first time on SDS-PAGE. From the purity of the samples run it is unlikely that other cellular components such as chromatin, cytoskeleton etc. were interfering with the running behaviour of proteins in CTAB-PAGE. The higher molecular species emerging in the earlier fractions suggest that the smear is at least partially attributed to an increase in molecular weight on those proteasomes. Again not all subunits (e.g. α7) showed modified species and smearing, however, they were found across a wide number of fractions suggesting that they were incorporated in proteasomes of different MWs.

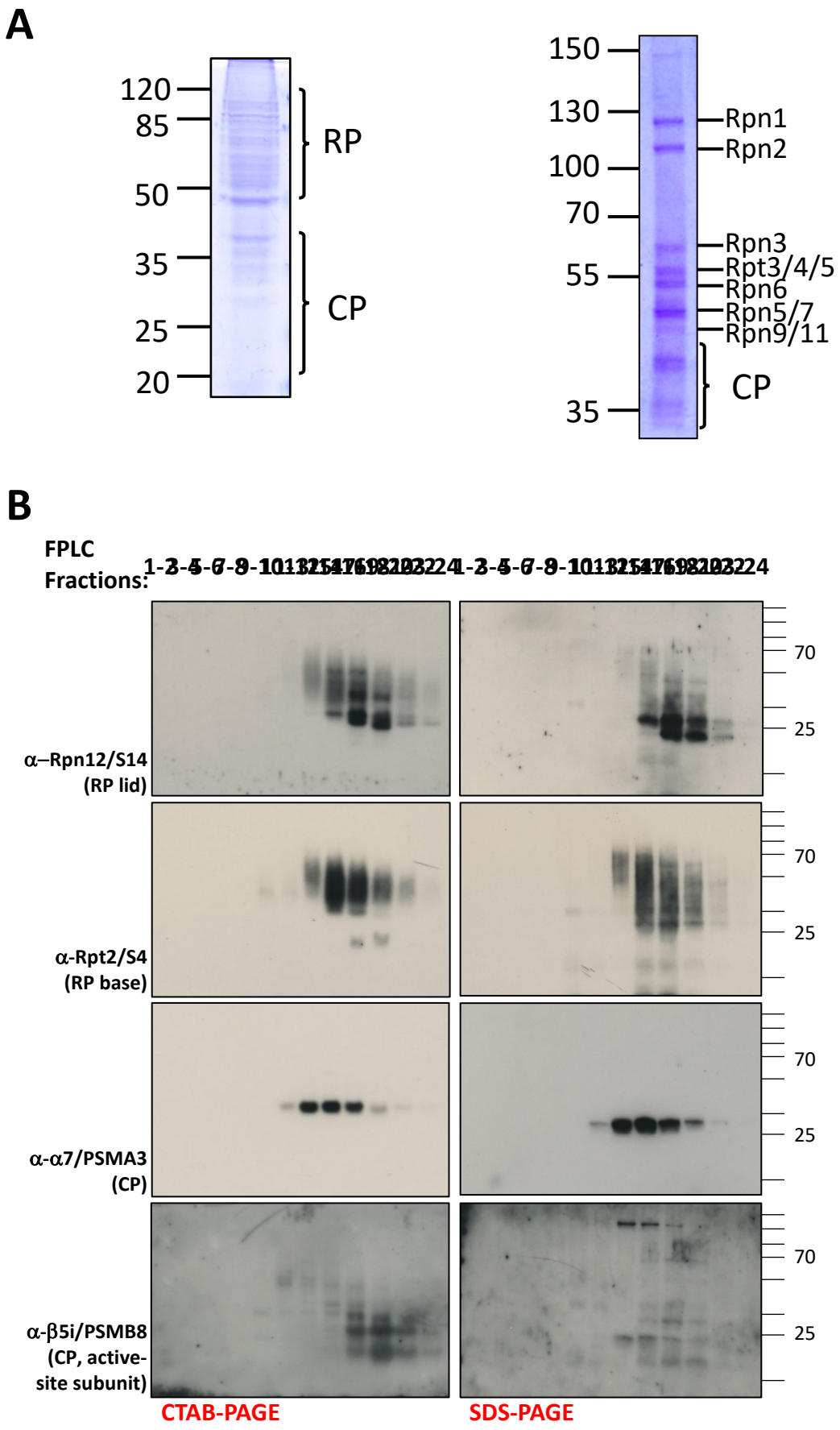

A
120
85
50
35
25
20
RP
CP
150
130
100
70
55
35
Rpn1
Rpn2
Rpn3
Rpt3/4/5
Rpn6
Rpn5/7
Rpn9/11
CP
B
FPLC Fractions:
α–Rpn12/S14 (RP lid)
α-Rpt2/S4 (RP base)
α-α7/PSMA3 (CP)
α-β5i/PSMB8 (CP, active-site subunit)
70
25
CTAB-PAGE
SDS-PAGE

Figure 3.6. Double purification of proteasomes by AP and FPLC techniques allows modified proteasomes to resolve on SDS-PAGE.

Nuclear human leukocyte proteasomes were affinity-captured from nuclear extract to purify them away from other nuclear components using a ubiquitin-like proteasome binding domain (UBL-His^6). A) Eluted proteasomes from the UBL capture was run on SDS-PAGE and stained with coomassie to visualise all proteins. The lower bands correspond to mostly Core Particle (CP) subunits and the higher molecular weight bands correspond to Regulatory Particle (RP) subunits. Another SDS-PAGE gel was run longer to better resolve RP subunits and labelled with likely band products. B) Eluted proteasomes were subjected to Superose6 FPLC size exclusion chromatography. FPLC fractions were analysed on both CTAB-PAGE and SDS-PAGE by Western blotting against proteasome subunits. N.B. FPLC yields fractions of highest MW to lowest.

To better confirm that the modified proteasome subunits mostly resided in the nucleus, primary leukocytes were fractionated as above and the proteasomes captured from both cytoplasmic and nuclear extracts using the same UBL capture release technique. The eluted proteasomes from both fractions were then subjected to FPLC size exclusion on a Superose6 column and fractions collected. Proteasome containing fractions 13-18 from each FPLC run (as well as samples from each UBL release, raw cytoplasmic and nuclear extracts, and whole lysate) was run on an SDS-PAGE gel and blotted for Rpt2 proteasome subunit (Figure 3.7). Unmodified Rpt2 was found in whole cell, cytoplasmic and nuclear fractions (indicated by the arrow), although modified Rpt2 only resided - and could only be captured - in the nuclear fraction (shown by the red bracket). In addition to the modified Rpt2 signal of the same size observed in Figure 3.6.B there was an addition of a larger molecular weight band of around 100 kDa that also represented a modified Rpt2 specie that was only isolated from the nucleus. Free UBL-His was also observed at 14 kDa, through cross reactivity with the Rpt2 antibody, most probably due to the huge amount of protein eluted off the loaded beads. The modified Rpt2 subunits were also detected after FPLC size exclusion chromatography, although the sample was diluted by the procedure.

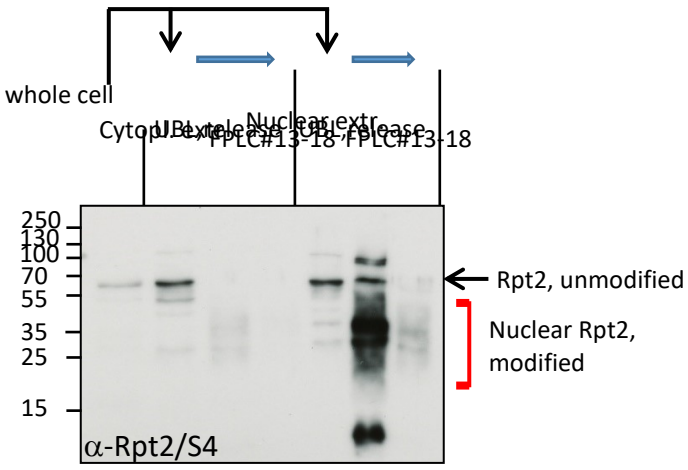


Figure 3.7. Modified species of Rpt2 are found mostly in the nucleus of the cell and can be still visualised after subsequent capture by UBL resin and FPLC purification.

Protein samples were taken from different stages of a large-scale nuclear human proteasome purification experiment, and run on SDS-PAGE. Western analysis was carried out by immunoblotting with an anti -Rpt2 proteasome antibody. Unmodified Rpt2 is indicated by an arrow, modified nuclear Rpt2 species are indicated with a red bracket.

3.4. Modified Proteasomes likely carry a charged polymer modification.

In order to further understand the biophysical properties of these modified proteasomes I first fractionated cells from the myeloma cell line OPM2 using the same cytoplasmic, nuclear isolation technique as in Figure 3.3. Proteasomes from each fraction were then isolated using GST-UBL loaded resin before eluting and running on a two dimensional electrophoresis system utilising iso-electric focusing (as stated in Method 2.7.3) before resolving by molecular weight using SDS-PAGE. Gels were transferred to PVDF membranes and stained using PonceauS reversible stain to visualise the large amount of eluted GST-UBL protein before being washed and probed with Rpt2 and Rpn12 antibodies Figure 3.8. The reactions were carried out twice with the blots in Figure 3.8 being representative. Additionally the same

preparation was run on IEF of a narrower range further confirming the focus of the prior blots.

Rpt2 probed 2D electrophoresis gel in Figure 3.8.i showed a number of dots present in both the cytosolic 2D and nuclear 2D blots corresponding to unmodified Rpt2, such as the three high molecular weight dots of roughly 60 kDa. As discussed previously the MW of proteasome subunits vary widely between different studies. Molecular weights of 49, 55, 62 kDa have all been shown (McIlwain, Berger, & Mak, 2013) Strikingly though, in the 2D Rpt2 blots there is a large amount of extra signal forming a diagonal focused ladder pattern on the proteasomes purified from nuclear lysate (red brackets). This was even more prominent when the same lysate was focused on a narrower pH 4-7 IEF strip. On both Figures 3.8.i and 3.8.iii a small amount of this diagonal laddering was present in the cytosolic blot, this is most probably due to a small amount of nuclear lysis or modified species that had not translocated to the nucleus. The membrane from Figure 3.8.i was also stripped and re-probed for Rpn12 subunit and again showed differences between the cytoplasmic and nuclear blots. The main Rpn12 band was evident in both the cytoplasmic and nuclear blots at ~ 28 kDa (predicted 30kDa). No significant change is observed to this main Rpn12 band, however a double band at ~70 kDa was shown to shift to a higher pH, but remain at the same MW in the nuclear blot (Yellow asterisk). Again showed the appearance of a diagonal stepped signal and one vertical stepped signal not present in the cytoplasmic focused gel shown by red brackets in Figure 3.8.ii. Although more is needed to identify the entire signal present on the blots the diagonal laddering is quite striking and indicative of a charged polymer modification where each monomer addition affects both the charge and MW of the protein. Tandem affinity purification should be carried out with elution not additionally eluting the UBL capture protein that at its high concentration shows background signal on the blots.

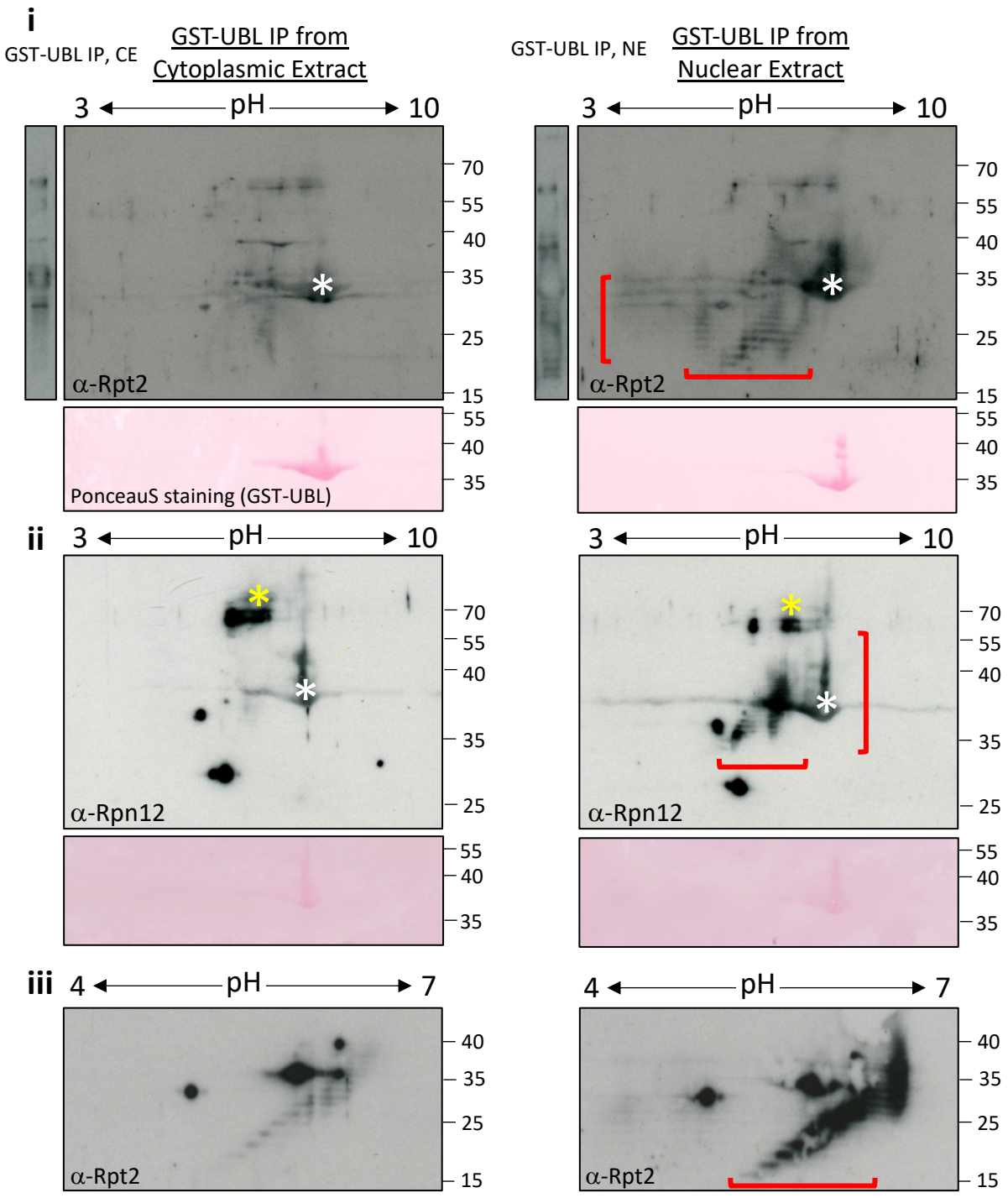


Figure 3.8. Two Dimensional electrophoresis of purified proteasomes show a charge and molecular weight shift of nuclear proteasome subunits.

GST-UBL captured proteasomes were captured from myeloma OPM2 cytoplasmic and nuclear extracts. The two samples were compared on two-dimensional iso-electric focusing/SDS-PAGE with an α-Rpn12 α-Rpt2 antibody. i) Shows GST-UBL captured

proteasomes from cytoplasmic and nuclear extracts focused to an iso-electric point on a pH 3-10 strip and subjected to a second SDS-PAGE dimension. The Western was then blotted with an α-Rpt2 antibody. ii) Shows GST-UBL captured proteasomes from cytoplasmic and nuclear extracts focused to an iso-electric point on a pH 3-10 strip and subjected to a second SDS-PAGE dimension. The Western was then blotted with an α-Rpn12 antibody. iii) Shows GST-UBL captured proteasomes from cytoplasmic and nuclear extracts focused to an iso-electric point on a pH 4-7 strip and subjected to a second SDS-PAGE dimension. The Western was then blotted with an α-Rpt2 antibody. The red brackets indicate signal from modified subunits. Care was taken to ensure that the iso-electric focusing was run to completion and that steady-state positions were reached. * Indicates a nonspecific signal due to the presence of a large amount of GST-UBL also shown in the PonceauS stained panels below.

Due to the diagonal laddering seen in the 2D blots suggesting that the modification could be a charged polymeric modification located in the nucleus, I investigated whether this smearing could represent tightly associated or covalently bound RNA or DNA. I first pooled fractions 15-16 containing the smear material from the FPLC run on Figure 3.6.B and then split it five ways. One was left as an input control whilst the other four were subjected to either Micrococcal nuclease, RNaseA/T1, RNase1 or RNaseH combination in the appropriate buffers and incubated at the optimal temperature for 2 h (as stated in Method 2.6). Due to the eluted material containing small amounts of EDTA, any cations required for the activity of the enzymes was added at a concentration that out competed the chelation effect of the EDTA.Reactions were stopped by the addition of SDS sample buffer and then run on SDS-PAGE before transferring and blotting for Rpt2 (Figure 3.9.i). There was, however, no observable change between the input with each treatment showing that there was no covalent modification or contamination by RNA or DNA.

Another charged polymeric nuclear modification is Poly-ADP-Ribose (PAR). To test if this could be attributed to the running behaviour of proteasome subunits, fractions 13-18 from FPLC purified proteasomes were pooled, split and subjected to a number of PAR hydrolysing enzymes as shown on Figures 3.9.ii-3.9.iii. These fractions again contained the smear material visualised in Figure 3.6.B. All enzymes were

commercially bought from suppliers stated in methods except for the orphan enzymes ADP-ribosylarginine hydrolase 2 variants 1 and 2 (ARH2.1 and ARH2.2) which were cloned into pET2a(+) bacterial expression vectors from HeLa cDNA and purified using Ni^{++}NTA resin as stated in Method 2.9.2.

The untreated fractions do resemble the FPLC SDS-PAGE blots in Figure 3.6.B showing the modifications are stable during freezing and storage at -80 °C as well as during the thawinf and carrying out of the mock reactions. ADP-ribosylarginine hydrolase 1 (ARH1), 2 variant 1 (ARH2.1), 2 variant 2 (ARH2.2) and 3 (ARH3) had no effect on the modified species compared to mock treated proteasomes (Figures 3.9.ii & 3.9.iii). However, poly(ADP-ribose) glycohydrolase (PARG) treated proteasomes showed a number of differences to Rpt2, Rpn12 and α7 subunits (lanes 3 & 6 of figures 3.9.ii and lanes 3-5 of Figure 3.9.iii). Both Rpt2 and Rpn12 blots curiously showed increased signal in the wells treated with PARG indicating increased antibody binding and detection of these subunits. Additionally, Rpn12 showed the appearance of a 55 kDa specie and additional smearing from ~45-130 kDa (lanes 3-5 of Figure 3.9.iii). Conversely the α7 blot showed reduction of signal of the main ~30 kDa band and appearance of slightly higher molecular smearing (Figures 3.9.ii and 3.9.iii). With all the blots there was however no cross reactivity of the antibody with the enzymes. Although shown to be mostly pure quantification of the viability of ARH2.1 and ARH2.2 to degrade substrate could not be quantified due to none known. It is therefore possible that these enzymes were lacking activity, although all effort was made not to degrade them and reactions were carried out in buffers supplemented with different cation composition. The reactions were carried out three times with the blots in Figure 3.9 being representative of all three experiments.

These could suggest that enzymes do have partial activity, but note that no complete collapse of the smear was possible with any combination of enzymes meaning that the modification is slightly different to the enzymes' natural substrate or that there were multiple modifications on these subunits and removal of PARG digestible modifications was not sufficient to collapse all modified subunits into a single band. Another possibility is that these enzymes may bind to the subunits but are not capable of hydrolysis causing an inceased shift in molecular size and retardation of migration behaviour.

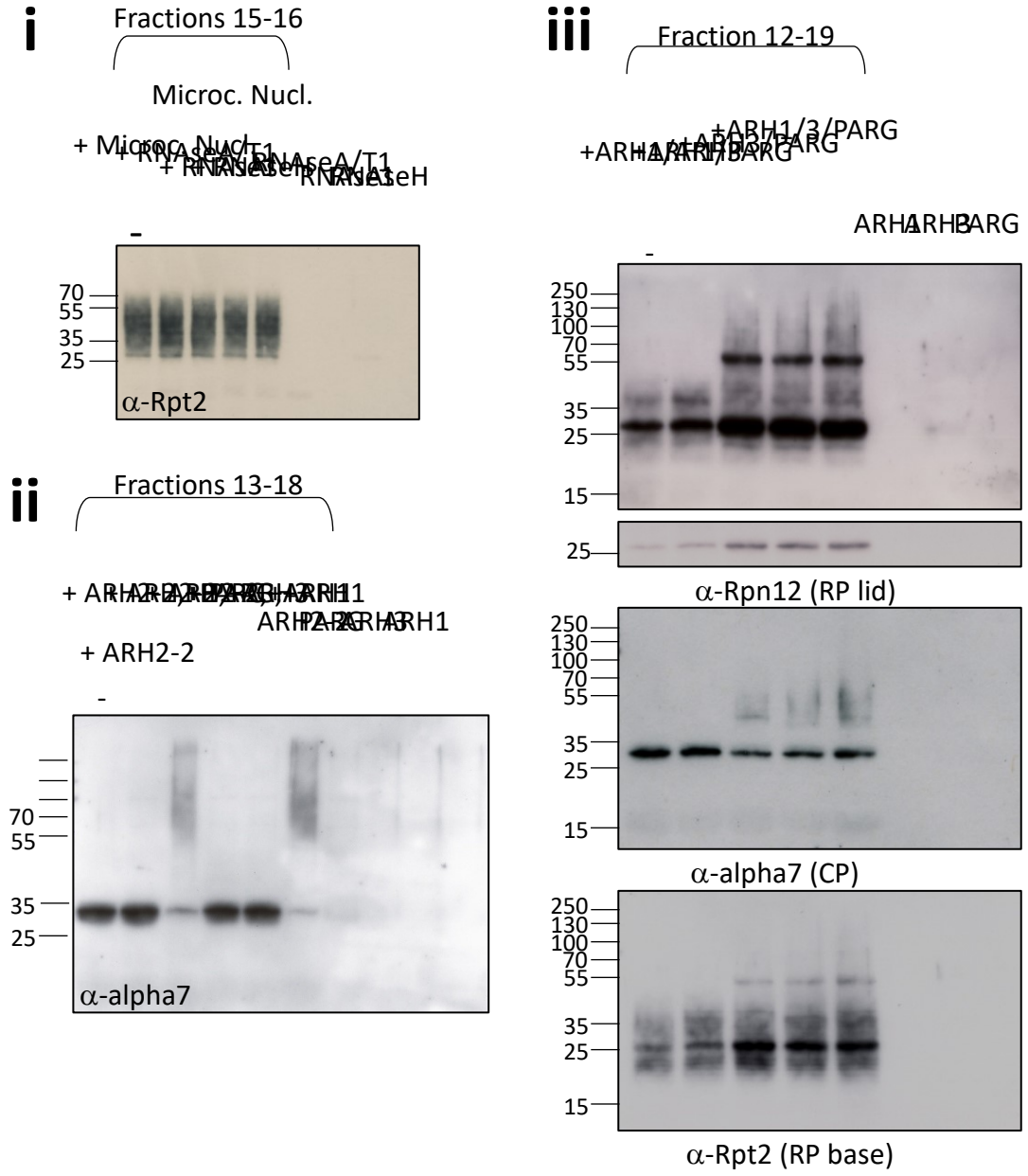


Figure 3.9. Enzymatic treatment of proteasome modifications.

Combined fractions from FPLC purification of UBL captured proteasomes were subjected to a number of enzymes with activity against DNA, RNA and PAR substrates. The fractions and enzymes used are shown above the lanes and the Westerns were

against the proteasome subunits stated per panel. Note the only changes observed were the lanes with PARG and the shift is towards an increase in MW.

Phosphodiesterase 1 from *C. adamanteus* venom has specificity for phosphodiester bonds in a wide range of substrates such as RNA/DNA/PAR. Proteasomes from FPLC fractions 13-18 were treated with PDE1 along with combinations of ARH3 and PARG and incubated for 1h at 37 °C. All treated and mock treated proteasomes were run on SDS-PAGE with enzyme controls, transferred and blotted for Rpt2 (Figure 3.10.i). Further testing of PDE1 as well as other DNA and RNA hydrolysing enzymes were tried on UBL captured proteasomes from OPM2 nuclear extract not subjected to FPLC size exclusion chromatography. These proteasomes were incubated with one or more enzyme in its appropriate buffer at 30/37 °C (dependant on the optimal enzyme temperature) for 1 h. Reactions were then run on SDS-PAGE and blotted with α-Rpt2 antibody Figure 3.10.ii.

In the first panel, all treated lanes had an apparent signal increase over the whole lane and shift of the diffuse signal upwards, this was more pronounced in the lanes treated with a combination of PDE1 and ARH3. The pattern of Rpt2 in the second and third panels was quite different to that of the first. This could be because the first panel used a small collection of FPLC fractions whereas the second and third were from whole cell lysate. Why the pattern of Rpt2 varies so extensively between UBL- captured proteasomes and proteasomes in whole cell lysate is still a problem. Interestingly PDE1 had a greater effect here with many of the minor modified bands disappearing with the retention of the main 55 kDa band. The predicted MW of Rpt2 is 49 kDa although, like most human proteasome subunits, the detection of proteasome subunits using SDS-PAGE rarely yield bands of the correct size. The disappearance of other bands and retention of the 55 kDa band could be unmodified Rpt2. However, this raise questions as to why no Rpt2 band of that height was visible in the FPLC purified blots. There are other proteasome subunits detected after FPLC suggesting that the signal is specific, although something is interfering with the normal migration is SDS-PAGE. Again, no cross reactivity of the antibody was seen in the enzyme only lanes. This shows that the higher MW smear is unlikely to be cross reactivity with the enzymes or degradation of the subunit, which would yield smaller bands.

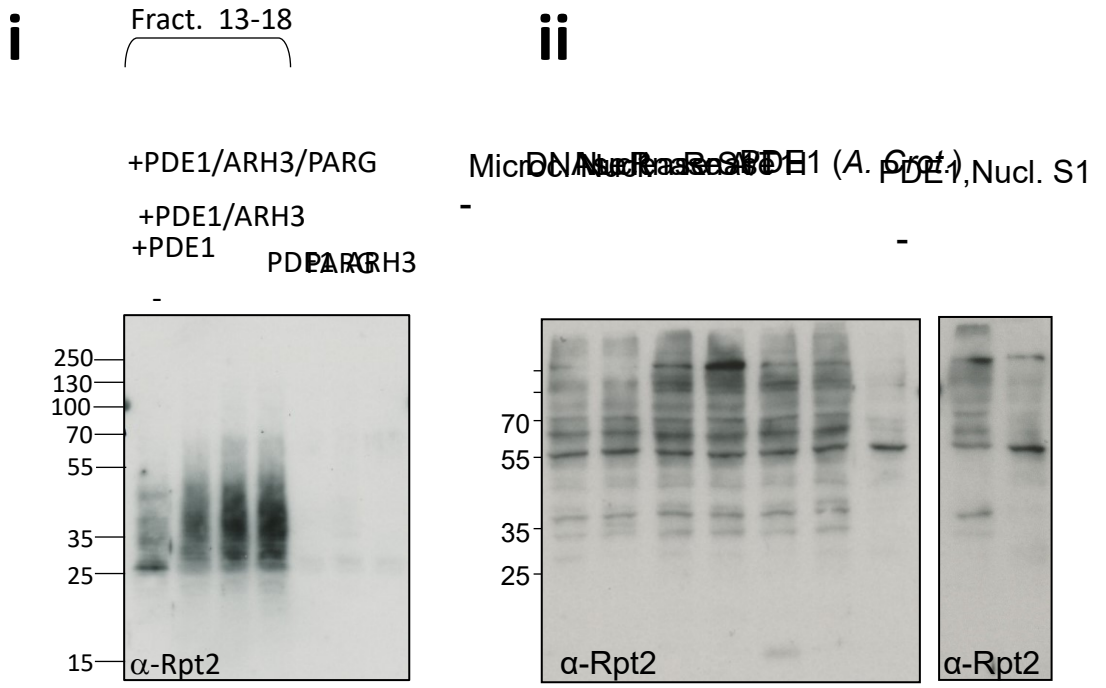


Figure 3.10. PDE1 has activity against modified Rpt2 subunits.

i) Fractions 13-18 from FPLC purification of UBL captured proteasomes were subjected to a number of enzymes with PAR hydrolysing activity (shown above each lane). Reactions were incubated at 37 °C for 1 h before being run on SDS-PAGE and blotted with an antibody against Rpt2 subunit of the RP. ii) UBL captured proteasomes from OPM2 nuclear extract were subjected to a number of enzymes with DNA, RNA and PAR hydrolysing activity (shown above each lane). Reactions were incubated at 30/37 °C for 1h before being run on SDS-PAGE and blotted with an antibody against Rpt2 subunit of the RP.

In order to see if proteasomes treated with S1 Nuclease and PDE1 enzymes, which had activity to the modified species of Rpt2, had any effect on the proteolytic activity of proteasomes, an *in vitro* ubiquitin degradation assay was utilised. A short model substrate was ubiquitinated as laid out in the methods, and the system confirmed in Appendix A. Proteasomes Ni^{++}NTA purified from OPM2 cells over expressing an His_6-2(StrepIITag)-TeV-Rpn11 protein construct (Method 2.9.1, Appendix C) were split and

treated on the beads with a combination of S1 Nuclease and PDE1 for 1 h at 37 °C. Beads were then washed once in PBS to remove added enzymes and proteasomes eluted with imidizol. Three different concentrations of proteasome were then added to the *in vitro* degradation assay along with mock treated controls and incubated for 1 h at 37 °C after which it was stopped by the addition of SDS-PAGE sample buffer and run on an SDS-PAGE gel alongside a substrate only lane. The gel was transferred and then blotted with an ubiquitin FK2 antibody (Figure 3.11). The reactions were only carried out once due to time limitations.

The smear of signal observed was due to the different levels of ubiquitination of the substrate. Comparison of the mock treated and S1 Nuclease/PDE1 treated proteasome lanes showed a slight/subtle difference in its ability to degrade the modified substrate as shown by a retention of α-Step signal in the 1x PDE1 treated proteasome lane. This was, however, not observable when excess proteasome was added as shown in the 3x proteasome lane. When even more proteasome was added 19.5 times that of the 1x proteasome treatment, processing of the ubiquitinated substrate was towards deubiquitination and not degradation as shown by the appearance of substrate only band of 15 kDa.

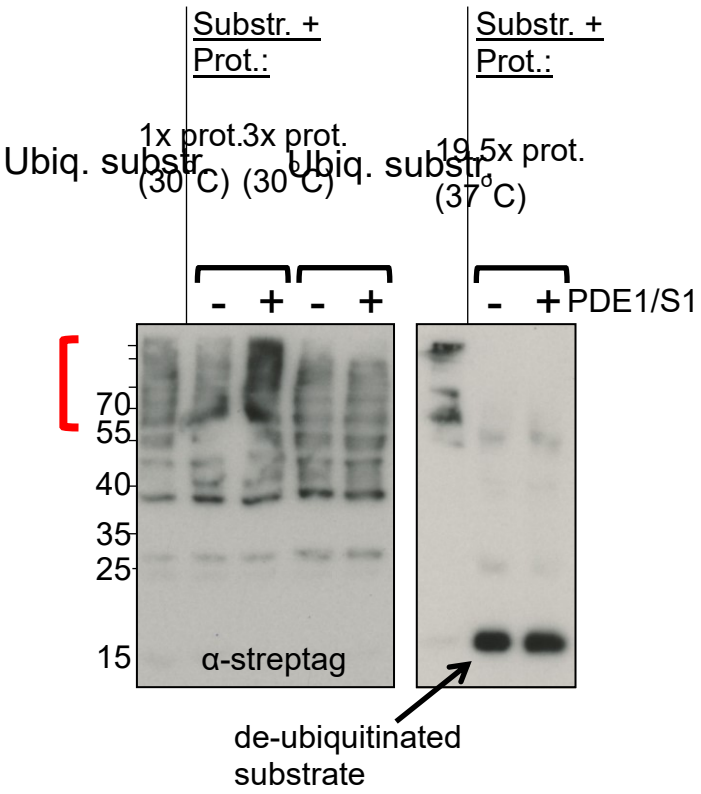


Figure 3.11. PDE1/S1 Nuclease treated proteasomes have no effect on their ability to degrade ubiquitinated proteins.

GST-UBL captured proteasomes were captured from myeloma OPM2 nuclear extract and treated with PDE1 and S1 nuclease. The treated proteasomes were added to a ubiquitinated substrate at three different concentrations and incubated for 1h before running on an SDS-PAGE gel and blotting for StepTag residing on the model substrate. The diffuse signal is due to the different levels of ubiquitination the substrate received and the band at ~16 kDa is deubiquitinated substrate.

3.5. Discussion

Continuing the work done by Dr M. Kleijnen and his lab member Ms Z Wang I show in this chapter that the diffuse smear material detected when running proteasome samples on CTAB-PAGE is most likely caused by extensively modified proteasome subunits most likely residing in the nucleus of the cell.

With the diffuse signal being retained through immunoprecipitation and FPLC purification size exclusion chromatography it shows that other proteins and cellular components are not the reason for the smear and that the smear is quite likely an extensive modification and not an artefact of CTAB-PAGE. Upon looking at the FPLC size exclusion blot, the fact that subunits such as α7 are found in these early fractions alongside the smears of Rpt2 and Rpn12 cements the facts that the modifications are real as any artefact in protein electrophoresis or off target effects of the antibodies would not explain why α7 was found in such a range of FPLC fractions unless it was incorporated in a range of hetrogeneric proteasomes.

SDS-PAGE, which is so indoctrinated as *the* protein electrophoresis system for resolving proteins by molecular weights, has meant many investigators have not even heard of the lesser known CTAB-PAGE system. This could also possibly be due to the slight difficulties in casting and running of CTAB-PAGE gels. In fact, even with extensive searching, no CTAB-PAGE compatible protein standard could be found that didn't contain SDS. Upon running a number of purified proteins on both systems, the proteins resolved in a similar manner. Yet the differences in the two systems could not be more pronounced than when looking at proteasome biology. Not only did modified proteasome subunits from unpurified samples fail to resolve on SDS-PAGE, upon fractionation of cells in Figure 3.2, cytoplasmic subunits barely showed up on the system. Only after UBL capture and enrichment did modified proteasome subunits start to migrate in to SDS-PAGE gels.

SDS has been recorded as having some unusual behaviour. Gel shifts, where proteins run at a different molecular weight, are relatively common. In fact, most proteasome subunits are subject to this. SDS-PAGE relies on the uniform coating of proteins with SDS detergent and generally binds to most proteins in a similar manner of around 1.1 - 2.2 g SDS/g. For some proteins though this SDS loading can be much higher or lower and ranges of 0.4-10g SDS/g protein have been published for membrane proteins

(Rath, Glibowicka, Nadeau, Chen, & Deber, 2009). Modification of amino acid residues are also known to cause shifts for example phosphorylation, acetylation, glycosylation to name a few (Georgieva & Sendra, 1999; Selcuk Unal, Zhao, Qiu, & Goldman, 2008). Interestingly this is not always the case, phosphorylation of the transcription factor c-Jun causes a shift on one serine residue whereas phosphorylation on an identical serine residue upstream does not (Morton, Davis, McLaren, & Cohen, 2003). Even a single amino acid change can cause molecular weights to shift a kilodalton or more (de Jong, Zweers, & Cohen, 1978; Panayotatos et al., 1993; Prudencio, Hart, Borchelt, & Andersen, 2009).

CTAB-PAGE is already recommended for looking at glycoproteins over SDS-PAGE electrophoresis due to its superior resolution and better detergent loading onto these proteins. From the investigations and results detailed in this chapter I also recommend its use in looking at all nuclear protein isolates at least in comparison to SDS-PAGE

The majority of protein processes such as translation, folding, modification and degradation occur in the cytoplasm of the cell so it would be logical for the majority of proteasomes to reside in this fraction and although I never directly looked at the amount of proteasomes residing in these fractions it is amazing to see how much extra material is detected in the nuclear fraction, this has been further shown by others (Arnold & Grune, 2002). However, relative levels can not be quantified here as other factors could lead to a selection bias such as the composition of CE and NE buffers when capturing. This suggests an important role of nuclear proteasomes. It is already known that proteasomes have a wider range of functions in the nucleus such as their interaction with chromatin, DNA and other nuclear components, but little is known about how this is accomplished (Bhat et al., 2008; F. Geng & Tansey, 2012; Kodadek, 2010; Kwak, Workman, & Lee, 2011; Walters et al., 2002)

Another interesting point not really investigated further here is the fact that capturing of proteasomes by the UBL domain of hPLIC2 seems to be biased towards nuclear proteasomes (Figure 3.7.). In this Figure the ratio of unmodified subunits to modified is severely different between Rpt2 found in the NE fraction to UBL captured proteasomes from the NE fraction. This could suggest a biological importance of these proteasomes in the relation between modified proteasomes and hPLIC2.

This causes one to question the methods utilised in raising antibodies against proteasome subunits. If UBL methods are used to capture proteasomes for use in raising antibodies and it itself is biased to particular species, how broad are the antibodies we use? This would have an effect on downstream IP capture and restrict the validity and complexity of this technique.

These modifications were found on most but not all 19S RP subunits tested. Rpt1, Rpt2, Rpt4, Rpn10 and Rpn12 showed extensive modifications compared to Rpt3 and Rpt5. I continued by focusing just on Rpt2 and Rpn12 regulatory subunits throughout the rest of the chapter.

2D electrophoresis of these two subunits confirmed great differences in these subunits when isolated from either the cytoplasm or nucleoplasm of myeloma cell lines. The most interesting was the appearance of a diagonal stripped ladder pattern, in the nuclear fractions, indicative of a polymeric charged modification. This further confirmed the validity of large charged modification that was observed on CTAB-PAGE on these subunits.

If this diffuse additional material is indeed due to large charged polymeric modifications this may also explain why they are unresolvable by SDS-PAGE. As mentioned earlier SDS-PAGE has been shown to lack in the resolution of proteins with negative polymeric modifications such as sialic acid moieties. The difficulty is that glycosylation modifications are huge and do notinteract with SDS in the same way as amino-acids in a peptide chain. As a result glycoproteins do not have equal loading of SDS-PAGE, and the terminal sugars are sometimes charged and further alter the charge to M_r ratio fundamental to SDS-PAGE electrophoresis. The result of these combined effects are often a huge smear on SDS-PAGE as the charge may repel detergent binding or even overwhelm the total negative SDS charge to restrict migration or even reverse it. The latter would also explain why CTAB-PAGE, which uses a detergent of opposite charge, would then be able to resolve such proteins.

A polymeric charged modification, however, does not explain why further purification allows for the running and resolving of these modifications in SDS-PAGE. Whether a reduction of other proteins competing for detergent allows better binding to the modified subunits or whether other cellular components were shielding the

modification and preventing SDS-PAGE resolution is still not understood and needs to be investigated further.

Attempted digestion of the modification on nuclear proteasomes was not conclusive, although some reactivity was observed with PAR hydrolysing enzymes PARG and PDE1 as well as the single stranded DNAase S1 nuclease. Although this modification differs from PAR it does share a number of characteristics and reactivity in enzymatic reactions, suggesting that the modifications observed may share some similarity to PAR but are distinct enough to prevent full cleavage. They could, however, share similar functions to PAR, which is important in directing DNA repair proteins to DNA (Beneke, 2012; Gibson & Kraus, 2012). PAR has also been shown to activate proteasomes to degrade oxidatively damaged histones and help in DNA repair (Arnold & Grune, 2002; Ullrich et al., 1999).

My identification of an SDS-PAGE-incompatible protein modification may also explain the difficulty in resolving the controversy as to whether RNA species, which early studies suggested are associated with proteasomes (then called prosomes) (Schmid et al., 1984), are bona fide components of proteasomes (Pamnani, Haas, Puhler, Sanger, & Baumeister, 1994). These modifications may account for the reported RNP-like density of prosomes/proteasomes, and our finding that SDS-PAGE fails to detect modified proteasomal subunits may explain the difficulty in resolving the controversy.

To fully confirm the findings of this chapter much more needs to be done. The nature and composition of all proteasome subunit modifications needs to be worked out. If the modification is nucleotide in nature P^{32} ATP could be fed to cells and radio labelling of proteasome subunits could be assessed. Chemical release of glycosylation modifications could be tried out, superseding the need for highly specific de-glycosylation enzymes. Only upon full removal of modifications and subsequent collapse of all proteasome subunits into a single band can the assumption that modification of the proteasome leads to these affects in SDS/CTAB-PAGE migration.

More has to be done to rule out the extraction method causing aggregation. Glycerol gradients could be used to get cleaner fractionation. It would however be hard to believe that aggregation occurs to proteasomes over other proteins and that denaturing by addition of SDS sample buffer and boiling would allow for clean release of some subunits such as α7 but not others. A major limitation is the use of His^6-Ubl

capture. Although UBL capture does pull proteasome particles down relatively cleanly the release by imidazole could release aspecific proteins binding to the Ni^{++} beads themselves. In addition to this, imidazole also releases the His^6-Ubl capture protein, that itself shows cross reactivity to a number of proteasome antibodies and made down stream analysis of some blots like that of 2D and capture blots hard to decipher. Cross linking of UBL to beads or using a two-step purification should be used. However, Ubl capture does not explain all of the smear material, which was evident in total lysate run on CTAB-PAGE, further suggesting that capture and fractionation plays no role in the smear observed.

CHAPTER 4 - Post translational modification of proteasome subunits change early after Bortezomib challenge.

Chapter 4: Post translational modification of proteasome subunits change early after Bortezomib challenge.

4.1. Introduction

Since the first use of proteasome inhibitors against myeloma many hypotheses have been presented to explain myeleoma's susceptibility to proteasome inhibition above that of other cancers and non-cancerous cells. Due to the nature of cancer's proliferation, the level of protein turnover by the proteasome (pertaining to cell cycle) is increased. Therefore, it has been hypothesised that proteasome inhibition would be lethal to all cancers due to the increased proteasome load. Multiple clinical trials and published papers have looked at proteasome inhibition in numerous cancers such as lung, prostate, and testicular. The a large proportion of these have been shown not to be significant and relatively large amounts of retractions of papers, due to spurious data, have occurred in recent years in some labs studying bortezomib's effects on cancers.

To explain why myeloma has sensitivity to proteasome inhibition over other cells the load versus capacity hypothesis was postulated (Bianchi et al., 2009). It states that myeloma cells have a higher load on the proteasome than other cell types due to the high secretion of M protein. This high secretion increases the load on the endoplasmic reticulum causing misfolding of the proteins, activating ERAD and targeting the proteins to the proteasome. There is, however, a number of conflicting arguments to this such as: why other highly secretory cells are immune to bortezomib (e.g. insulin secretion in the beta cells of the pancreas); why over half of patients with myeloma are already resistant to proteasome inhibitors; why inhibition of *only* two out of six active sites of the proteasome is so detrimental to the degradation of proteins; and why proteasome inhibition does not correlate to protein degradation.

Although a lot of work has been done on inhibition of proteasomes by agents such as Bortezomib and Epoxomicin on *in vivo* and *in vitro* systems, relatively little has been done looking at the early kinetics of inhibition of these agents.

Kisselev et al. 2006 show that, at least in HeLa cells, the levels of proteasome inhibition do not correlate with the inhibition of protein breakdown and that the other sites help maintain protein breakdown levels with the Trypsin-Like (T-Like) site achieving increased activation upon Chymotrypsin-Like (CT-Like) activity inhibition.

In this chapter, I look at the early kinetics of proteasome inhibition by Bortezomib and other proteasome inhibitory agents focusing on the inhibition of the CT-Like site in the first 24 h after treatment. A discrepancy is found in the level of inhibition of proteasomes in cell lysate and purified proteasome populations to that of proteasome inhibition within cells.

Upon further testing this could not be attributed to caspase activation, increased binding of proteasome inhibitor over time or even cell death initiation as read by AnnexinV staining. However, proteasome inhibition by Bortezomib, Epoxomicin or the vinyl sulfone inhibitor Ada-K(Biotin)-Ahx_3-L_3-VS (VS-Biotin) did show a change in the patterning of modified proteasome subunits

Work done in this chapter has been subsequently published (Pitcher et al., 2014, 2015) copies of which can be found at the back of this thesis (APPENDIX E).

4.2.1. Measurement of CT-Like activity upon Bortezomib treatment.

I first chose to investigate the first 10 h of inhibition of the CT-Like active site by Bortezomib in various human cell lines of differing Bortezomib sensitivity. A time course was set up using the Bortezomib-sensitive myeloma cell lines RPMI-8226 & NCI-H929 as well as the Bortezomib-insensitive cell lines A549, lung carcinoma, and Jurkat acute lymphoblastic leukaemia. The cells were all treated with 10 nM Bortezomib or a DMSO solute control. Cells were then harvested from each of the treatments of the four cell lines every two hours over the first ten hours of treatment. The cells were then lysed in Proteasome Activity Buffer (PAB) and the lysate split with one fraction receiving a 20 μM Bortezomib dose to inhibit all CT-Like activity of the proteasome. The site specific substrate Suc-LLVY-AMC was then added to each sample and the fluorescent intensity read every 20 s over a 1 h time period. Rates calculated from the gradient of the graph. The activity of 20 μM Bortezomib-treated lysate that corresponded to aspecific protease activity was subtracted from both the DMSO and 10 nM Bortezomib readings and the activities normalised to each timepoint's DMSO control Figure 4.1. (Method 2.8.2). The experiment was carried out twice with three replicates per experimental repeat.

The two myeloma cell lines RPMI-8226 and NCI-H929 showed a steady decrease in activity to nearly 5 % at 10 hours, whilst the Bortezomib insensitive cell lines A549, lung carcinoma, and Jurkat, chronic lymphoid leukaemia, showed a similar decrease over the first 4 hours but then levelled off to keep their remaining CT-Like activity above 20 %. This could be explained by a number of hypotheses such as different cell permeability of bortezomib, different binding affinity of bortezomib, or different levels of turnover of the proteasome, and shows some of the first evidence for different CT-Like site responses of inhibition between Bortezomib sensitive and insensitive cells.

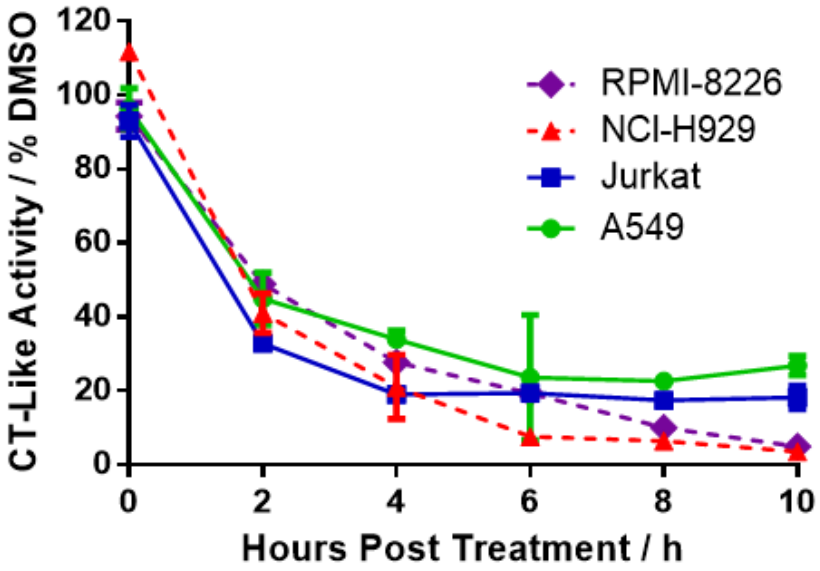


Figure 4.1. CT-Like active site inhibition of various human cell-lines over the first 24 h of Bortezomib treatment.

NCI-H929, RPMI-8226, Jurkat and A549 cells were treated with 10 nM Bortezomib or DMSO and the CT-Like activity measured and plotted as a percent of the DMSO control at 0, 2, 4, 6, 8 & 10 h post treatment. Bars represent mean ± SEM, n=2.

In order to investigate the level of CT-Like inhibition where load on the proteasome outweighs capacity, the myeloma cell line NCI-H929 was treated in duplicate with 10 nM Bortezomib or DMSO solute control at 0, 2, 4, 6, 8, 10 and 24 h. Bortezomib treated cells and DMSO control cells were lysed at the end of the experiment in PAB and the lysate split with one fraction receiving a 20 μM Bortezomib dose to inhibit all CT-Like activity of the proteasome. The site specific substrate Suc-LLVY-AMC was then added to each sample and the fluorescent intensity read every 20 s over a 1 h time period. Rates calculated from the gradient of the graph. The activity of 20 μM Bortezomib treated lysate that corresponded to aspecific protease activity was subtracted from both the DMSO and 10 nM Bortezomib readings and the activities normalised to each timepoint's DMSO control (Method 2.8.2). Cells left over from the proteasome activity assay where counted and 2 x 10^5 cells were run on each lane of the CTAB-PAGE gel

before Western probing with an anti Ubiquitin antibody to visualise total ubiquitinated proteins (Figure 4.2).

In Figure 4.2 the CT-Like activity of the proteasomes from 10 nM Bortezomib treated cells decreased quite rapidly from its maximum of 111.87 % of control at time 0, down to 41.02 %, 21.09 %, 7.64 %, 6.47 %, 3.50 % and 0.27 % at 2, 4, 6, 8, 10 and 24 h. Larger variation in the DMSO control at time 0 is likely to have skewed the treated time point and therefore the maxima is likely to be around the 100% level. The ubiquitin blot showed a smear corresponding to signal from every ubiquitinated protein in the cell. Only at around 6 h did the amount of ubiquitin signal in the Bortezomib treated cells exceed that of the DMSO treated cells, indicating that only at around ~80 % inhibition of the CT-Like active site did demand exceed the rate of degradation.

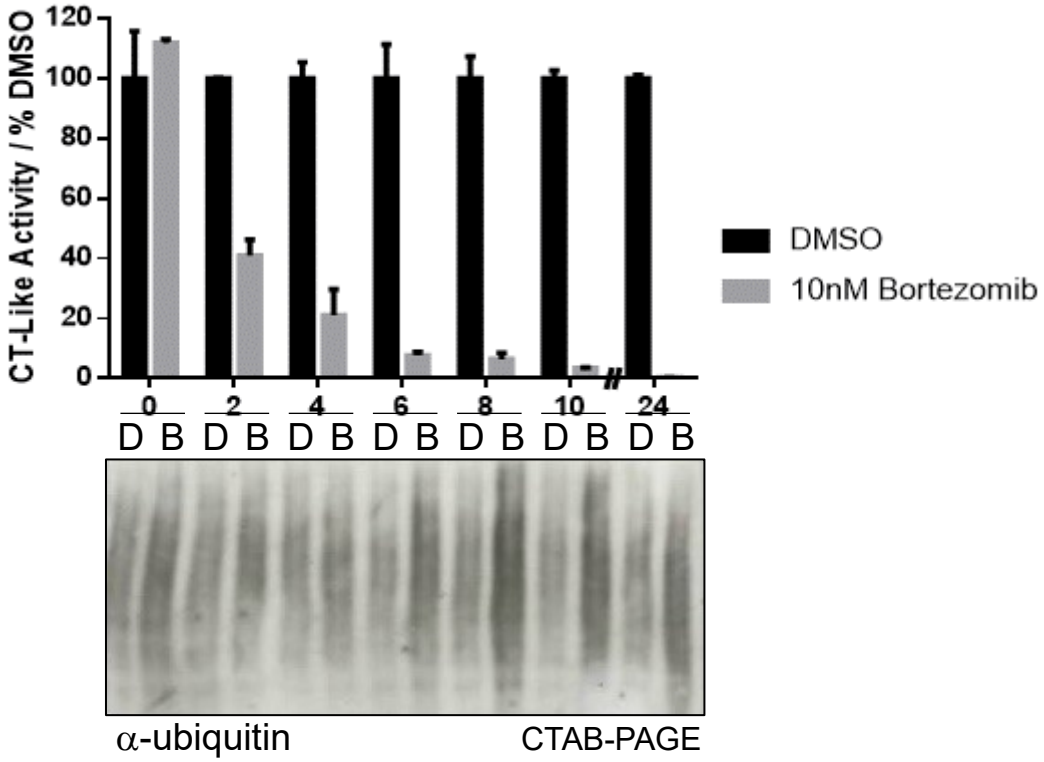


Figure 4.2. Inhibition of the CT-Like active site of intracellular proteasomes over the first 24 h of Bortezomib treatment.

NCI-H929 cells were treated with 10 nM Bortezomib or DMSO and the CT-Like activity measured and plotted as a percent of the DMSO control at 0, 2, 4, 6, 8, 10 & 24 h post

treatment (top panel). Bars represent Mean activity ± SEM, n=2. Lysate from the same samples was also run on CTAB-PAGE and the Western blotted for ubiquitin conjugates as shown in (bottom panel).

To test if the drop in proteasome activity was due to Bortezomib binding and not due to any feedback from other pathways in response to bortezomib, NCI-H929 cells were first lysed in PAB to disrupt any cellular processes. The lysate was then split and left on ice and each hour 10 nM Bortezomib was added to duplicate samples and an equal volume of DMSO to another duplicate. On the sixth hour, corresponding to t=0, 20 μM Bortezomib was added instead of the regular concentration alongside the regular DMSO treated samples. Immediately after the high dose Bortezomib treatment CT-Like activity of every sample was measured by the addition of the site specific Suc-LLVY-AMC fluorescent substrate and the fluorescent intensity read (Method 2.8.2). Each sample was then normalised to its times DMSO control and plotted as a percent of this value (Figure 4.3).

Treatment with 10 nM Bortezomib did produce a reduction in the CT-Like activity of proteasomes from lysed cells although the activity did not continue to fall and was relatively level throughout all the time points with only a 13-16 % reduction. This suggests that the continued decrease in activity of the proteasome within treated live cells was likely to be due to intracellular processes amplifying the direct inhibition by bortezomib or possibly cell diffusion. The 20 μM treated lysate showed a complete reduction in activity, meaning that the activity that remained in the 10 nM Bortezomib samples was not attributable to aspecific protease activity. This in comparison with Figures 4.1 & 4.2 this finding suggests additional cellular mechanisms that result in the inhibition of intracellular proteasomes.

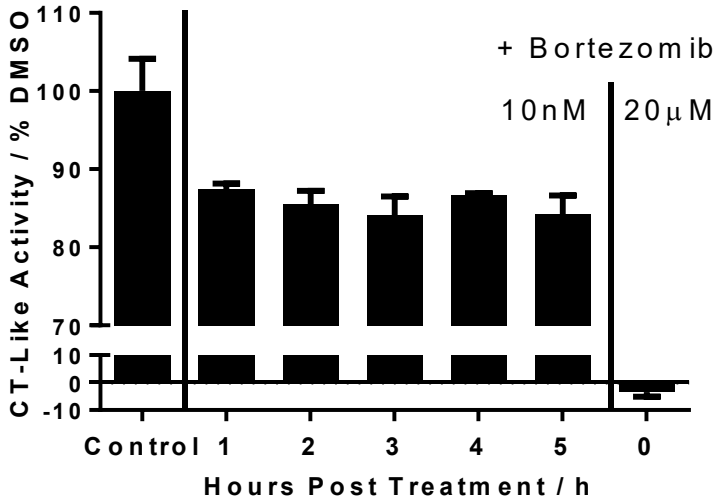


Figure 4.3. Inhibition of the CT-Like active site over the first 24 h of Bortezomib treatment.

NCI-H929 cells were first lysed and the lysate treated with 10 nM Bortezomib for 1, 2, 3, 4 & 5 hours. CT-Like activity measured by a site specific fluorescent substrate and plotted as a percent of the matching DMSO timepoint. 20 μM Bortezomib was added at timepoint 0 to measure aspecific protease activity, of which non was recorded. DMSO plotted is representative of 1-5 h mean. Bars represent Mean activity ± SEM, n=2.

To further support the above result, I tested the inhibition of human and yeast proteasomes purified from other cellular components that might amplify the inhibition by Bortezomib. Proteasomes from the human cell line OPM2 were purified as stated in Methods 2.4.6 and yeast proteasomes as stated in Methods 2.3.3. These proteasomes were then treated in duplicate with either 10 nM Bortezomib, DMSO or 20 μM Bortezomib, to measure aspecific protease activity, and incubated for 2, 4, and 6 h at 30 °C. After this time the CT-Like activity was read by addition of Suc-LLVY-AMC site specific fluorescent substrate. Aspecific protease activity, measured by the 20 μM Bortezomib treated samples, was then subtracted from the DMSO and 10 nM Bortezomib treated samples, and the 10 nM Bortezomib treated samples normalised to DMSO control and plotted Method 2.8.2 (Figure 4.4).

Activity in the yeast purified samples treated with 10 nM Bortezomib saw a modest decrease in activity of between 14-21 %, similar to that of human proteasomes in lysate (Figure 4.3), and was relatively level though out all time points. Proteasomes purified from the OMP2 cell line that were treated with 10 nM Bortezomib saw a greater reduction in comparison to the yeast of 49-61 % and also saw a slight reduction over time between the 2 h sample and the 4 h samples. This drop could be due to a number of reasons, such as the stability of the human proteasome complex at this temperature, the purification of proteasomes away from stabilising factors, the reduction of ATP in solution resulting in disassembly or due difficulty in purifying human proteins in one step yielded low levels of protease. In both cases the level of inhibition of purified proteasomes did not continue to fall like those proteasomes that resided in treated cells.

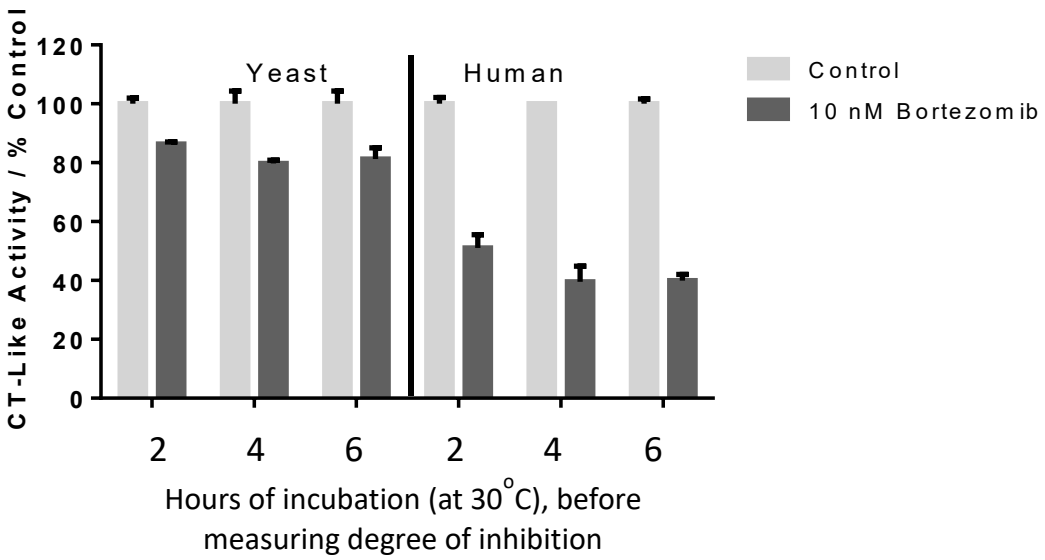


Figure 4.4. Inhibition of the CT-Like active site of purified yeast or human proteasomes over the first 6 h of Bortezomib treatment.

Proteasomes purified by affinity capture techniques from yeast or human cells were treated with 10 nM Bortezomib and incubated at 30 °C for 2, 4 or 6 h. CT-Like proteasome activity was measured by degradation of a fluorescent substrate Suc-LLVY-AMC at 30 °C for yeast, 37 °C for human and normalised to the DMSO control. Bars represent Mean activity ± SEM, n=2.

4.2.2. Investigation into whether caspase activity plays a role in proteasome activity shutdown.

To test to see if the activation of caspase could explain the continued reduction in CT-Like activity of intracellular proteasomes, I first treated NCI-H929 cells with 10 nM Bortezomib or DMSO. Both lots of treated cells were then harvested at 8, 10, 12, 14, 16, 18 and 24 hours before being lysed and their lysate run on SDS-PAGE gel. Western analysis was done by probing against the active form of caspase 3 using a anti cleaved caspase 3 antibody and anti Poly ADP-Ribose polymerase (PARP) antibody, a substrate of caspase 3 and indicator of caspase activation (Figure 4.5). Caspase 3 is an executioner of apoptosis (McIlwain et al., 2013).

The appearance of a cleaved caspase 3 band corresponding to the active form of caspase 3 was only visible after 10 h treatment with Bortezomib. Cleaved PARP shown by the appearance of the lower molecular weight band also only appeared after 10 h Bortezomib treatment, and still showed the full length band at this timepoint showing that caspase 3, that cleaves PARP on activation, had only just become active. Caspase 3 therefore could not play a role in the continued shutdown of proteasomes seen in (Figure 4.1) where the CT-Like activity had almost been fully inhibited by this time. This suggests that he continued drop in proteasome activity is lethal to the cells and triggers caspase activation and apoptosis as oppose to caspase activation leading to the continued decline in proteasome activity being a result of caspase cleavage of the proteasome.

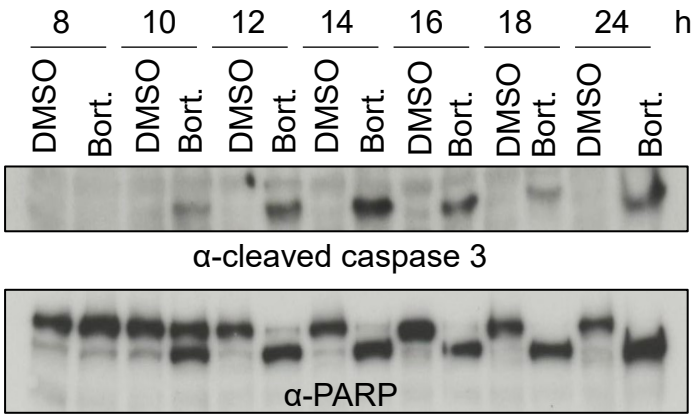


Figure 4.5. Inhibition of the CT-Like active site over the first 24 h of Bortezomib treatment.

NCI-H929 cells were treated with 10 nM Bortezomib or DMSO and samples collected and lysed at 8, 10, 12, 14, 16, 18 & 24 h after treatment. Lysate was run on SDS-PAGE gel and probed for the active/cleaved caspase 3 or for a caspase 3 substrate Poly-ADP ribose polymerase (PARP).

To further confirm that caspase activation does not lead to the decrease in proteasome activity observed, I treated NCI-H929 cells with either 10 nM Bortezomib alone or in combination with a Caspase Inhibitor Set III. The Caspase Inhibitor Set III contained Caspase-1 Inhibitor, Z-YVAD-FMK, Caspase-2 Inhibitor, Z-VDVAD-FMK, Caspase-3 Inhibitor, Z-DEVD-FMK, Caspase-5 Inhibitor, Z-WEHD-FMK, Caspase-6 Inhibitor, Z-VEID-FMK, Caspase-8 Inhibitor, Z-IETD-FMK, Caspase-9 Inhibitor, Z-LEHD-FMK, Caspase-Family Inhibitor, Z-VAD-FMK used all together each at a concentration of 4 μM. DMSO and Caspase inhibitor set controls were also set up alongside at the same concentration. Cells were harvested at 0, 2, 4, 6, 8 and 24 hours after treatment and CT-Like activity measured as stated in Method 2.8.2 and plotted against DMSO control, the activities were plotted as seen in Figure 4.6. As Inhibition of caspases using this concentration on these cells have shown full inhibition and is further backed up by the latter Figure 4.13.

There was no observable difference in the CT-Like activity in proteasomes treated with either 10 nM Bortezomib or cells treated with 10 nM Bortezomib in combination with the caspase inhibitor set. The caspase inhibitor set alone also showed no significant

difference in activity compared to DMSO showing that the inhibitor set itself did not affect the CT-Like activity recorded. This suggests that caspase activation plays no role in the continued decrease of proteasome activity observed in the first 24 hours.

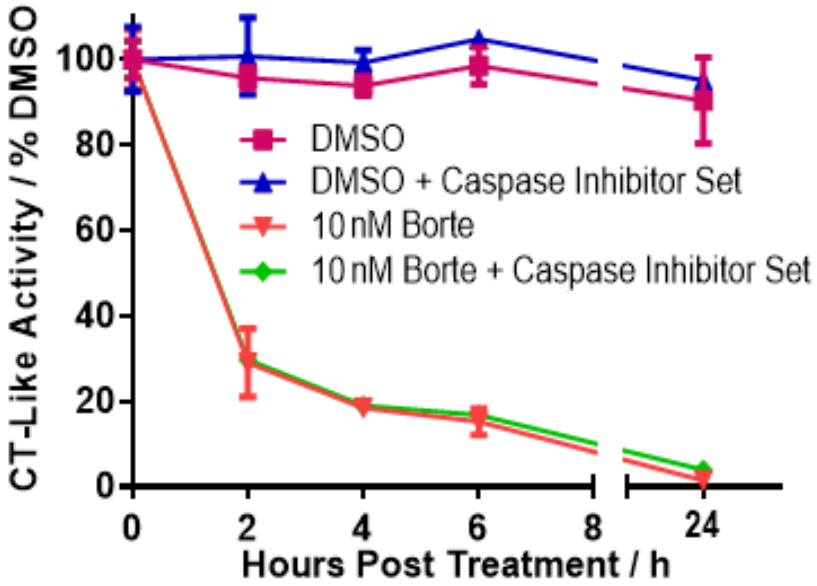


Figure 4.6. Assessing whether caspase inhibition rescues severe CT-Like inhibition in the first 24 h of Bortezomib treatment.

NCI-H929 cells were treated with either 10 nM Bortezomib or DMSO with or without addition of a broad caspase inhibitor set. CT-Like activity was measured by degradation of a fluorescent substrate Suc-LLVY-AMC at 37 °C and normalised to the DMSO control. Data represented as mean ± SEM (n = 2 per value)

To further test whether cell death responses play a role in proteasome activity shut down, NCI-H929 cells were treated with a lethal 10 nM Bortezomib dose and collected at 8, 10, 12, 14, 16, 18 and 24 hours after treatment. The cells were then stained using AnnexinV-AMC and viability dye 4',6-diamidino-2-phenylindole (DAPI) and run through a flow cytometer to read fluorescent intensities of each cell (Method 2.5.2). Cell death was measured by either AnnexinV and/or DAPI positivity whereas live cells was measured by the negativity of both markers (see gating strategy Appendix D). The percentage of live cells was then plotted as shown in Figure 4.7.

Early and late apoptosis was only shown to initiate at around 10 hours post Bortezomib treatment, showing that this was much later than the initial proteasome activity decrease and therefore is unlikely to play a role in the severe shutdown CT-Like site seen.

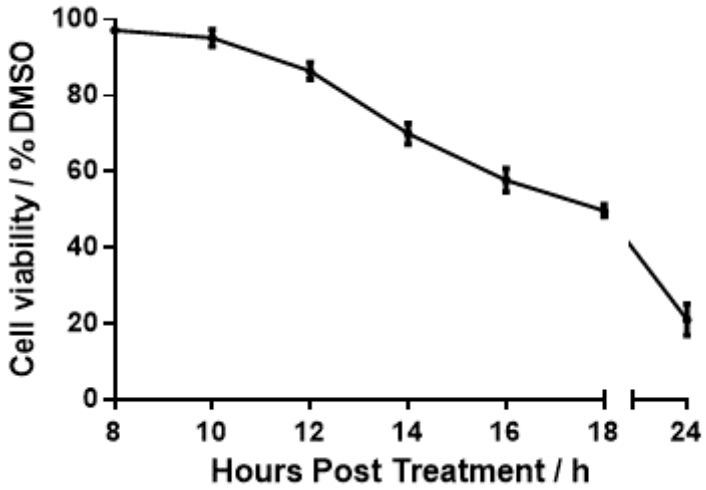


Figure 4.7. Cell viability of NCI-H929 cells upon lethal 10 nM Bortezomib challenge over time.

NCI-H929 cells were treated with 10 nM Bortezomib and collected at 8, 10, 12, 14, 16, 18 and 24. Live cells were calculated by percentage of AnnexinV/DAPI double negative cells to total cells. Points represent Mean activity ± SEM, n=2.

4.2.3. Investigation into active-site occupation over time by proteasome Inhibitors.

Another possibility for the continued decrease in CT-like activity is continued binding and inhibition of the CT-Like site by Bortezomib due to continued cell permeability or due to proteasomes slowly becoming available after degradation of a protein substrate preventing inhibition. To investigate this, a biotinylated vinyl sulfone proteasome inhibitor Ada-K(Biotin)-Ahx$_3$-L$_3$-VS (VS-Biotin), that inhibits the three active sites of the proteasome equally, was used at a 10 μM concentration (level of inhibition comparable to 10 nM Bortezomib) to treat NCI-H929 cells along with a DMSO solute control. VS-Biotin forms covalent bonds with all catalytic threonine's of the proteasome similar to Bortezomib, but without the specificity to the CT-Like active site. Cells from both treatments were collected at 0, 2, 4 and 6 hours and split to measure the CT-like activity via use of the site specific Suc-LLVY-AMC fluorescent substrate (Method 2.8.2), whilst the other half run on a SDS-PAGE gel for Western analysis. The Western was probed for the proteasome active sites being biotinylated by the VS-Biotin with use of a streptavidin conjugated to HRP as well as antibodies against the α7 proteasome core subunit and pro-caspase3 (Figure 4.8).

The activity of the VS-Biotin inhibitor treated cells was similar to that of cells treated with Bortezomib, with the CT-like activity decreasing over the first 6 hours down to around 10 %. However, occupation of the VS-Biotin inhibitor decreased over this time with the highest biotin signal observed in the two-hour treatment reducing and levelling off by 4 hours. This was however not due to reduction in proteasome particles as shown by the α7 signal that remained steady throughout the experiment. Pro-caspase 3 shows no activation of caspase by loss of signal.

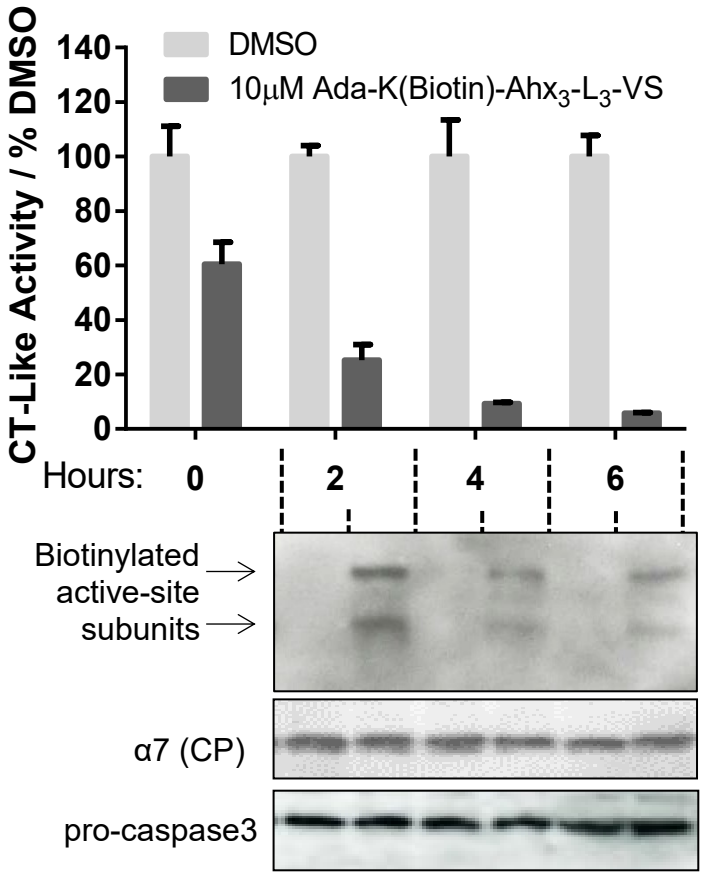


Figure 4.8. Inhibition and occupation of the CT-Like active site by a biotinylated vinyl sulfone inhibitor over the first 6 h of treatment.

NCI-H929 were treated with 10 μM Ada-K(Biotin)-Ahx_3-L_3-VS biotinylated vinyl sulfone inhibitor or DMSO control and lysed at 0, 2, 4 and 6 h post treatment. The CT-Like activity measured by fluorescent readout of Suc-LLVY-AMC cleavage and plotted as percent of DMSO control. Bars represent Mean activity ± SEM, n=2. at the same timepoints lysate was run on SDS-PAGE.

4.2.4. Investigation into whether proteasome modifications play a role in its inhibition upon PI treatment.

To investigate whether the modification of proteasome subunits that was observed in Chapter 3 could play a role in the shutdown of proteasome activity, NCI-H929 cells were treated with 0, 2, 5, 10, 20, 50 or 100 nM of Bortezomib and harvested 24 h after treatment. Lysate was then run on a CTAB-PAGE gel (Method 2.7.2) and Western blotted for proteasome subunits Rpn12, Rpt2 and β5i (Figure 4.9).

Changes to the pattern of all three proteasome subunits investigated occurred at the >5 nM Bortezomib treated cells, the lethal dose for this cell line. In all three blots the main, highest intensity, band still remained unchanged but a number of the minor species of higher MW disappeared, with appearance of medium and low molecular weight species. Again, the pattern of each western blot resembled that of Figures 3.10 and 3.11 where whole cell lysate was run, but different to the observations seen when purified proteasomes were run such as in Figure 3.6.B. As CTAB-PAGE does not have a commercial protein standard the MW of each change can't be calculated but the changes are evident on challenge on the cells with a lethal dose.

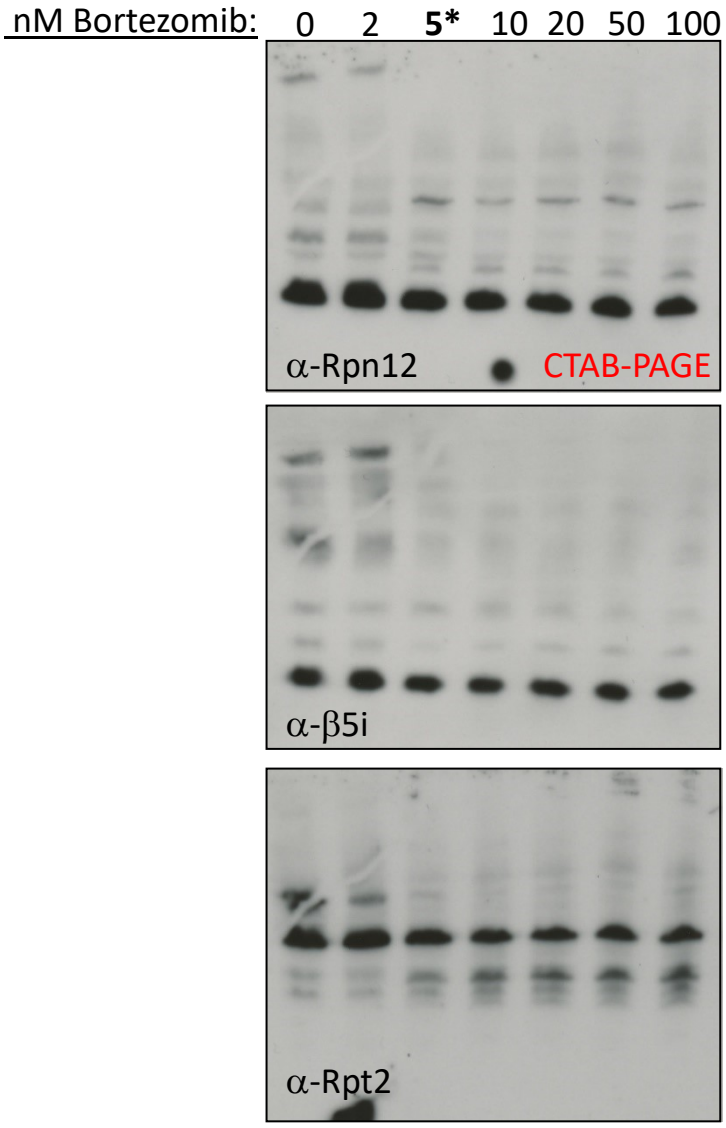


Figure 4.9. Investigation to see if Bortezomib plays a role in proteasome subunit modification changes.

NCI-H929 cells were treated with 0, 2, 5, 10, 20, 50 or 100 nM Bortezomib and lysed 24 h after treatment. Lysate was run on CTAB-PAGE and Western analysis of Rpn12, Rpt2 and β5i was carried out. The LD^{50} for the NCI-H929 cell line used is 5 nM as indicated by asterisk. Note the change of pattern of each blot in the > 5 nM samples.

To investigate if the effects of Bortezomib on changing the modification of proteasome subunits was early enough to cause the proteasome shutdown seen, a time course was set up using LD^{50} concentration of either Bortezomib or Epoxomicin.

NCI-H929 cells were treated with either 10 nM Bortezomib or 20 nM Epoxomicin and cells collected at time points 0, 1, 2, 3, 4, 5, and 6 hours for Bortezomib or 0, 1 and 2 h for Epoxomicin. Epoxomicin is another proteasome inhibitor, it inhibits the active sites of the proteasome to a similar extent to bortezomib, but utilises an epoxyketone rather than a boronic acid to for covalent links with the catalytic threonine's residing in the active site. Cells were lysed in CTAB-RIPA buffer and lysate run on CTAB-PAGE electrophoresis system (Method 2.7.2). Both gels were transferred to PVDF membrane and probed for the Rpn12 regulatory subunit of the proteasome (Figure 4.10), that had shown to be the most extensively modified in Chapter 3.

In both blots banding pattern was again similar to the other Rpt12 blots from whole cell lysate e.g. Figure 4.9. The an appearance of a mid-weight band (black arrow) was visible in the early hours of treatment at 3 hours for Bortezomib and 2 hours after Epoxomicin treatment shown by black arrow. Bortezomib treated cells also showed the disappearance of a high molecular weight band from 3 hours onwards, shown by red arrow. This was the earliest observable change that could coincide with the severe shutdown of proteasomes investigated this chapter.

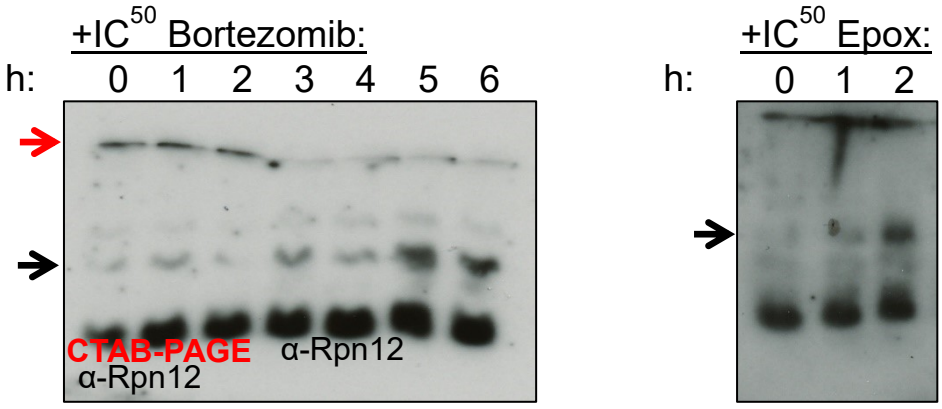


Figure 4.10. Changes in modified Rpn12 subunits in the early hours after Proteasome inhibition.

NCI-H929 cells were treated with a lethal dose of the proteasome inhibitors Bortezomib (5 nM) or Epoxomicin (10 nM). Cells were then lysed at 0, 1, 2, 3, 4, 5, and 6 h after Bortezomib treatment or 0, 1 and 2 h after Epoxomicin and run on CTAB-PAGE. Rpn12 Western analysis was carried out. Black arrow corresponds to appearance of medium MW Rpn12 signal and red arrow the disappearance of high MW Rpn12 signal.

To test whether the appearance of this medium molecular weight and disappearance of the higher molecular weight band was a true phenotype upon Bortezomib treatment, NCI-H929 cells were treated with either 10 nM Bortezomib, 20 mM Epigallocatechin gallate (EGCG), a combination of both or treated with a DMSO solute control. Cells were harvested for 24 hours after treatment, lysed, and ran on CTAB-PAGE before Western analysis of Rpn12 proteasome sub unit Figure 4.11. EGCG is known to counteract the effects of Bortezomib by reacting with Bortezomibs boronic acid group. Again the appearance of a medium MW band (black arrow) and disappearance of a high MW band (red arrow) was seen in the Bortezomib only lane and negated in the lane treated with both EGCG and Bortezomib indicating that these are true Bortezomib effects. However, there was a disappearance of a third band upon bortezomib treatment that was prevented by the co treatment of ECGC. This could be due to a bortezomib independent process, and potentially caspase cleavage.

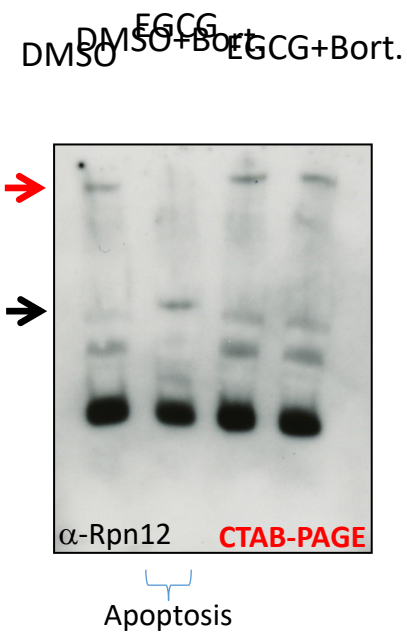


Figure 4.11. Bortezomib mediated changes to Rpn12 are prevented by addition of EGCG.

NCI-H929 cells were treated with a lethal dose of the proteasome inhibitor Bortezomib (5 nM) for 24 h with or without the addition of 20 mM EGCG. Singularly treated DMSO and EGCG lanes act as controls. Cells were then lysed and run on CTAB-PAGE. Rpn12 Western analysis was carried out. Note the Bortezomib mediated changes in lane two are prevented upon co-treatment with EGCG lane four.

To further test proteasome inhibitors' ability to cause changes to the pattern of proteasome subunits resolved by CTAB-PAGE protein electrophoresis I tested the effect of Epoxomicin and VS-Biotin inhibitors effect on the pattern in modified species resolved by CTAB-PAGE. NCI-H929 cells were treated with either 0, 0.31, 1.25, 5 or 20 nM Epoxomicin with or without the addition of 20 mM EGCG. A second experiment was set up with 0, 0.01, 0.1, 1, and 10 μM VS-Biotin inhibitor also with or without the addition of 20 mM ECGC. All cells were harvested after 24 hours of treatment, lysed, and run on CTAB-PAGE. The Epoxomicin Western was probed for Rpn12 subunit (Figure 4.12.i & 4.12.ii) whilst the VS-Biotin inhibitor Western was additionally probed

with a streptavidin-HRP antibody and an antibody against the β5i proteasome catalytic subunit (Figure 4.12.ii).

Only upon a lethal concentration of Epoxomicin and VS-Biotin inhibitors did an observable change in the pattern of Rpn12 and β5i occur. The streptavidin-HRP again showed binding of the VS-Biotin inhibitor to the catalytic active sites of the proteasome in a dose dependent manner. The addition of EGCG that ablated Bortezomib activity had no effect on these two inhibitors suggesting that the changes are not specific to Bortezomib and unlikely to be off target due to the different chemistries of the different inhibitors.

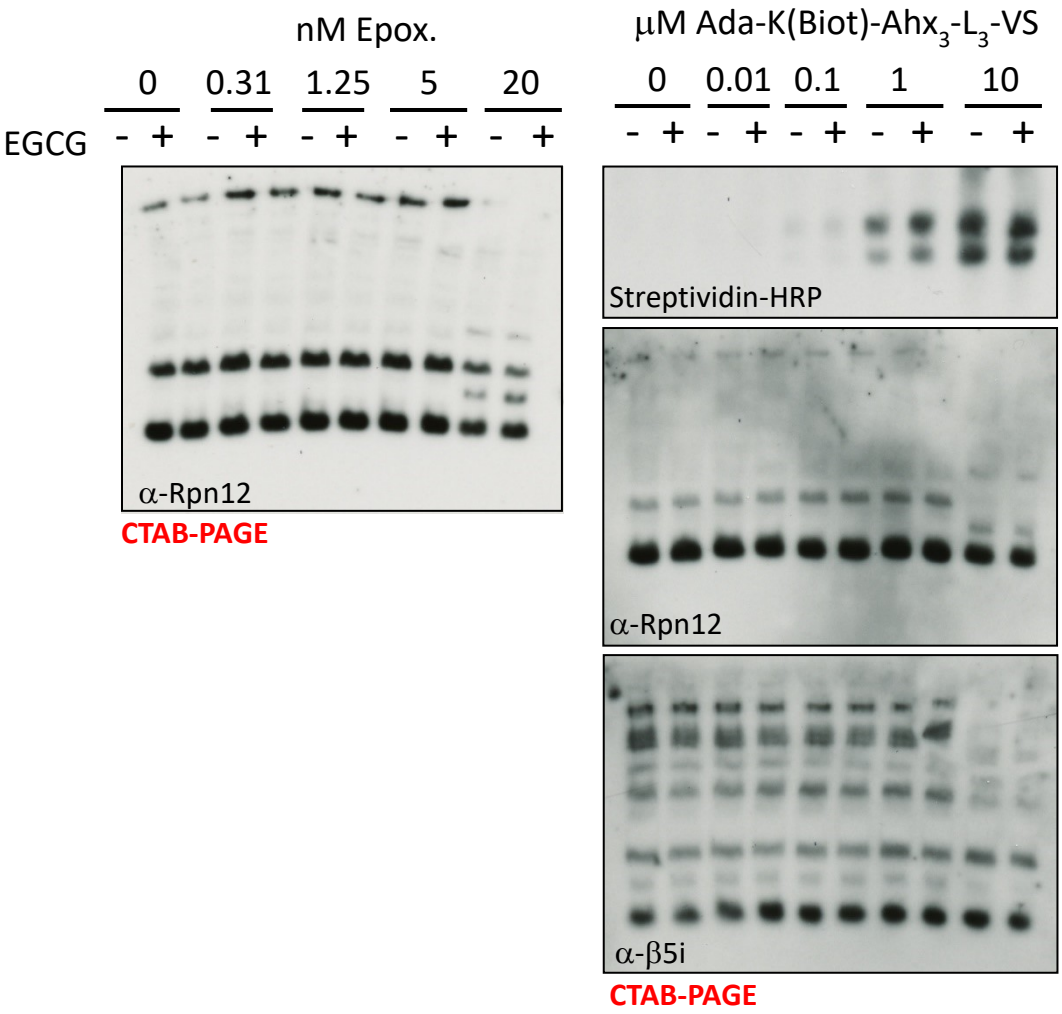


Figure 4.12. EGCG has no effect on proteasome inhibitor mediated changes.

NCI-H929 cells were treated with a varied dose of the proteasome inhibitor Epoxomicin or Ada-K(Biot)-Ahx3-L3-VS with or without the addition of 20 mM EGCG for 24 h. Cells were then lysed and run on CTAB-PAGE. Rpn12 Western analysis was carried out. Note that co-treatment with ECGC does not prevent the changes seen with Epox and VS-Biotin.

To investigate if cleavage of proteasome subunits by caspase was cause for the pattern change of a number of proteasome subunits seen on CTAB-PAGE on addition of a lethal Bortezomib challenge, NCI-H929 cells were treated with either 10 nM Bortezomib, 4 μM of each caspase inhibitor from Caspase inhibitor set III or a combination of both alongside DMSO solute control. After 24 hours of treatment cells were then lysed and run on CTAB-PAGE gel before Western analysis with Rpn10, Rpn12, Rpt2 or β5i antibodies Figure 4.13.

The pattern seen in each of the four westerns against proteasome subunits changed from the DMSO control lane to the lanes treated with bortezomib. The bortezomib treated lane showed many bands appear and disappear in comparison to the control lane. However, when one compares this to the lane treated with both bortezomib and caspase family inhibitor set there are less changes suggesting that the caspase family inhibitor set was able to prevent some changes through its action of caspase inhibition. Indeed the lane treated with the caspase inhibitor set only did not show any changes in comparison to the DMSO control, confirming that the caspase inhibitor set had no effect on proteasomes on its own. All of this taken together suggests that there are a number of changes contributed to bortezomib treatment (red arrows), however some of these changes are indeed due to caspase activation (black arrows). The caspase inhibitor set however does not prevent apoptosis activation and therefore bortezomib changes could still be explained by other proteolysis mechanisms such as autophagy.

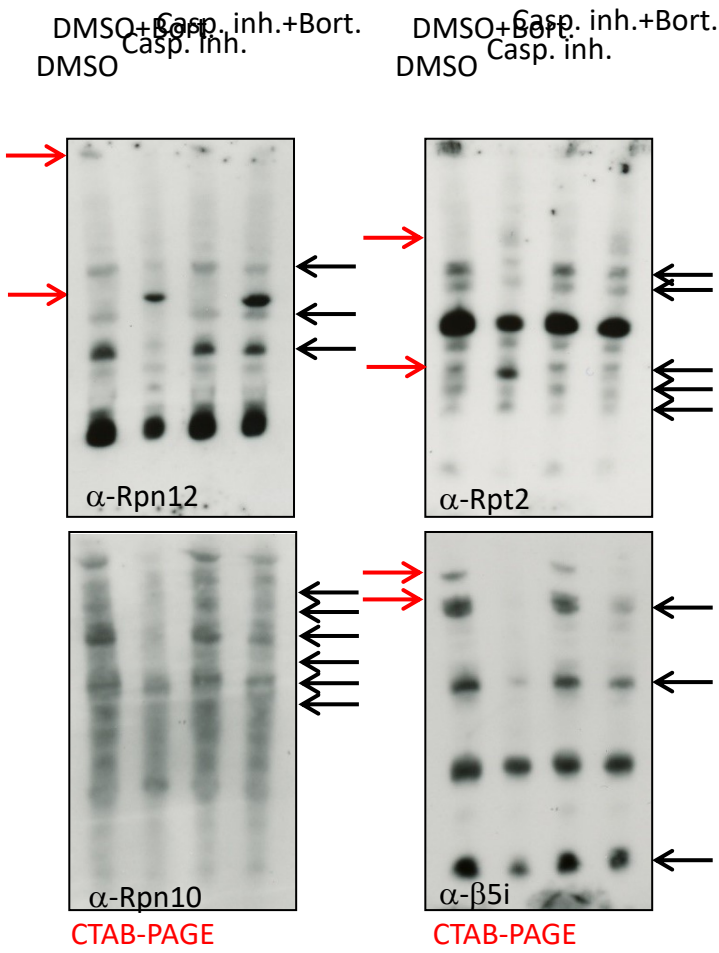


Figure 4.13. Deciphering the changes to proteasome subunits caused by Bortezomib or intracellular caspase activation.

NCI-H929 cells were treated with 10 nM Bortezomib alone or in combination with 4 μM of each caspase inhibitor from Caspase Inhibitor Set III (Enzo). DMSO solute and caspase inhibitor controls were also setup and run alongside. After 24 h the cells were lysed and run on CTAB-PAGE. Western analysis was carried out on Rpn12, Rpt2, Rpn10 and β5i. Red arrow correspond to Bortezomib mediated changes whilst black arrows correspond to the changes from caspase activity.

In the previous chapter it was found that the modification of proteasome subunits was mostly restricted to the nucleus of the cell. To investigate if Bortezomib treatment had any effect on the localisation of modified proteasomes subunits a capture of His^6-2(StrepIITag)-TeV-Rpn11 tagged proteasomes were purified from fractionated treated OPM2 cells. OPM2 cells over expressing a Rpn11 tag subunit (Method 2.9.1) cells were treated with 10 nM Bortezomib or DMSO solute control for 24 hours before being fractionated using a detergent cytosolic lysis technique before subsequent high salt nuclear extraction (Method 2.4.5), and then subsequent purification by Ni^{++}NTA pulldown to enable analysis by SDS-PAGE. The fractions from the control and Bortezomib treated cells was then run on an SDS-PAGE gel. Western analysis was then carried out using Rpn11, Rpn10, Rpt4, Rpt5, Rpt2 and β5i antibodies.

Just as in chapter 3 enrichment by this capture technique allowed for resolution of modified subunits by SDS-PAGE. It was observed in all the Westerns analysed the majority of modified subunits occurred in the nuclear fraction. Although it was seen that the intensity of these subunits or particular modified species changed on the addition of Bortezomib. For Rpn11 and β5i modified species normally located in the nucleus were also find in the cytoplasm of Bortezomib treated samples.

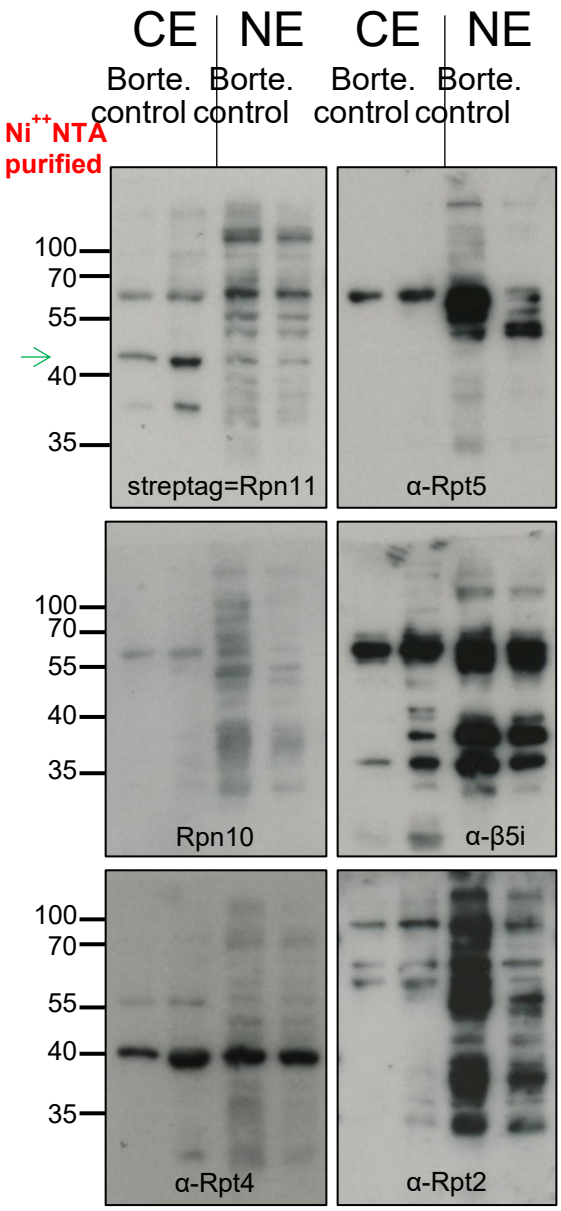


Figure 4.14. Affinity purification of proteasomes using incorporated His^6 tagged RPN11 from cytosolic and nuclear lysate of H929 cells treated with/without 10 nM Bortezomib.

NCI-H929 cells were treated with a lethal dose of 5 nM Bortezomib or DMSO solute control after which the cells were fractionated using a detergent cytosolic lysis technique before a high salt nuclear extraction. Nickel resin was used to capture the His^6 tagged Rpn11 subunit. Western analysis was carried out on Rpn11 (through strep tag), Rpn10, Rpt4, Rpt5, Rpt2 and β5i subunits. CE= Cytosolic Extract, NE= Nuclear Extract

4.3. Discussion

The findings detailed in this chapter have revealed important abnormalities in the current literature on how Bortezomib acts within cells. Agents such as Bortezomib work by the difference of drug sensitivity of target cells, such as myeloma, compared to other non-malignant cells in the body. The proteolytic function of the proteasome is fundamental to the degradation of intracellular proteins and its inhibition is toxic to all cell types.

As discussed in the introduction chapter the mechanism by which Bortezomib kills cells such as myeloma has been much disputed. Rationales for this, such as NF-κB pathway that relies on the degradation of IκBα by the proteasome has now been disproven as a mechanism for its toxicity (Hideshima et al., 2009). The prevailing theory is that the higher workload of protein production and degradation within myeloma cells puts strain on the proteasome that even a modest inhibition of would be lethal (Bianchi et al., 2009).

As Bortezomib requires about 24 h incubation to cause cell death in Myeloma cells relatively little had been done at the earlier stages of inhibition, and when investigations had been done very few timepoints had been looked at. To investigate myelomas sensitivity to Bortezomib further I first decided to go back to basics and look at the rate of inhibition of the CT-Like active site of the proteasome upon Bortezomib treatment over the first 24 h concentrating mainly on the first 10 h post treatment. When comparing multiple cell lines, it was evident that this inhibition of the CT-Like site was one that followed a similar kinetic profile over the first four hours of treatment. After this point Bortezomib insensitive cells CT-Like activity levelled off with around 20 % remaining, whilst the Myeloma cell lines RPMI-8226 and NCI-H929 CT-Like activity continued to reduce for a further 6 hours to near full inhibition. This suggests that the sensitivity of myeloma cells to Bortezomib over that of other cells may not just be due to a small free level of proteasome inhibition, but due to a different response to Bortezomib causing severe shutdown of CT-Like activity.

From treating various myeloma cell lines with Bortezomib and looking at CT-Like inhibition as well as accumulation of ubiquitinated proteins it suggested that myeloma cell lines have a greater free capacity than suggested by Bianchi et al., 2009. Accumulation of ubiquitin conjugates, showing insufficient proteasome activity, only

exceeded the control treated cells at 8 h where the level of CT-Like activity was lower than 20 %. This was the same level at which the CT-Like activity of insensitive cells levelled off and remained above. Interestingly measurement of proteasome inhibition of peripheral blood cells also shows that these cells only show an 80 % reduction of CT-Like activity upon intravenous (IV) treatment at doses lethal to myeloma cells. This lead to an interesting question as to why myeloma cells act differently upon Bortezomib treatment, and what the cause of this continued inhibition above that of Bortezomib treatment in other cell types. Visualisation of ubiquitin conjugates by Western analysis is a standard method to show when the load on the proteasome outweighs that of the capacity of the proteasome and is used by many others in the field (Haglund et al., 2014; Kessler et al., 2001). Recently over expression of GFP tagged ubiquitin, has allowed for the quantification of ubiquitin conjugates accumulation via flow cytometry (Masucci et al., 2000).

If myeloma cells were to have such different levels of inhibition due to cellular processes, disrupting these before treatment would allow for one to measure the true direct effects of Bortezomib from binding. Upon looking at inhibition of CT-Like activity in NCI-H929 myeloma cells lysed prior to treatment it was evident that the level of inhibition was substantially different to that of proteasome inhibition within cells reaching only 10 % compared to complete inhibition seen within cells. As expected the maximum level of inhibition was reached quickly as there were no cellular membranes to be crossed. Additional analysis of treatment of proteasomes enriched from other cellular components appeared similar, with yeast proteasomes obtain only a 15-20 % reduction. However, proteasomes purified from human cells showed a greater level of inhibition of around 60 % at 4 hours before levelling off. Although this time dependant inhibition of purified human proteasomes was higher than expected compared to the human lysate treated proteasomes and yeast purified proteasomes this was most likely partly due to the stability of human purified proteasomes when incubated 30 °C. The raw data did show a decrease in activity of both Bortezomib and DMSO treated proteasomes at a level much greater level than that of the yeast treated proteasomes, most probably due to the unstable nature of human proteasomes. Although a titration of Bortezomib was not carried out on purified proteasomes it is common knowledge within our lab that to fully inhibit the CT-Like activity of the proteasome to measure aspecific protease activity a concentration of around 20 μM is required around 2,000

times that needed to fully inhibit the same activity within cells. Although a different organism, from a different kingdom, yeast has widely been used as a model for proteasome biology. Proteasomes are relatively homologous between these two organisms and the core particle subunits share a great level of homology. It has always been a question as to why inhibition of proteasomes within *S. cerevisiae* has been so difficult to achieve with concentrations of 100,000 times that of human dosage being needed. Even with the knockout of efflux drug pumps Bortezomib concentrations of around 125 μM are required to kill these cells (Fleming et al., 2002). The data strongly suggests that there are is more at play than just simple diffusion and active site binding by Bortezomib and secondary mechanisms maybe amplifying these changes seen in human cells, with myeloma cells hyper sensitive to these changes.

Caspase activation has been shown to contribute to the shutdown of proteasome activity upon cell death activation (Adrain, Creagh, Cullen, & Martin, 2004; Sun et al., 2004). This was found to be restricted to the regulatory particle subunits Rpn2, Rpn10 and Rpt5 with the core particle showing no cleaved products upon cell death. These cleavage events of the RP further perturbs cellular processes and causes cataclysmic events that further drive apoptosis to completion. Most of these events were mediated by caspase 3 with lesser effects by caspase 9 and caspase 7 as shown by individual caspase inhibitors' prevention of cleavage products.

In this chapter I investigated whether these known cleavage events that inhibit the proteasome could play a role in the inhibition of the CT-Like activity observed in the first 10 hours of treatment. Looking at cleaved caspase 3 (the active form of this caspase and executioner of apoptosis) as well as cleaved Poly-ADP-Ribose Polymerase a substrate of caspase 3 it was evident that caspase 3 activation occurred at 10 hours after Bortezomib treatment shown by the appearance of both cleaved proteins. Further analysis of caspase effects on proteasome activity was shown again to have no effect. A Caspase inhibitor set that inhibited Caspase 1, 2, 3, 5, 6, 8, 9, as well as an inhibitor of the broad family of Caspases, showed no recovery of proteasome inhibition by Bortezomib. This showed no recovery in the shutdown of the Proteasome overserved compared to cells treated with Bortezomib alone. This confirms what was stated in Adrain et al., 2004; Sun et al., 2004 that caspase mediated inhibition of the proteasome is a late event seen upon apoptosis initiation and therefore although caspases may play a role in the shutdown of proteasomes in the later stages

of apoptosis it does not explain the shutdown of CT-Like activity in the first 10 hours post treatment. The percentage of dead cells upon Bortezomib treatment as measured by the positivity of AnnexinV and/or DAPI also showed that this was in fact the case and that caspase activation coincided with the first reduction in percentage of live cells at 10 h.

Work done by (Clemens et al., 2015) showed that Bortezomib concentration within cells exceeds that of the media surrounding it and there is active transport of the drug over the cellular membrane by the anion-transporting polypeptide 1B1. Although I showed in experiments that the maximum inhibition of that concentration of Bortezomib in lysate or purified is fast and reached within 2 hours in lysate or purified proteasomes, this recent finding could explain why the activity continues to fall within cells. Although lacking the facility to directly measure intra and extracellular concentration of Bortezomib, I came up with a novel way of investigating the problem by looking at relative levels of active site occupation of biotinylated VS-Biotin inhibitor. After finding a concentration that resulted in a similar level of CT-Like inhibition to that of 10 nM Bortezomib treatment, I looked at the inhibition of the CT-Like site by VS-Biotin as well as doing Western analysis on the same cells. The occupation of the catalytic subunits was shown by the signal from a Streptavidin-HRP probed Western that directly measures biotinylation of the active sites by covalent binding of the VS-Biotin proteasome inhibitor. The decrease in signal of biotinylated active sites, from its maximum at 2 hours, showed that for this inhibitor there is no additional binding after its maximum at two hours, even though the inhibition of CT-Like activity continued to decrease after this time. The level of maximum inhibition of proteasomes by VS-Biotin in cells correlates with the maximum level of inhibition seen on purified yeast proteasomes and cell lysate treated with Bortezomib and is further evidence that proteasome shutdown past 2 h post treatment is due to a secondary mechanism and not that of direct proteasome inhibitor binding. Western analysis of the α7 subunit of the proteasome also ruled out decrease in activity from a reduction in the number of proteasome particles. This also suggests that Bortezomib and other proteasome inhibitors follow the fashion as VS-Biotin with a minimal level of direct inhibition followed by secondary mechanism of proteasome inhibition.

From work done in the previous chapter and published in Pitcher et al. 2014; Pitcher et al. 2015, it was shown that the subunits of the proteasome, especially that of the

regulatory particle is heavily modified by a still uncharacterised charged polymer modification. This was only resolvable utilising the protein electrophoresis system CTAB-PAGE or visible via normal SDS-PAGE technique upon enrichment of the proteasome away from other cellular components. In this chapter it was shown that upon a lethal Bortezomib concentration the pattern of a number of proteasome subunits on CTAB-PAGE changed and this was linked to the LD^{50} of the cell line with concentration lower showing that of the control. I also show that upon a lethal dose of Bortezomib and Epoxomicin there are changes in the CTAB-PAGE resolvable modifications of at least Rpn12, although others were not tested, at around 2 hours after treatment. This is the earliest change that has been observed upon proteasome inhibition, earlier than the accumulation of ubiquitinated protein at 8 hours post treatment and correlates with the maximum level of active site occupation shown by VS-Biotin at 2 hours. Although still unproven the changes observed could explain the continued shut down of proteasome activity after the maximum level of proteasome inhibitor binding at observed at the same time. How these modifications could inhibit the proteasome further is still unknown, although the modification could affect many attributes of proteasome biology such as preventing binding of activators, changing the kinetics of proteolysis by conformational changes to the active sites, disassembly of the complex or RP to CP etc. this however is not due to reduction in proteasome particles as shown by α7 Western analysis.

Previous research done by Golden et al. 2009 showed that the polyphenol EGCG reacts with the boronic acid group of Bortezomib which is essential for the covalent binding and inhibition of the CT-Like active site. Upon treating cells with a lethal Bortezomib dose or in combination with EGCG it was apparent that the boronic acid residue of Bortezomib is required for the apparent changes in modification of the Rpn12 subunit suggesting it is direct proteasome inhibition that causes these secondary changes rather than off target effects from a different part of the bortezomib molecule. This would also make sense as Epoxomicin, which has a different chemistry to Bortezomib, also shows these changes upon treatment. A treatment of cells with Epoxomicin or VS-Biotin again showed changes to the Rpn12 and β5i sub units upon a lethal dose and were unaffected by the addition of EGCG showing that EGCG reactivity is specific to Bortezomib and that all proteasome inhibitors effect modifications upon the proteasome itself.

Although these modification changes were shown to occur at 2 hours after treatment and before the onset of caspase 3 I tested to see whether any of these changes could be attributed to caspase and not that of Bortezomib. It was shown that upon treatment with Bortezomib a number of changes occurred in the Rpn12, Rpt2, Rpn10, and β5i subunits. With cells treated with the same caspase inhibitor set as before it was noted that some of these changes were due to caspase cleavage, in the later hours, but on Rpn12, Rpt2 and β5i there were a number of Bortezomib only mediated changes. This further confirms the Bortezomib plays a role in the regulation of the modification of Proteasomes. Kleijnen et al. 2007 published that occupation of the catalytic sub units by Bortezomib induces a conformational change in the proteasome that stabilises the RP-CP interaction. Modification of the Proteasome could be down to this conformational change allowing access to residues on the proteasomes normally hidden from modifying enzymes during the normal proteolysis process of the proteasome. There is a possibility that modification may be due to activation of a modification pathway due to build-up of regulatory proteins normally degraded by the proteasome, although due to the fact that the accumulation of Ubiquitinated proteins occurred at 8 hours and the changes to the modification of proteasome sub units, at least Rpn12, occurred at 2 hours makes it unlikely. The fact that multiple Proteasome inhibitors of different chemistries caused these changes in proteasome sub units also makes it unlikely that it is due to off target effects of these drugs.

4.3.1. Proposed mechanism of proteasome inhibition

From the results presented in this chapter I now propose a new mechanism of action of Bortezomib on myeloma cells depicted in Figure 4.15. Prior to Bortezomib treatment proteasomes are ordered with those that are extensively modified residing in the nucleus of the cell. The demand for degradation (light blue shading) of ubiquitinated proteins is around 20 % with plenty of free activity. When an IC^{50} concentration of Bortezomib is administered, it enters the cell and occupies a small number of CT-Like active sites (shown by red stars) reducing its activity and the CT-Like activity falls by around 10 – 20 %. At around 2 hours after treatment, modification of the proteasome occurs through a currently unknown mechanism. At some point within the next eight hours misregulation of proteasomes also happens and some nuclear proteasomes

translocated to the cytoplasm. Whether this is due to cell cycle arrest in as of yet unclear. The proteasome activity continues to decrease as proteasomes are modified further until around 10 hours post treatment when the proteasome capacity reduces to levels lower than required for normal degradation of ubiquitinated proteasomes. At this point caspase's especially caspase 3 causes irreversible cleavage of the proteasome and cell death is inevitable.

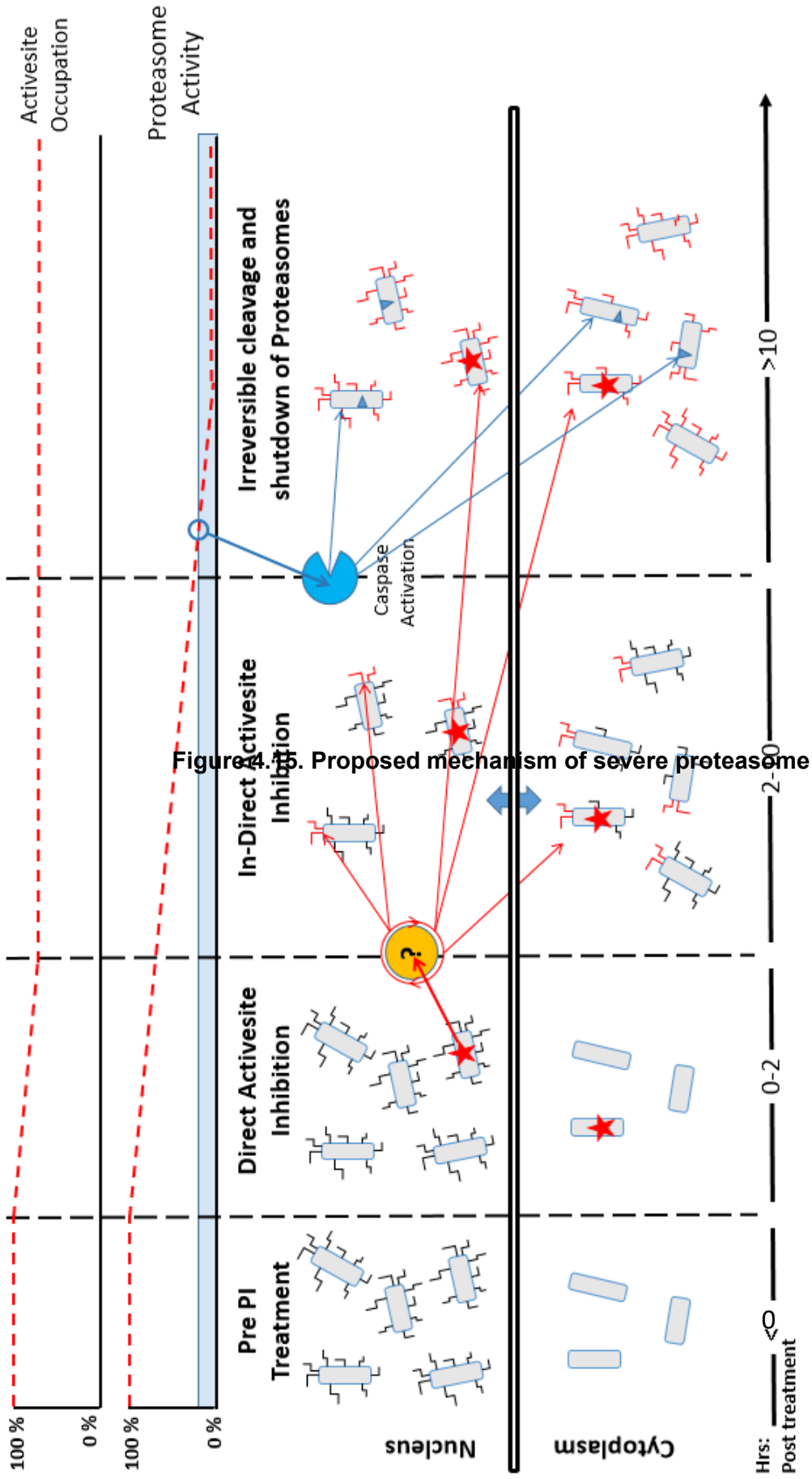


Figure 4.15. Proposed mechanism of severe proteasome inhibition upon treatment w

4.4. Future Work

This intriguing new model of action by proteasome inhibitors such as Bortezomib opens up a whole avenue of additional questions. Firstly, work needs to be done to fully understand what these modifications are and which enzymes are responsible in its production and addition to proteasome subunits. Mass-spec has been challenging in the discovery of charged modifications, there is potential that a top down approach using LC-MS could yield better results. If the modification isn't detectable then fragments missing in the detection would narrow down the amino acids that might harbour the modification and could be narrowed down and confirmed by mutagenesis. Finding the exact nature of the modifications would require either chemical analysis of the modifications. Cells treated with radio labelled compounds such as [γ-^{32}P] ATP, [32P] NAD, [C^{14}] D-Glucose etc. could yield radiolabelled proteasome subunits, allowing for narrowing down of the chemistry of the modification. Due to the rapid kinetics of most enzymes there is little possibility that affinity purification of proteasomes may pulldown enzymes involved in these changes.. One major obstacle is that the modifications observed presented as one pattern when run as total cell lysate and a separate pattern when the proteasomes were purified away from other cellular components. Further work is needed to understand what this cause is and to better standardise the method of PAGE techniques for proteasome subunit western analysis.

As multiple myeloma cells are so sensitive to proteasome inhibitors it is reasonable to hypothesise that the modification of proteasomes within these cells is hyper-activated and further work is needed to look at the appearance of these modifications in other cell lines insensitive to Bortezomib and whether there are differences in the level, onset and persistence of these modification compared to that of Myeloma cells. As Bortezomib is not a curative agent and resistance to the therapy occurs in greater than 98 % of patients it would be interesting to observe whether these changes are still apparent in samples taken from patients with relapsing MM. Although some drug resistance has been shown to be due to mutations in the act of site of the proteasome this is rarely the case in patients and therefore it is essential to investigate whether resistance occurs due to changes in the modifications outlined in this and the previous chapter.

CHAPTER 5 - Development of Allosteric proteasome inhibitors.

Chapter 5: Development of Allosteric proteasome inhibitors.

5.1 Introduction

Novel therapeutics can be discovered via two main methods, blind drug discovery or targeted approaches. Blind drug discovery, such as high throughput screening, utilises a library of pre-synthesised compounds. Each compound is either used in binding assays against a particular target enzyme or against a particular cell line or cancer. Targeted approaches take known substrates or binding partners of a protein of interest and modify them to still allow for binding but to interfere with the normal function of that enzyme in the cell. The proteasome has many binding partners as described in Chapter 1 although currently no therapies target the proteasome by allosteric inhibition. Inhibitors such as bortezomib work by having a peptide like back bone that mimics the CT-Like substrate allowing for specificity, and a boronic acid group that causes covalent bonding to the catalytic threonine of the active site.

In our lab a phage display technique was utilised to identify forty seven peptides of seven amino acid in length that were able to bind to human and/or yeast proteasomes that were complexed with a number of different molecules such as ATP, ADP and/or bortezomib. The process to take these peptide sequences to stable and targeted therapeutics that could interfere with proteasome biology in the cell causing lethality in myeloma is long and complex. A number of processes have to be overcome before this new drug can be marketed. Firstly, although the peptide sequences were found by binding to proteasomes, this needed to be further confirmed in pulldowns utilising the peptide and, more importantly, the effect on proteasome biology had to be measured. Due to the nature of the phage display library utilising phage viruses much larger than the proteasome core it was known that these peptides bound to the outside of the proteasome and therefore would not directly interfere with the proteolytic active sites. The proteasome is a complex piece of cellular machinery that does not just carry out proteolysis of proteins but also is thought to partake in gene transcription in the nucleus. These and other functions may be perturbed by direct binding of peptides to the outside of the proteasome that compete with normal binding partners.

Conformational changes from the allosteric binding of peptides could also change the kinetics of the proteasome, it has been shown that during proteolysis of a protein the proteasome undergoes two structural confirmations that alternate and is thought to help translocate the protein through the proteolytic core (Matyskiela et al., 2013). Bortezomib binding to the CT-like active site has also been shown to lock the proteasome in a single conformational position (Maurits F Kleijnen et al., 2007), this could also explain why even though 4 out of 6 active sites are still available the proteasome activity is perturbed far greater than expected (Kisselev et al., 2006). Other binding partners such as PA28, PA200 and PA700, are shown to directly modulate the activity of the proteasome via binding to its outer surface. This further suggests that allosteric drug binding to the proteasome could be a potential mechanism of proteasome inhibition. Others have identified small peptides that inhibit the proteasome both in vitro and in vivo, although none have been developed therapies. The peptide PR-39 was discovered in the intestine of pigs and was first identified to have antibacterial properties. Later it was shown to bind to the α7 subunit of the core particle inhibiting the proteolytic activity of the 20S proteasome allosterically as well as disrupting the proper engagement of the core and regulatory particles (Maria Gaczynska et al., 2003). Another identified allosteric proteasome inhibitor is 5-amino-8-hydroxyquino-line. It was shown by NMR to bind to the inner core in a non-competitive manor again to the α7 subunit (X. Li et al., 2010). Because of the nature of allosteric inhibitors, and their target not being the proteolytic active sites, there is great possibility of them being used synergistically or after resistance has developed from Bortezomib treatment. In fact 5-amino-8-hydroxyquino-line has been proven to overcome resistance to Bortezomib in cultured cell lines (X. Li et al., 2010).

Once the binding of the peptides has been confirmed and its effect on proteasomes through readouts of proteasome activity via site specific fluorogenic substrates or poly-ubiquitin substrate degradation, the optimisation of the peptide can be carried out. The main obstacles to overcome in drug development are stability, cell permeability, minimising off target effects, potency, toxicity and excretion. Each optimisation is a balance between ensuring that the promotion of one factor is not to the detriment of another.

As overviewed in Peptidomimetics in Organic and Medicinal Chemistry (Guarna et al., 2014) the normal procedure of optimisation starts with size reduction of the peptide in

question. Multiple variants are created with the loss of one or more amino acids from the C and N termini and their function assessed. The smallest variant that retains the function of the original molecule is then taken forward for further optimisation. The next step is to find the key amino acids within the peptide that imply its required activity. This is done by a process called alanine scanning where each amino acid is substituted for an alanine and each variant tested. Due to alanine not having any side chains, and being the simplest amino acid, the loss of function of a derivative confirms that the amino acid substituted by alanine is essential to its function. Next, D-amino acid scanning is carried out. This shift of configuration results in a different arrangement of side chains giving insight into the bioactive conformations as well as increasing stability through prevention of amino acid cleavage by L-amino specific proteases. Next, derivatives are created with N-methylation of each amide bond; this is done for multiple reasons. Firstly, it identifies which amino acid acts as a hydrogen bonding donor when interacting with its target enzyme such receptor. Secondly, the creation of this tertiary amide bond helps create rigidity in the backbone of the peptide preventing cis/trans equilibrium. Lastly, demethylation of the amide bond also helps in stability to proteolytic cleavage of the amide bond. The information from these changes allow for identification of which amino acids are essential so that unessential amino acids can be changed to screen for increases in potency and cell permeability.

Although not carried out during this thesis due to time restraints the next steps would be to take the peptidomimetic variants to look for off-target binding using immobilised peptides to capture binding partners, followed by: mass spectroscopy, specificity of the compound for killing myeloma cells over non-cancerous cells, toxicity of the compound in vivo, and finally to look at modes of excretion, half life and dosing.

In this chapter I carry on the research into developing a novel allosteric proteasome inhibitor. Work done prior to my commencement by Dr R. Babb had found a number of seven amino acid peptides that bound to the proteasome by using a phage display technique. Further work by Mr K Tzortzis carried out the first analysis on what the minimum core sequence would be to achieve inhibition of proteasomes ability to degrade ubiquitinated substrate. I carried on this work by testing a number of increasingly peptidomimetic variants of this starting peptide on its ability of kill myeloma cell lines. A number of changes were found to be beneficial to the toxicity of myeloma cells or the inhibition of purified proteasome and the potency of the drug was

reduced fourfold over three rounds of optimisation. It was also shown that the optimised compound may have a preference to actively dividing cells.

Peptide sequences have been anonymised due to the ongoing optimisation and development of these compounds.

5.2. Identification of proteasome binding peptides

Work done by past lab member Dr Rebbecca Babb utilised a phage display library to find peptides that bound to the outside of the proteasome. In brief proteasomes were purified from *S. cerevisiae*, expressing Rpn11-Tev-ProteinA tag, utilising an IgG loaded resin and then cleaved off using tobacco etch virus protease. Human proteasomes were purified from HeLa cells using the UBL domain of hPLIC2/ubiquilin2. The proteasomes were then treated with ADP, ADP+ATP or ADP+Bortezomib and bound to plates ready for phage capture. A pre-compiled M13 phage display library (Ph.D.™-7 Phage Display Peptide Library, NEB) that contained 10^9 variations of the seven amino acid terminus of the minor coat protein P3 phage protein was then precleared with either resin or treated proteasomes and the remaining phage virus' added to the captured treated proteasomes. Unbound particles were removed by washing before the bound particles eluted. The eluted particles were then added to plated *E. coli*, before the viral plaques picked and genome sequencing to identify the phage peptide. The number of times the phage was found was also recorded and a table was created showing the most promising peptides and the conditions they were found in Table 5.1. Note that peptide 12 and 15 was found in multiple conditions. Other peptides showed a similar conserved sequence.

Proteasome Envelope-interacting peptide screen		
Source of proteasome:	Yeast *S. cerevisiae (Rpn11-TeV tagged)*	Homo sapiens (HeLa lysate)
Experimental conditions	**Peptides identified, number of times found**	
Preclear resin **Binding: proteasome+ADP**	Peptide 1 19x Peptide 2 13x Peptide 3 10x Peptide 4 5x Peptide 5 3x Peptide 6 3x Peptide 7 2x Peptide 8 2x Peptide 9 2x Peptide 10 2x	Peptide 17 6x Peptide 15 5x Peptide 18 2x Peptide 12 2x Peptide 19 3x Peptide 20 2x
Preclear: proteasome+ADP **Binding: proteasome/ADP+ATP**	Peptide 11 2x Peptide 12 2x Peptide 13 2x	Peptide 21 2x Peptide 22 2x Peptide 23 2x
Preclear: proteasome/ADP **Binding:** **proteasome/ADP+Bortezomib**	Peptide 14 3x Peptide 15 2x Peptide 16 2x	Peptide 24 2x Peptide 25 2x Peptide 26 2x Peptide 27 2x

Table 5.1. List of peptides identified from phage display capture of differently treated human and yeast proteasomes.

Human and yeast proteasomes were purified and immobilised (yeast: on IgG beads using the Rpn11-TeV-ProtA tag, and human proteasomes by binding to UBL domain immobilized either on glutathione-sepharose beads or Ni^{++}NTA beads. A phage display library was then precleared before being added to the immobilised proteasomes. Non-binding phage particles were removed by washing and the remaining phage's sequenced to identify the seven amino acid binding sequence. The number of times each peptide was found is also displayed next to the anonymised peptide names. Two of the peptides peptide 15 and peptide 12 were found in multiple conditions. Summary of work done by Dr R Babb.

To confirm that the peptides identified bound to the proteasome Dr Rebbeca Babb then used beads loaded with Peptide 15, the second most frequent peptide found in the human binding experiment and also found in yeast proteasomes treated with ADP+Bortezomib, as well as two peptide sequences that did not appear from the capture experiment. They were then incubated in HeLa lysate, washed and eluted.

Total cell lysate as well as elutant from the two control peptides and Peptide 15 were then run on SDS-PAGE and blotted for Rpn1 and Rpn10 RP subunits and α7 CP subunit Figure 5.1.

Both blots showed specific signal that was confined to the lysate and Peptide 15 elutant lanes, but aberrant from the control peptide lanes meaning that Peptide 15 was indeed able to bind to full intact proteasomes in a strong enough manner to pull down proteasomes from lysate.

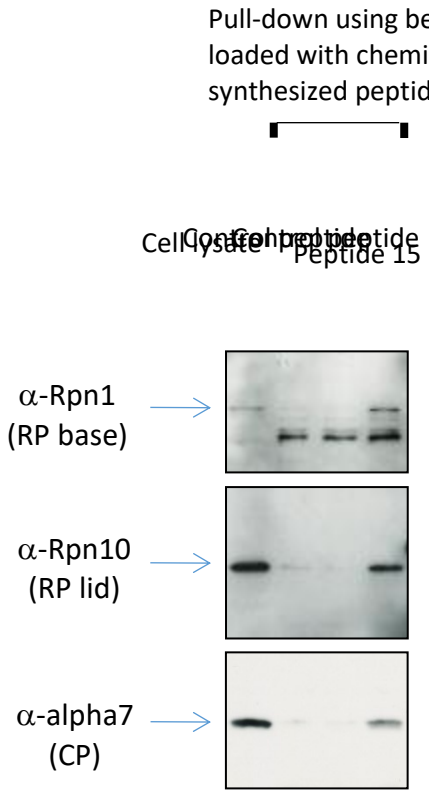


Figure 5.1. Capture of human proteasomes using Peptide 15 identified from Phage display experiment.

Peptide 15 identified from phage display experiments was loaded onto resin along with two control peptides not found to bind. Loaded beads were then incubated in lysate from NCI-H929 cells before the beads eluted and run on SDS-PAGE alongside whole cell lysate. Specific signal was shown by arrows. Note signal corresponding to proteasome subunits was only found in lysate and Peptide 15 elutant. Work was carried out by past lab member Dr. R Babb

5.3. Identification the minimal core inhibitory residues.

All the peptides identified from the phage display experiments were seven amino acids in length with a triple glycine followed by single lysine residue. To identify the minimal core sequence that could exhibit inhibitory activity on the proteasome truncated forms of Peptide 15 were created and work done by Mr Konstantinos Tzortzis utilised the ubiquitin degradation system (Method 2.8.1.) to see what each truncation event would have on the proteasomes ability to degrade a model ubiquitinated substrate Figure 5.2.. Proteasome Activity Assays using short fluorescent site specific substrates could not be carried out as we were unaware if the peptides effect would be on the catalytic active site or the numerous activities of the regulatory particle and due to the small size of the florecent substrates used in these assays, no RP activity is needed for it to enter the catalytic lumen of the proteasome.

Inhibition of the proteasome as shown by retention of the strep signal was pretty minor in the full length peptide. Truncations increased the inhibitory effect of the peptide whilst some residues such as amino acid seven were essential for its inhibitory activity. Amino acids three to seven were the most essential and even though there were slight increases in the inhibitory effect of an amino acid retention to either side. In some lanes an emergence of a substrate only band ~14 kDa indicated to the presence of de-ubiquitination activity but no substrate degradation this was mostly restricted to the amide modified C-terminus of the peptide.

I decided to take forward the 3-7 amino acid truncation as it was essential to start with the smallest peptide variant to increase its chances of cell permeability.

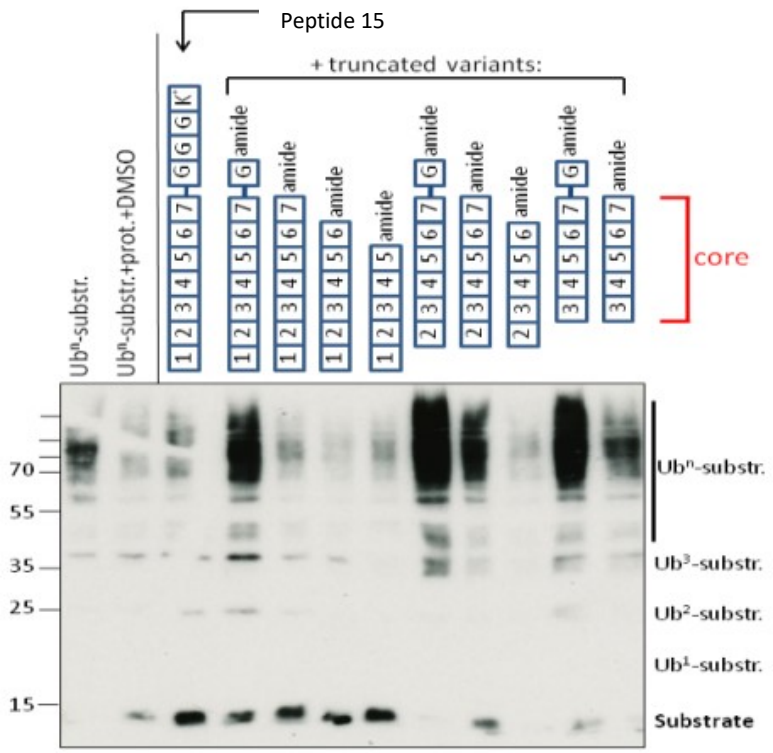


Figure 5.2. Finding the minimal inhibitory core sequence of peptide 15.

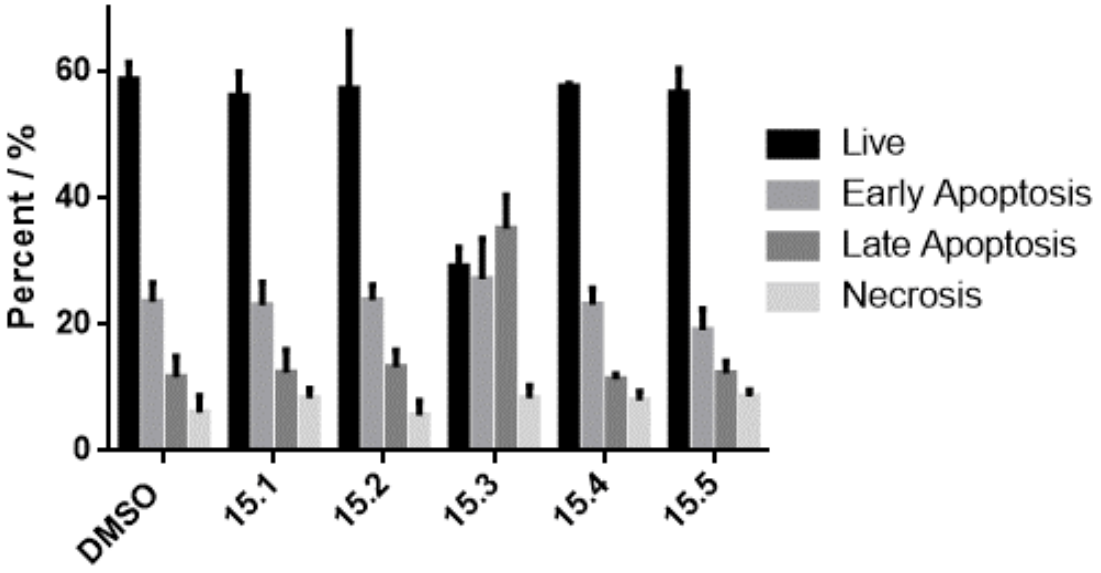
Proteasomes were incubated with full length and truncations forms of Peptide 15. The pre-incubated proteasomes were then added to a model ubiquitnated substrate and the reaction carried out for 1 h. The reaction was stopped and run on SDS-PAGE. The blot detects the strep tag present on the substrate. Inhibition is shown by the retention of the strep signal. Note the emergence of a substrate only band in some lanes indicating de-ubiquitination but no substrate degradation.

5.4. First Round Optimisation.

N.B. From this point forward the core residues 3-7 have been renamed 1-5 for simplicity in explaining where further modifications have been carried out.

For the next round of optimisation, acetylation of the N terminus of the first amino acid and a mixture of D isomers of some of the amino acids were synthesised, bottom of Figure 5.3. As the size of the peptide was getting small enough and because cell permeability is a harder process to optimise I decide to test the lethality of the next round of peptides on RPMI-8226 myeloma cells. 150 μM of each of the new peptides was added to wells containing roughly 2.5 $x10^5$ cells/ml. Cell were then incubated for 24 h before being harvested and AnnexinV/DAPI stained (Method 2.5.1) the florescence was read and the percentage of each population plotted Figure 5.3. Live cells were quantified as $AnnexinV^-/DAPI^-$, Early Apoptosis as $AnnexinV^+/DAPI^-$, Late Apoptosis $AnnexinV^+/DAPI^+$ and Necrosis as $AnnexinV^-/DAPI^+$ (gating strategy Appendix D).

The results showed that acetylation of the first amino acid and substitution of residues three and four with its D isoforms showed an increase in cell death. Whether this was due to cell permeability or increased inhibition of the proteasome, is not investigated here. Off target effects could not be ruled out although the main apoptotic mechanism is thought to be due to proteasome inhibition due to the strong binding and inhibition seen *ex vivo.*



Trunc. 15	H – 1 – 2 – 3 – 4 – 5 – NH_2
MK15.1	Ac – 1 – 2 – 3^D – 4 – 5 – NH_2
MK15.2	Ac – 1 – 2 – 3 – 4^D – 5 – NH_2
MK15.3	Ac – 1 – 2 – 3^D – 4^D – 5 – NH_2
MK15.4	H – 1 – 2 – 3^D – 4^D – 5 – NH_2
MK15.5	H – 1^D – 2^D – 3^D – 4^D – 5^D – NH_2

Figure 5.3. First round optimisation of the 5-mer core.

Top Panel RPMI-8226 myeloma cells were treated with 150 μM of each peptide for 24 h. After which time the cells were harvested and their apoptosis state measured by AnnexinV/DAPI staining. Bars represent mean ± SEM, n=3

Bottom Panel The top line shows the truncated core sequence of Peptide 15 with the variants shown below. Ac = Acetylation, NH_2 = Amide, X^D = D-isoform of amino acid

5.5. Second Round Optimisation.

In the next round of optimisation, the best compound from Figure 5.3, compound 15.3, was further modified to either methylate the third or fourth amide bond or to substitute the first second or fifth amino acid for another. To investigate whether this round of modifications had any effect on the potency, yeast proteasomes were incubated with 1 mM to 3 nM of each compound before being added to a reaction mixture containing a ubiquitinated substrate (Method 2.8.1). The reactions were incubated for 1 h at 30 °C before being stopped by the addition of SDS loading buffer and being run on an SDS-PAGE gel. Western analysis was then carried out against the strep tag on the protein substrate. Reactions were repeated twice due to the limited amount of peptide synthesised.

The top blot from the addition of the 1st round optimised compound showed strong inhibition, as measured by signal retention, to around the 3 μM. A number of modifications to this compound such as methylation of the 3rd or 4th amide bond or substitution of the 1st or 5th amino acid increased the potency with inhibition being seen to as low as 3 nM. It was therefore decided to take this first optimised compound (MK15.6) for further optimisation.

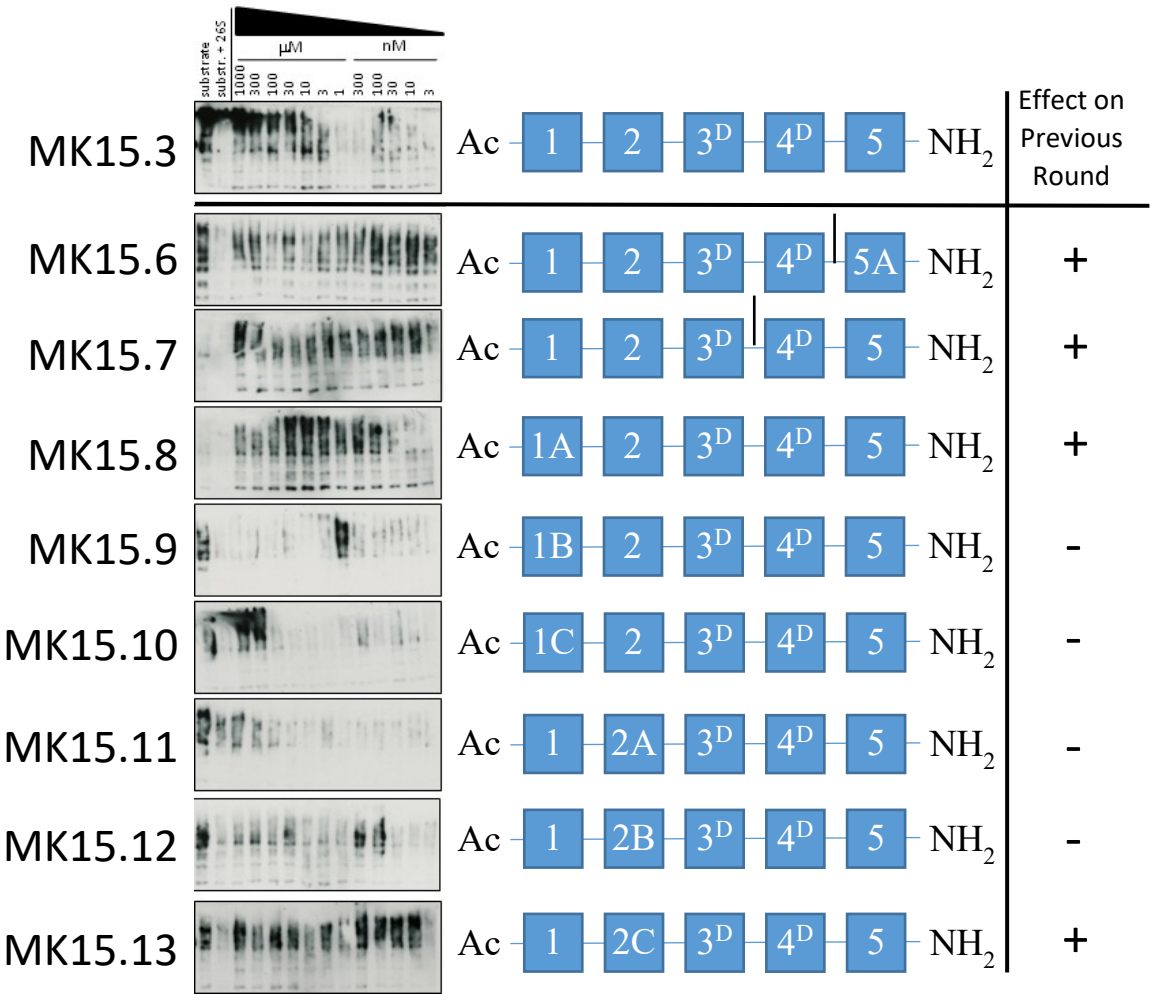


Figure 5.4. Investigating the potency of 2nd round optimisation.

Left Panel Proteasomes purified from yeast were treated with different levels of the compound variants shown above. The proteasomes were then added to an ubiquitinated substrate and the reaction left for 1 h. Reactions were then run on SDS-PAGE gels and Western analysis for the strep tag of the substrate was carried out. The first lane in each blot shows signal from substrate only and second after digestion with untreated proteasomes. Inhibition was observed by the retention of signal. N=2

Right Panel The top line shows the truncated core sequence of Peptide 15 with the variants shown below. Ac = Acetylation, NH_2 = Amide, X^D = D-isoform of amino acid, vertical sticks show methylation of amide bond

5.6. Third Round Optimisation.

Whereas the previous compounds had been commercially purchased the purity of these agents had not been ascertained. A collaboration was setup with Prof. Steven Ballet of the Vrije Universiteit Brussel, Belgium to synthesise highly pure peptidomimetic compounds. Dr Cecilia Betti a postdoctoral fellow in Prof. Ballet's lab carried out all further synthesis of the peptidomimetic compounds. All further compounds were also subjected to HPLC purification.

In this round of optimisation, the MK15.6 compound from Figure 5.4 was further modified to either methylate the amide bond or to modify the first, second or fifth amino acids with a variety of groups or non-organic elements, bottom panel Figure 5.5. to investigate the lethality of these variants RPMI-8226 myeloma cells were treated with 150 μM of each of the new peptides was added to wells containing roughly 2.5 $x10^5$ cells/ml. Cell were then incubated for 24 h before being harvested and AnnexinV/DAPI stained (Method 2.5.1) the fluorescence was read and live cells plotted as a percent of $AnnexinV^-/DAPI^-$ over total cells Figure 5.4.

Although all compounds showed a slight change in viability to the control these were not significant However, BC-MK5 showed a significant change from around 85 % to 52 %, it did however show a large variability and error of ± 22 %.

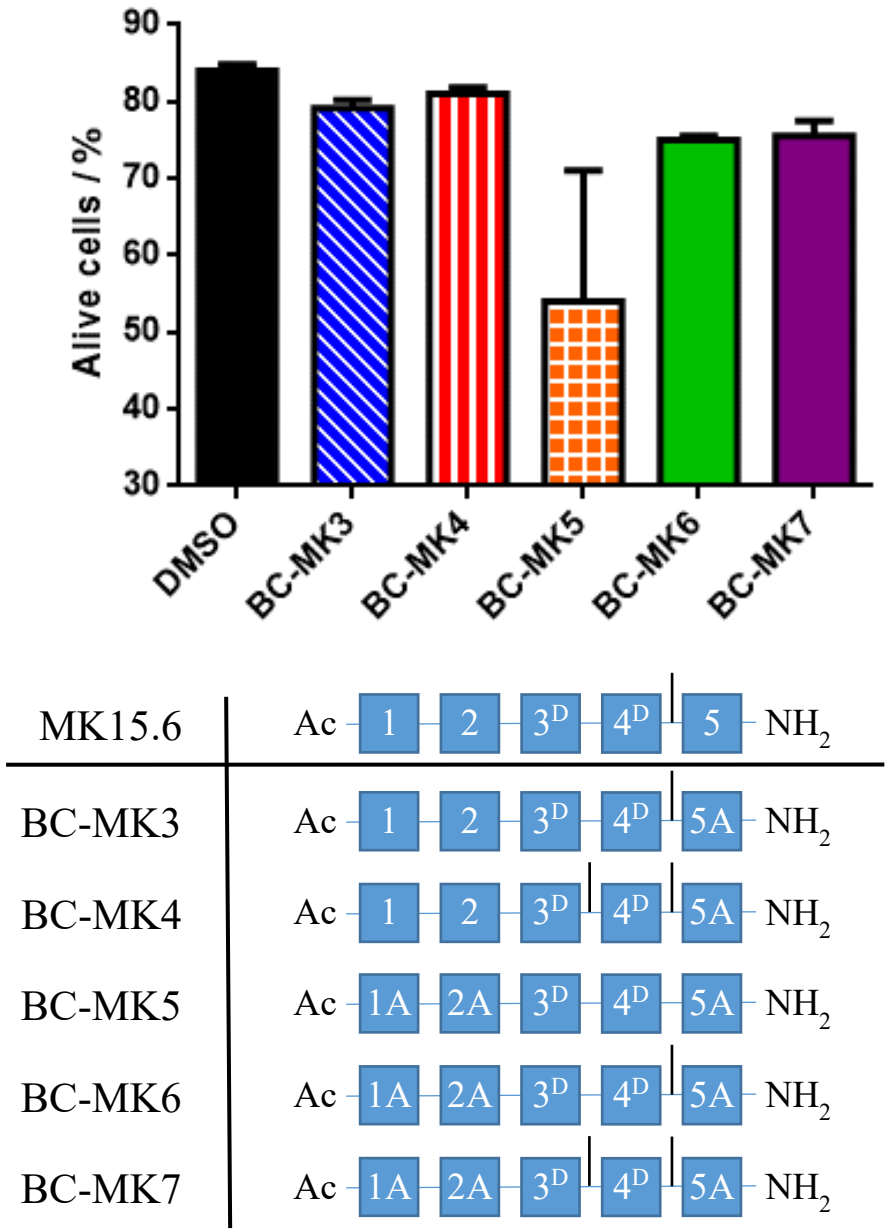


Figure 5.5. Viability as measured by AnnexinV/DAPI staining of NCI-H929 cells treated with 150 μM peptide.

Top Panel, RPMI-8226 myeloma cells were treated with 150 μM of each peptide for 24 h. After which time the cells were harvested and their apoptosis state measured by AnnexinV/DAPI staining. Bars represent mean ± SEM, n=2.

Bottom Panel, The top line shows compound MK15.6 the best candidate from the previous round with its the variants shown below. Ac = Acetylation, NH_2 = Amide, X^D = D-isoform of amino acid, vertical sticks show methylation of amide bond and A,B,C… denote changes of amino acids or variation of side chain.

We observed unexpected variability in the lethality of BC-MK5 between experiments as shown but large standard errors seen in previous experiment Figure 5.5. As experiments were not carried out on the same day after feeding, it was hypothesised that the feeding regime could be playing a role in the effectiveness of the compound. To investigate this RPMI-8226 cells were left unfed for 72h after which cells were either spun down and resuspended to the same concentration in the same 'old' media or with a percentage of new media. Other cells weren't spun down prior and media was carefully removed from the top of the well and then new media added before the cells resuspended. Cells were then plated into new flat bottom or U bottom plates and half treated with 200 μM BC-MK5 or same volume of DMSO. 48h after treatment the cells were collected and viability was measured by flow cytometry. The percent of live cells was then plotted as shown in Figure 5.6

Due to the extremely limited quantities of BC-MK5 synthesised and the need for the compound to be used as a comparison in future experiments, only one replicate was carried out. The results are deemed to be a true effect as the patterns between treated and control cells in the non-spun cells were similar to the spun cells, albeit it to a lesser degree. Interestingly the cells that received only 25 % new media showed the greatest cell death, but this was not due to starvation of cells, as cells that received no new media were relatively immune to the effects of BC-MK5. There was also no significant drop in viability between the untreated of each condition and the viability before setup, also showing no cell death from cell starvation. This could suggest that there needs to be some stimulation by growth factors present in new media, but not an extreme dilution of autocrine factors secreted by the cells themselves to cause the cells to be under stimulated. Myeloma cells are known to proliferate slowly in culture, the cells undergo lengths of time in quiescence. During quiescence the load on the proteasome is much lower, possibly explaining why the correct stimulation may release the cells from quiescence and allow for greater effects of proteasome inhibitors. Another possibility is that cell permeability or active transport of the peptide is also effected by culturing conditions, although more work is needed to investigate these findings.

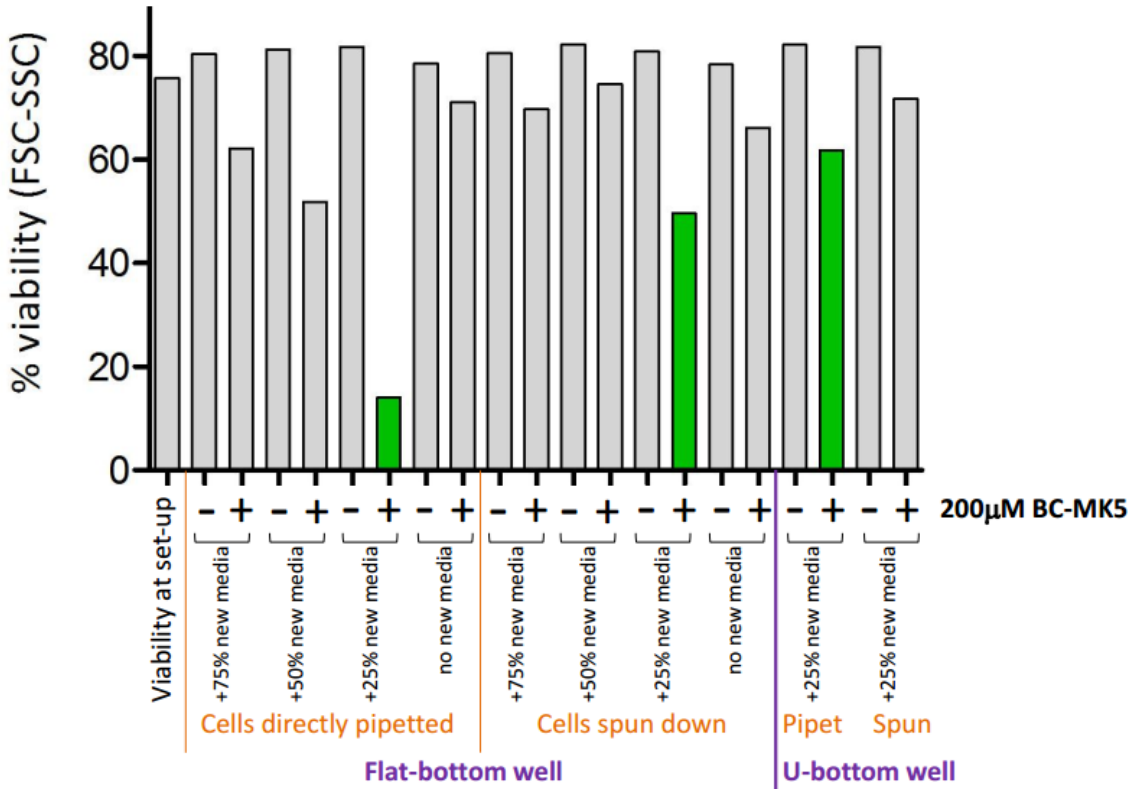


Figure 5.6. Effect of media change on BC-MK5 toxicity.

RPMI-8226, cells were not fed for 3 days before treatment before a percentage of their media was changed either by centrifuging and resuspension or by careful removal of the media at the top of the well. Cells were re-plated at the same concentration and treated with DMSO or 200 µM for a further 48 h. Bars represent single experimental values.

With BC-MK5 showing promising effects in killing myeloma cell lines a small titration range was carried out to find a dose that would allow comparison of further modifications. To investigate this RPMI-8226 myeloma cells left unfed for 72 h before ¼ of their media changed. The cells were then plated and treated with 600, 400, 200, 100, 50 or 25 µM BC-MK5 or DMSO for 48 h. Cells were then stained by AnnexinV/DAPI (Method 2.5.1) and fluorescent intensity measure by flow cytometry. Viability was calculated by a percentage of $AnnexinV^-/DAPI^-$ over all cells.

From this it was seen that BC-MK5 worked in a dose dependent manor. The new feeding regime showed tight standard error bars and showed effects of the drug down

to 50 μM with 25 μM showing no difference to the DMSO control. Because of this a 100 μM peptide concentration was deemed suitable for future experiments.

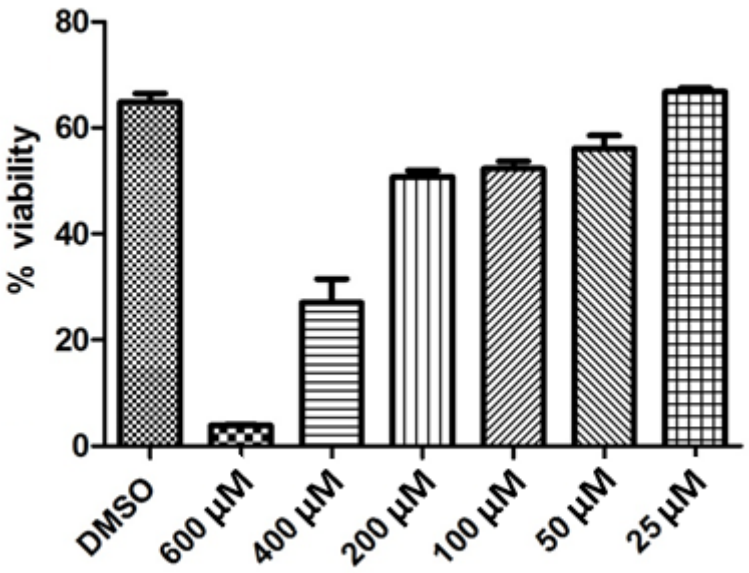


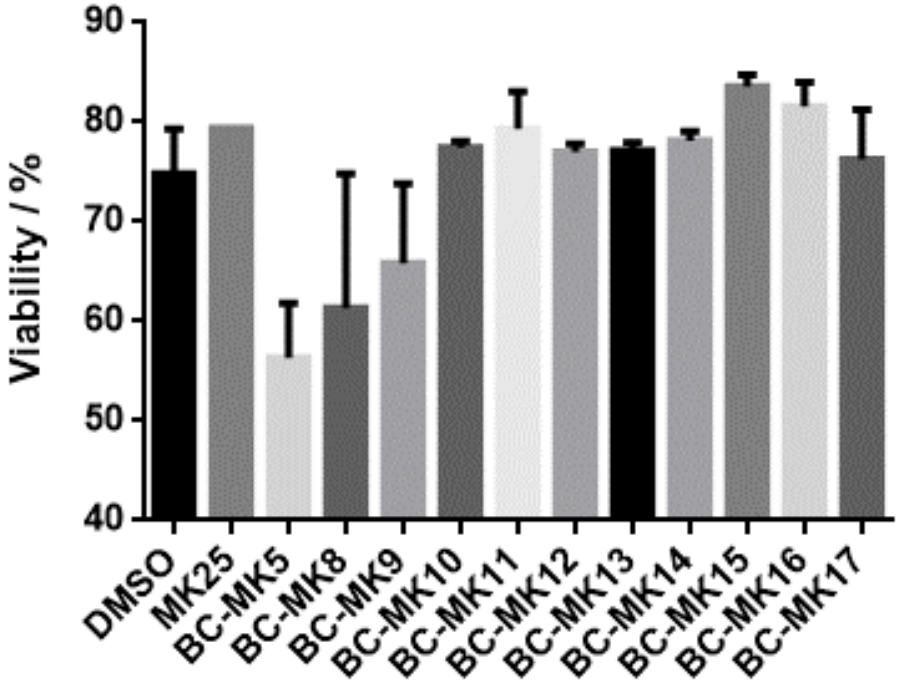
Figure 5.7. Titration of BC-MK5 on RPMI-8226 myeloma cells.

RPMI-8226 cells were treated with varying concentration of BC-MK5 for 48h before being harvested and the viability of each culture measured by a percentage of AnnexinV$^-$/DAPI$^-$ over total cells. Bars represent mean with ±SEM n=2

5.7. Fourth Round Optimisation.

The next round of optimisation focused on modification and substitution of amino acids of BC-MK5 as well as methylation of some amide bonds, bottom panel Figure 5.8. To investigate if any of these changes enhanced the inhibition each of these compounds were added to RPMI-8226 cells at a concentration of 100 μM and the cells incubated for 48 h. Cells were then harvested stained by AnnexinV/DAPI (Method 2.5.1) and fluorescent intensity measure by flow cytometry. Viability was calculated by a percentage of $AnnexinV^-/DAPI^-$ over all cells.

The changes to BC-MK5 in this round of optimisation did not play a significant enhancement of the drug. BC-MK5 still showed the greatest cell death with a drop in viability from ~76 % down to ~57 % whilst the others either ablated the activity or significantly reduced it.



BC-MK5	Ac–1A–2A–3^{D}–4^{D}–5A–NH_2
BC-MK8	Ac–1B–2A–3^{D}–4^{D}–5A–NH_2
BC-MK9	Ac–1A–2B–3^{D}–4^{D}–5A–NH_2
BC-MK10	Ac–1B–2A–3^{D}–4^{D}–5A–NH_2
BC-MK11	Ac–1A–2B–3^{D}–4^{D}–5A–NH_2
BC-MK12	Ac–1A–2A–3^{D}–4^{D}–5B–NH_2
BC-MK13	Ac–1A–2A–3^{D}–4^{D}–5C–NH_2
BC-MK14	Ac–1A–2A–3^{D}–4A–5A–NH_2
BC-MK15	Ac–1B–2A–3^{D}–4A–5A–NH_2
BC-MK16	Ac–1A–2B–3^{D}–4A–5A–NH_2
BC-MK17	Ac–1A–2A–3^{D}–4A–5A–NH_2

Figure 5.8. Testing derivatives of BC-MK5 on the ability to kill RPMI-8226 cells.

Top Panel, RPMI-8226 myeloma cells were treated with 100 μM of each peptide for 48 h. After which time the cells were harvested and their apoptosis state measured by AnnexinV/DAPI staining. Bars represent mean ± SEM, n=2.

Bottom Panel, The top line shows compound BC-MK5 the best candidate from the previous round with its the variants shown below. Ac = Acetylation, NH_2 = Amide, vertical sticks show methylation of amide bond and A,B,C… denote changes of amino acids or variation of side chain.

5.8. Fifth Round Optimisation.

The next modification was the incorporation of a silylated proline termed Silaproline in place of the proline residue. A schematic of the modified sequence will not be shown as to keep the anomaly of the proline residue in the sequence. Due to the synthesis method used a racemic mixture of the compound was produced with a chiral centre between the primary carbon and carboxylic acid (Figure 5.9). The racemic mixtures were partially purified from one another by HPLC purification and termed BC-MK18a and BC-MK18b.

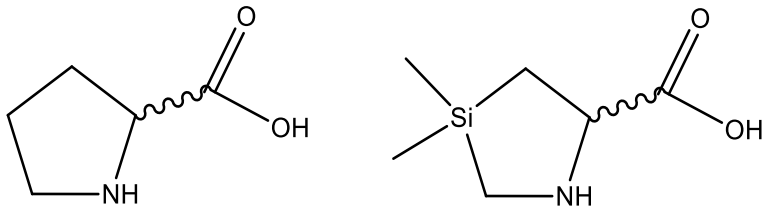


Figure 5.9. Structures or L/D-Proline and L/D-Silaproline.

The left hand side structure shows racemic proline amino acid while the right hand side shows racemic silaproline. Note that the forth carbon in the pyrrolidine ring has been substituted for a di-methylated silicon atom.

To investigate if silaproline had any effect on the toxicity of the compound to myeloma cells each of these compounds along with BC-MK5 were added to RPMI-8226 cells at a concentration of 200, 100, 30 and 10 µM and the cells incubated for 48 h. Cells were then harvested viability was measured by a percentage of side scatter SSc^{Low} over all cells (Gating method Appendix D).

BC-MK18b did show enhanced toxicity in RPMI-8226 cells with complete killing at 200 µM and a slight reduction of 2 % over BC-MK5 at 100 µM. BC-MK18a did seem to outperform BC-MK5 at the 200 µM concentration although at 100 µM its toxicity was worse than that of BC-MK5 and its overall effect is most probably insignificant. With

BC-MK18b showing enhanced activity to BC-MK5 the main racemic variant should be identified.

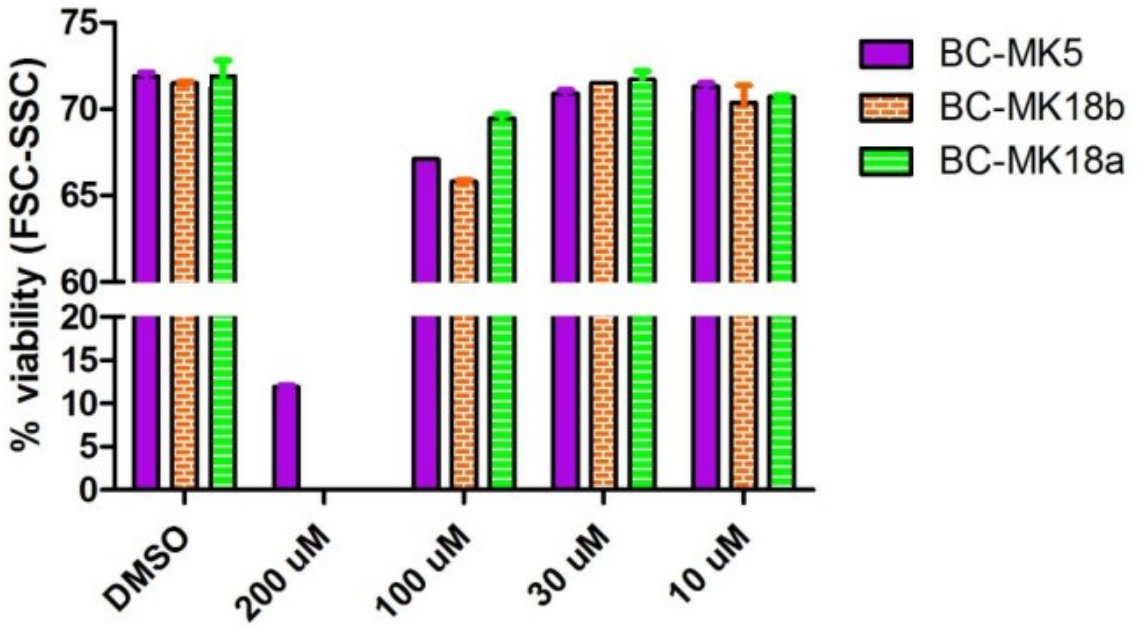


Figure 5.10. Viability of OPM-2 cells after 48h treatment with peptide variants.

OPM-2 cells were treated with 10, 30, 100 or 200 μM of BC-MK5 or silaproline variants BC-MK18a or BC-MK18b alongside DMSO control. After 48 h cells were harvested and cell viability measured as a percent of side scatter $(SSC)^{Low}$ over total cells.

To further investigate whether this novel collection of proteasome inhibitor derivatives only target cells that are in a particular state. Cell cycle analysis was carried out in response to compound treatment. RPMI-8226 cells were treated with either 1.65, 6.25, 25 or 100 μM of BC-MK5 or silaproline variants BC-MK18a or BC-MK18b or DMSO control for 24 h. Vybrant DyeCycle Violet Stain that binds in a non-toxic manor to DNA was then added to the cell culture media and the cells left for a further 45 min. Flow cytometry was carried out and the cell state for each cell was read by the intensity of signal from the dye in the 450/50 filter corresponding to the amount of DNA present. Live cells were gated by FSc^{High} SSc^{Low} population and the different cell states were gated as shown in Appendix D.

The cell state assay showed that each drug effected the cells in a similar manor, which is not surprising with them all being derivatives of one another. The effect of each peptide to proportion of cells residing in G0/G1, S and G2/M states was concentration dependant with higher concentrations producing a greater effect. The overall effect of these peptide derivatives is a loss of cells from the S phase and increase of cells in the G0/G1. Cells in the G2/M phase were relatively unaffected. As dead cells were excluded from analysis the loss of a certain population would increase the ratio of the other populations even though the cell number may remain unchanged. It is therefore likely that the main change seen is a loss of S Phase. Why these peptides have effects on a particular cell state is unknown although the proteasome is known to play a major role in the regulation of the cell cycle as summarised in Introduction 1.9.1.

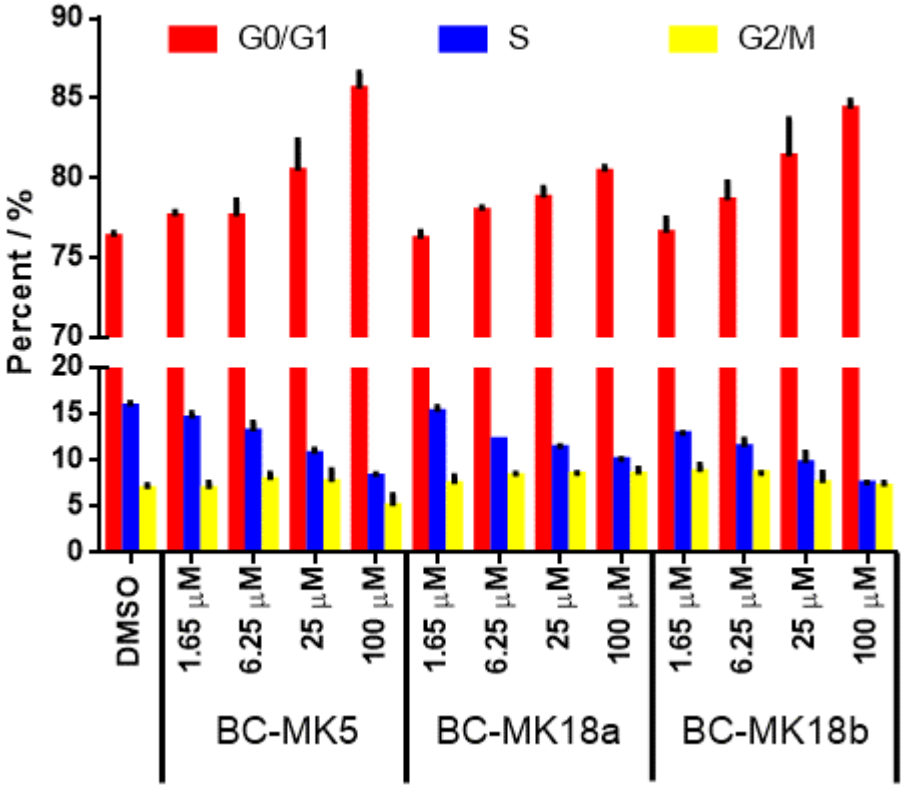


Figure 5.11. Viability of OPM-2 cells after 48h treatment with peptide variants.

OPM-2 cells were treated with 1.65, 6.25, 25 or 100 μM of BC-MK5 or silaproline variants BC-MK18a or BC-MK18b alongside DMSO control. After 48 h cells were harvested and the cell state was measured by addition of Vybrant DyeCycle Violet Stain.

5.9. Discussion.

For traditional proteasome inhibition, therapeutics such as Bortezomib, Carfilzomib and Ixazomib are being used in the clinic for treatment of myeloma. These compounds all directly bind to the catalytic threonine of the chymotrypsin, and to a lesser degree other, proteolytic active sites of the proteasome. A small number of other studies had shown that inhibition of the proteasome could be carried out by allosteric binding of inhibitors to the alpha subunits of the proteasome (Maria Gaczynska et al., 2003; X. Li et al., 2010). The proteasome is a complex cellular machine, degradation of ubiquitinated proteins requires not just the catalytic core but also the recognition of the ubiquitin chain by Rpn10 and Rpn13, cleavage by Rpn11 as well as an ATP mediated translocation of the protein into the catalytic lumen of the core particle by Rpt1, 2, 6, 3, 4, & 5. Disruption or knockout of a number of these subunits are lethal or cause serious growth defects. In addition, the proteasome is believed to play multiple roles in gene transcription, some of which are non-proteolytic and restricted to the RP (Nickell et al., 2009; Sakata et al., 2012; Tomko et al., 2010; Verma et al., 2002). It is therefore a sensible assumption that allosteric inhibition may be a good target for proteasome inhibition by inhibition protein processing into the catalytic lumen, by disruption of gene regulation or by causing conformational changes in the CP catalytic pockets specificity, ability or kinetics to breakdown substrates.

In this chapter I continued to develop a novel allosteric proteasome inhibitor. The identification via phage display yielded multiple binding peptides and although I only took one peptide along. This peptide was chosen as previous work had already shown it’s ability to bind and pulldown proteasomes as well as showing minor inhibitory effects. For this peptide a minimal core inhibitory sequence was found by truncations on either end. Substitution of the third and fourth residues for their corresponding D-isomers was found to be beneficial in the potency of the compound in inhibiting proteasomes. Further analysis focused on the ability to kill cells rather than potency in inhibiting proteasomes. This was due to the fact that the core sequence was now known to inhibit proteasomes and further enhancement to increase its inhibitory effects on purified proteasomes may be detrimental to the permeability of the drug and therefore would negate its effectiveness.

With the lead compound being a small peptide it was important to try and reduce its ability to be degraded by peptidases. Synthesis was done by the expertise of Dr Cecilia Betti. A number of modifications were carried out to reduce protease susceptibility as well as to increase cell permeability, such as methylation of the amide bond or substitutions of the side chains to produce unnatural amino acids. The strategy is of peptidomimetic optimisation is to improve target affinity, to retain biological activity and to improve membrane-permeability and protease-resistance.

Cell permeability is a more difficult thing to optimise. Obviously the structure of the molecule cannot change drastically without detriment to the effect of the drug and therefore, changes were carried out to slightly alter the amino acids one by one. There are three major classes of cell penetrating peptides cationic, amphipathic and hydrophobic, reviewed in Milletti, 2012 so the changes were mostly to enhance the property of that residue. Examples such as methylation of side chains, nitration or sulfonation of aromatic rings.

Silaproline had been shown to increase cell permeability 20 fold (Pujals et al., 2006) mostly due to a 14 fold increase in hydrophobicity (Cavelier et al., 2002). Upon changing the proline residue in the peptide to that of a silaproline residue the toxicity shown was significant at 100 μM only showed a slight improvement and was not greatly significant. An overview of the changes can be found in Figure 5.12.

It is interesting that the feeding regime plays such an important role in the killing of the cells. Data from multiple experimental repeats also showed that the higher the viability of the cells the greater effect of the peptide (Data not shown). This together suggests that the peptide has enhanced lethality in actively cycling cells. In fact, by investigating the cell cycle state of treated cells, I found that BC-MK5 and the silaproline variants BC-MK18a, BC-MK18b all increased the percentage of cells in G^0/G^1 phase in a dose-dependent manner while decreasing the S phase percentage. This would indicate that those cells in S phase where being killed off by the action of the drug giving a greater percentage to those in the stationary G^0/G^1 phase.

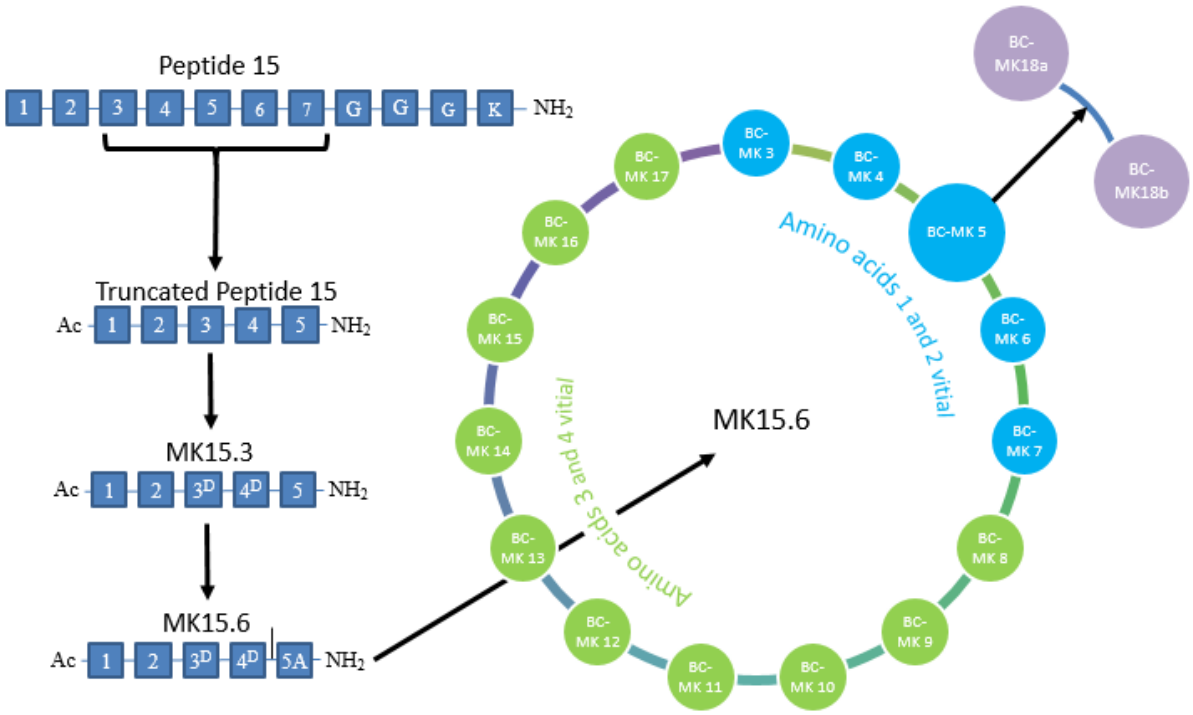


Figure 5.12. Overview of Peptide 15 optimisation.

Schematic showing each round of optimisation of peptide 15 with emphasis on the optimisation of MK15.6 to BC-MK5, BC-MK18a/b.

5.10. Future Work.

Unfortunately, due to the small amounts of peptides synthesised, there were limitations to the number of different assays that could be performed. Furthermore, the development was time consuming due to the need to wait for the results from the testing of each derivative before the next round could be decided and the start of synthesis begun.

Although the potency of this drug was increased over the course of these optimisation rounds, the concentration at which you saw a total killing of myeloma cells was still quite high at between 25 – 100 μM. Further modifications should be carried out to see if there was possibility of decreasing this further, especially modifications which restrict conformational freedom of the compounds.

Little has been done to investigate the other peptides on the list identified from phage display techniques. Peptide 17 was found more times in the phage experiments on human proteasomes so maybe a better candidate. The others although they were found fewer times the ability of them to penetrate the cell or be resistant to metabolic degradation may make them more suitable candidates.

After the most potent drug had been synthesised further work would be needed to test the candidate *in vivo.* Human myeloma engrafted NOD/scid/gamma (NSG) mice could be used to test the compounds ability to shrink tumour as a standalone agent or in combination with other proteasome inhibitors. This would also allow to test for toxicity and the drugs mode of metabolism and excretion.

It is also important to understand the mechanism of action. Where does it bind? How does this cause inhibition? Single-particle cryo-EM studies may yield further insight in the docking sites of these small-molecule compounds. This would provide information as to whether the peptide binds to a known binding pocket of a proteasome partner, may explain the inhibitory activity on the proteasome, or may just show a conformational change or lock of the proteasome into a conformation that may prevent proteolysis.

CHAPTER 6 – Discussion and Conclusion.

Chapter 6: Discussion and Conclusion.

6.1. Discussion

The development of new treatments for myeloma has increased survival rate substantially over the past two decades. However, life expectancy following treatment remains poor, with a mean of six years. The development of Bortezomib in the early 2000's greatly increased life expectancy through uses as a second-line treatment and/or in a combination therapy for conditioning before stem cell transplantation.

The discovery and subsequent investigations into the UPP have shown that it is a highly conserved and important pathway for all eukaryotes. Severe/complete inhibition of the proteasome is known to be lethal to any human cell. In addition, disease-specific dysfunctions in the UPP are known to exist, raising the prospect of more targeted interference. For example, it has been proposed that inhibition or activation of substrate-specific E3 enzymes may be curative in a number of disorders such as Parkinson's disease. In MM, the role the proteasome plays in the biology of the disease is still to a large degree speculative. A number of competing hypotheses have emerged as to why MM has the greatest sensitivity to PI. Although some hypotheses have been disproven, like of the role proteasome inhibition plays on NF-κB activation, those that still remain like that of Load vs Capacity are challenging to confirm or disprove and are likely to remain at the forefront of speculation until greater understanding of the proteasome biology of this disease is achieved. With resistance to bortezomib occurring in all patients and the lack of curative therapies to this the most common haematological malignancy, new therapies are drastically needed. It is also important to fully understand why bortezomib firstly has selective lethality in MM through better understanding of its mechanism, which in turn may also help decipher the mechanism by which resistance develops in this disease,

6.1.1. Post-translational modification of proteasome subunits, unresolvable by SDS-PAGE

The first aim of my thesis was to investigate a novel modification that had been identified by Dr Kleijnen and a previous member of the Kleijnen Group, Ms Z. Wang. They had found that a number of proteasome subunits, when blotted on CTAB-PAGE Western blots, showed a large amount of diffuse signal, higher than the main defined band for each subunit. This, however, was not visible when Western analysis was carried out on the standard SDS-PAGE protein electrophoresis system. Following on from this, they described how this smear material could be separated from the defined band by using a simple detergent lysis technique. Subsequent work indicated that the smear was confined to the nucleus of the cell, as shown by the use of a simple cytoplasmic and nuclear extraction technique. The fact that the diffuse smear material could be separated from the defined band material strongly suggested that the smear was from a distinct modified species and not an artefact due a lab error or incomplete loading of detergent, which may affect mobility of proteins in the gel leading to multiple bands or smear.

I continued to expand on this work by first confirming that CTAB-PAGE under my technique and laboratory conditions was able to resolve proteins. CTAB-PAGE's ability to resolve monomeric as well as its ability to dissociate multimeric proteins was shown to be equal to that of SDS-PAGE. In fact, the fractionation carried out by Ms Wang also showed that some proteasome subunits, at least those from cytoplasmic extraction, were able to be resolved as a single band. Single bands were also seen in Westerns probed for lamin B2 (used as a cell fractionation control). As yeast proteasomes have such a high homology and have been used extensively as a model system in the understanding of the UPP, I investigated if proteasomes that resided in the nucleus of yeast also showed this diffuse signal when run on CTAB-PAGE. However, this was not the case and suggested this was either a modification of more complex eukaryotes or simply that yeast do not harbour this modification on their proteasomes. This could explain why this observation has not been seen before as requires human proteasomes to be resolved on CTAB-PAGE and not the commonly used SDS_PAGE.

Upon subjecting nuclear proteasomes (captured, from the nuclear extract of primary human leukocytes using the UBL domain of hPLIC/ubiquilin 2) to FPLC size exclusion

chromatography, the modified proteasomes could be resolved by both CTAB and SDS-PAGE systems. This observation is hard to explain although it could suggest that other nuclear components prevent these modified species from resolving on SDS-PAGE, or that a concentrated sample is required to resolve them. The signal from a selection of proteasome subunits could be detected in a wide number of fractions. Rpn12 and Rpt2 showed the diffuse smear throughout these fractions with a slight reduction in molecular weight from the early to late fractions. This suggested that the modification on the proteasome that causes this diffuse smearing also altered the molecular weight of the proteasome, making the proteasome particle measurably larger as more extensively modified proteasomes emerge from the Superose6 column first. The smear material corresponded mostly to RP subunits and was not present on all subunits of the proteasome. Some subunits such as α7 did not show modified smear material but were also found in a wide range of fractions, indicating that non-modified subunits are also incorporated into these modified proteasomes.

The UBL capture method may also have helped with the visualisation of these modified proteasomes on SDS-PAGE. When looking at an Rpt2 Western blot of whole cell lysate, CE, NE, as well as UBL capture from CE and NE, modified Rpt2 was highly enriched by UBL capture from the same fraction. This however, was not seen in the UBL capture from the CE. The ratio of unmodified subunit signal to that of modified changed to bias the modified subunits after capture with UBL domain of hPLIC. This could mean that the UBL domain binds stronger to modified proteasomes and that these modifications may play a role in UBL binding and hPLIC biology. Further work is needed to test this hypothesis. However if UBL does select for modified subunits, this could explain why UBL enrichment allows for visualisation of the modified smear material on SDS-PAGE.

Proteasomes purified from both the cytoplasm and nucleus of OPM2 myeloma cells were also subjected to two-dimensional gel electrophoresis, specifically by focusing the proteins by their iso-electric point and then in the second dimension by SDS or CTAB-PAGE. The nuclear fraction showed an extensive ‘diagonal laddering’ signal. This was indicative of a charged polymeric modification that both changes the size and charge of the protein upon each monomer addition. This could explain the nucleotide-like density reported in the purification of prosomes (proteasomes) (Schmid et al., 1984), described finding which at the time was controversial (Baumeister et al.,

1998). More work needs to be carried out to identify the nature of all the signal from the 2D western blots. The large amount of signal that corresponds to UBL capture protein is not optimal and may be hiding specific signal behind it. Better capture methods such as utilising a tandem affinity purification where more than one capture/release is used may be beneficial not only to clean up the prep but also to remove UBL signal via a second capture. The diagonal laddering that is observed is likely to be specific to proteasome analysis due to the fact that it is largely present in the nuclear isolation even though UBL capture was the same through both cytoplasmic and nuclear extractions.

Due to the location of this modification, and the likelihood of the modification being polymeric and charged in nature, I first ruled out covalently bonded or tightly bound DNA and RNA. Purified proteasomes were incubated with a selection of DNase and RNase enzymes that both cut single and double strands. No changes were observed with these enzymes on reducing the modified smear seen with some subunits on CTAB-PAGE. Another modification that is known to reside on nuclear proteasomes is that of poly-(ADP)-Ribose (Ullrich et al., 1999). This was also ruled out as being the cause for the higher molecular weight smear as digestion with PDE1, ARH1, ARH2 (variants 1 & 2), ARH3 and PARG did not fully collapse the modified species into an unmodified band. Both variants of ARH2 were cloned, expressed and purified in-house. With no known substrate available confirmation that the purified enzyme prep had activity could not be confirmed. Multiple buffers were tried although no activity was seen with these enzymes. There was slight activity with PARG, which yielded a more intense signal possibly due to increased antibody binding from small PAR chain removal, as well as an effect on the migration of subunits upon PDE1 treatment. PDE1 created more diffuse signal above the unmodified band, this could be due to enzyme binding but incomplete digestion. One potential limitation of PDE1 treatment was the purity of the PDE1 enzyme prep. This crude enzyme prep was isolated from rattlesnake venom and therefore has the potential to be contaminated with other proteases and enzymes that may affect the proteasome prep and yield the results seen by the PDE1 treatment. An inhibitor should be used to prevent PDE1 changes to confirm that these changes are specific to the enzyme itself. Our current working hypothesis, based on preliminary enzymatic digestion experiments carried out by another member of the lab, is that the nuclear modification on proteasomes may be a

nuclear glycosaminoglycan. Note that glycosaminoglycan is not present in more primitive eukaryotes such as yeast, which dovetails with our observation that yeast nuclear proteasomes are not modified. Further effort is needed to test this hypothesis properly.

6.1.2. Post-translational modification of proteasome subunits change early after Bortezomib challenge

Upon trying to delve into the early kinetics of proteasome inhibition with Bortezomib treatment, I firstly noted that inhibition of the CT-Like active site is a lot more severe than expected from predicted models. A selection of different cell lines showed similar inhibition of this site in the first 8 hours. However, after this time the cells that were resistant to Bortezomib retained ~20 % CT-Like activity, while the sensitive myeloma cells continued to reduce their activity until the CT-Like site was fully inhibited. It was always thought that proteasomes respond equally regardless of whether they reside in sensitive or resistant cells, this difference shows the first evidence that sensitivity could be due to how Bortezomib inhibits the proteasome and not the remaining free activity of the proteasome have in different cell types.

When looking at the levels of polyUb conjugates within the cell it was only after ~8 h treatment, when the level of CT-Like inhibition dropped past this ~20 % remaining threshold, that the levels of poly-ubiquitinated proteins increased, showing that demand for proteasome function was outweighing capacity. This was in direct disagreement with the most prevailing theory on myeloma's sensitivity to Bortezomib, as not only was a large degree of inhibition observed (not minimal inhibition as hypothesised), but a greater level of inhibition of proteasomes was observed in myeloma cell lines compared to other resistant cell lines. Thus, it is not that a small level of inhibition is enough to overload the UPP in myeloma, but rather that cells experience unexpectedly severe proteasome shutdown. With the most severe inhibition being observed in those cell lines that are Bortezomib-sensitive, showing a level of inhibition that that would kill any cell type.

If in MM cells Bortezomib had an increased inhibitory effect on proteasome function, this could be due to a secondary cellular mechanism. Upon treating lysed cells with Bortezomib, the reduction in CT-Like activity was only 10-15 %. This correlated with

inhibition of purified proteasomes from yeast. Purified human proteasomes showed a greater level of inhibition of around 40 % but did not continue to decrease over time and did not show a complete inhibition as observed in cells. This partial response to Bortezomib observed when treating purified proteasomes or proteasomes residing in lysate was surprising. As Bortezomib works by direct active-site inhibition and is not known to effect upstream processing of the proteasome, it should therefore inhibit intracellular and purified proteasomes equally. However this mild inhibition suggests that a secondary mechanism that enhances the inhibition of bortezomib is the cause of the servear inhibition of proteasomes.

The reason for increased shutdown of proteasome activity in myeloma cell lines, and not in Bortezomib-insensitive cell lines, could not be put down to caspase activation or cell death, which both occurred at 10 h. Increased binding of PI was also ruled out, as - although the CT-Like activity continued to decrease - no increased active-site labelling of proteasome particles was observed. In fact, the opposite happened as a reduction of active-site occupation by VS-Biotin was observed. There was, however, a change to the CTAB-PAGE resolvable modifications (observed in chapter 3) upon PI treatment. The changes observed were to the modified subunit species rather than the unmodified subunits of the nuclear proteasomes, mostly RP subunits, with disappearance of some bands and appearance of others showing very early (2 h) after treatment with PIs. Although some of these changes could be put down to caspase activation, inhibition of intracellular caspases in combination with a lethal dose of Bortezomib still yielded a number of PI-mediated changes. The severe shutdown of proteasomes within the cells compared with that of proteasomes that reside in lysate or purified away from other cellular components suggest that the shutdown is not direct inhibition via bortezomib. If bortezomib caused these changes directly the same level of inhibition would be expected almost instantaneously in lysate, due to the lack of cell diffusion required.

The concept of bortezomib inhibiting the proteasome via two separate mechanisms may seem farfetched. However, disruption of proteolysis via proteasome inhibition disrupts a huge number of cell processes allowing for hyperactivation of protein modifying enzymes. Many proteins within the cell are activated/inhibited by modification, particularly phosphorylation, indeed, the activity of the proteasome is also known to be affected by a number of posttranslational modifications. Relatively

recently, a number of complex modifications have been shown to directly inhibit the proteasome. In cells that have high oxidative stress, like those of plasma and myeloma cells, 4-hydroxy-2-nonenal is shown to covalently bind to proteasomes, upon which both the trypsin-like and caspase-like activities of the proteasome are severely diminished (Okada et al., 1999). This could explain why the chymotrypsin-like active site is the most important target for inhibition, being the most active site in cells that have high oxidative stress. It could also explain why disruption of proteolysis could further enhance this mechanism creating stronger inhibitory effects within the cell.

The 26S proteasome is known to be modified by O-GlcNAc transferase. O-GlcNAc is known to modify Rpt2 subunit where it inhibits the activity of the 19S regulatory unit, specifically affecting the ATPase activity of a number of 19S base subunits (Zhang et al., 2003). This further confirms that large modifications of this nature can inhibit the activity of the proteasome, and corresponds with preliminary data within our lab that suggests that at least some of the modifications observed on proteasome subunits could indeed be glycosaminoglycans like O-GlcNAc.

6.1.3. Development of Allosteric proteasome inhibitors

In addition to modification of proteasome subunits which regulate proteasome function, a number of other proteins interact with the outside of the proteasome, changing and regulating its activity. The third aim of my project was to investigate whether molecules that bound to the outside of the proteasome could regulate its function and shows lethality in MM cells. Work had been done prior to my PhD commencement that identified a number of peptides, seven amino acids in length, which bound to the proteasome under a number of physiological conditions and were confirmed to be able to pull down proteasomes from cell lysate. A single peptide that was identified was carried forward for optimisation and testing as a novel allosteric inhibitor. The core inhibitory sequence corresponded to the amino acids 3-7 in the original sequence were taken forward to be optimised. Working alongside an organic chemist collaborator, modifications were carried out such as: substitution of amino acid isomers, methylation of amide bonds, and adaption of amino acid variable regions to form unnatural amino acids. These variants of the original peptide were able to inhibit the degradation of a model ubiquitin substrate by purified human proteasomes. The

most potent variant of these was shown to be able to kill myeloma cells at a 25 μM. Interestingly, I found that the state the cells were in when treated with this peptide does influence the effectiveness of this compound. The effect of the compound was greatest when a quarter of the media the cells resided in was changed. Not changing the media or changing 100 % of the media resulted in very little death when the compound was added. This suggested that it was not due to serum or amino acid starvation, nor due to dilution of cytokines and cell produced factors, but was likely a balance of the two. Performing a cell cycle analysis of cells treated with differing concentrations of the compound showed that the percentage of cells in the S phase decreased with higher concentrations of compound, whereas the percentage of cells found in the G_0/G_1 phase increased. Both the feeding regime and cell cycle analysis equally point to the drug being particularly potent in cells that are actively proliferating. Whether this is due to more internalisation of the drug or because of the increased proteasome load during progression through the cell cycle is unknown.

Bortezomib is not known to be selective in killing cells within a certain phase within their cell cycle, it is therefore peculiar that a different proteasome inhibitor would have this effect. However, one has to realise that the mechanism of this agent is not the same as that of bortezomib and as such may cause cytotoxicity via a different mechanism. By binding to the outside of the proteasome, this novel peptide could indeed have stronger effects on other properties than that of proteolysis such as the proteasome's role as transcription complex or with chromatin remodelling.

6.2. Limitations of Study

Working on a large complex such as the proteasome creates many technical difficulties. Whereas posttranslational modification analysis of smaller singular proteins can be done via mutagenesis of the most commonly modified residues, this is harder when looking at a complex of over 33 proteins.

The antibodies used in this study were thought to be specific, although cross reactivity was seen with UBL capture blots, where the UBL protein was visible in westerns with a number of proteasome antibodies. No cross reactivity was seen with any of the enzymes utilised to degrade the PTMs of the proteasome and therefore it is likely that this cross reactivity was due to the extremely excessive amounts of UBL protein eluted from the capture beads. Expresion of tagged proteasome subunits may be useful in confirming that the signal is specific, if the smear is also seen by detection against the tagged epitope.

Enrichment of human proteasomes was done by UBL capture. This utilises the UBL domain of hPLIC, which binds to S5A/Rpn10, and therefore captures only 26S proteasomes and not those that are capped with different activators or core particles alone. By investigating how only 26S proteasomes respond to bortezomib information maybe lost on how different proteasome complexes respond.

The nuclear and cytoplasmic extraction technique was able to extract proteins within these two compartments, however, to confirm that this technique itself does not cause the findings observed, cell fractionation could be done via a different method, such as density gradient centrifugation, which does not utilise two buffers and therefore proteins from the different compartments of the cell would be subjected to the same treatment throughout capture. This is unlikely to have any effect as the smear observed on CTAB-PAGE was evident before fractionation when whole cell lysate was run and could be separated from single, unmodified species using the two buffer fractionation system.

FPLC purification was done utilising an old system. Although the Sepharose6 column was brand new, UV and conductivity analysis could not be carried out and therefore samples from each fraction were run on western to show successful separation. This method of size exclusion chromatography works well for large modifications on singular proteins, although the size of the proteasome complex means that even large

modifications only produce a small percentage mass difference. A better separation could have been achieved using an ion exchange column. This utilises the charge of a particular protein or complex and an ion concentration gradient that elutes the capture proteins dependent on their charge. If the modification on the proteasomes was indeed charged, this would allow much greater separation between those that were modified and those that were not.

The complexity we had in removing the modification on the proteasome subunits was due to a number of factors. The modification was unknown; simple, easily removable modifications, such as DNA, RNA, ubiquitin, were ruled out, and the fact that the subunits may be harbouring multiple modifications of different types meant that a singular PTM digestion might not achieve complete resolution of proteasome subunits into a singular band.

There was a large variation of the smear material between blots. Although most changes were due to the differences in running of whole cell lysate or UBL captured proteasomes. Why the smear would change between whole cell lysate and UBL purified proteasomes run on CTAB-PAGE may also suggest the same reason by these two samples run on SDS-PAGE also show differences, with a lack of smear material observed when whole cell lysate was run on SDS-PAGE.

6.3. Future Work

The work done in this thesis has opened up other avenues for investigation. The modification identified in Chapter 3 and further characterised in Chapter 4 has to be identified and its biological function deciphered. Initial attempts during this thesis to detect the modification via mass spectroscopy (MS) were unsuccessful due to the purity of the samples and the charge of the modification effecting the flight into the detector. A top-down approach could yield better results utilising LC-MS and reporting on the regions of the proteins that are likely modified. Further studies utilising nuclear magnetic resonance (NMR) could yield the structure of this modification, whereas single amino acid substitutions could help identify the exact residues that harbour this modification.

The mechanism by which Bortezomib works and the full function of the proteasome in myeloma and other cells is far from being fully understood. Mechanisms in which MM cells become resistant to Bortezomib have not been understood in patients with relapsing MM. From this thesis work, it has become evident that proteasomes undergo enhanced inhibition through a second mechanism as yet unknown. It is this that could be playing a fundamental role in the susceptibility of MM cells to Bortezomib, as well as potentially playing a role in its resistance. It is therefore essential to decipher what impact these modifications have, and how they can be manipulated, via targeting with therapeutics to create new therapies or to enhance current therapies.

The development of an allosteric inhibitor as described in Chapter 5 has a long way to go before being a viable therapy for the treatment of MM. Although a fourfold enhancement to the potency was achieved throughout the rounds of optimisation, further modification could yield a more potent compound. Other peptides identified in the phage display experiment could also achieve greater levels of inhibition, due to the different chemistries, allowing for different modifications as well as potentially allowing for increased cell permeability. After identifying the most potent variant of this compound, studies would have to be done on its effectiveness in treating myeloma in an in-vivo system. NSG mice that have been engrafted with human myeloma cancer could be used to understand the effectiveness of the drug as well as the toxicity, and the metabolism and half-life of the drug in a biological system.

6.4. Conclusions

In conclusion, I have established and presented from my experimentation a number of findings that were previously unknown to science. Firstly, the discovery of a posttranslational modification on nuclear proteasomes which interferes with SDS-PAGE analysis. Although the exact nature of this modification was not deciphered, further analysis suggested it to be charged and polymeric in nature. The modification was mostly restricted to the nucleus and may play a role in the nuclear processes of proteasomes such as translation and chromatin remodelling. I further demonstrate how bortezomib and other proteasome inhibitors achieve a severe level of proteasome inhibition as shown by the discrepancy between the severe inhibition of *intra cellular* proteasomes vs moderate inhibition of purified proteasomes. This severe level of inhibition is greater in cells that are sensitive to bortezomib treatment and shows some of the first differences between sensitive and resistant cells. The severe inhibition is greatest in sensitive cells and has been shown not to be due to increased drug binding, caspase activation or cell death. However modifications of proteasome subunits change within 2 h after treatment with PIs and are a more likely cause for the excessive intracellular inhibition of proteasome we observed. These changes to CTAB resolvable modified subunits only occur with a lethal dose and occurs 2 h after treatment, showing an early secondary change in response to PI that may explain a secondary mechanism for the increased inhibition of proteasomes *in vivo*. This severe level of inhibition is contrary to the load vs capacity model where it is hypothesised that only a small level of inhibition is required to cause cell death in myeloma. I however show that contrary to a small level of inhibition, myeloma cells undergo severe inhibition. Understanding of this modification could allow for targeting of the different processes of the proteasome and the mechanism by which resistance pursues. If the modification of proteasomes is linked to the level of inhibition and sensitivity of myeloma to PI, manipulation of the modification could prevent resistance or re-sensitise cells to PI.

Finally, I showed that allosteric inhibition of the proteasome by a small 5-mer peptidomeric compound is capable of inhibiting substrate degradation with purified proteasomes and capable of killing myeloma cells *in vitro.* This shows that allosteric proteasome inhibitors be a valid target for proteasome inhibition and myeloma therapies. Allosteric inhibition could also allow for synergistic inhibition of the

proteasome along with traditional proteasome inhibitors and help prevent resistance mechanism through a secondary inhibitory mechanism.

APPENDIX A - Confirmation of *in vitro* degradation System

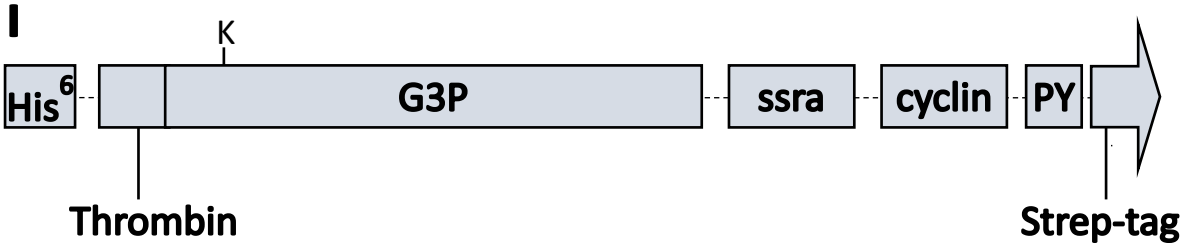
Appendix A - Confirmation of *in vitro* degradation System

The components of the *in vitro* degradation system were expressed and purified as stated in 2.8.1. Samples from each of the components purified were run on SDS-PAGE and total protein stained using Coomassie-R250 (Figure A.ii). All show a major band of the correct size although the purity of E1 was low, but was to be expected as mentioned by Dr Andreas Martin upon gifting of the system.

Ubiquitination of the model substrate was done as stated in method 2.8.1. A reaction mixture was made up of E1, E2, E3, ATP, Ub and the model substrate and incubated for 1 h at 30 ºC. Other control reactions were set up such as substrate only tube and full ubiquitination mixture which was left on ice for 1 h as well as a reaction mixture lacking the E1 enzyme. After the reactions had taken place a small amount was run on SDS-PAGE and the gel stained for total protein with Coomassie-R250 (Figure A.1.iii). Only the reaction containing all components incubated at 30 ºC showed a reduction of the Ub and substrate only band and the appearance of multiple bands correlating to the multiple levels of ubiquitinated substrate.

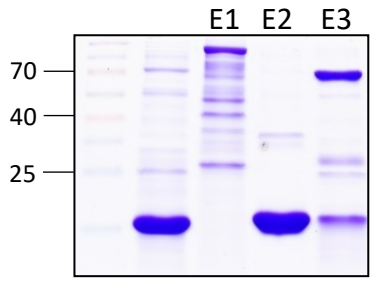
The substrate was purified from the other ubiquitinating enzymes and free Ub using its StrepTag as shown in the substrates domain topology Figure A.1.i. To confirm that purified proteasomes were able to degrade the ubiquitinated substrate, purified yeast proteasomes (Method 2.3.3.) were added to the ubiquitinated substrate as stated in 2.8.1. Substrate only and proteasome only tubes were also mock treated and after 45 min at 30 ºC the reactions were split and run on two SDS-PAGE gels. One gel was transferred and the western blotted for the StrepTag on the substrate before being stripped and blotted for PolyUb. The second gel was stained for total protein using Coomassie-R250 (Figure A.1.iv). In the blot against the StrepTag of the substrate the signal seen in the substrate only lane virtually disappeared in the third lane where proteasome was also added, showing that the substrate was successfully degraded by the proteasome. The next blot showed that the ubiquitin signal remained although a downwards shift was observed between substrate only and substrate + proteasome lanes. This indicates that the full chain is cleaved off and the ubiquitin chains are not hydrolysed any further. The schematic shows the overall process of the removal of the ubiquitin chain and degradation of the substrate into small peptide sequences.

i



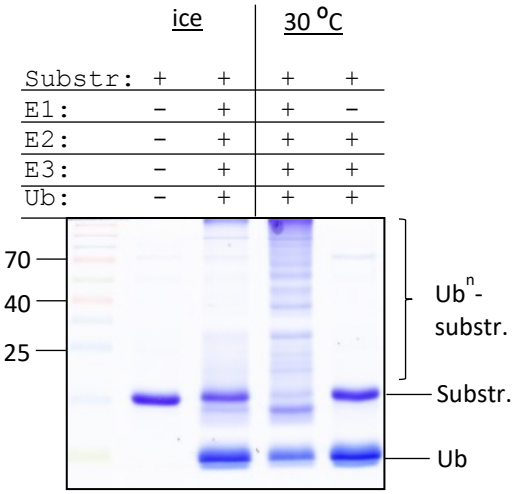
ii

Purified components

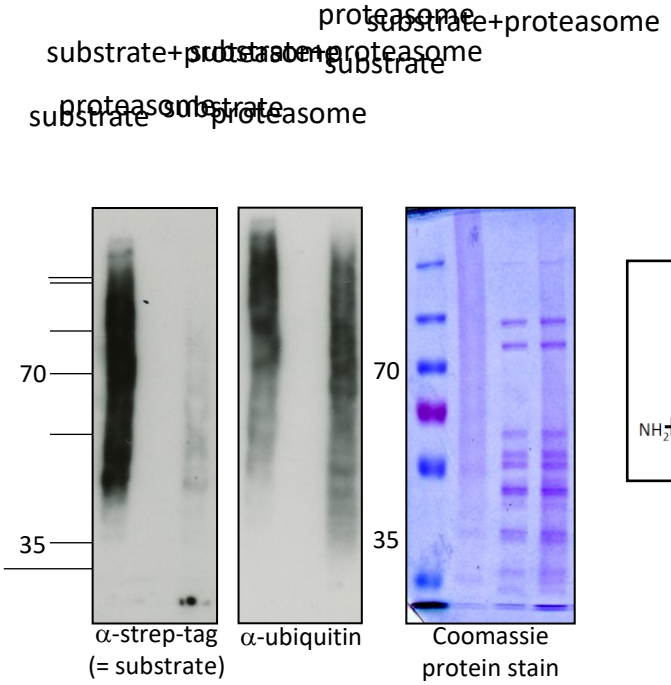


iii

In vitro ubiquitination



iv



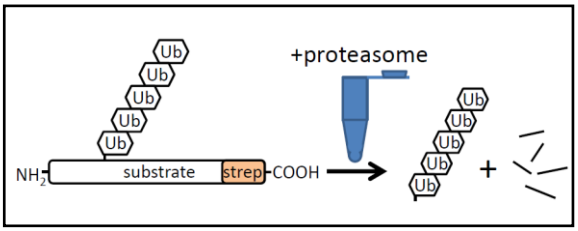
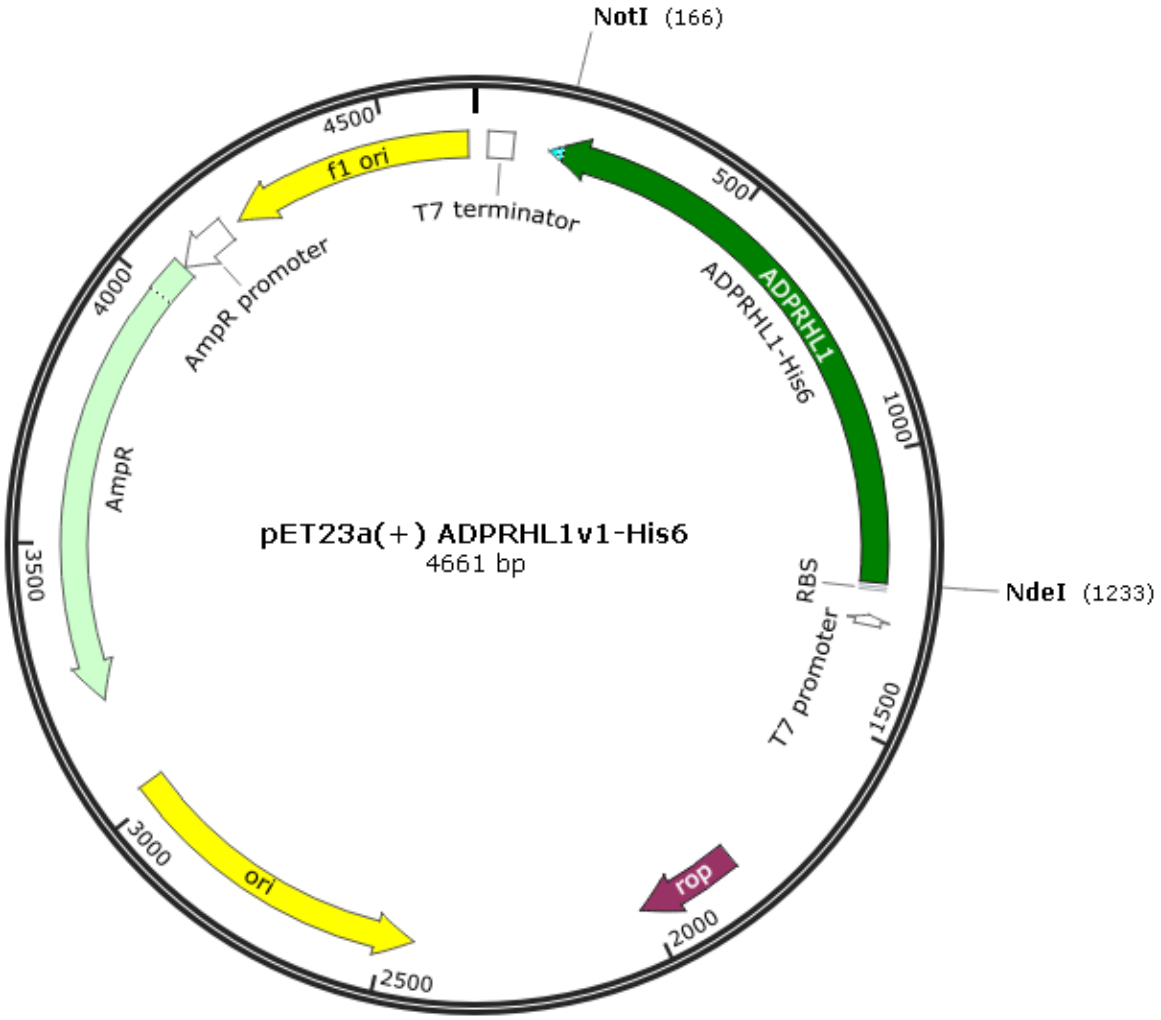


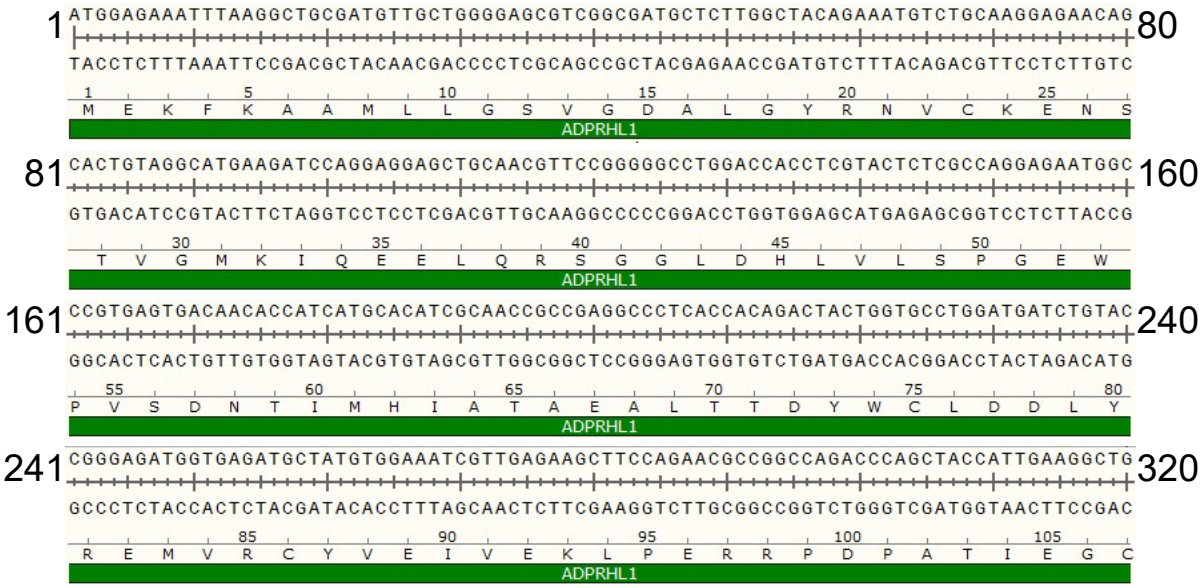
Figure A.1. Testing the ubiquitination of a model substrate and its ability to be degraded by proteasomes.

i) Shows the domain topology of the model substrate kindly gifted by Dr A Martin.His^6 and StrepTag's were used for purification of the substrate away from other bacterial proteins and ubiquitination reaction. An antibody against the StrepTag was also used to detect the substrate by Western analysis. K depicts the lysine ubiquitinated. ii) SDS-PAGE gel of the purified components needed for the ubiquitination of the model substrate. Stained with Coomassie-R250. iii) Coomassie-R250 stained SDS-PAGE gel of the ubiquitination of the substrate. Note that all components are required and the reaction has to be incubated at 30 ºC for ubiquitination to occur. High molecular weight smear indicated the different levels of ubiquitination of the substrate. iv) Shows the ability of proteasomes to degrade the substrate. The substrate and proteasome were incubated at 30 ºC for 45 min before being run on an SDS-PAGE gel with substrate only and proteasome only controls. Westerns were blotted for StrepTag on the model substrate (Note the disappearance of the signal showing degradation of the substrate) and ubiquitin (Note the shift downwards of ubiquitin smear. Indicative of removal of polyUb chain off substrate) Schematic shows overall process happening when ubiquitinated substrate is incubated with proteasome.

APPENDIX B - Plasmid and sequence maps for ADPRHL1 variant 1 + 2 bacterial over expression plasmids

I. ADPRHL1 variant 1 -His6 Bacterial Overexpression Plasmid





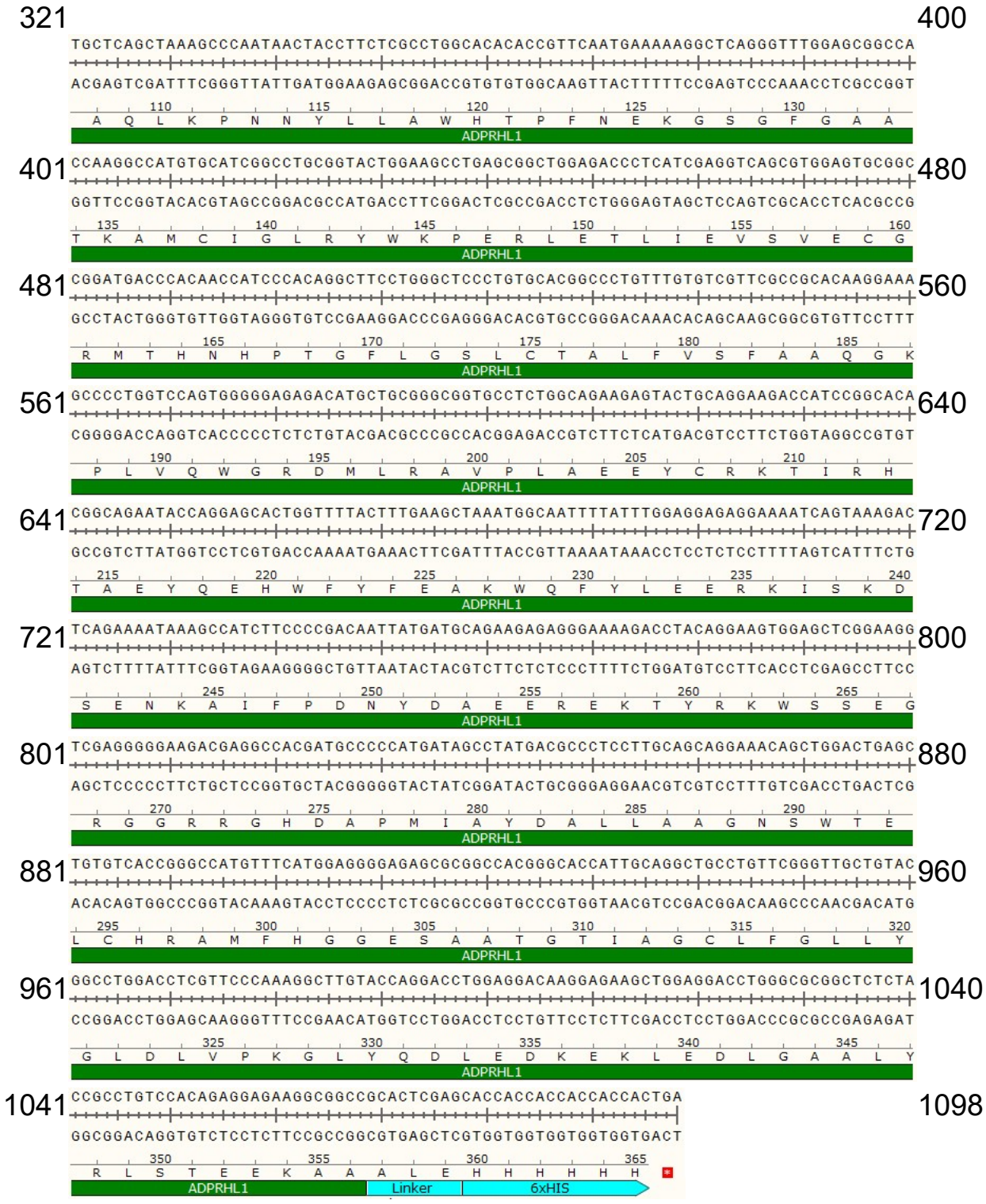
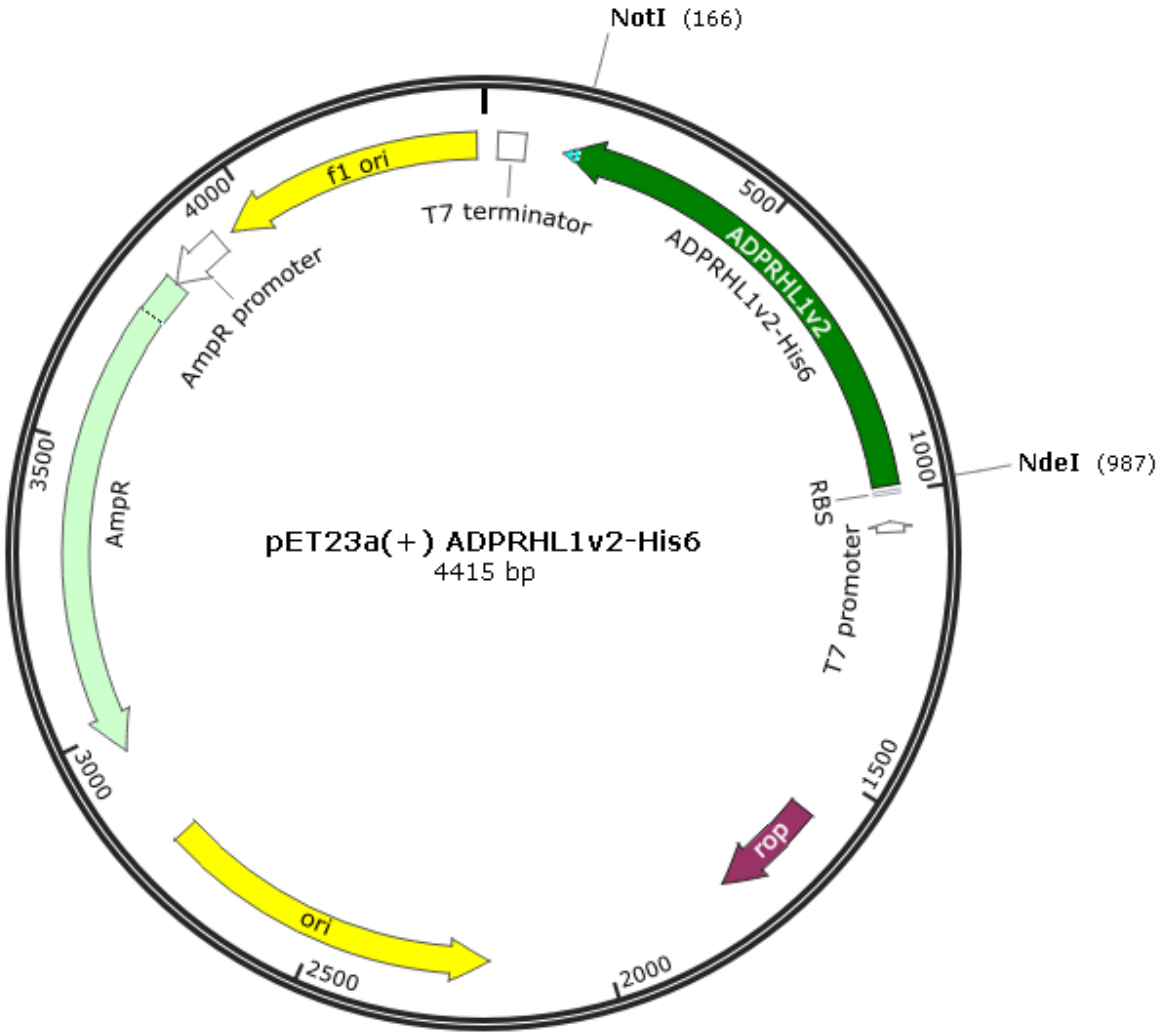

321
400
TGCTCAGCTAAAGCCCAATAACTACCTTCTCGCCTGGCACACACCGTTCAATGAAAAAGGCTCAGGGTTTGGAGCGGCCA
ACGAGTCGATTTCGGGTTATTGATGGAAGAGCGGACCGTGTGTGGCAAGTTACTTTTTCCGAGTCCCAAACCTCGCCGGT
110 115 120 125 130
A Q L K P N N Y L L A W H T P F N E K G S G F G A A
ADPRHL1
401
CCAAGGCCATGTGCATCGGCCTGCGGTACTGGAAGCCTGAGCGGCTGGAGACCCTCATCGAGGTCAGCGTGGAGTGCGGC
480
GGTTCCGGTACACGTAGCCGGACGCCATGACCTTCGGACTCGCCGACCTCTGGGAGTAGCTCCAGTCGCACCTCACGCCG
135 140 145 150 155 160
T K A M C I G L R Y W K P E R L E T L I E V S V E C G
ADPRHL1
481
CGGATGACCCACAACCATCCCACAGGCTTCCTGGGCTCCCTGTGCACGGCCCTGTTTGTGTCGTTCGCCGCACAAGGAAA
560
GCCTACTGGGTGTTGGTAGGGTGTCCGAAGGACCCGAGGGACACGTGCCGGGACAAACACAGCAAGCGGCGTGTTCCTTT
165 170 175 180 185
R M T H N H P T G F L G S L C T A L F V S F A A Q G K
ADPRHL1
561
GCCCCTGGTCCAGTGGGGGAGAGACATGCTGCGGGCGGTGCCTCTGGCAGAAGAGTACTGCAGGAAGACCATCCGGCACA
640
CGGGGACCAGGTCACCCCCTCTCTGTACGACGCCCGCCACGGAGACCGTCTTCTCATGACGTCCTTCTGGTAGGCCGTGT
190 195 200 205 210
P L V Q W G R D M L R A V P L A E E Y C R K T I R H
ADPRHL1
641
CGGCAGAATACCAGGAGCACTGGTTTTACTTTGAAGCTAAATGGCAATTTTATTTGGAGGAGAGGAAAATCAGTAAAGAC
720
GCCGTCTTATGGTCCTCGTGACCAAAATGAAACTTCGATTTACCGTTAAAATAAACCTCCTCTCCTTTTAGTCATTTCTG
215 220 225 230 235 240
T A E Y Q E H W F Y F E A K W Q F Y L E E R K I S K D
ADPRHL1
721
TCAGAAAATAAAGCCATCTTCCCCGACAATTATGATGCAGAAGAGAGGGAAAAGACCTACAGGAAGTGGAGCTCGGAAGG
800
AGTCTTTTATTTCGGTAGAAGGGGCTGTTAATACTACGTCTTCTCTCCCTTTTCTGGATGTCCTTCACCTCGAGCCTTCC
245 250 255 260 265
S E N K A I F P D N Y D A E E R E K T Y R K W S S E G
ADPRHL1
801
TCGAGGGGGAAGACGAGGCCACGATGCCCCCATGATAGCCTATGACGCCCTCCTTGCAGCAGGAAACAGCTGGACTGAGC
880
AGCTCCCCCTTCTGCTCCGGTGCTACGGGGGTACTATCGGATACTGCGGGAGGAACGTCGTCCTTTGTCGACCTGACTCG
270 275 280 285 290
R G G R R G H D A P M I A Y D A L L A A G N S W T E
ADPRHL1
881
TGTGTCACCGGGCCATGTTTCATGGAGGGGAGAGCGCGGCCACGGGCACCATTGCAGGCTGCCTGTTCGGGTTGCTGTAC
960
ACACAGTGGCCCGGTACAAAGTACCTCCCCTCTCGCGCCGGTGCCCGTGGTAACGTCCGACGGACAAGCCCAACGACATG
295 300 305 310 315 320
L C H R A M F H G G E S A A T G T I A G C L F G L L Y
ADPRHL1
961
GGCCTGGACCTCGTTCCCAAAGGCTTGTACCAGGACCTGGAGGACAAGGAGAAGCTGGAGGACCTGGGCGCGGCTCTCTA
1040
CCGGACCTGGAGCAAGGGTTTCCGAACATGGTCCTGGACCTCCTGTTCCTCTTCGACCTCCTGGACCCGCGCCGAGAGAT
325 330 335 340 345
G L D L V P K G L Y Q D L E D K E K L E D L G A A L Y
ADPRHL1
1041
CCGCCTGTCCACAGAGGAGAAGGCGGCCGCACTCGAGCACCACCACCACCACCACTGA
1098
GGCGGACAGGTGTCTCCTCTTCCGCCGGCGTGAGCTCGTGGTGGTGGTGGTGGTGACT
350 355 360 365
R L S T E E K A A A L E H H H H H H *
ADPRHL1
Linker
6xHIS

Figure B.1. Plasmid map and confirmed sequence of ADP-ribosylhydrolase like 1 (ADPRHL1) transcript variant 1

ADPRHL1 variant 1 which encodes the ARH2 variant 1 gene was amplified from HeLa cDNA using Forward (5'-TACATATGGAGAAATTTAAGGCTGCGATGTTGC-3') and reverse (5'-AAGCGGCCGCCTTCTCCTCTGTGGACAGGCGGTAG-3') primers and cloned into pET2a(+) vector using *Nde*I and *Not*I restriction sites. Sequence confirmed by sanger sequencing.

II. ADPRHL1 variant 2 -His6 Bacterial Overexpression Plasmid





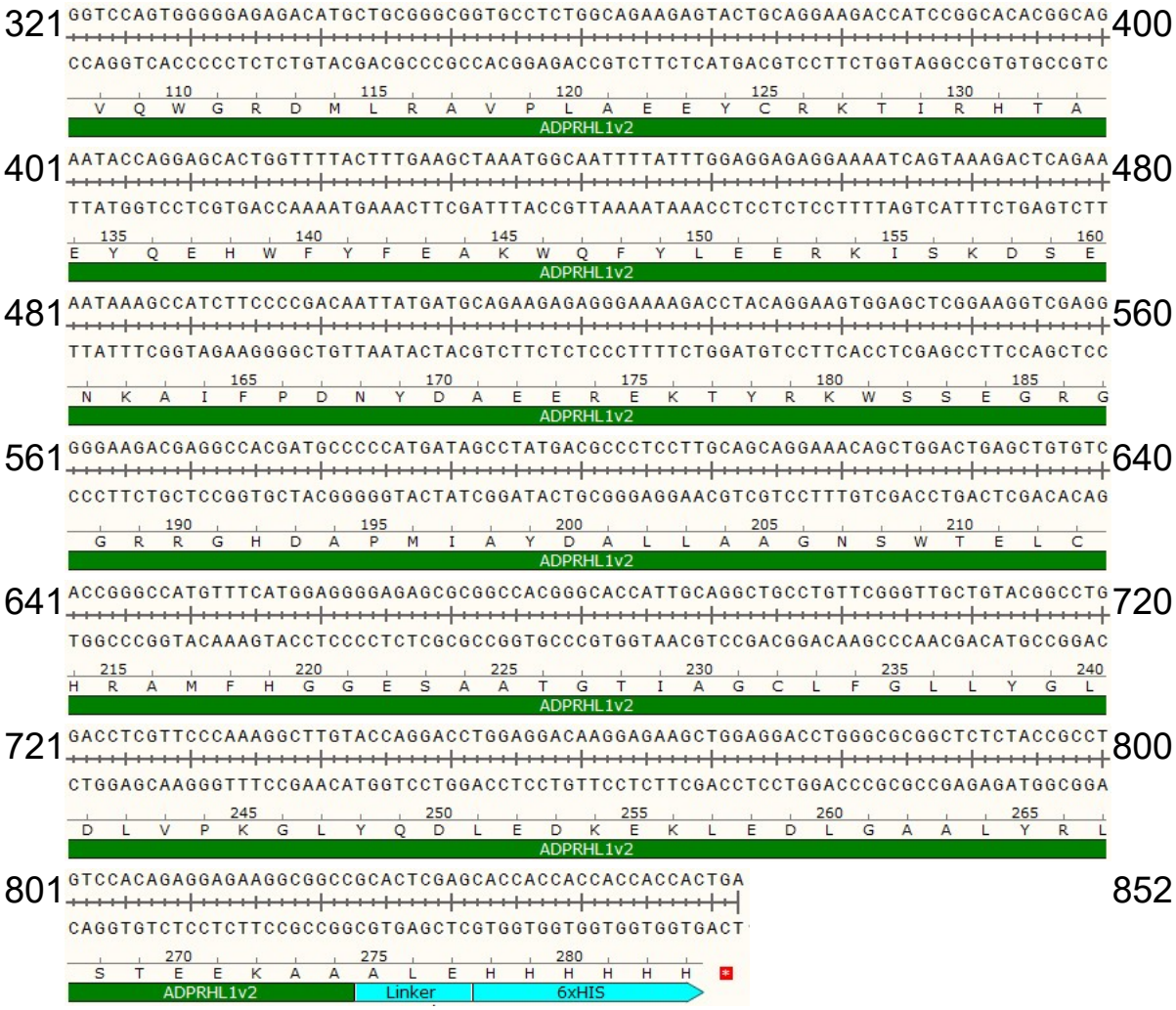
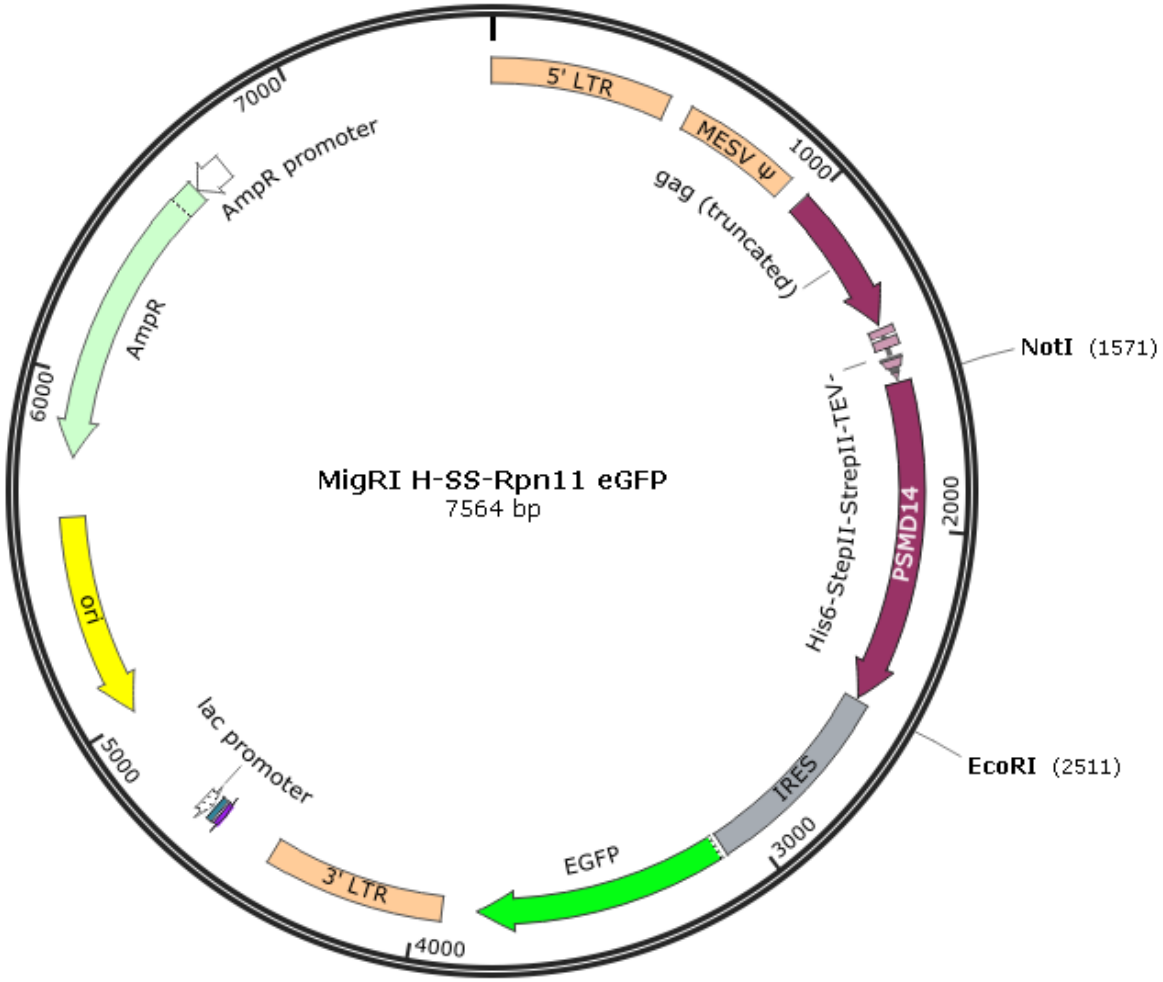


Figure B.2. Plasmid map and confirmed sequence of ADP-ribosylhydrolase like 1 (ADPRHL1) transcript variant 2

ADPRHL1 variant 2 which encodes the ARH2 variant 2 gene was amplified from HeLa cDNA using Forward (5'- TACATATGGTGAGATGCTATGTGGAAATCG -3') and reverse (5'- GGGCGGCCGCCTTCTCCTCTGTGGACAGGCGGTAG -3') and cloned into pET2a(+) vector using *Nde*I and *Not*I restriction sites. Sequence confirmed by sanger sequencing.

APPENDIX C- Creation of an OPM2 cell line over expressing a tagged Rpn11 subunit


MigRI H-SS-Rpn11 eGFP
7564 bp
5' LTR
MESV Ψ
gag (truncated)
NotI (1571)
His6-StepII-StrepII-TEV-
PSMD14
EcoRI (2511)
IRES
EGFP
3' LTR
lac promoter
ori
AmpR
AmpR promoter
1000
2000
3000
4000
5000
6000
7000


1 atgcatcatcaccatcaccactacgtgactttatggagccatccgcagtttgaaaaaggcggcggcagcggcggcggcag 80
tacgtagtagtggtagtggtgatgcactgaaatacctcggtaggcgtcaaacttttccgccgccgtcgccgccgccgtc
M H H H H H H Y V T L W S H P Q F E K G G G S G G G S
6xHis
Strep-Tag II
81 cggcggcggcagctggagccatccgcagtttgaaaaaggcagcgcggcgagcgagaacctctacttccagggccGCGGCC 160
gccgccgccgtcgacctcggtaggcgtcaaacttttccgtcgcgccgctcgctcttggagatgaaggtcccggCGCCGG
G G G S W S H P Q F E K G S A A S E N L Y F Q G R G
Strep-Tag II
TEV
161 GCATGGACAGACTTCTTAGACTTggaggaggtatgcctggactgggccaggggccacctacagatgctcctgcagtggac 240
CGTACCTGTCTGAAGAATCTGAAcctcctccatacggacctgacccggtccccggtggatgtctacgaggacgtcacctg
R M D R L L R L G G G M P G L G Q G P P T D A P A V D
PSMD14
241 acagcagaacaagtctatatctcttccctggcactgttaaaaatgttaaaacatggccgtgctggagttccaatggaagt 320
tgtcgtcttgttcagatatagagaagggaccgtgacaatttttacaattttgtaccggcacgacctcaaggttaccttca
T A E Q V Y I S S L A L L K M L K H G R A G V P M E V
PSMD14
321 tatgggtttgatgcttggagaatttgttgatgattataccgtcagagtgattgatgtgtttgctatgccacagtcaggaa 400
atacccaaactacgaacctcttaaacaactactaatatggcagtctcactaactacacaaacgatacggtgtcagtcctt
M G L M L G E F V D D Y T V R V I D V F A M P Q S G
PSMD14

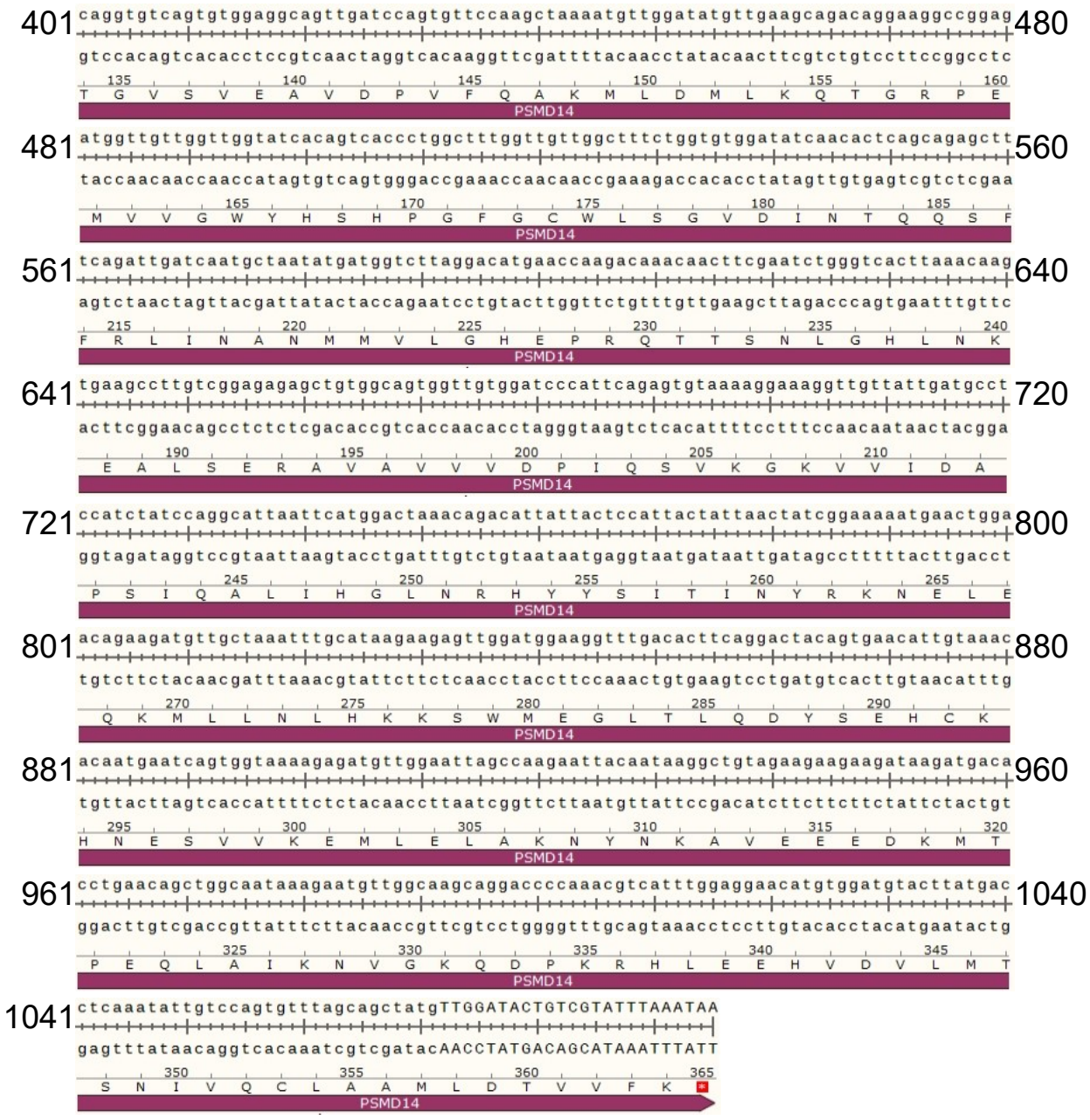


Figure C.1. Plasmid map and confirmed sequence of His^{6}-2(StrepIITag)-TeV-PSMD14 retroviral expression plasmid

Cloning of construct was done in two steps. Firstly, the annealing of two pairs of oligos (making up the tag sequence) and subsequent three-way ligation into *Bgl*II:*Xho*I linearised vector. Secondly Amplification of PSMD14 encoding Rpn11 before being ligated in frame into MigRI now containing the tag using *Eco*RI and *Not*I restriction sites. Sequence confirmed by sanger sequencing

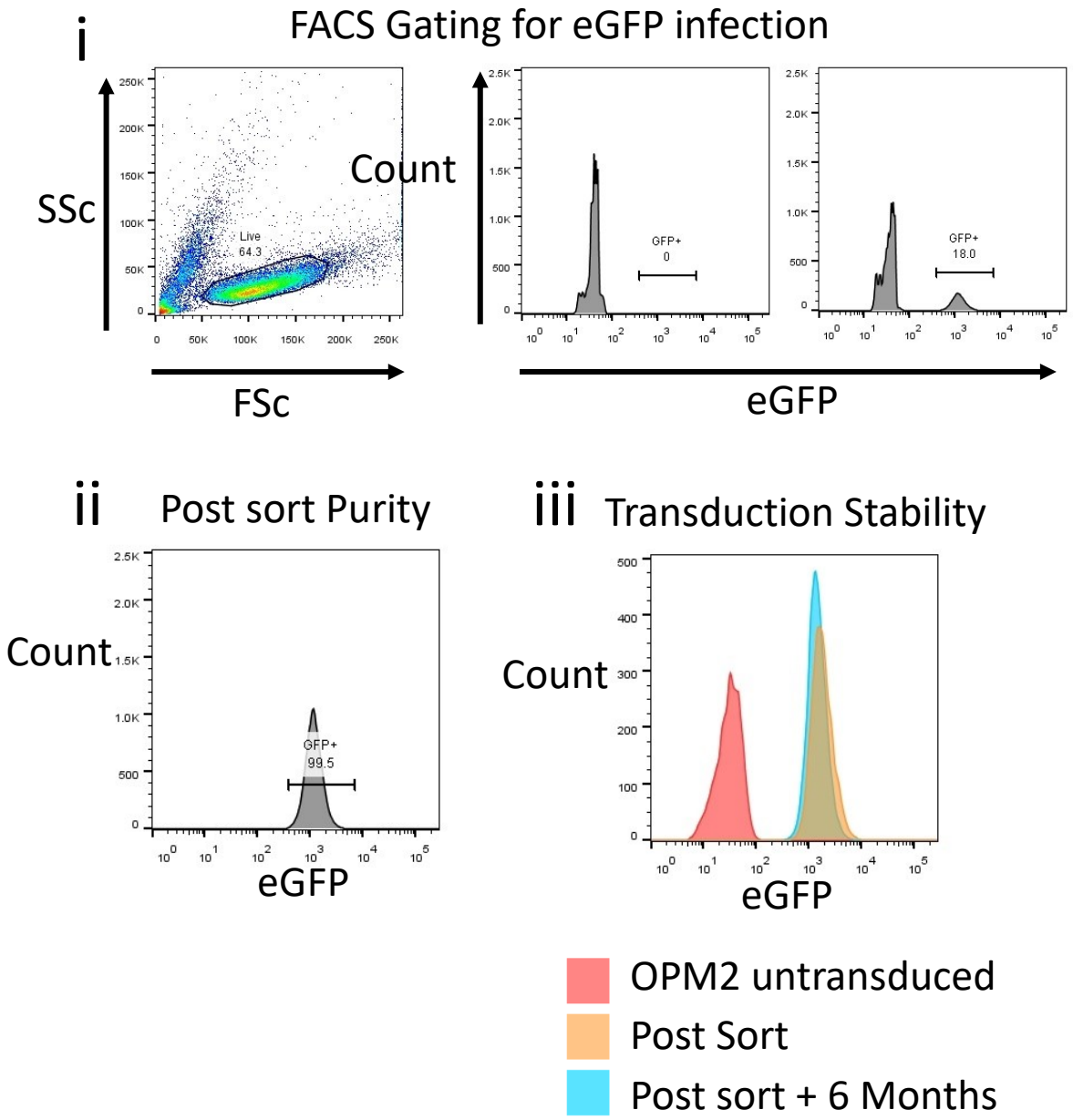
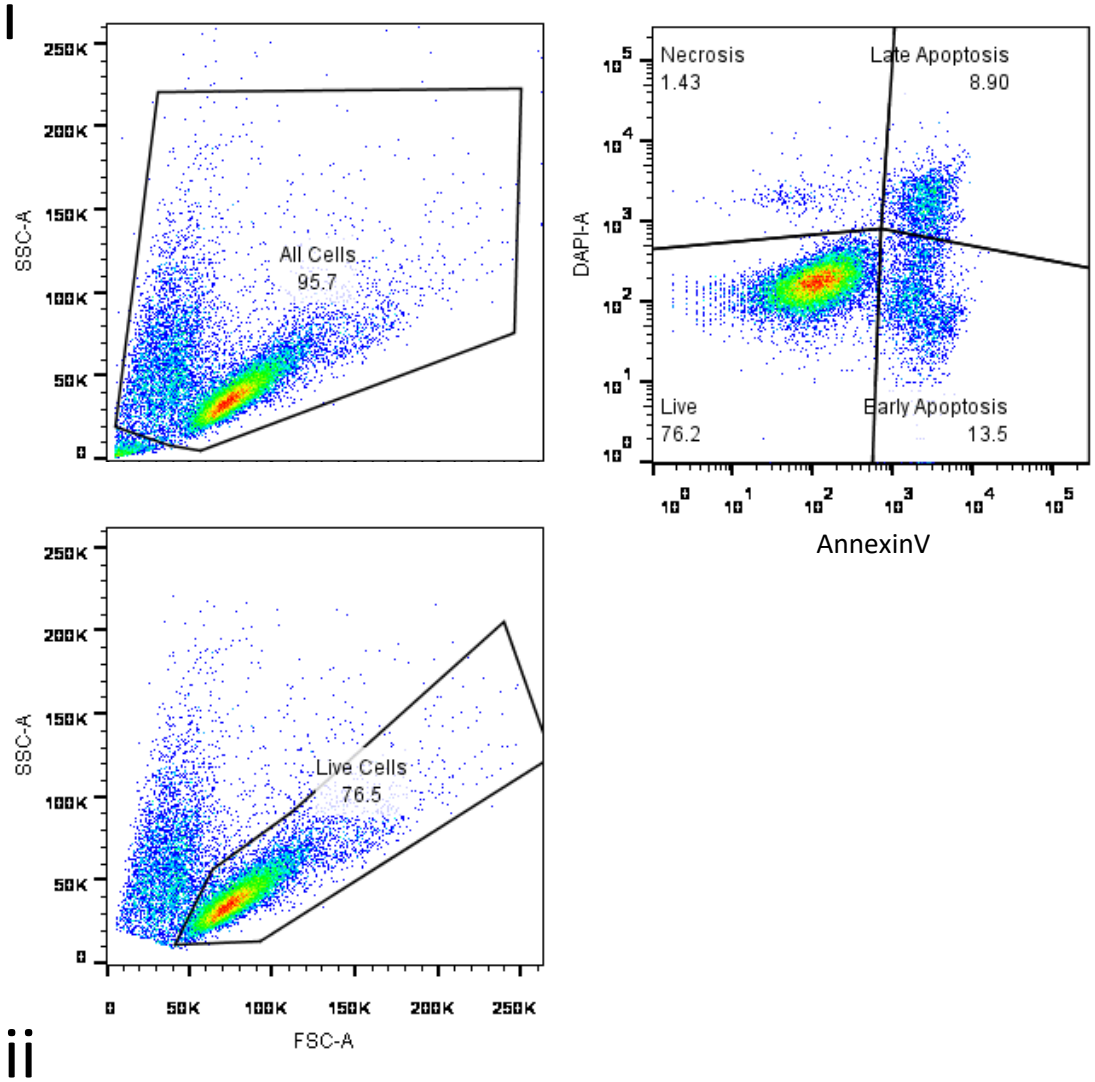


Figure C.2. FACS Gating strategy, Purity and stability analysis

i) Shows the sorting of the His^6-2(StrepIITag)-TeV-Rpn11 transduced cells. Gating was first done on the live cells (Forward Scatter $(FSc)^{HIGH}$ Side Scatter $(SSc)^{LOW}$). The next two plots show untransduced cells whilst the right shows the His^6-2(StrepIITag)-TeV-Rpn11 transduced cells with an 18 % transduction efficiency, and GFP^+ gating. ii) Shows the purity of the cells after sorting. iii) Shows the stability of the cells grown for 6 months to that of a recently thawed vial from sort compared to non transduced OPM2 myeloma cells.

APPENDIX D - Flow cytometry Gating Strategy

i


SSC-A
All Cells
95.7
DAPI-A
Necrosis
1.43
Late Apoptosis
8.90
Live
76.2
Early Apoptosis
13.5
AnnexinV
Live Cells
76.5
FSC-A

ii

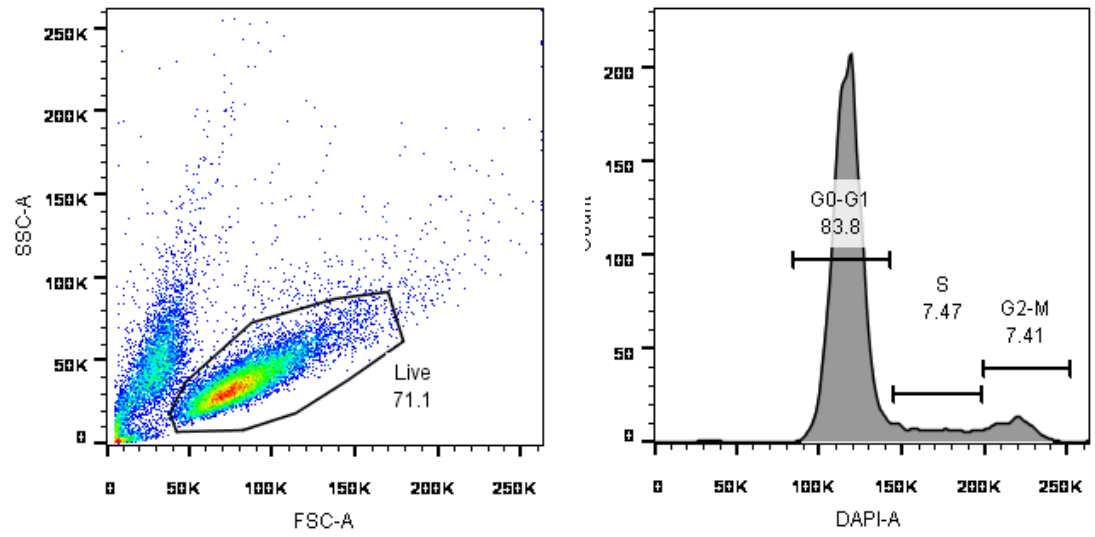

SSC-A
Live
71.1
FSC-A
G0-G1
83.8
S
7.47
G2-M
7.41
DAPI-A

Figure D.1. Gating strategies for flow cytometric analysis of cells

i) Shows the gating done for cell viability. Cells are first gated on both the live and dead populations, removing the $FSc^{LOW}SSc^{LOW}$ events correlating to cell fragments. To the AnnexinV/DAPI staining the live, early apoptotic, late apoptotic and necrotic cells were gated as shown in the right panel. For those cells whose viability was measure by simple FSc/SSc the first gating was done identically, then the live cells were gated on the FSc^{HIGH} SSc^{LOW} population. Note the similarity of the Live percentages done both ways on the same sample. ii) For the cell cycle analysis was carried out by first gating on the live cells FSc^{HIGH} SSc^{LOW} and then gating on the three different populations as shown in the right panel.

APPENDIX E - Published Papers

Biochimica et Biophysica Acta 1844 (2014) 2222–2228

Contents lists available at ScienceDirect

Biochimica et Biophysica Acta

journal homepage: www.elsevier.com/locate/bbapap

Nuclear proteasomes carry a constitutive posttranslational modification which derails SDS-PAGE (but not CTAB-PAGE)

David S. Pitcher [a], Kate de Mattos-Shipley [a], Ziming Wang [a], Konstantinos Tzortzis [a], Katerina Goudevenou [a], Helen Flynn [b], Georg Bohn [a], Amin Rahemtulla [a], Irene Roberts [a], Ambrosius P. Snijders [b], Anastasios Karadimitris [a], Maurits F. Kleijnen [a,*]

[a] Centre for Haematology, Division of Experimental Medicine, Faculty of Medicine, Imperial College London, Hammersmith Campus, Commonwealth Building 4th Floor, Du Cane Road, London W12 0NN, United Kingdom
[b] London Research Institute, Clare Hall Laboratories, Blanche Lane, South Mimms, Potters Bar EN6 3LD, United Kingdom

ARTICLE INFO

Article history:
Received 29 April 2014
Received in revised form 22 August 2014
Accepted 24 August 2014
Available online 2 September 2014

Keywords:
CTAB-PAGE
Proteasome
ADP-ribose
Ubiquitin
Nuclear biology
Apoptosis

ABSTRACT

We report that subunits of human nuclear proteasomes carry a previously unrecognised, constitutive posttranslational modification. Subunits with this modification are not visualised by SDS-PAGE, which is used in almost all denaturing protein gel electrophoresis. In contrast, CTAB-PAGE readily visualises such modified subunits. Thus, under most experimental conditions, with identical samples, SDS-PAGE yielded gel electrophoresis patterns for subunits of nuclear proteasomes which were misleading and strikingly different from those obtained with CTAB-PAGE. Initial analysis indicates a novel modification of a high negative charge with some similarity to polyADP-ribose, possibly explaining compatibility with (positively-charged) CTAB-PAGE but not (negatively-charged) SDS-PAGE and providing a mechanism for how nuclear proteasomes may interact with chromatin, DNA and other nuclear components.

© 2014 Elsevier B.V. All rights reserved.

1. Introduction

Most denaturing protein gel electrophoresis is done using SDS-PAGE, discontinuous sodium dodecyl sulphate polyacrylamide gel electrophoresis [1], due to its ease-of-use and reliability [2]. Although some posttranslational modifications may affect the migration behaviour of proteins on SDS-PAGE, *e.g.* N-linked glycosylation, SDS-PAGE is believed to, and generally does, faithfully represent the composition of complex protein mixtures [2]. However, we now report a novel modification of nuclear proteasomes that prevents SDS-PAGE from visualising the proteasomal subunits. By way of further background, proteasomes [3,4] are 2.5 MDa protease complexes, located in the cytoplasm and nucleus, which degrade ubiquitin-marked protein substrates. There is an alternative to SDS-PAGE, the much less used CTAB (cetyl trimethyl ammonium bromide)-PAGE system [5,6]. We report that, unlike SDS-PAGE, CTAB-PAGE *does* visualise these modified subunits of nuclear proteasomes. Thus, for nuclear proteins, combined use of SDS-PAGE and CTAB-PAGE may be required to capture sample complexity. Initial analysis into the nature of the posttranslational modification indicates that the modification shares several characteristics with, but also is distinct from, classical ADP-ribose chains.

* Corresponding author.
E-mail address: m.kleijnen@imperial.ac.uk (M.F. Kleijnen).

2. Materials and methods

2.1. Antibodies, chemicals, enzymes, western blotting, tissue culture

The following is a list of commercial antibodies and their corresponding manufacturers: α-Rpn10/S5a (MoAb S5a-18, BML-PW9250), α-Rpn12/S14 (PAb, BML-PW8815), α-20S α7 (MoAb LN43, BML-PW8110), α-20S α6 (MoAb MCP20, BML-PW8100), α-Rpt1/S7 (MoAb MSS1-104, BML-PW8825), α-Rpt2/S4 (PAb, BML-PW8305), α-Rpt3/S6b (PAb, BML-PW8175), α-Rpt4/S10b (MoAb p42-23, PW8830), α-Rpt5/S6a (MoAb TBP1-19, PW8770), α-'core' CP subunits (PAb, PW8155), α-β5i/LMP7 (PAb, PW8355), α-ubiquitin (FK2, PW8810), and α-poly(ADP-ribose) (PAb 96-10-04, ALX-210-890-R100) are from Enzo Lifesciences. α-Rpn1/S2 (539166) is from Calbiochem. α-Lamin B2 (MoAb, ab8983) is from Abcam. α-SMARCB1/Ini1 (PAb, sc-13055) is from Santa Cruz. α-Ubiquilin1 (MoAb, 377700) is from Invitrogen.

Bortezomib is from Millennium/Takeda. Epoxomicin and Ada-K(Biot)-Ahx3-L3-VS are from Enzo Lifesciences. Doxorubicin, vinblastin, cycloheximide, and epigallocatechin gallate (EGCG) are from Sigma-Aldrich. Micrococcal nuclease, RNaseA/T1, RNaseH and RNAse1 are from Fermentas/Thermo Scientific. Antibodies against yeast proteasome are from Dr. Daniel Finley, Harvard Medical School. The α-Dbf11 antibody is from Dr. Christian Speck, CSC-MRC London. We generated β-glucanase (*Oerskovia xanthineolytica*) using an *Escherichia coli* strain

http://dx.doi.org/10.1016/j.bbapap.2014.08.013
1570-9639/© 2014 Elsevier B.V. All rights reserved.

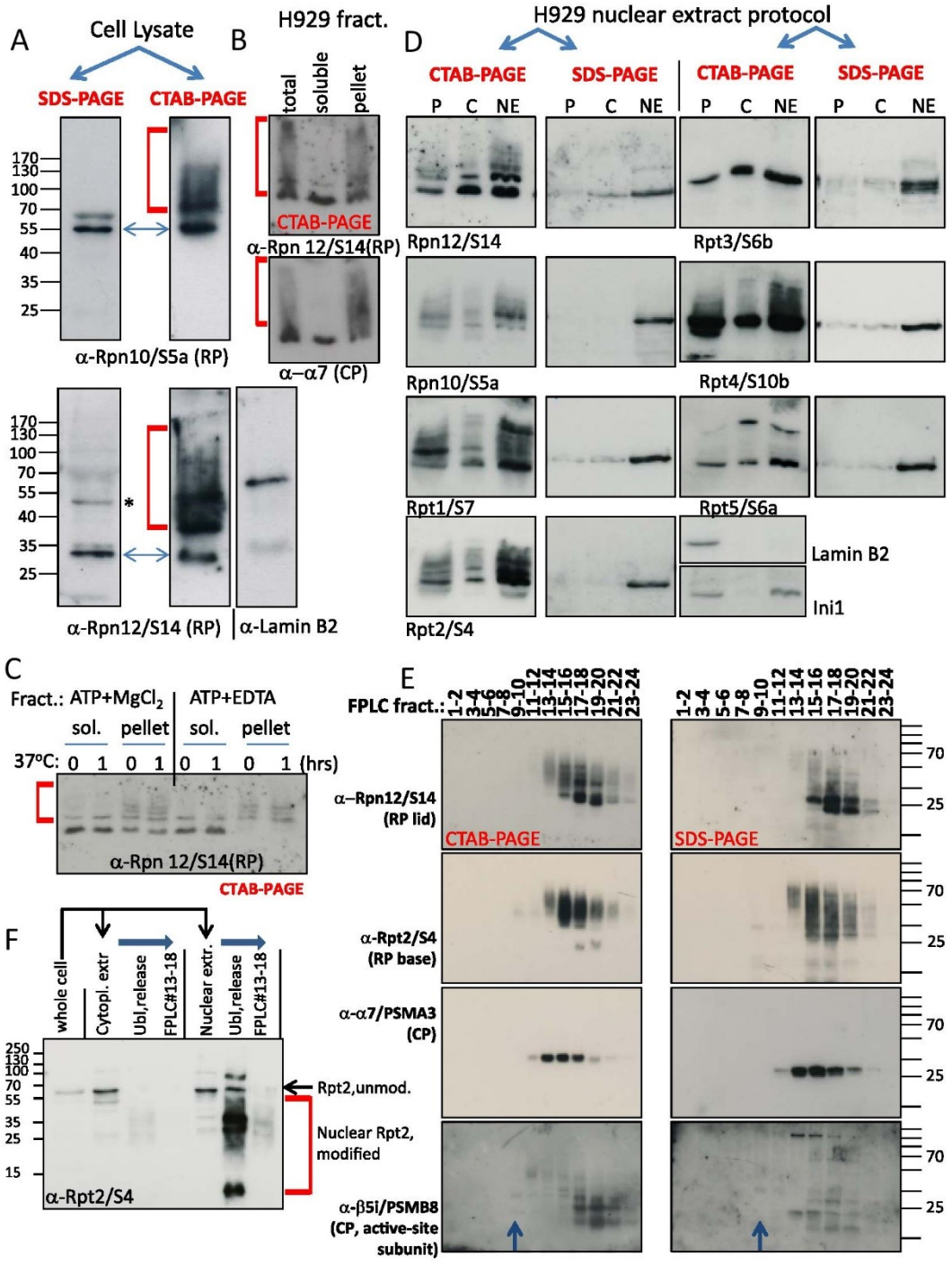


Fig. 1. A proteasome modification that correlates with subcellular localization. (A) Lysate from KMS12-BM myeloma cells was split and run on SDS and CTAB PAGE systems, before being blotted for proteasome subunits. Red brackets indicate signal unique to CTAB-PAGE. Note that CTAB-PAGE is not inherently prone to smearing: not all proteins we tested migrated as a smear (*e.g.* LaminB2, Fig. 1A; Ini1, Rpt3, Fig. 1D), and lanes with a CTAB-PAGE-unique smear also contained sharply focused bands. (B) NCI-H929 myeloma cells were subjected to subcellular fractionation, and fractions were analysed by Western blotting against proteasome subunits using CTAB-PAGE. Red brackets indicate CTAB-PAGE unique signal. (C) Presence of divalent cations in fractionation buffer affects CTAB-PAGE pattern. NCI-H929 myeloma cells were fractionated using a cytosol extraction buffer containing either $MgCl_2$ or EDTA. Fractions were kept on ice or incubated at 37 °C for 1 h, after which they were analysed using CTAB-PAGE and Western blotting with an α-Rpn12/S14 proteasome subunit antibody. (D) Cell fractionation of NCI-H929 cells was extended with a nuclear extraction step. All fractions were split and subjected to CTAB-PAGE and SDS-PAGE, and analysed by Western blotting against proteasome subunits. P = pellet remaining after nuclear extraction, C = cytosolic extract, NE = nuclear extract. Notice that although the same protein was loaded on both systems, SDS-PAGE doesn't display all of the species observed in CTAB-PAGE. The fractionation protocol (Materials and methods, Section 2.1) normalises for cell number: lanes contain the amount of protein extracted or remaining in pellet per equal number of cells. In addition, by employing a very efficient stripping procedure [7], the same membrane is used for all antibodies, thus eliminating pipetting variation between panels. (E) Nuclear human proteasomes were affinity-captured from nuclear extract with a ubiquitin-like proteasome binding domain (Ubl-His_6), released, and subjected to Superose6 FPLC fractionation. FPLC fractions were analysed on both CTAB-PAGE and SDS-PAGE by Western blotting against proteasome subunits. Arrows indicate a Blue Dextran FPLC marker band. (F) Protein samples were taken from different stages of a large-scale nuclear human proteasome purification experiment, and immunoblotted with an α-Rpt2 proteasome antibody. Unmodified Rpt2 is indicated by an arrow, modified nuclear Rpt2 species are indicated with a red bracket.

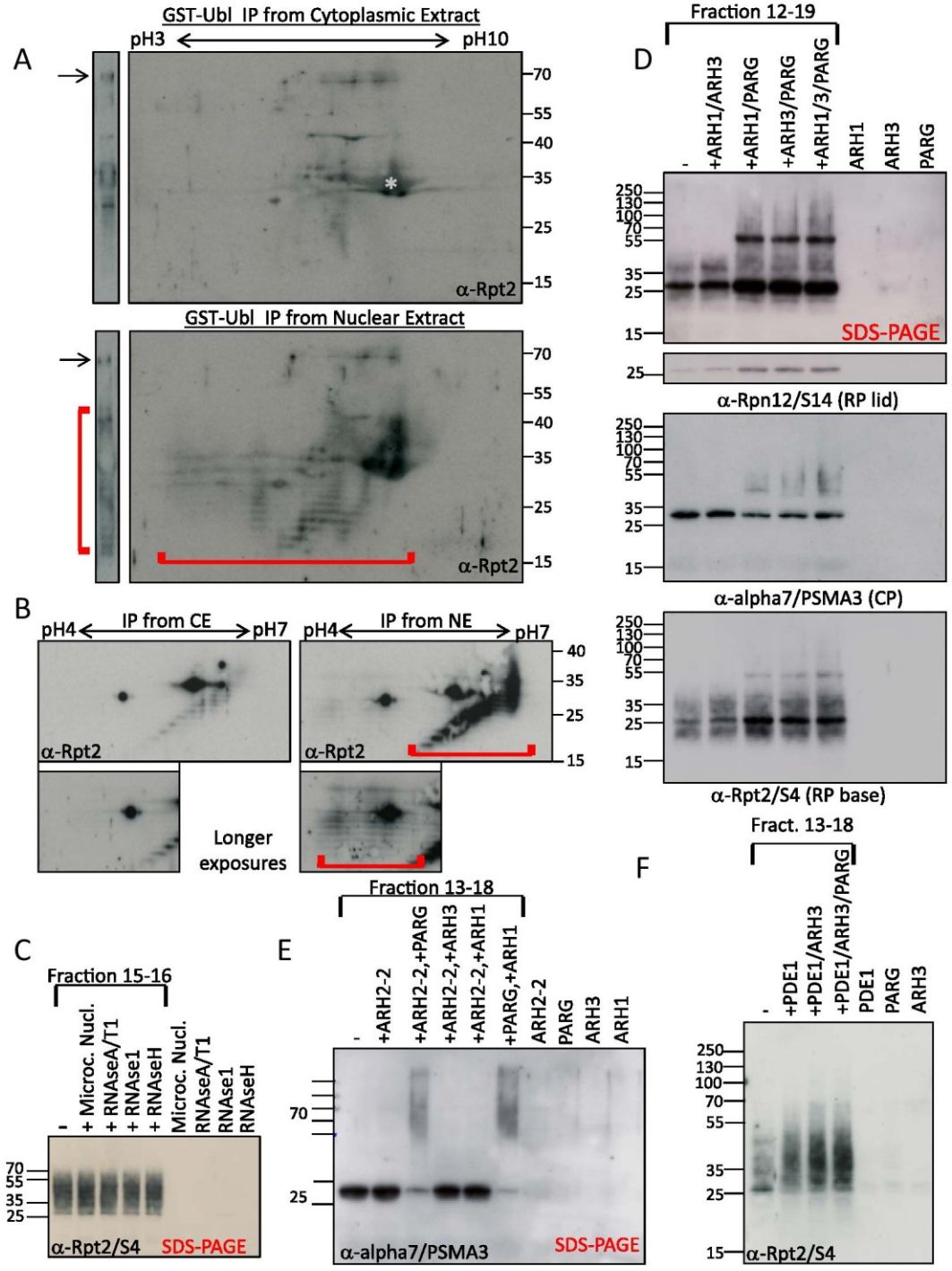


Fig. 2. The constitutive modification of proteasomes shares several characteristics with – but is distinct from – poly(ADP)-ribose. (A) Proteasomes were captured, using GST-Ubl (see also Fig. S2), from both cytoplasmic extract and subsequent nuclear extract of myeloma OPM2 cells. The two samples were compared on two-dimensional isoelectric focusing/SDS-PAGE with an α-Rpt2 antibody. The red brackets indicate where nucleus-extracted, modified Rpt2 focuses in a pH 3–10 linear gradient. Care was taken to ensure that the isoelectric focusing was run to completion and that steady-state positions were reached. * Indicates a nonspecific signal due to the presence of a large amount of GST-Ubl (see corresponding PonceauS staining in Fig. S3A). (B) Experiment as in (A), but this time samples were analysed on a narrow-range pH 4–7 gradient. A longer exposure of the left part of the gel is shown underneath to highlight the 'striated' focusing phenotype. (C) Nuclear proteasomes were captured with Ubl-His_6 and further purified by FPLC, as in Fig. 1E. Combined proteasome FPLC fractions 13–18 were incubated with nucleotide modification enzymes Micrococcal Nuclease, RNaseA/T1 mixture, RNAse1 and RNaseH. Samples were run on SDS-PAGE, and analysed by Western blot using an α-Rpt2/S4 proteasomal subunit antibody. (D) Pooled FPLC fractions 12–19 were incubated with combinations of PAR hydrolysing enzymes PARG, ARH1 and ARH3. Subsequently, samples were analysed by SDS-PAGE and Western blotting using several antibodies against proteasomal subunits. PAR enzyme-dependent changes in subunit patterns were observed for Rpn12, α7 and Rpt2. Prior to re-probing, the membrane was checked after stripping [7] and found to be void of signal. (E) The orphan PAR enzyme ARH2, for which no substrate is known as yet, does not affect the migration behaviour of the α7 proteasome subunit. Two isoforms of ARH2 were cloned and tested, neither of which had activity; shown here is ARH-2.2. (F) FPLC fractions were incubated with phosphodiesterase 1 (PDE1), ARH3 and PARG. Samples were run on SDS-PAGE, and analysed by Western blot using an α-Rpt2/S4 proteasomal subunit antibody.

material and that it persisted *in isolation*. Most of the main-band material was NP40-extractable (cytosolic), whereas the CTAB-PAGE-unique bands were found in the nuclear pellet and could be separated further from chromatin and the nuclear architecture using a nuclear extraction step (Fig. 1D) [8]. EDTA in the fractionation buffer improved separation of the main band from the collection of high-molecular-weight

bands, bands which were then stable and immune even to prolonged incubation at 37 °C (Fig. 1C). A subsequent high-salt nuclear extraction step removed about half of the proteasomes from the nuclear pellet; we used the chromatin remodelling complex component SMARCB1/Ini1 as positive control and Lamin B2 as negative control (Fig. 1D). Note that it was *not* the nuclear environment in which proteasomes reside in at the moment of encountering CTAB in the lysis buffer that determined their subunits' migration behaviour on CTAB-PAGE: CTAB-PAGE-unique bands persisted when proteasomes were extracted away from chromatin and nuclear architecture prior to exposure to CTAB (Fig. 1D) and, in the case of yeast *Saccharomyces cerevisiae*, nuclear and cytosolic proteasome subunits migrated identically on CTAB-PAGE (below, Fig. S4C).

Additional validation that CTAB-PAGE-unique bands corresponded to true protein species came from identifying experimental conditions under which *also* SDS-PAGE could visualise the CTAB-PAGE-unique bands, thus uncoupling visualisation of protein species from use of a particular PAGE system. While Fig. 1D's sub-cellular fractionation experiment still revealed a striking discrepancy between the *same* samples' SDS-PAGE and CTAB-PAGE patterns, further purification steps led to a convergence of each proteasome subunit pattern on both PAGE systems. Importantly, with increased purification, the SDS-PAGE pattern started to resemble the CTAB-PAGE pattern, rather than the other way around (Fig. 1E,F). Thus, on SDS-PAGE, nuclear proteasome subunits *also* migrated as collections of multiple species, on the condition that these proteasomes were sufficiently purified. Briefly, proteasomes were captured from primary human leukocytes using a resin-immobilised ubiquitin-like (Ubl) domain of hPLIC2/Ubiquilin2 [10,13,14], then further purified using FPLC size-exclusion chromatography (Fig. 1E). CTAB-PAGE analysis of purified nuclear proteasomes showed extensive modification of the Regulatory Particle (RP) subunits Rpn12 and Rpt2, and the β5i Core Particle (CP) subunit, as before; by contrast, the CP subunit α7 migrated as a single band (see also Fig. 2C,D). Surprisingly, unlike in the experiments described above, analysis of *purified* nuclear proteasomes by SDS-PAGE gave virtually identical results to those seen with CTAB-PAGE (Fig. 1E). One interpretation why SDS-PAGE – with increasing sample purification – starts to yield CTAB-PAGE patterns, is that modified nuclear proteasomes interact with other components of the nuclear extract and that this interaction prevents SDS-PAGE from visualising proteasomes. Consistent with this interpretation, when analysing samples taken over the course of a single purification procedure, modified proteasomes were only visible on SDS-PAGE in samples taken *after* the Ubl-capturing step (Fig. 1F), indicating that sample complexity is 'masked' in unpurified lysate or extract mixtures. Interestingly, in Fig. 1F, the Ubl domain [10,13] did not capture unmodified Rpt2 from the cytoplasmic extract; we found this to be the result of the particular construct [10,11] and buffer conditions used (Fig. S2). In sum, CTAB-PAGE detected human proteasomes that are located in a distinct sub-cellular location, most likely in the nucleus (although a tightly-bound cytosolic or cytoskeletal location could not formally be excluded, and relative distribution of proteasomes between fractions may depend to some extent on fractionation procedure), and that carry constitutive modifications which are largely incompatible with SDS-PAGE analysis.

In order to understand why CTAB, but not SDS-PAGE visualised proteins modified in this manner, we sought to identify the nature of the posttranslational modification. We used a GST-Ubl [11] construct to capture proteasomes from either cytoplasmic or subsequent nuclear extract (Fig. S2), and compared these by two-dimensional isoelectric focusing (IEF)/SDS-PAGE. The posttranslational modification substantially changed focusing of proteasomal subunits, even in a wide-range pH 3–10 gradient (Figs. 2A, S3). The modification imparted a complex focusing phenotype, including (1) a 'striated' rather than punctuate focusing pattern (even in a narrow pH range, Fig. 2B, and with steady-state focusing achieved), and (2) diagonal 'slanting' towards the acidic pole (Fig. 2B). The pronounced effects of the posttranslational modification on the pI of proteasomal subunits strongly suggest that it carries a charge (and, in the case of the population slanting towards the acidic pole, a negative charge) [15]. It was not DNA or RNA (Fig. 2C). We found that the modification of nuclear proteasomes shared several characteristics with, but also is distinct from, classical ADP-ribose chains (poly(ADP-ribosyl) – PAR – chains) [16,17]. PAR is a nuclear modification of high negative charge, which could explain relative incompatibility with (negatively-charged) SDS-PAGE. Characteristics shared with PAR include: (1) sensitivity to the PAR hydrolytic enzymes PARG, ARH1, ARH2 and ARH3. Incubation with these enzymes, alone or in combination, altered the Western blot patterns of several proteasome subunits (Fig. 2D,E). Most of the changes reflected activity of PARG, which hydrolyses ribose–ribose linkages between coupled ADP-ribose units in PAR chains (Fig. 2D). Note that, even though we used standard SDS-PAGE rather than CTAB-PAGE (as was possible with *purified* nuclear proteasomes as substrate), PAR-hydrolysing enzymes had unusual effects on migration of proteasome subunits. These include apparent upward migration and increased signal intensity, in part due to PARG-facilitated entry of modified proteasome subunits into the SDS-PAGE gel (Fig. 1F). A direct comparison on SDS-PAGE of cytosolic *versus* (purified) nuclear Rpt2 showed that nuclear Rpt2 migrated with an apparent molecular weight range below that of unmodified, cytosolic Rpt2, as may be expected from a highly negatively-charged protein modification (Figs. 1F, 2B). (2) Sensitivity to venom phosphodiesterase I (PDE1). PDE1 hydrolyses pyrophosphate bonds of ADP-ribose units in PAR, and also changed the Rpt2 pattern (Fig. 2F) [18]. (3) α-PAR antibodies immunoprecipitated proteasomal antigens and, *vice versa*, proteasome antibodies immunoprecipitated PAR-reactive antigens (Fig. S4B). We found that an alternative approach, using biotin-NAD^+ for metabolic labelling, was not feasible, because living cells did not take up biotin-NAD^+ nor could we use digitonin-permeabilised cells for our constitutively-present modifications. (4) Yeast proteasomes, which lack PAR [19], were unmodified on CTAB-PAGE (Fig. S4C). However, the modification of human nuclear proteasomes also differs from PAR in several respects: (1) complete resolution of modified nuclear proteasomes into single subunit bands using PAR enzymes was never achieved (Fig. S4A), even when combined and under a wide variety of experimental conditions. (2) The nuclear proteasome modification is *constitutively* present, whereas standard PAR chains on substrates are generally transient, short-lived and synthesised in response to stress at sites of *e.g.* DNA damage [16,17]. Interestingly, the constitutive modification of nuclear proteasomes we report here expands on what is already known, namely that *standard* PAR transiently activates nuclear proteasomes to degrade oxidatively damaged histones [8,17,20] and regulates proteasome assembly in the nucleus *via* modification of assembly factor PI31 [21]. Because PDE1/PAR enzyme treatment was only partially effective against the proteasome modification (Fig. S4A), it has not yet been possible, despite various attempts, to obtain a mass spectrometry signature.

Finally, we identified a physiological process which induces changes in CTAB-PAGE detectable proteasome modifications. It has been reported that, during apoptosis, activated caspases cut once in each of three proteasome subunits. These cleavage events were visualised with SDS-PAGE [22,23]. However, we now report, that changes to proteasome structure during apoptosis are far more dramatic: CTAB-PAGE-unique subunit species of multiple proteasome subunits changed dramatically during apoptosis, as observed when treating cells with a lethal dose of Bortezomib *versus* control- or sub-IC50-treated cells (Fig. 3A). The same was observed when using apoptosis-inducing compounds which are not proteasome inhibitors (Figs. 3C, S6A), or proteasome inhibitors other than Bortezomib (Fig. S5). Most, but not all, of these changes were caspase-dependent, because caspase inhibitors prevented many, though not all, of these changes (Fig. 3B). Interestingly, by comparing eight human cell lines on CTAB-PAGE, we found that proteasome modification patterns can vary to some extent (Fig. S6B). We are currently studying how this modification affects proteasome function.

In sum, we found that nuclear proteasome subunits carry a post-translational modification which makes those subunits invisible to

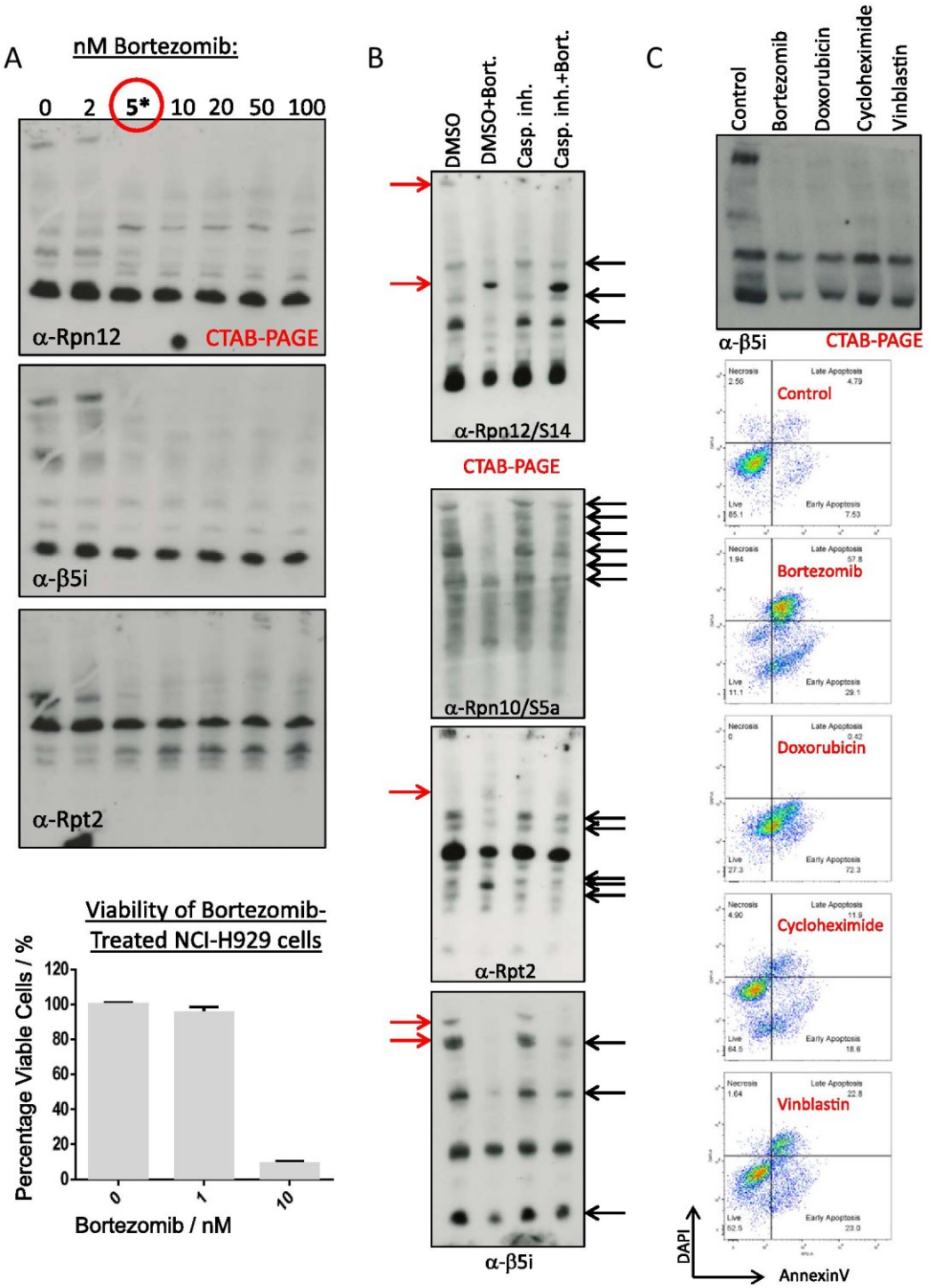


Fig. 3. The constitutive modification of proteasomes changes in response to a physiological stimulus. (A) Western blot analysis of the effects of a Bortezomib concentration range on the CTAB-PAGE patterns of several proteasome subunits. NCI-H929 myeloma cells were treated with the indicated Bortezomib concentrations for 24 h, after which total cell lysate was analysed by CTAB-PAGE and Western blot. (Asterisk denotes IC50 value for the NCI-H929 cell line used.) The bottom panel shows that Bortezomib between 1 and 10 nM induces apoptosis in these cells, as determined by AnnexinV–7AAD staining. (B) Western blot analysis of the effects of Bortezomib (20 nM) and a caspase inhibitor cocktail on the CTAB-PAGE pattern of proteasome subunits. Indicated with red and black arrows are Bortezomib-induced changes in the CTAB-PAGE pattern which are caspase-independent and caspase-mediated, respectively. (C) Myeloma OPM2 cells were treated for 29 h with Bortezomib (250 nM), doxorubicin (10 μg/ml), cycloheximide (500 μg/ml), or vinblastin (10 μg/ml). Cell viability was assessed by Annexin V/DAPI, and total cell lysate was analysed by CTAB-PAGE.

SDS-PAGE. We identified an alternative system that overcomes this problem (CTAB-PAGE), and gained insight into the nature of the modification leading to a possible explanation for observed PAGE compatibilities. Finally, we identified the first example of specific biology involving CTAB-PAGE detectable protein modifications.

Even though the constitutive modifications of nuclear proteasomes differ from classical PAR chains, their sharing of some characteristics suggests a possible function for these modifications in proteasome biology. Nuclear proteasomes are known to have a variety of nuclear functions [24–28]; they must interact with chromatin, DNA and other

nuclear components, but little is known about how this is accomplished. In general, when PAR chains are present, they recruit *e.g.* PAR-binding repair proteins to DNA and chromosomes [16,17]. In analogy, we hypothesise that proteins in nuclear processes capture the (constitutive) CTAB-PAGE-detectable modifications on nuclear proteasomes, thereby recruiting proteasome function to *e.g.* gene expression, even under non-stress conditions.

Our identification of an SDS-PAGE-incompatible protein modification may also explain the difficulty in resolving the controversy as to whether RNA species, which early studies suggested are associated with proteasomes (then called *prosomes*) [29], are bona fide components of proteasomes [30]. These modifications may account for the reported RNP-like density of prosomes/proteasomes, and our finding that SDS-PAGE fails to detect modified proteasomal subunits may explain the difficulty in resolving the controversy. Our data suggest that CTAB-PAGE should be used routinely in nuclear biology to ascertain whether or not a protein of interest is similarly modified.

Acknowledgements

We would like to thank Andy Porter, Valentina Caputo, James Crawley, David Lane, Gerald Cohen, Daniel Finley, Neema Sofaer and Jeroen Roelofs for comments and scientific discussions.

Funding: This research was supported by Leukaemia Lymphoma Research UK (LLR Grant 10016 to MFK, LLR Gordon Piller Studentship award Grant 11043 to MFK/AK/DP), and by the NIHR Biomedical Research Centre at Imperial College NHS Trust, London.

Appendix A. Supplementary data

Supplementary data to this article can be found online at http://dx.doi.org/10.1016/j.bbapap.2014.08.013.

References

[1] U.K. Laemmli, Cleavage of structural proteins during the assembly of the head of bacteriophage T4, Nature 227 (5259) (1970) 680–685.
[2] J.E. Coligan, Current protocols in protein science, John Wiley and Sons, New York, 1996. (p. <1- > (loose-leaf)).
[3] D. Finley, Recognition and processing of ubiquitin–protein conjugates by the proteasome, Annu. Rev. Biochem. 78 (2009) 477–513.
[4] G.C. Lander, et al., Complete subunit architecture of the proteasome regulatory particle, Nature 482 (7384) (2012) 186–191.
[5] R. Atkins, R. Tuan, Cetyltrimethylammonium bromide discontinuous gel electrophoresis of proteins, in: J. Walker (Ed.), The Protein Protocols Handbook, Humana Press, 2002, pp. 87–103.
[6] R.J. Simpson, CTAB-PAGE, Cold Spring Harb. Protoc. 2010 (4) (2010) (pdb.prot5412).
[7] Y.-G. Yeung, E.R. Stanley, A solution for stripping antibodies from polyvinylidene fluoride immunoblots for multiple reprobing, Anal. Biochem. 389 (1) (2009) 89–91.
[8] E. Bakondi, et al., Age-related loss of stress-induced nuclear proteasome activation is due to low PARP-1 activity, Free Radic. Biol. Med. 50 (1) (2011) 86–92.
[9] M.F. Kleijnen, et al., Stability of the proteasome can be regulated allosterically through engagement of its proteolytic active sites, Nat. Struct. Mol. Biol. 14 (12) (2007) 1180–1188.
[10] K.J. Walters, et al., Structural studies of the interaction between ubiquitin family proteins and proteasome subunit S5a, Biochemistry 41 (6) (2002) 1767–1777.
[11] M.F. Kleijnen, R.M. Alarcon, P.M. Howley, The ubiquitin-associated domain of hPLIC-2 interacts with the proteasome, Mol. Biol. Cell 14 (9) (2003) 3868–3875.
[12] P. Holden, W.A. Horton, Crude subcellular fractionation of cultured mammalian cell lines, BMC Res. Notes 2 (2009) 243.
[13] H. Besche, et al., Isolation of mammalian 26S proteasomes and p97/VCP complexes using the ubiquitin-like domain from HHR23B reveals novel proteasome-associated proteins, Biochemistry 48 (2009) 2538–2549.
[14] M.F. Kleijnen, et al., The hPLIC proteins may provide a link between the ubiquitination machinery and the proteasome, Mol. Cell 6 (2) (2000) 409–419.
[15] E. Gianazza, Isoelectric focusing as a tool for the investigation of posttranslational processing and chemical modifications of proteins, J. Chromatogr. A 705 (1995) 67–87.
[16] S. Beneke, Regulation of chromatin structure by poly(ADP-ribosyl)ation, Front. Genet. 3 (2012) 169.
[17] B.A. Gibson, W.L. Kraus, New insights into the molecular and cellular functions of poly(ADP-ribose) and PARPs, Nat. Rev. Mol. Cell Biol. 13 (7) (2012) 411–424.
[18] O. Hayaishi, K. Ueda, Poly(ADP-ribose) and ADP-ribosylation of proteins, Annu. Rev. Biochem. 46 (1977) 95–116.
[19] Z. Tao, P. Gao, H.-W. Liu, Studies of the expression of human poly(ADP-ribose) polymerase-1 in *Saccharomyces cerevisiae* and identification of PARP-1 substrates by yeast proteome microarray screening, Biochemistry 48 (49) (2009) 11745–11754.
[20] O. Ullrich, et al., Poly-ADP ribose polymerase activates nuclear proteasome to degrade oxidatively damaged histones, Proc. Natl. Acad. Sci. U. S. A. 96 (11) (1999) 6223–6228.
[21] P. Cho-Park, H. Steller, Proteasome regulation by ADP-ribosylation, Cell 153 (2013) 614–627.
[22] X.-M. Sun, et al., Caspase activation inhibits proteasome function during apoptosis, Mol. Cell 14 (1) (2004) 81–93.
[23] C. Adrain, et al., Caspase-dependent inactivation of proteasome function during programmed cell death in *Drosophila* and man, J. Biol. Chem. 279 (35) (2004) 36923–36930.
[24] K.P. Bhat, et al., The 19S proteasome ATPase Sug1 plays a critical role in regulating MHC class II transcription, Mol. Immunol. 45 (8) (2008) 2214–2224.
[25] F. Geng, W.P. Tansey, Similar temporal and spatial recruitment of native 19S and 20S proteasome subunits to transcriptionally active chromatin, Proc. Natl. Acad. Sci. U. S. A. 109 (16) (2012) 6060–6065.
[26] F. Geng, S. Wenzel, W.P. Tansey, Ubiquitin and proteasomes in transcription, Annu. Rev. Biochem. 81 (2012) 177–201.
[27] T. Kodadek, No splicing, no dicing: non-proteolytic roles of the ubiquitin–proteasome system in transcription, J. Biol. Chem. 285 (4) (2010) 2221–2226.
[28] J. Kwak, J.L. Workman, D. Lee, The proteasome and its regulatory roles in gene expression, Biochim. Biophys. Acta 1809 (2) (2011) 88–96.
[29] H.P. Schmid, et al., The prosome: an ubiquitous morphologically distinct RNP particle associated with repressed mRNPs and containing specific ScRNA and a characteristic set of proteins, EMBO J. 3 (1) (1984) 29–34.
[30] V. Pamnani, et al., Proteasome-associated RNAs are non-specific, Eur. J. Biochem. 225 (2) (1994) 511–519.

EBioMedicine 2 (2015) 642–648

Contents lists available at ScienceDirect

EBioMedicine

journal homepage: www.ebiomedicine.com

Original Article

Bortezomib Amplifies Effect on Intracellular Proteasomes by Changing Proteasome Structure☆

David S. Pitcher, Kate de Mattos-Shipley, Konstantinos Tzortzis, Holger W. Auner, Anastasios Karadimitris, Maurits F. Kleijnen *

Centre for Haematology, Division of Experimental Medicine, Faculty of Medicine, Imperial College London, Hammersmith Campus, Commonwealth Building 4th Floor, Du Cane Road, London W12 0NN, United Kingdom

ARTICLE INFO

Article history:
Received 7 May 2015
Accepted 7 May 2015
Available online 28 May 2015

Keywords:
Multiple myeloma
Proteasome
Bortezomib
CTAB-PAGE
Posttranslational modification

ABSTRACT

The proteasome inhibitor Bortezomib is used to treat multiple myeloma (MM). Bortezomib inhibits protein degradation by inactivating proteasomes' active-sites. MM cells are exquisitely sensitive to Bortezomib – exhibiting a low-nanomolar IC^{50} – suggesting that *minimal* inhibition of degradation suffices to kill MM cells. Instead, we report, a low Bortezomib concentration, contrary to expectation, achieves severe inhibition of proteasome activity in MM cells: the degree of inhibition exceeds what one would expect from the small proportion of active-sites that Bortezomib inhibits. Our data indicate that Bortezomib achieves this severe inhibition by triggering secondary changes in proteasome structure that further inhibit proteasome activity. Comparing MM cells to other, Bortezomib-resistant, cancer cells shows that the degree of proteasome inhibition is the greatest in MM cells and only there leads to proteasome stress, providing an explanation for why Bortezomib is effective against MM but not other cancers.

© 2015 The Authors. Published by Elsevier B.V. This is an open access article under the CC BY license (http://creativecommons.org/licenses/by/4.0/).

1. Introduction

The proteasome inhibitor (PI) Bortezomib is used as a first- and second-line treatment of multiple myeloma (MM) (Anderson et al., 2011). Proteasomes' (Finley, 2009; Lander et al., 2012) main function is to degrade ubiquitinated proteins in a controlled manner (Bedford et al., 2011; Finley, 2009; Glickman and Ciechanover, 2002). Proteasomes are comprised of a cylindrical core particle (CP) capped at each end by a regulatory particle (RP) (Lander et al., 2012; He et al., 2012). The RP captures and denatures ubiquitin-marked protein substrates, and translocates their unfolded polypeptide chains towards proteolytic active-sites in the CP's lumen (Finley, 2009). CP contains three types of active-sites, each of which comprises a peptide-docking area and an exposed catalytic threonine. PIs including Bortezomib prevent protein hydrolysis by forming covalent adducts with the catalytic threonines of the active-sites (Groll et al., 2009; Beck et al., 2012). Some proteasome activity is necessary for any cell to live (Heinemeyer et al., 1997), not just MM cells (Craxton et al., 2012; Suraweera et al., 2012).

Although the Bortezomib concentrations at which cells of different cancers die differ widely, from low nanomolar to high micromolar IC^{50} concentrations, cells of the (incurable) B-cell malignancy MM are exquisitely sensitive (Shabaneh et al., 2013), hence Bortezomib's success in treatment of MM (Anderson et al., 2011). Intriguingly, Bortezomib at its low IC^{50} concentration causes only a small reduction in proteasomes' ability to degrade proteins (Kisselev et al., 2006; Shabaneh et al., 2013). The reduction is small because Bortezomib preferentially inhibits the chymotrypsin-like (CT-Like) active-site, but – at IC^{50} – does not inhibit the caspase-like and trypsin-like active-sites (Fig. S2A) (Kisselev et al., 2006); however, protein substrates can be hydrolysed by any of the three types of active-sites (Kessler et al., 2001; Kisselev et al., 2006). Thus, the question arises why minimal inhibition of proteasome function suffices to induce apoptosis in MM but not in Bortezomib-insensitive cells. Several explanations have been proposed, including high proteasome workload in MM cells (Bianchi et al., 2009; Meister et al., 2007; Shabaneh et al., 2013).

We report that, surprisingly, a (low) IC^{50} Bortezomib challenge – which in-vitro minimally inhibits proteasomes – in living MM cells severely inhibits proteasomes' hydrolytic activity. Our data suggest that, in living MM cells, a Bortezomib-induced structural change in the

☆ Research in context: Bortezomib and other proteasome inhibitors can treat multiple myeloma, a blood cancer arising from plasma B-cells, but few other cancers. It has been unclear why Bortezomib kills myeloma cells at concentrations so low that only partial inhibition of proteasomes is expected, and why Bortezomib cannot kill most other cancer cells. We now report that Bortezomib achieves unexpectedly severe inhibition of intracellular proteasomes, by triggering structural changes in these which further depress activity. Thus, Bortezomib 'punches above its weight' and achieves unexpectedly severe – sometimes lethal – levels of proteasome inhibition. The greatest inhibition happens exactly in cells from cancers which Bortezomib can treat.

* Corresponding author.
E-mail address: m.kleijnen@imperial.ac.uk (M.F. Kleijnen).

http://dx.doi.org/10.1016/j.ebiom.2015.05.016
2352-3964/© 2015 The Authors. Published by Elsevier B.V. This is an open access article under the CC BY license (http://creativecommons.org/licenses/by/4.0/).

proteasome (Pitcher et al., 2014) is responsible for this severe degree of proteasome inhibition.

2. Experimental procedures

Antibodies from Enzo Life Sciences: α-ubiquitin (FK2, PW8810), α-cleaved caspase 3 (PAb, ADI-AAS-103), α-20S α7 (MoAb LN43, BML-PW8110), α-Rpn12/S14 (PAb, BML-PW8815), α-Rpn10/S5a (MoAb S5a-18, BML-PW9250), α-Rpt5/S6a (MoAb TBP1-19, PW8770), α-Rpt4/S10b (MoAb p42-23, PW8830), α-Rpt2/S4 (PAb, BML-PW8305), and α-β5i/LMP7 (PAb, PW8355). Antibodies from other sources: α-streptag (Qiagen, MoAb 34850), α-PARP (CellSignalling, PAb, #9542) and α-procaspase3 (CellSignalling, PAb, #9661). CTAB-PAGE as described (Pitcher et al., 2014; Simpson, 2010). Additional Reagents: Ada-K(Biotin)-Ahx_3-L_3-VS, epoxomicin (Enzo LifeSciences), Bortezomib (Millennium/Takeda), Streptactin resin (Qiagen, 30004), Ni^{++}NTA resin (Sigma-Aldrich, His Select HF Nickel Affinity Gel, H0537 (Fig. 2c), or His Select agarose, P2266). AnnexinV/7AAD apoptosis staining (EBioscience 88-8007-74) was used to assess cell viability. Enzymes: DNase1, micrococcal nuclease, RNaseA/T1, RNaseH, S1 nuclease and RNAse1 (Fermentas/Thermo), PDE1 from *Crotalus adamanteus* venom (Sigma, P3243-1VL). Caspase Inhibitor Set III (Enzo Life Sciences, ALX-850-227-KI01), used at 1:500 dilution = 4 μM. Antibodies were diluted in PBS + 0.5% Tween20 for Western blotting, PVDF membranes were re-probed multiple times (Yeung and Stanley, 2009). Myeloma cell lines NCI-H929, KMS12-BM, RPMI-8226, OPM2, and the T-lymphocyte Jurkat cell line, were grown in RPMI (Sigma), supplemented with 10% v/v FBS, and 1% v/v Pen/strep. Cell fractionation procedure as described (Pitcher et al., 2014). For fractionation, a cytosol extraction (CE) buffer (25 mM Tris–HCl [pH 7.8], 5 mM $MgCl_2$/EDTA, 1 mM ATP/ADP, 2 mM DTT, 150 mM NaCl, 0.1 or 0.5% NP-40/IGEPAL) and nuclear extraction (NE) buffer (Bakondi et al., 2011) (20 mM HEPES [pH 7.4], 420 mM NaCl, 0.5 mM EDTA, 0.5 mM EGTA, 1 mM DTT, 1 tablet of inhibitor cocktail (Roche, 11-873-580-001) per 50 ml) were used. When using the NE for subsequent affinity-purification, 2 volumes of H_2O were added to 1 volume NE to reduce the NaCl concentration to physiological levels. For non-fractionated lysate, cell pellets snap-frozen in LN and stored at −80 °C were resuspended and combined in 10× volume of CE buffer and passed through a NanoDeBEE (BEE international) homogeniser at 19,000 PSI. Proteasome activity was measured basically as described (Kisselev and Goldberg, 2005; Vilchez et al., 2012), using fluorogenic proteasome substrates Suc-LLVY-AMC, Ac-RLR-AMC, Ac-GPLD-AMC (Enzo Life Sciences) for the three types of active-site. Cells were lysed in proteasome activity assay buffer (50 mM Tris–HCl, pH 7.5, 250 mM sucrose, 5 mM $MgCl_2$, 0.5 mM EDTA, 2 mM ATP and 1 mM DTT) by passing cells through a 29 G needle ten times. Fluorescence (380 nm excitation, 460 nm emission) was monitored continuously on a microplate fluorometer for 1 h at 37 °C. To measure for the presence of free 20S proteasomes, 0.015% SDS was added to the proteasome activity assay buffer (Fig. S2C). For each well, a second was set up with the addition of 40 mM Bortezomib; any activity in the Bortezomib wells was subtracted from corresponding wells to compensate for unspecific protease activity. The ubiquitinated substrate (G3P) (Matyskiela et al., 2013) was kindly provided by Dr Andreas Martin, and used as described. In-vitro degradation with purified yeast (Fig. S4) and human (Fig. 3C,D) proteasomes was done in PBS supplemented with 2.5 mM ATP, 2.5 mM $MgCl_2$, 2.5 mM DTT, and 10% DMSO in a total volume of 20 μl. Reaction was performed for 1 h either at 30 °C or 37 °C (Fig. 3C,D), after which the reaction was stopped by addition of 20 μl 2× SDS sample buffer and boiled.

Graphs were produced using Graph pad Prism 6. Data plotted were mean of replicates, with error bars plotted of the standard error of mean (SEM).

Research was supported by Leukaemia Lymphoma Research UK (LLR Grant10016 to MFK, LLR Gordon Piller Studentship award Grant11043 to MFK, AK, DP), by an MRC-Imperial Confidence-in-Concept (ICiC) grant to MFK, and by the NIHR Biomedical Research Centre at Imperial College NHS Trust, London.

3. Results

NCI-H929 MM cells were challenged with a lethal (10 nM) Bortezomib concentration for varying lengths of time. Cells were then lysed and an artificial fluorogenic peptide substrate was used to measure proteasomes' hydrolytic activity (Fig. 1a). Over 0–6/8 h, CT-like activity declined continually to almost nothing. Only when it was nearly absent (<10%), after 6–8 hour incubation, was an increase in ubiquitin conjugate levels observed; intracellular accumulation of ubiquitinated proteins indicates that proteolytic workload exceeds proteasome capacity, accumulation being a phenotype which integrates other regulatory mechanisms in the cell including deubiquitinating enzyme activity (Fig. 1a; see also Fig. S1A). However, when cells were first lysed and then challenged with 10 nM Bortezomib, only a 40% reduction in proteasomal (CT-like) activity was observed (Fig. S2A: 61.5% CT-like activity left, and as previously reported (Kisselev et al., 2006)). A much stronger-than-expected in-vivo inhibitory effect was also observed for the other types of proteasomal active-sites (Figs. S2E;S2C).

Predictable explanations for Bortezomib's severe inhibition of proteasomes' activity in MM cells did not apply: (1) severe inhibition was not due to prolonged incubation, because exposing *purified* proteasomes in the test tube to 10 nM Bortezomib for longer periods of time still showed modest inhibition in line with Fig. S2A (Figs. 1B; Fig. S1B) (Bianchi et al., 2009; Kisselev et al., 2006; Shabaneh et al., 2013). Furthermore, we identified a MM cell line, RPMI-8226, in which CT-like proteasome activity dropped very rapidly, within 2 h, to <10% (Fig. 1e); this time-frame approaches that of the in-vitro test using cell lysate (Fig. S2A), but in-vitro 61.5% of activity remains. (2) Although 10 nM Bortezomib induced apoptosis, and apoptosis is known to inhibit proteasomes via caspase activation (Sun et al., 2004; Adrain et al., 2004), caspase activation was not responsible for the observed proteasome inhibition: inhibition preceded caspase activation (Fig. 1c), occurred when caspase inhibitors were present (Fig. 1d), cells were alive until 10 h post-challenge as measured by Annexin-V staining (Fig. S2B), and there was a non-myeloma, T-lymphocyte cell line that did not die with 10 nM Bortezomib but in which proteasome activity still dropped well beyond expectation to ~20% (Figs. 1F,S2D; see also lung carcinoma A549 cells: Fig. S2D). (3) Severe inhibition was not because MM cells actively pumped in and/or retained Bortezomib to establish a 10–100 fold higher (Fig. S2A) intracellular Bortezomib concentration. We used the irreversible biotinylated inhibitor Ada-K(Biotin)-Ahx_3-L_3-VS (Kessler et al., 2001) to simultaneously measure inhibition of activity and the degree to which active-sites were inhibited, i.e. biotinylated (Kessler et al., 2001). We observed in-vivo a discrepancy between active-site inhibition and reduction in hydrolytic activity of those active-sites (Fig. 2a).

We now report a structural change in the proteasome which does correlate with Bortezomib-triggered early shutdown of proteasomal activity: Bortezomib-triggered early changes in posttranslational modifications on proteasomal subunits. We recently reported that human nuclear proteasomes carry a constitutive, CTAB-PAGE-detectable, post-translational modification that, in some respects, resembles poly(ADP)-ribose (Pitcher et al., 2014). We reported that exposing MM cells to Bortezomib induced changes in these CTAB-PAGE-detectable proteasome modifications, exactly at Bortezomib's IC^{50} concentration and above (Pitcher et al., 2014). Fig. 2b – CTAB-PAGE analysis of total cell lysate – shows that changes in these modifications of the proteasomal Rpn12 subunit occur between 1 h (RPMI-8226) and 4 h (H929) of PI challenge. To examine these Bortezomib-triggered changes in finer detail, we combined cell fractionation with affinity-purification of human proteasomes. (Purification is a technical trick that enables modified subunits to also become compatible with, and visible on, SDS-PAGE (Pitcher et al., 2014).) We generated retrovirally-transduced OPM2 MM cells, which expressed a Rpn11 subunit tagged N-terminally with

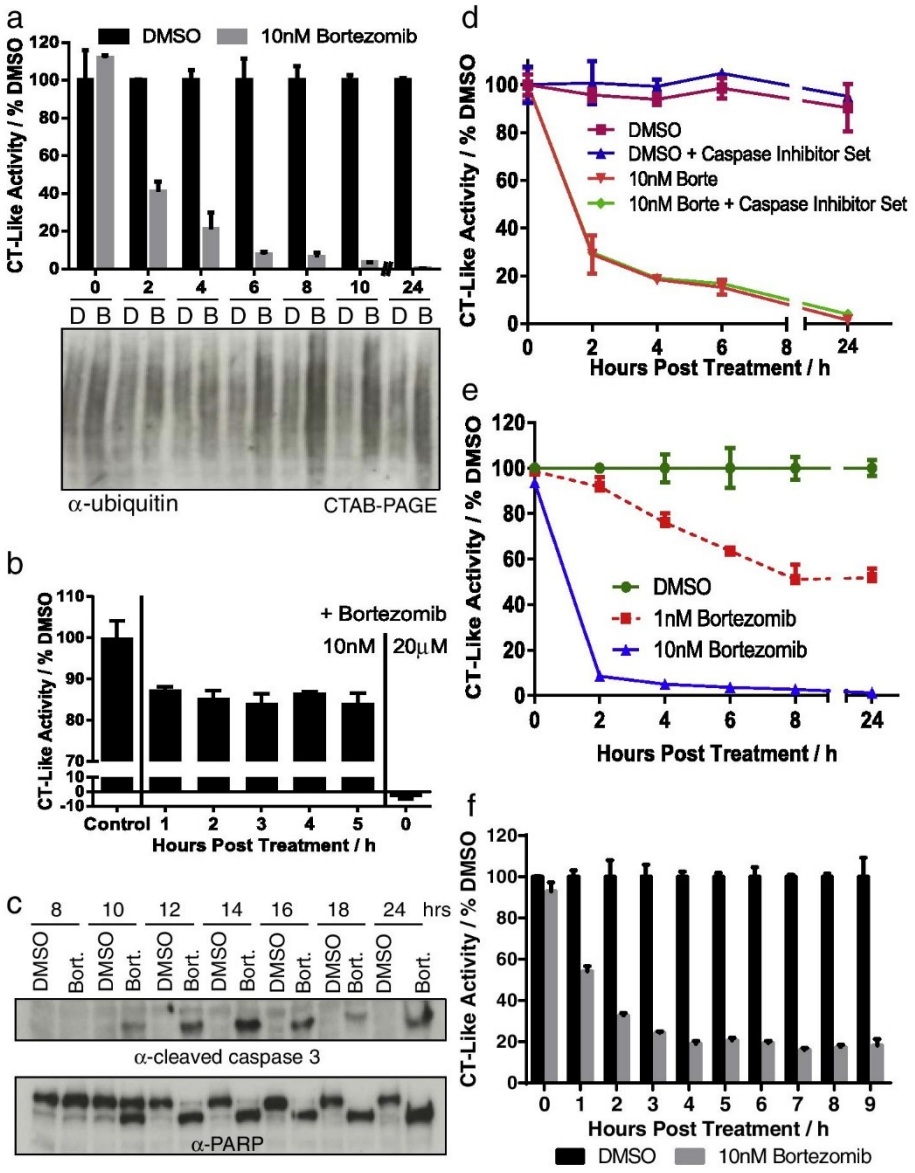


Fig. 1. Exposing myeloma cells to a lethal Bortezomib concentration leads to much greater inhibition of proteasomal hydrolytic activity in-vivo than is seen with cell lysate or purified proteasomes. (a) Measuring over time the effects on CT-like proteasome activity in Bortezomib-sensitive multiple myeloma cells (NCI-H929) after a 10 nM Bortezomib challenge (n = 2 per value). For the same time points, the degree of accumulation of ubiquitin conjugates in NCI-H929 cell lysate is visualised (see also Fig. S1A). Data represented as mean ± SEM. (b) Measuring the level of inhibition of purified human *26S* proteasomes following pre-incubation with 10 nM Bortezomib from 1 to 5 h at 4 °C (CT-Like activity was measured using Suc-LLVY-AMC at 37 °C). Data represented as mean ± SEM. Fig. S1B: experiment done also with yeast *26S* proteasomes, and with higher pre-incubation temperature. (c) Time course experiment with NCI-H929 cells, looking at caspase 3 activation and PARP cleavage (Substrate of Caspase 3), following a 10 nM Bortezomib challenge. (d) Investigating the effect of caspase inhibitors on Bortezomib's ability to shut down over time CT-Like activity in NCI-H929 cells. For experimental procedure, and validation that the procedure indeed inhibited caspases, see (Pitcher et al., 2014). Data represented as mean ± SEM (n = 2 per value). (e) Measuring over time the effects on CT-like proteasome activity in Bortezomib-sensitive multiple myeloma cells (RPMI-8226) after a DMSO, 1 nM (sub-lethal) and 10 nM (lethal) Bortezomib challenge. Data represented as mean ± SEM (n = 2 per value). (f) Measuring over time the effects on CT-like proteasome activity in the Bortezomib-insensitive T lymphocyte Jurkat cell line. Annexin-V staining showed that this 10 nM Bortezomib challenge did *not* induce cell death in the Jurkat cells. Data represented as mean ± SEM. See also Figs. S1,S2.

a His_6–StrepII–StrepII–TEV-affinity cassette. Cell fractionation and then affinity-purification (using streptactin or Ni^{++}NTA) showed that subunits from specifically nuclear proteasomes are extensively modified, as we reported previously (Pitcher et al., 2014) (Fig. 2c: Rpn11 subunit, detected with anti-streptag antibody). Repeating this fractionation-then-affinity-purification procedure, but this time after OPM2 cells had been treated with 20 nM (lethal) Bortezomib for up to 5–7 h, showed that patterns of modified subunits changed (Fig. 2d,e). These changes' characteristics depended on the particular proteasome subunit that was analysed. Generalising, these changes involved (A) a reduction in complexity for nuclear proteasomes (e.g. Rpt5, Rpn12), and/or (B) the appearance of modified subunit species in the cytosol fraction (e.g. β5i, Rpn12). (A) and (B) raise the possibility that severe inhibition of proteasome activity in total lysate (Fig. 1) may result from changes in proteasome structure which happen both in the cytosolic and nuclear compartments of the cell after cells are challenged with Bortezomib. We are currently investigating the exact nature of the proteasome modifications.

In order to test directly if changes in these proteasome modifications affect proteasome function, we first searched for commercial enzyme preparations that can digest the modifications of nuclear proteasomes. We discovered that a combination of venom phosphodiesterase-1 and S1 nuclease was efficient in trimming these modifications and collapsing modified Rpt2 species into its correct subunit-size species (Fig. 3A). Next,

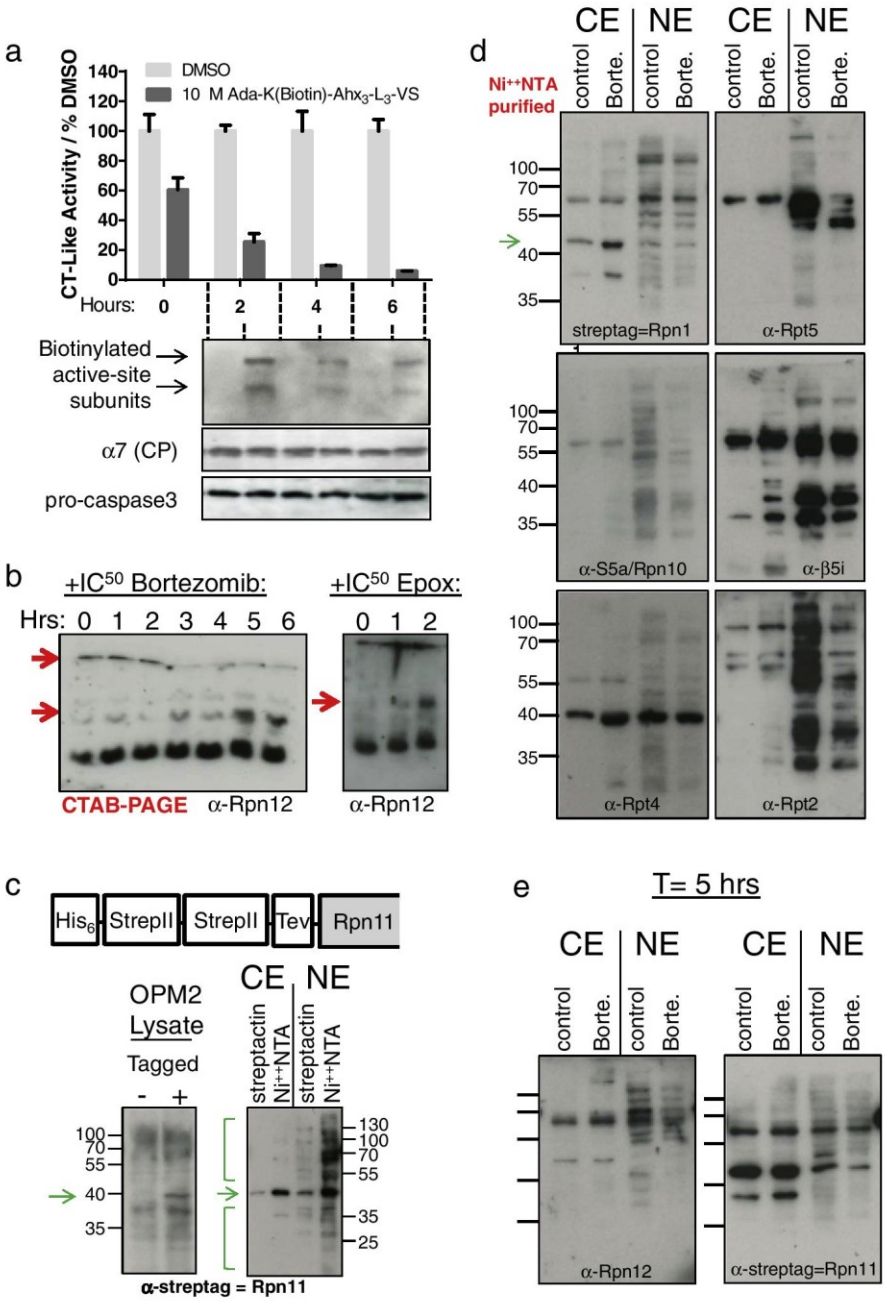


Fig. 2. Bortezomib's inhibition of proteasomal active-sites triggers changes in the structure of intracellular proteasomes. (a) Investigating the active-site occupation by proteasome inhibitor Ada-K(Biotin)-Ahx_3-L_3-VS, and proteasome activity remaining. NCI-H929 cells were incubated with 10 μM inhibitor for several hours, after which they were harvested and analysed for levels of inhibited/biotinylated active-sites, overall proteasome activity and pro-caspase-3 status (n = 2 per value). While the level of inhibited active-sites did not increase over time (and in fact was less in the 4- and 6-hour samples), we observed a steady decline in the activity of the CT-like active-sites in these samples. Ada-K(Biotin)-Ahx_3-L_3-VS-treated cells remained alive, as determined by Annexin-V/7AAD staining, for up to 10 h, and procaspase-3 levels stayed constant for the same time. Data represented as mean ± SEM. (b) NCI-H929 cells were incubated with 10 nM Bortezomib, RPMI-8226 cells with 20 nM epoxomicin, cells were lysed at specific time points and run on CTAB-PAGE (Pitcher et al., 2014). The resulting western was blotted for Rpn12. Note the changes in Rpn12 patterning over time upon lethal PI challenge. (c) OPM2 MM cells were retrovirally transduced to overexpress the Rpn11 proteasome subunit bearing an N-terminal affinity-tag (see schematic). Western blotting (left panel) of whole-cell lysate from transduced/non-transduced OPM2 cells using an α-streptag antibody shows expression of the tagged subunit (expected size Rpn11 + Tag = 35.6 kDa + 9 kDa = 44.6 kDa). Using this tagged MM cell line, the Western Blot panel on the right shows affinity-purification of proteasomes from both cytosolic (CE) and subsequent nuclear (NE) extract by Ni^{++}NTA or Streptactin capture. Extraction done as described (Pitcher et al., 2014), using 0.1% NP40 in CE buffer. Note that the many modified nuclear species of Rpn11 cannot be visualised on SDS-PAGE unless purified, and thus – after purification – appear on gel 'out of nowhere' (compare 'total lysate' panel on the left with purified 'CE/NE proteasome' panel on the right, green brackets), as reported previously (Pitcher et al., 2014). (d) Tagged proteasomes were affinity-captured with Ni^{++}NTA from CE and NE from 7-hour control- (PBS) or Bortezomib-treated (20 nM) Rpn11-tagged OPM2 cells. These proteasomes were run on SDS-PAGE, and then blotted for various proteasomal subunits. Extraction done as described (Pitcher et al., 2014), but CE buffer contained 0.5% NP40. (e) Same as in (d), but cells were harvested – and proteasomes were captured – after only 5 h of incubation with Bortezomib. See also Fig. S3.

we combined this enzyme protocol with an in-vitro proteasome-mediated proteolysis assay, which uses a ubiquitinated model protein as substrate (Matyskiela et al., 2013) (Figs. 3B, S4). We scaled up cell growth and affinity-purified proteasomes from total (i.e. including nuclear) lysate. Proteasomes bound to affinity-resin were mock-treated or treated with PDE1/S1 at a sub-optimal (20 °C) temperature, after which resin was washed to remove enzymes. Next, proteasomes were eluted to generate a control and a PDE1/S1-treated proteasome

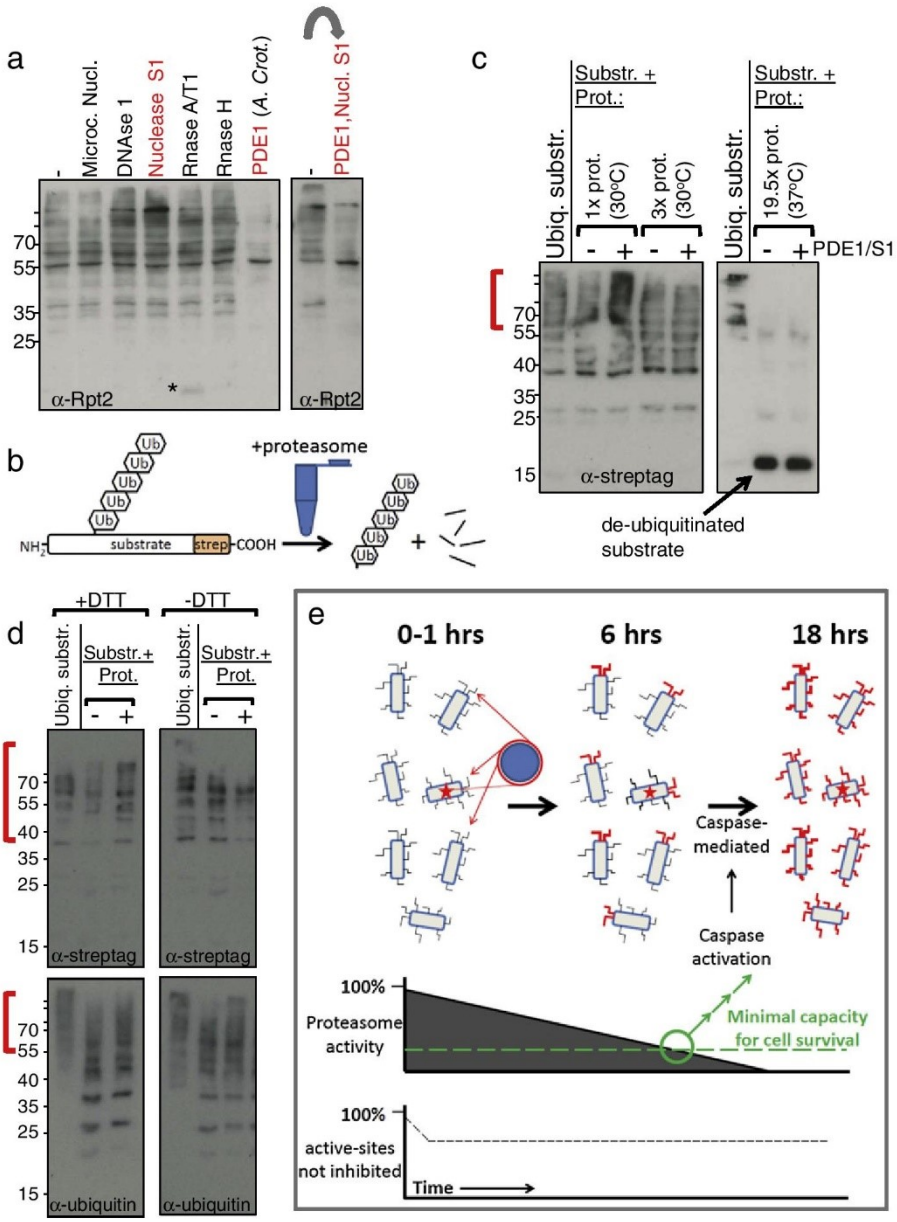


Fig. 3. Manipulating proteasome modifications changes proteasome function. (a) Affinity-purified nuclear proteasomes were incubated with the indicated enzymes for 1 h at 37 °C, subjected to SDS-PAGE, and analysed by Western Blot for proteasome subunit Rpt2. (b) Schematic presentation of the in-vitro proteasome-mediated proteolysis assay, which uses a ubiquitinated model protein as substrate (Matyskiela et al., 2013). In this system, proteasomes degrade the protein substrate while releasing the multiubiquitin chains in intact form (Fig. S4D). (c) Human proteasomes from Rpn11-tagged OPM2 cells were affinity-purified by Ni^{++}-NTA agarose capture of the His_6 domain. Half the prep was incubated on the beads in reaction buffer, while the other with reaction buffer and PDE1 + S1 combination, for 50 min at 20 °C before being eluted in 250 mM Imidizole-PBS. Varying relative amounts of proteasomes/substrate 1×, 3× were added to G3P model substrate and incubated for 1 h at 30 °C (in the presence of ATP, $MgCl_2$ and DTT) before running on SDS-PAGE and blotted against the Strep domain on the model substrate. Panel on the right: incubated at 37 °C and 19.5× proteasomes to substrate. (d) As in (c), but comparing enzyme-treated and control-treated proteasomes for ability to degrade ubiquitinated protein substrate in reducing (+DTT) and oxidizing reaction conditions. Analysis is done using streptag (substrate) and ubiquitin antibodies. (e) We propose the following model of how PIs virtually shut down proteolysis in cells while inhibiting few active-sites throughout. 2 h after exposing myeloma cells to an IC^{50} Bortezomib challenge (5–10 nM), only a small proportion of active-sites have been inhibited (red star). This proportion does not increase and, as a result, proteolysis is, in this initial period, almost unaffected due to uninhibited active-sites. However, over the next several hours, proteasomes' CTAB-PAGE-detectable modifications change (red), causing proteasome activity to decline. When proteolysis falls below the level required for life, caspases are activated and cells go through programmed cell death. See also Fig. S4.

preparation. Most subunits of PDE1/S1-treated versus untreated proteasomes were very similar, but for example Rpn12 showed pronounced differences (Fig. S3). We then incubated the proteasome preparations with a ubiquitinated model protein (Matyskiela et al., 2013) (Fig. S4) in order to assess the ability of these proteasome preparations to process a ubiquitinated substrate. At low proteasome/substrate ratio at 30 °C, the PDE1/S1-treated proteasomes were impaired in degrading ubiquitinated substrate (Fig. 3C). However, increasing the ratio overcame this defect, with both preparations degrading substrate equivalently. At even higher proteasome/substrate ratio, and at 37 °C, proteasomes processed the substrate towards deubiquitination rather than degradation, and again both preparations behaved equivalently (Fig. 3B). In addition, we found that changes in the redox state of the reaction conditions uncovered qualitative differences between enzyme-treated and untreated proteasomes (Fig. 3D): in the oxidizing conditions minus DTT, enzyme-treated proteasomes removed streptag epitope (i.e. substrate) more efficiently than untreated proteasomes but did not shift down the ubiquitin signal correspondingly, indicating that these enzyme-treated

proteasomes only partially digested the substrate protein – starting from the tagged carboxyterminus – before premature release. In contrast, under reducing conditions, untreated proteasomes were more efficient in degrading substrate than enzyme-treated proteasomes (see also Fig. 3C). In sum, our data indicate that, under certain experimental conditions, changes in proteasome modifications affect proteasome function, thereby strengthening the case that Bortezomib-triggered changes in proteasome modifications within cells also affect proteasome function.

4. Discussion

In summary, our data reveal a dramatic inhibition of proteasome activity in MM cells after a (low) IC^{50} Bortezomib challenge, and suggest that this inhibition is the *compound* result of, first, inhibition of a subset of active-sites, and, second, structural changes in the proteasome which further impair hydrolytic activity (Fig. 3E). Engagement of PIs with active-sites changes proteasome conformation and stabilizes the (distant) CP–RP (Kleijnen et al., 2007; Park et al., 2008) and RP-hPLIC/ubiquilin (Kleijnen et al., 2000) interactions, thus providing a possible signalling mechanism into the cell that may enable active-site inhibition to directly trigger activation of the cellular machinery that then changes the posttranslational modifications of the proteasomes. Whereas it has been very difficult to explain why MM cells die from a nanomolar IC^{50} Bortezomib challenge when assuming that the modest level of proteasome inhibition observed in-vitro holds true in-vivo (Bianchi et al., 2009; Kisselev et al., 2006; Shabaneh et al., 2013), it is not surprising that a myeloma cell with over 95% CT-inhibition and observable proteasome stress (i.e. accumulation of ubiquitin conjugates, Fig. 1a) will undergo apoptosis. In addition, our data show that Bortezomib, in cancer cells which are Bortezomib-resistant, does not achieve the same degree of proteasome inhibition as in (Bortezomib-sensitive) MM cells (Figs. 1F, S2D), thus providing a molecular mechanism explaining what differentiates MM from most other cancers which Bortezomib cannot treat. Please note that our data indicate that a high proteasome workload in MM cells (Bianchi et al., 2009; Meister et al., 2007; Shabaneh et al., 2013) cannot be the primary reason for MM cells' sensitivity to Bortezomib: for this explanation to work, all proteasomes in a cell would need to be fully engaged – with no spare capacity left – in order for a minimal inhibition of proteasomes to produce proteasome stress; instead, we observed that MM cells have much spare proteasome capacity, and that reducing capacity even to 20% still did not yield proteasome stress (Fig. 1a). Understanding the cellular mechanism via which Bortezomib amplifies its effect on proteasome function may enable future intervention to re-sensitize Bortezomib-resistant cells to treatment.

Authorship contributions

DSP designed, performed research, analysed data, and wrote manuscript. KdM-S, KT designed, performed research and analysed data. HWA, AK designed research and analysed data. MFK designed, performed research, analysed data, and wrote manuscript.

Disclosure of conflicts of interest

The authors declare that they have no conflict of interest.

Acknowledgements

The authors would like to thank Prof. Irene Roberts for helpful discussions.

Appendix A. Supplementary data

Supplementary data to this article can be found online at http://dx.doi.org/10.1016/j.ebiom.2015.05.006.

References

Adrain, C., Creagh, E.M., Cullen, S.P., Martin, S.J., 2004. Caspase-dependent inactivation of proteasome function during programmed cell death in Drosophila and man. J. Biol. Chem. 279, 36923–36930.
Anderson, K.C., Richardson, P.G., Ghobrial, I.M., 2011. Bortezomib in the Treatment of Multiple Myeloma. Springer, Basel.
Bakondi, E., Catalgol, B., Bak, I., Jung, T., Bozaykut, P., Bayramicli, M., Ozer, N.K., Grune, T., 2011. Age-related loss of stress-induced nuclear proteasome activation is due to low PARP-1 activity. Free Radic. Biol. Med. 50, 86–92.
Beck, P., Dubiella, C., Groll, M., 2012. Covalent and non-covalent reversible proteasome inhibition. Biol. Chem. 393, 1101–1120.
Bedford, L., Lowe, J., Dick, L.R., Mayer, R.J., Brownell, J.E., 2011. Ubiquitin-like protein conjugation and the ubiquitin–proteasome system as drug targets. Nat. Rev. Drug Discov. 10, 29–46.
Bianchi, G., Oliva, L., Cascio, P., Pengo, N., Fontana, F., Cerruti, F., Orsi, A., Pasqualetto, E., Mezghrani, A., Calbi, V., Palladini, G., Giuliani, N., Anderson, K.C., Sitia, R., Cenci, S., 2009. The proteasome load versus capacity balance determines apoptotic sensitivity of multiple myeloma cells to proteasome inhibition. Blood 113, 3040–3049.
Craxton, A., Butterworth, M., Harper, N., Fairall, L., Schwabe, J., Ciechanover, A., Cohen, G.M., 2012. NOXA, a sensor of proteasome integrity, is degraded by 26S proteasomes by an ubiquitin-independent pathway that is blocked by MCL-1. Cell Death Differ. 19, 1424–1434.
Finley, D., 2009. Recognition and processing of ubiquitin–protein conjugates by the proteasome. Annu. Rev. Biochem. 78, 477–513.
Glickman, M.H., Ciechanover, A., 2002. The ubiquitin–proteasome proteolytic pathway: destruction for the sake of construction. Physiol. Rev. 82, 373–428.
Groll, M., Huber, R., Moroder, L., 2009. The persisting challenge of selective and specific proteasome inhibition. J. Pept. Sci. 15, 58–66.
He, J., Kulkarni, K., Da Fonseca, P.C.A., Krutauz, D., Glickman, M.H., Barford, D., Morris, E.P., 2012. The structure of the 26S proteasome subunit Rpn2 reveals its pc repeat domain as a closed toroid of two concentric alpha-helical rings. Structure 20, 513–521.
Heinemeyer, W., Fischer, M., Krimmer, T., Stachon, U., Wolf, D.H., 1997. The active sites of the eukaryotic 20 S proteasome and their involvement in subunit precursor processing. J. Biol. Chem. 272, 25200–25209.
Kessler, B.M., Tortorella, D., Altun, M., Kisselev, A.F., Fiebiger, E., Hekking, B.G., Ploegh, H.L., Overkleeft, H.S., 2001. Extended peptide-based inhibitors efficiently target the proteasome and reveal overlapping specificities of the catalytic beta-subunits. Chem. Biol. 8, 913–929.
Kisselev, A.F., Goldberg, A.L., 2005. Monitoring activity and inhibition of 26S proteasomes with fluorogenic peptide substrates. Methods Enzymol. 398, 364–378.
Kisselev, A.F., Callard, A., Goldberg, A.L., 2006. Importance of the different proteolytic sites of the proteasome and the efficacy of inhibitors varies with the protein substrate. J. Biol. Chem. 281, 8582–8590.
Kleijnen, M.F., Shih, A.H., Zhou, P., Kumar, S., Soccio, R.E., Kedersha, N.L., Gill, G., Howley, P.M., 2000. The hPLIC proteins may provide a link between the ubiquitination machinery and the proteasome. Mol. Cell 6, 409–419.
Kleijnen, M.F., Roelofs, J., Park, S., Hathaway, N.A., Glickman, M., King, R.W., Finley, D., 2007. Stability of the proteasome can be regulated allosterically through engagement of its proteolytic active sites. Nat. Struct. Mol. Biol. 14, 1180–1188.
Lander, G.C., Estrin, E., Matyskiela, M.E., Bashore, C., Nogales, E., Martin, A., 2012. Complete subunit architecture of the proteasome regulatory particle. Nature 482, 186–191.
Matyskiela, M.E., Lander, G.C., Martin, A., 2013. Conformational switching of the 26S proteasome enables substrate degradation. Nat. Struct. Mol. Biol. 20, 781–788.
Meister, S., Schubert, U., Neubert, K., Herrmann, K., Burger, R., Gramatzki, M., Hahn, S., Schreiber, S., Wilhelm, S., Herrmann, M., Jack, H.-M., Voll, R.E., 2007. Extensive immunoglobulin production sensitizes myeloma cells for proteasome inhibition. Cancer Res. 67, 1783–1792.
Park, E., Lee, J.W., Eom, S.H., Seol, J.H., Chung, C.H., Nov 28 2008. Binding of MG132 or deletion of the Thr active sites in HslV subunits Increases the affinity of HslV protease for HslU ATPase and makes this interaction nucleotide-independent. J. Biol. Chem. 283 (48), 33258–33266. http://dx.doi.org/10.1074/jbc.M805411200 (Epub 2008 Oct 6).
Pitcher, D.S., De Mattos-Shipley, K., Wang, Z., Tzortzis, K., Goudevenou, K., Flynn, H., Bohn, G., Rahemtulla, A., Roberts, I., Snijders, A.P., Karadimitris, A., Kleijnen, M.F., 2014. Nuclear proteasomes carry a constitutive posttranslational modification which derails SDS-PAGE (but not CTAB-PAGE). Biochim. Biophys. Acta 1844, 2222–2228.
Shabaneh, T., Downey, S., Goddard, A., Screen, M., Lucas, M., Eastman, A., Kisselev, A., 2013. Molecular basis of differential sensitivity of myeloma cells to clinically relevant bolus treatment with Bortezomib. PLoS One 8.
Simpson, R.J., Apr 2010. CTAB-PAGE. Cold Spring Harb. Protoc. 2010 (4), 460–462. http://dx.doi.org/10.1101/pdb.prot5412 (pdb.prot5412).
Sun, X.-M., Butterworth, M., Macfarlane, M., Dubiel, W., Ciechanover, A., Cohen, G.M., 2004. Caspase activation inhibits proteasome function during apoptosis. Mol. Cell 14, 81–93.

Suraweera, A., Munch, C., Hanssum, A., Bertolotti, A., 2012. Failure of amino acid homeostasis causes cell death following proteasome inhibition. Mol. Cell 48, 242–253.

Vilchez, D., Boyer, L., Morantte, I., Lutz, M., Merkwirth, C., Joyce, D., Spencer, B., Page, L., Masliah, E., Berggren, W.T., Gage, F.H., Dillin, A., 2012. Increased proteasome activity in human embryonic stem cells is regulated by PSMD11. Nature 489, 304–308.

Yeung, Y.-G., Stanley, E.R., 2009. A solution for stripping antibodies from polyvinylidene fluoride immunoblots for multiple reprobing. Anal. Biochem. 389, 89–91.

REFERENCES

Adams, J., Palombella, V. J., Sausville, E. A., Johnson, J., Destree, A., Lazarus, D. D., … Elliott, P. J. (1999). Proteasome inhibitors: a novel class of potent and effective antitumor agents. *Cancer Research*, *59*(11), 2615–22. Retrieved from http://cancerres.aacrjournals.org/content/59/11/2615.abstract

Adrain, C., Creagh, E. M., Cullen, S. P., & Martin, S. J. (2004). Caspase-dependent inactivation of proteasome function during programmed cell death in Drosophila and man. *The Journal of Biological Chemistry*, *279*(35), 36923–30. https://doi.org/10.1074/jbc.M402638200

Aguilera, M., Oliveros, M., Martínez-Padrón, M., Barbas, J. A., & Ferrús, A. (2000). Ariadne-1: A vital drosophila gene is required in development and defines a new conserved family of RING-finger proteins. *Genetics*, *155*(3), 1231–1244.

Alao, J. P. (2007). The regulation of cyclin D1 degradation: roles in cancer development and the potential for therapeutic invention. *Molecular Cancer*, *6*, 24. https://doi.org/10.1186/1476-4598-6-24

Alexander, D. D., Mink, P. J., Adami, H. O., Cole, P., Mandel, J. S., Oken, M. M., & Trichopoulos, D. (2007). Multiple myeloma: A review of the epidemiologic literature. *International Journal of Cancer*. https://doi.org/10.1002/ijc.22718

Alvarez Sedó, C., Baronio, M., Nodar, F., Mancisidor, I., Wojcik, C., & Rawe, V. (2012). Proteasome dynamics during oocyte maturation and their relationship with cytoplasmic morphology. *Fertility and Sterility*, *98*(3), S153. https://doi.org/10.1016/j.fertnstert.2012.07.565

Andersen, J. S., Lyon, C. E., Fox, A. H., Leung, A. K. L., Lam, Y. W., Steen, H., … Lamond, A. I. (2002). Directed proteomic analysis of the human nucleolus. *Current Biology*, *12*(1), 1–11. https://doi.org/10.1016/S0960-9822(01)00650-9

Arnold, J., & Grune, T. (2002). PARP-mediated proteasome activation: A co-ordination of DNA repair and protein degradation? *BioEssays*, *24*(11), 1060–1065. https://doi.org/10.1002/bies.10179

Attal, M., Harousseau, J.-L., Facon, T., Guilhot, F., Doyen, C., Fuzibet, J.-G., … Myélome, I. F. du. (2003). Single versus double autologous stem-cell transplantation for multiple myeloma. *The New England Journal of Medicine*, *349*(26), 2495–2502. https://doi.org/10.1056/NEJMoa032290

Avet-Loiseau, H., Gerson, F., Magrangeas, F., Minvielle, S., Harousseau, J. L., &

Bataille, R. (2001). Rearrangements of the c-myc oncogene are present in 15% of primary human multiple myeloma tumors. *Blood*, *98*(10), 3082–3086. https://doi.org/10.1182/blood.V98.10.3082

Bakondi, E., Catalgol, B., Bak, I., Jung, T., Bozaykut, P., Bayramicli, M., … Grune, T. (2011). Age-related loss of stress-induced nuclear proteasome activation is due to low PARP-1 activity. *Free Radical Biology & Medicine*, *50*(1), 86–92.

Bastians, H., Topper, L. M., Gorbsky, G. L., & Ruderman, J. V. (1999). Cell cycle-regulated proteolysis of mitotic target proteins. *Mol Biol Cell*, *10*(11), 3927–3941. https://doi.org/10.1091/mbc.10.11.3927

Baumeister, W., Walz, J., Zühl, F., & Seemüller, E. (1998). The proteasome: Paradigm of a self-compartmentalizing protease. *Cell*. https://doi.org/10.1016/S0092-8674(00)80929-0

Beneke, S. (2012). Regulation of chromatin structure by poly(ADP-ribosyl)ation. *Front Genet*, *3*, 169. https://doi.org/10.3389/fgene.2012.00169

Bensinger, W. (2014). Allogeneic Stem Cell Transplantation for Multiple Myeloma. *Hematology/Oncology Clinics of North America*. https://doi.org/10.1016/j.hoc.2014.06.001

Besche, H. C., Sha, Z., Kukushkin, N. V., Peth, A., Hock, E. M., Kim, W., … Goldberg, A. L. (2014). Autoubiquitination of the 26S Proteasome on Rpn13 Regulates Breakdown of Ubiquitin Conjugates. *EMBO Journal*, *33*(10), 1159–1176. https://doi.org/10.1002/embj.201386906

Beyette, J. R., & Mykles, D. L. (1992). Immunocytochemical localization of the multicatalytic proteinase (Proteasome) in crustacean striated muscles. *Muscle & Nerve*, *15*(9), 1023–1035. https://doi.org/10.1002/mus.880150907

Bhat, K. P., Turner, J. D., Myers, S. E., Cape, A. D., Ting, J. P. Y., & Greer, S. F. (2008). The 19S proteasome ATPase Sug1 plays a critical role in regulating MHC class II transcription. *Molecular Immunology*, *45*(8), 2214–2224.

Bianchi, G., Oliva, L., Cascio, P., Pengo, N., Fontana, F., Cerruti, F., … Cenci, S. (2009). The proteasome load versus capacity balance determines apoptotic sensitivity of multiple myeloma cells to proteasome inhibition. *Blood*, *113*(13), 3040–3049. https://doi.org/10.1182/blood-2008-08-172734

Bochtler, M., Ditzel, L., Groll, M., Hartmann, C., & Huber, R. (1999). The

proteasome. *Annu Rev Biophys Biomol Struct*, *28*, 295–317. https://doi.org/10.1146/annurev.biophys.28.1.295

Bose, S., Stratford, F. L. L., Broadfoot, K. I., Mason, G. G. F., & Rivett, A. J. (2004). Phosphorylation of 20S proteasome alpha subunit C8 (alpha7) stabilizes the 26S proteasome and plays a role in the regulation of proteasome complexes by gamma-interferon. *The Biochemical Journal*, *378*(Pt 1), 177–84. https://doi.org/10.1042/BJ20031122

Boyd, K. D., Ross, F. M., Walker, B. A., Wardell, C. P., Tapper, W. J., Chiecchio, L., … Morgan, G. J. (2011). Mapping of chromosome 1p deletions in myeloma identifies FAM46C at 1p12 and CDKN2C at 1p32.3 as being genes in regions associated with adverse survival. *Clinical Cancer Research*, *17*(24), 7776–7784. https://doi.org/10.1158/1078-0432.CCR-11-1791

Brown, R. D., Pope, B., Gibson, J., Murray, A., Sze, D., Hart, D., & Joshua, D. (2000). Dendritic cells from patients with myeloma are numerically normal but functionally defective due to tgfβl and il-10 inhibition of the upregulation of cd80 expression after hucd40lt stimulation. *Blood*, *96*(11 PART I), 161a.

Burroughs, A. M., Jaffee, M., Iyer, L. M., & Aravind, L. (2008). Anatomy of the E2 ligase fold: Implications for enzymology and evolution of ubiquitin/Ub-like protein conjugation. *Journal of Structural Biology*, *162*(2), 205–218. https://doi.org/10.1016/j.jsb.2007.12.006

Campanero, M. R., & Flemington, E. K. (1997). Regulation of E2F through ubiquitin-proteasome-dependent degradation: stabilization by the pRB tumor suppressor protein. *Proceedings of the National Academy of Sciences of the United States of America*, *94*(6), 2221–2226. https://doi.org/10.1073/pnas.94.6.2221

Cancer Research UK. (2015). Cancer Research UK. Myeloma Statistics. Retrieved June 2, 2016, from http://www.cancerresearchuk.org/health-professional/cancer-statistics/statistics-by-cancer-type/myeloma

Catzavelos, C., Bhattacharya, N., Ung, Y. C., Wilson, J. A., Roncari, L., Sandhu, C., … Slingerland, J. M. (1997). Decreased levels of the cell-cycle inhibitor p27Kip1 protein: prognostic implications in primary breast cancer. *Nature Medicine*, *3*(2), 227–230. https://doi.org/10.1038/nm0297-227

Catzavelos, C., Tsao, M. S., DeBoer, G., Bhattacharya, N., Shepherd, F. A., &

Slingerland, J. M. (1999). Reduced expression of the cell cycle inhibitor p27Kip1 in non-small cell lung carcinoma: a prognostic factor independent of Ras [In Process Citation]. *Cancer Res*, *59*(3), 684–688.

Cavelier, F., Vivet, B., Martinez, J., Aubry, A., Didierjean, C., Vicherat, A., & Marraud, M. (2002). Influence of silaproline on peptide conformation and bioactivity. *Journal of the American Chemical Society*, *124*(12), 2917–2923. https://doi.org/10.1021/ja017440q

Chang, H., Qi, X., Jiang, a, Xu, W., Young, T., & Reece, D. (2010). 1P21 Deletions Are Strongly Associated With 1Q21 Gains and Are an Independent Adverse Prognostic Factor for the Outcome of High-Dose Chemotherapy in Patients With Multiple Myeloma. *Bone Marrow Transplantation*, *45*(1), 117–121. https://doi.org/10.1038/bmt.2009.158

Cheng, M., Olivier, P., Diehl, J. A., Fero, M., Roussel, M. F., Roberts, J. M., & Sherr, C. J. (1999). The p21(Cip1) and p27(Kip1) CDK “inhibitors” are essential activators of cyclin D-dependent kinases in murine fibroblasts. *The EMBO Journal*, *18*(6), 1571–83. https://doi.org/10.1093/emboj/18.6.1571

Chiarle, R., Budel, L. M., Skolnik, J., Frizzera, G., Chilosi, M., Corato, A., … Inghirami, G. (2000). Increased proteasome degradation of cyclin-dependent kinase inhibitor p27 is associated with a decreased overall survival in mantle cell lymphoma. *Blood*, *95*(2), 619–26. Retrieved from http://www.bloodjournal.org/content/95/2/619.abstract

Child, J. A., Morgan, G. J., Davies, F. E., Owen, R. G., Bell, S. E., Hawkins, K., … Selby, P. J. (2003). High-Dose Chemotherapy with Hematopoietic Stem-Cell Rescue for Multiple Myeloma. *New England Journal of Medicine*, *348*(19), 1875–1883. https://doi.org/10.1056/NEJMoa022340

Chng, W. J., Kumar, S., VanWier, S., Ahmann, G., Price-Troska, T., Henderson, K., … Fonseca, R. (2007). Molecular dissection of hyperdiploid multiple myeloma by gene expression profiling. *Cancer Research*, *67*(7), 2982–2989. https://doi.org/10.1158/0008-5472.CAN-06-4046

Ciechanover, a, Heller, H., Elias, S., Haas, a L., & Hershko, a. (1980). ATP-dependent conjugation of reticulocyte proteins with the polypeptide required for protein degradation. *Proceedings of the National Academy of Sciences of the*

United States of America, *77*(3), 1365–1368. https://doi.org/10.1073/pnas.77.3.1365

Clemens, J., Seckinger, A., Hose, D., Theile, D., Longo, M., Haefeli, W. E., … Weiss, J. (2015). Cellular uptake kinetics of bortezomib in relation to efficacy in myeloma cells and the influence of drug transporters. *Cancer Chemotherapy and Pharmacology*, *75*(2), 281–291. https://doi.org/10.1007/s00280-014-2643-1

Cuervo, A. M., Palmer, A., Rivett, A. J., & Knecht, E. (1995). Degradation of proteasomes by lysosomes in rat liver. *European Journal of Biochemistry*, *227*(3), 792–800. Retrieved from http://www.ncbi.nlm.nih.gov/pubmed/7867640

D 'Amato, R. J., Loughnan, M. S., Flynn, E., & Folkman, J. (1994). Thalidomide is an inhibitor of angiogenesis (fibroblast growth factor/rabbit cornea). *Proc. Natl. Acad. Sci. USA*, *91*, 4082–4085. https://doi.org/10.1073/pnas.91.9.4082

Dawson, T. M., & Dawson, V. L. (2010). The role of parkin in familial and sporadic Parkinson's disease. *Movement Disorders : Official Journal of the Movement Disorder Society*, *25 Suppl 1*(0 1), S32-9. https://doi.org/10.1002/mds.22798

de Ávila, A. L. R., Krepischi, A. C. V., Moredo, L. F., Aguiar, T. F. M., da Silva, F. C., de Sá, B. C. S., … Carraro, D. M. (2014). Germline CDKN2A mutations in Brazilian patients of hereditary cutaneous melanoma. *Familial Cancer*, *13*(4), 645–649. https://doi.org/10.1007/s10689-014-9736-1

de Jong, W. W., Zweers, A., & Cohen, L. H. (1978). Influence of single amino acid substitutions on electrophoretic mobility of sodium dodecyl sulfate-protein complexes. *Biochemical and Biophysical Research Communications*, *82*(2), 532–539. https://doi.org/10.1016/0006-291X(78)90907-5

Demo, S. D., Kirk, C. J., Aujay, M. A., Buchholz, T. J., Dajee, M., Ho, M. N., … Bennett, M. K. (2007). Antitumor activity of PR-171, a novel irreversible inhibitor of the proteasome. *Cancer Research*, *67*(13), 6383–6391. https://doi.org/10.1158/0008-5472.CAN-06-4086

Deshaies, R. J., & Joazeiro, C. A. (2009). RING domain E3 ubiquitin ligases. *Annu Rev Biochem*, *78*, 399–434. https://doi.org/10.1146/annurev.biochem.78.101807.093809

Dhodapkar, M. V, Geller, M. D., Chang, D. H., Shimizu, K., Fujii, S.-I., Dhodapkar, K. M., & Krasovsky, J. (2003). A reversible defect in natural killer T cell function

characterizes the progression of premalignant to malignant multiple myeloma. *The Journal of Experimental Medicine*, *197*(12), 1667–76. https://doi.org/10.1084/jem.20021650

Dib, A., Gabrea, A., Glebov, O. K., Bergsagel, P. L., & Kuehl, W. M. (2008). Characterization of MYC translocations in multiple myeloma cell lines. In *Journal of the National Cancer Institute - Monographs* (pp. 25–31). https://doi.org/10.1093/jncimonographs/lgn011

Diehl, J. A., Zindy, F., & Sherr, C. J. (1997). Inhibition of cyclin D1 phosphorylation on threonine-286 prevents its rapid degradation via the ubiquitin-proteasome pathway. *Genes and Development*, *11*(8), 957–972. https://doi.org/10.1101/gad.11.8.957

Duberg, A. S., Nordstroem, M., Toerner, A., Reichard, O., Strauss, R., Janzon, R., … Ekdahl, K. (2005). Non-Hodgkin's lymphoma and other nonhepatic malignancies in Swedish patients with hepatitis C virus infection. *Hepatology*, *41*(3), 652–659.

El-Deiry, W. S., Harper, J. W., O 'connor, P. M., Ei-Deiry, W. S., Velculescu, V. E., Canman, C. E., … Howard, Y. W.]. (1994). WAF1/CIP1 Is Induced in p53-mediated G1 Arrest and Apoptosis. *Cancer Res [CANCER RESEARCH*, *54*(54), 1169–1174. Retrieved from http://cancerres.aacrjournals.org/content/54/5/1169.long

Enenkel, C., Lehmann, A., & Kloetzel, P.-M. (1999). GFP-labelling of 26S proteasomes in living yeast: insight into proteasomal functions at the nuclear envelope/rough ER. *Molecular Biology Reports*, *26*, 131–135. https://doi.org/10.1023/A:1006973803960

Fehlker, M., Wendler, P., Lehmann, A., & Enenkel, C. (2003). Blm3 is part of nascent proteasomes and is involved in a late stage of nuclear proteasome assembly. *EMBO Reports*, *4*(10), 959–63. https://doi.org/10.1038/sj.embor.embor938

Fergusson, J., Landon, M., Lowe, J., Dawson, S. P., Layfield, R., Hanger, D. P., & Mayer, R. J. (1996). Pathological lesions of Alzheimer's disease and dementia with Lewy bodies brains exhibit immunoreactivity to an ATPase that is a regulatory subunit of the 26S proteasome. *Neuroscience Letters*, *219*(3), 167–170. https://doi.org/10.1016/S0304-3940(96)13192-X

Fleming, J. A., Lightcap, E. S., Sadis, S., Thoroddsen, V., Bulawa, C. E., &

Blackman, R. K. (2002). Complementary whole-genome technologies reveal the cellular response to proteasome inhibition by PS-341. *Proceedings of the National Academy of Sciences of the United States of America*, *99*(3), 1461–6. https://doi.org/10.1073/pnas.032516399

Fonseca, R., Blood, E., Rue, M., Harrington, D., Oken, M. M., Kyle, R. A., … Greipp, P. R. (2003). Clinical and biologic implications of recurrent genomic aberrations in myeloma. *Blood*, *101*(11), 4569–4575. https://doi.org/10.1182/blood-2002-10-3017

Gaczynska, M., Osmulski, P. A., Gao, Y., Post, M. J., & Simons, M. (2003). Proline- and arginine-rich peptides constitute a novel class of allosteric inhibitors of proteasome activity. *Biochemistry*, *42*(29), 8663–8670. https://doi.org/10.1021/bi034784f

Gaczynska, M., Rock, K. L., & Goldberg, A. L. (1993). Gamma-interferon and expression of MHC genes regulate peptide hydrolysis by proteasomes. *Nature*, *365*(6443), 264–267. https://doi.org/10.1038/365264a0

Geng, F., & Tansey, W. P. (2012). Similar temporal and spatial recruitment of native 19S and 20S proteasome subunits to transcriptionally active chromatin. *Proceedings of the National Academy of Sciences of the United States of America*, *109*(16), 6060–6065.

Geng, J., & Klionsky, D. J. (2008). The Atg8 and Atg12 ubiquitin-like conjugation systems in macroautophagy. “Protein modifications: beyond the usual suspects” review series. *EMBO Reports*, *9*(9), 859–64. https://doi.org/10.1038/embor.2008.163

Georgieva, E., & Sendra, R. (1999). Mobility of Acetylated Histones in Sodium Dodecyl. *Analytical Biochemistry*, *402*, 399–402. https://doi.org/10.1006/abio.1999.4050

Gibson, B. A., & Kraus, W. L. (2012). New insights into the molecular and cellular functions of poly(ADP-ribose) and PARPs. *Nature Reviews Molecular Cell Biology*, *13*(7), 411–424.

Gille, C., Goede, A., Schlöetelburg, C., Preißner, R., Kloetzel, P. M., Göbel, U. B., & Frömmel, C. (2003). A comprehensive view on proteasomal sequences: Implications for the evolution of the proteasome. *Journal of Molecular Biology*,

326(5), 1437–1448. https://doi.org/10.1016/S0022-2836(02)01470-5

Goedert, J. J., Coté, T. R., Virgo, P., Scoppa, S. M., Kingma, D. W., Gail, M. H., … Biggar, R. J. (1998). Spectrum of AIDS-associated malignant disorders. *Lancet*, *351*(9119), 1833–1839. https://doi.org/10.1016/S0140-6736(97)09028-4

Golden, E. B., Lam, P. Y., Kardosh, A., Gaffney, K. J., Cadenas, E., Louie, S. G., … Schonthal, A. H. (2009). Green tea polyphenols block the anticancer effects of bortezomib and other boronic acid-based proteasome inhibitors. *Blood*, *113*(23), 5927–5937.

Goldstein, G., Scheid, M., Hammerling, U., Schlesinger, D. H., Niall, H. D., & Boyse, E. A. (1975). Isolation of a polypeptide that has lymphocyte-differentiating properties and is probably represented universally in living cells. *Proceedings of the National Academy of Sciences of the United States of America*, *72*(1), 11–5. https://doi.org/10.1073/pnas.72.1.11

Groettrup, M., Kirk, C. J., & Basler, M. (2010). Proteasomes in immune cells: more than peptide producers? *Nature Reviews. Immunology*, *10*(1), 73–8. https://doi.org/10.1038/nri2687

Groettrup, M., Pelzer, C., Schmidtke, G., & Hofmann, K. (2008). Activating the ubiquitin family: UBA6 challenges the field. *Trends in Biochemical Sciences*. https://doi.org/10.1016/j.tibs.2008.01.005

Guarna, A., Trabocchi, A., Guarna, A., Trabocchi, A., Guarna, A., & Trabocchi, A. (2014). Peptidomimetics in Organic and Medicinal Chemistry. *Peptidomimetics in Organic and Medicinal Chemistry: The Art of Transforming Peptides in Drugs*, (April), 259. https://doi.org/10.1002/9781118683033

Haglund, C., Mohanty, C., Fryknäs, M., D'Arcy, P., Larsson, R., Linder, S., & Rickardson, L. (2014). Identification of an inhibitor of the ubiquitin–proteasome system that induces accumulation of polyubiquitinated proteins in the absence of blocking of proteasome function. *MedChemComm*, *5*(3), 376. https://doi.org/10.1039/c3md00386h

Harris, J. L., Alper, P. B., Li, J., Rechsteiner, M., & Backes, B. J. (2001). Substrate specificity of the human proteasome. *Chemistry & Biology*, *8*(12), 1131–1141. https://doi.org/10.1016/S1074-5521(01)00080-1

Hattori, N., Shimura, H., Kubo, S., Kitada, T., Wang, M., Asakawa, S., … Mizuno, Y.

(2000). Autosomal recessive juvenile parkinsonism: a key to understanding nigral degeneration in sporadic Parkinson's disease. *Neuropathology : Official Journal of the Japanese Society of Neuropathology*, *20 Suppl*(May), S85–S90. https://doi.org/10.1046/j.1440-1789.2000.00312.x

Hendil, K. B. (1988). The 19 S multicatalytic "prosome" proteinase is a constitutive enzyme in HeLa cells. *Biochemistry International*, *17*(3), 471–478.

Hideshima, T., Ikeda, H., Chauhan, D., Okawa, Y., Raje, N., Podar, K., … Anderson, K. C. (2009). Bortezomib induces canonical nuclear factor-kappaB activation in multiple myeloma cells. *Blood*, *114*(5), 1046–52. https://doi.org/10.1182/blood-2009-01-199604

Hipp, M. S., Kalveram, B., Raasi, S., Groettrup, M., & Schmidtke, G. (2005). FAT10, a ubiquitin-independent signal for proteasomal degradation. *Molecular and Cellular Biology*, *25*(9), 3483–3491. https://doi.org/10.1128/MCB.25.9.3483-3491.2005

Hirano, H., Kimura, Y., & Kimura, A. (2016). Biological significance of co- and post-translational modifications of the yeast 26S proteasome. *Journal of Proteomics*. https://doi.org/10.1016/j.jprot.2015.11.016

Hong, L., Huang, H.-C., & Jiang, Z.-F. (2014). Relationship between amyloid-beta and the ubiquitin–proteasome system in Alzheimer's disease. *Neurological Research*, *36*(3), 276–282. https://doi.org/10.1179/1743132813Y.0000000288

Hsu, W.-L., Preston, D. L., Soda, M., Sugiyama, H., Funamoto, S., Kodama, K., … Mabuchi, K. (2013). The incidence of leukemia, lymphoma, and multiple myeloma among atomic bomb survivors: 1950 – 2001. *Radiation Research*, *179*(3), 10.1667/RR2892.1. https://doi.org/10.1667/RR2892.1

Huibregtse, J. M., Scheffner, M., Beaudenon, S., & Howley, P. M. (1995). A family of proteins structurally and functionally related to the E6-AP ubiquitin-protein ligase. *Proceedings of the National Academy of Sciences of the United States of America*, *92*(7), 2563–2567. https://doi.org/10.1073/pnas.92.7.2563

Hutchison, C. a, Batuman, V., Behrens, J., Bridoux, F., Sirac, C., Dispenzieri, A., … Sanders, P. W. (2012). The pathogenesis and diagnosis of acute kidney injury in multiple myeloma. *Nature Reviews. Nephrology*. https://doi.org/10.1038/nrneph.2011.168

Isasa, M., Katz, E. J., Kim, W., Yugo, V., González, S., Kirkpatrick, D. S., … Crosas, B. (2010). Monoubiquitination of RPN10 Regulates Substrate Recruitment to the Proteasome. *Molecular Cell*, *38*(5), 733–745. https://doi.org/10.1016/j.molcel.2010.05.001

Keats, J. J., Reiman, T., Maxwell, C. A., Taylor, B. J., Larratt, L. M., Mant, M. J., … Pilarski, L. M. (2003). In multiple myeloma, t(4;14)(p16;q32) is an adverse prognostic factor irrespective of FGFR3 expression. *Blood*, *101*(4), 1520–1529. https://doi.org/10.1182/blood-2002-06-1675

Kessler, B. M., Tortorella, D., Altun, M., Kisselev, A. F., Fiebiger, E., Hekking, B. G., … Overkleeft, H. S. (2001). Extended peptide-based inhibitors efficiently target the proteasome and reveal overlapping specificities of the catalytic beta-subunits. *Chemistry & Biology*, *8*(9), 913–929.

Khor, B., Bredemeyer, A. L., Huang, C.-Y., Turnbull, I. R., Evans, R., Maggi, L. B., … Sleckman, B. P. (2006). Proteasome activator PA200 is required for normal spermatogenesis. *Molecular and Cellular Biology*, *26*(8), 2999–3007. https://doi.org/10.1128/MCB.26.8.2999-3007.2006

Kisselev, A. F., Callard, A., & Goldberg, A. L. (2006). Importance of the different proteolytic sites of the proteasome and the efficacy of inhibitors varies with the protein substrate. *The Journal of Biological Chemistry*, *281*(13), 8582–8590. https://doi.org/M509043200 [pii]10.1074/jbc.M509043200

Kleijnen, M. F., Alarcon, R. M., & Howley, P. M. (2003). The ubiquitin-associated domain of hPLIC-2 interacts with the proteasome. *Mol Biol Cell*, *14*(9), 3868–3875. https://doi.org/10.1091/mbc.E02-11-0766E02-11-0766 [pii]

Kleijnen, M. F., Roelofs, J., Park, S., Hathaway, N. A., Glickman, M., King, R. W., & Finley, D. (2007). Stability of the proteasome can be regulated allosterically through engagement of its proteolytic active sites. *Nat Struct Mol Biol*, *14*(12), 1180–1188. https://doi.org/nsmb1335 [pii]10.1038/nsmb1335

Kleijnen, M. F., Roelofs, J., Park, S., Hathaway, N. a, Glickman, M., King, R. W., & Finley, D. (2007). Stability of the proteasome can be regulated allosterically through engagement of its proteolytic active sites. *Nature Structural & Molecular Biology*, *14*(12), 1180–1188. https://doi.org/10.1038/nsmb1335

Kloetzel, P.-M. (2001). Antigen processing by the proteasome. *Nature Reviews*

Molecular Cell Biology, *2*(3), 179–188. https://doi.org/10.1038/35056572

Knowlton, J. R., Johnston, S. C., Whitby, F. G., Realini, C., Zhang, Z., Rechsteiner, M., & Hill, C. P. (1997). Structure of the proteasome activator REGalpha (PA28alpha). *Nature*, *390*(6660), 639–643. https://doi.org/10.1038/37670

Kodadek, T. (2010). No Splicing, no dicing: non-proteolytic roles of the ubiquitin-proteasome system in transcription. *The Journal of Biological Chemistry*, *285*(4), 2221–2226.

Koike, M., Sekigawa, I., Okada, M., Matsumoto, M., Iida, N., Hashimoto, H., & Oshimi, K. (2002). Relationship between CD4+/CD8+ T cell ratio and T cell activation in multiple myeloma: Reference to IL-16. *Leukemia Research*, *26*(8), 705–711. https://doi.org/10.1016/S0145-2126(01)00192-8

Komander, D., Clague, M. J., & Urbé, S. (2009). Breaking the chains: structure and function of the deubiquitinases. *Nature Reviews. Molecular Cell Biology*, *10*(8), 550–563. https://doi.org/10.1038/nrm2731

Korinek, V., Barker, N., Morin, P. J., van Wichen, D., de Weger, R., Kinzler, K. W., … Clevers, H. (1997). Constitutive transcriptional activation by a beta-catenin-Tcf complex in APC-/- colon carcinoma. *Science (New York, N.Y.)*, *275*(5307), 1784–1787. https://doi.org/10.1126/science.275.5307.1784

Kulkarni, M., & Smith, H. E. (2008). E1 ubiquitin-activating enzyme UBA-1 plays multiple roles throughout C. elegans development. *PLoS Genetics*, *4*(7). https://doi.org/10.1371/journal.pgen.1000131

Kwak, J., Workman, J. L., & Lee, D. (2011). The proteasome and its regulatory roles in gene expression. *Biochimica et Biophysica Acta*, *1809*(2), 88–96.

Kyle, R. A., & Rajkumar, S. V. (2008). Multiple myeloma. *Blood*. https://doi.org/10.1182/blood-2007-10-078022

Kyle, R. A., Therneau, T. M., Rajkumar, V. S., Offord, J. R., Larson, D. R., Plevak, M. F., & Melton, L. J. (2002). A LONG-TERM STUDY OF PROGNOSIS IN MONOCLONAL GAMMOPATHY OF UNDETERMINED SIGNIFICANCE. *The New England Journal of Medicine*, *346*(8), 564–569.

Lander, G. C., Estrin, E., Matyskiela, M. E., Bashore, C., Nogales, E., & Martin, A. (2012). Complete subunit architecture of the proteasome regulatory particle. *Nature*, *6*(7384), 6–13. https://doi.org/10.1038/nature10774

Lee, S. H., Park, Y., Yoon, S. K., & Yoon, J. B. (2010). Osmotic stress inhibits proteasome by p38 MAPK-dependent phosphorylation. *Journal of Biological Chemistry*, *285*(53), 41280–41289. https://doi.org/10.1074/jbc.M110.182188

Leone, P. E., Walker, B. A., Jenner, M. W., Chiecchio, L., Dagrada, G., Protheroe, R. K. M., … Morgan, G. J. (2008). Deletions of CDKN2C in multiple myeloma: Biological and clinical implications. *Clinical Cancer Research*, *14*(19), 6033–6041. https://doi.org/10.1158/1078-0432.CCR-08-0347

Li, W., Bengtson, M. H., Ulbrich, A., Matsuda, A., Reddy, V. A., Orth, A., … Joazeiro, C. A. P. (2008). Genome-wide and functional annotation of human E3 ubiquitin ligases identifies MULAN, a mitochondrial E3 that regulates the organelle's dynamics and signaling. *PLoS ONE*, *3*(1). https://doi.org/10.1371/journal.pone.0001487

Li, X., Wood, T. E., Sprangers, R., Jansen, G., Franke, N. E., Mao, X., … Schimmer, A. D. (2010). Effect of noncompetitive proteasome inhibition on bortezomib resistance. *Journal of the National Cancer Institute*, *102*(14), 1069–1082. https://doi.org/10.1093/jnci/djq198

Liu, Y., Huang, X., He, X., Zhou, Y., Jiang, X., Chen-Kiang, S., … Xu, G. (2015). A novel effect of thalidomide and its analogs: suppression of cereblon ubiquitination enhances ubiquitin ligase function. *FASEB Journal : Official Publication of the Federation of American Societies for Experimental Biology*, *29*(12), 4829–39. https://doi.org/10.1096/fj.15-274050

Loda, M., Cukor, B., Tam, S. W., Lavin, P., Fiorentino, M., Draetta, G. F., … Pagano, M. (1997). Increased proteasome-dependent degradation of the cyclin-dependent kinase inhibitor p27 in aggressive colorectal carcinomas. *Nature Medicine*, *3*, 231–234. https://doi.org/10.1038/nm0297-231

Lokireddy, S., Kukushkin, N. V., & Goldberg, A. L. (2015). cAMP-induced phosphorylation of 26S proteasomes on Rpn6/PSMD11 enhances their activity and the degradation of misfolded proteins. *Proceedings of the National Academy of Sciences of the United States of America*, *112*(52), E7176-85. https://doi.org/10.1073/pnas.1522332112

Lu, H., Zong, C., Wang, Y., Young, G. W., Deng, N., Souda, P., … Ping, P. (2008). Revealing the dynamics of 20S proteasome phosphoproteome: A combined CID

and ETD approach 10.1074/mcp.M800064-MCP200. *Mol Cell Proteomics*, M800064--MCP200. Retrieved from http://www.mcponline.org/cgi/content/abstract/M800064-MCP200v1

Ludwig, H., Pohl, G., & Osterborg, A. (2004). Anemia in multiple myeloma. *Clinical Advances in Hematology & Oncology : H&O*.

Luo, Y., Hurwitz, J., & Massagué, J. (1995). Cell-cycle inhibition by independent CDK and PCNA binding domains in p21Cip1. *Nature*, *375*, 159–161. https://doi.org/10.1038/375159a0

Machiels, B. M., Henfling, M. E., Broers, J. L., Hendil, K. B., & Ramaekers, F. C. (1995). Changes in immunocytochemical detectability of proteasome epitopes depending on cell growth and fixation conditions of lung cancer cell lines. *European Journal of Cell Biology*, *66*(3), 282–92. Retrieved from http://www.ncbi.nlm.nih.gov/pubmed/7539747

Masucci, M. G., Dantuma, N. P., Lindsten, K., Glas, R., & Jellne, M. (2000). Short-lived green fluorescent proteins for quantifying ubiquitin/proteasome-dependentproteolysis in living cells. *Nature Biotechnology*, *18*(5), 538–543. https://doi.org/10.1038/75406

Mattsson, K., Pokrovskaja, K., Kiss, C., Klein, G., & Szekely, L. (2001). Proteins associated with the promyelocytic leukemia gene product (PML)-containing nuclear body move to the nucleolus upon inhibition of proteasome-dependent protein degradation. *Proceedings of the National Academy of Sciences of the United States of America*, *98*(3), 1012–7. https://doi.org/10.1073/pnas.031566998

Matyskiela, M. E., Lander, G. C., & Martin, A. (2013). Conformational switching of the 26S proteasome enables substrate degradation. *Nature Structural & Molecular Biology*, *20*(7), 781–8. https://doi.org/10.1038/nsmb.2616

McGarry, T. J., & Kirschner, M. W. (1998). Geminin, an inhibitor of DNA replication, is degraded during mitosis. *Cell*, *93*(6), 1043–1053. https://doi.org/10.1016/S0092-8674(00)81209-X

McGrath, J. P., Jentsch, S., & Varshavsky, a. (1991). UBA 1: an essential yeast gene encoding ubiquitin-activating enzyme. *The EMBO Journal*, *10*(1), 227–236.

McIlwain, D. R., Berger, T., & Mak, T. W. (2013). Caspase functions in cell death and

disease. *Cold Spring Harbor Perspectives in Biology*. https://doi.org/10.1101/cshperspect.a008656

Metzger, M. B., Hristova, V. A., & Weissman, A. M. (2012). HECT and RING finger families of E3 ubiquitin ligases at a glance. *Journal of Cell Science*, *125*(3), 531–537. https://doi.org/10.1242/jcs.091777

Michelle, C., Vourc'H, P., Mignon, L., & Andres, C. R. (2009). What was the set of ubiquitin and ubiquitin-like conjugating enzymes in the eukaryote common ancestor? *Journal of Molecular Evolution*, *68*(6), 616–628. https://doi.org/10.1007/s00239-009-9225-6

Milletti, F. (2012). Cell-penetrating peptides: Classes, origin, and current landscape. *Drug Discovery Today*. https://doi.org/10.1016/j.drudis.2012.03.002

Moll, U. M., & Petrenko, O. (2003). The MDM2-p53 interaction. *Molecular Cancer Research : MCR*, *1*(14), 1001–8. https://doi.org/10.1016/s0092-8674(00)81871-1

Morgan, G. J., Johnson, D. C., Weinhold, N., Goldschmidt, H., Landgren, O., Lynch, H. T., … Houlston, R. S. (2014). Inherited genetic susceptibility to multiple myeloma. *Leukemia*, *28*(3), 518–24. https://doi.org/10.1038/leu.2013.344

Morton, S., Davis, R. J., McLaren, A., & Cohen, P. (2003). A reinvestigation of the multisite phosphorylation of the transcription factor c-Jun. *EMBO Journal*, *22*(15), 3876–3886. https://doi.org/10.1093/emboj/cdg388

Murata, S., Sasaki, K., Kishimoto, T., Niwa, S. -i., Hayashi, H., Takahama, Y., & Tanaka, K. (2007). Regulation of CD8+ T Cell Development by Thymus-Specific Proteasomes. *Science*, *316*(5829), 1349–1353. https://doi.org/10.1126/science.1141915

Nickell, S., Beck, F., Scheres, S. H., Korinek, A., Forster, F., Lasker, K., … Baumeister, W. (2009). Insights into the molecular architecture of the 26S proteasome. *Proceedings of the National Academy of Sciences of the United States of America*, *106*(29), 11943–11947. https://doi.org/0905081106 [pii]\r10.1073/pnas.0905081106

Nucci, M., & Anaissie, E. (2009). Infections in patients with multiple myeloma in the era of high-dose therapy and novel agents. *Clinical Infectious Diseases : An Official Publication of the Infectious Diseases Society of America*, *49*(8), 1211–

25. https://doi.org/10.1086/605664

Okada, K., Wangpoengtrakul, C., Osawa, T., Toyokuni, S., Tanaka, K., & Uchida, K. (1999). 4-Hydroxy-2-nonenal-mediated impairment of intracellular proteolysis during oxidative stress. Identification of proteasomes as target molecules. *Journal of Biological Chemistry*, *274*(34), 23787–23793. https://doi.org/10.1074/jbc.274.34.23787

Olink-Coux, M., Arcangeletti, C., Pinardi, F., Minisini, R., Huesca, M., Chezzi, C., & Scherrer, K. (1994). Cytolocation of prosome antigens on intermediate filament subnetworks of cytokeratin, vimentin and desmin type. *Journal of Cell Science*, *107 (Pt 3*, 353–66. Retrieved from http://www.ncbi.nlm.nih.gov/pubmed/7516340

Orlowski, R. Z., Stinchcombe, T. E., Mitchell, B. S., Shea, T. C., Baldwin, A. S., Stahl, S., … Soignet, S. L. (2002). Phase I trial of the proteasome inhibitor PS-341 in patients with refractory hematologic malignancies. *Journal of Clinical Oncology*, *20*(22), 4420–4427. https://doi.org/10.1200/JCO.2002.01.133

Osmulski, P. A., Hochstrasser, M., & Gaczynska, M. (2009). A Tetrahedral Transition State at the Active Sites of the 20S Proteasome Is Coupled to Opening of the ??-Ring Channel. *Structure*, *17*(8), 1137–1147. https://doi.org/10.1016/j.str.2009.06.011

Osmulski, P. a, & Gaczynska, M. (2013). Rapamycin allosterically inhibits the proteasome. *Molecular Pharmacology*, *84*(1), 104–13. https://doi.org/10.1124/mol.112.083873

Oyajobi, B. O. (2007). Multiple myeloma/hypercalcemia. *Arthritis Research and Therapy*, *9*(Suppl.1), 1–6. https://doi.org/10.1186/ar2168

Palmer, A., Mason, G. G., Paramio, J. M., Knecht, E., & Rivett, A. J. (1994). Changes in proteasome localization during the cell cycle. *Eur J Cell Biol*, *64*(1), 163–175.

Palmer, A., Rivett, A. J., Thomson, S., Hendil, K. B., Butcher, G. W., Fuertes, G., & Knecht, E. (1996). Subpopulations of proteasomes in rat liver nuclei, microsomes and cytosol. *Biochem. J*, *316*, 401–407.

Pamnani, V., Haas, B., Puhler, G., Sanger, H. L., & Baumeister, W. (1994). Proteasome-associated RNAs are non-specific. *European Journal of*

Biochemistry / FEBS, *225*(2), 511–519.

Panayotatos, N., Radziejewska, E., Acheson, A., Pearsall, D., Thadani, A., & Wong, V. (1993). Exchange of a single amino acid interconverts the specific activity and gel mobility of human and rat ciliary neurotrophic factors. *Journal of Biological Chemistry*, *268*(25), 19000–19003.

Pear, W. S., Miller, J. P., Xu, L., Pui, J. C., Soffer, B., Quackenbush, R. C., … Baltimore, D. (1998). Efficient and rapid induction of a chronic myelogenous leukemia-like myeloproliferative disease in mice receiving P210 bcr/abl-transduced bone marrow. *Blood*, *92*(10), 3780–3792. https://doi.org/10.1016/0092-8674(84)90077-1

Petersen, B. O., Wagener, C., Marinoni, F., Kramer, E. R., Melixetian, M., Denchi, E. L., … Helin, K. (2000). Cell cycle – and cell growth – regulated proteolysis of mammalian CDC6 is dependent on APC – CDH1. *Genes & Development*, (Diffley 1996), 2330–2343. https://doi.org/10.1101/gad.832500.ORC

Pitcher, D. S., de Mattos-Shipley, K., Tzortzis, K., Auner, H. W., Karadimitris, A., & Kleijnen, M. F. (2015). Bortezomib Amplifies Effect on Intracellular Proteasomes by Changing Proteasome Structure. *EBioMedicine*, *2*(7), 642–648.

Pitcher, D. S., De Mattos-Shipley, K., Wang, Z., Tzortzis, K., Goudevenou, K., Flynn, H., … Kleijnen, M. F. (2014). Nuclear proteasomes carry a constitutive posttranslational modification which derails SDS-PAGE (but not CTAB-PAGE). *Biochimica et Biophysica Acta - Proteins and Proteomics*, *1844*(12), 2222–2228.

Pitzer, F., Dantes, A., Fuchs, T., Baumeister, W., & Amsterdam, A. (1996). Removal of proteasomes from the nucleus and their accumulation in apoptotic blebs during programmed cell death. *FEBS Letters*, *394*(1), 47–50. https://doi.org/10.1016/0014-5793(96)00920-9

Piva, R., Cancelli, I., Cavalla, P., Bortolotto, S., Dominguez, J., Draetta, G. F., & Schiffer, D. (1999). Proteasome-dependent degradation of p27/kip1 in gliomas. *Journal of Neuropathology and Experimental Neurology*, *58*(7), 691–696. Retrieved from http://www.sciencedirect.com/science/article/B6WVB-45D9803-4PK/1/b5ec41a37f0e665db9a6381015aad076

Prideaux, S. M., Conway O'Brien, E., & Chevassut, T. J. (2014). The genetic architecture of multiple myeloma. *Advances in Hematology*.

https://doi.org/10.1155/2014/864058

Prudencio, M., Hart, P. J., Borchelt, D. R., & Andersen, P. M. (2009). Variation in aggregation propensities among ALS-associated variants of SOD1: Correlation to human disease. *Human Molecular Genetics*, *18*(17), 3217–3226. https://doi.org/10.1093/hmg/ddp260

Pujals, S., Fernández-Carneado, J., Kogan, M. J., Martinez, J., Cavelier, F., & Giralt, E. (2006). Replacement of a proline with silaproline causes a 20-fold increase in the cellular uptake of a pro-rich peptide. *Journal of the American Chemical Society*, *128*(26), 8479–8483. https://doi.org/10.1021/ja060036c

Rabl, J., Smith, D. M., Yu, Y., Chang, S. C., Goldberg, A. L., & Cheng, Y. (2008). Mechanism of Gate Opening in the 20S Proteasome by the Proteasomal ATPases. *Molecular Cell*, *30*(3), 360–368. https://doi.org/10.1016/j.molcel.2008.03.004

Rajkumar, S. V., Dimopoulos, M. A., Palumbo, A., Blade, J., Merlini, G., Mateos, M. V., … Miguel, J. F. S. (2014). International Myeloma Working Group updated criteria for the diagnosis of multiple myeloma. *The Lancet Oncology*. https://doi.org/10.1016/S1470-2045(14)70442-5

Rath, A., Glibowicka, M., Nadeau, V. G., Chen, G., & Deber, C. M. (2009). Detergent binding explains anomalous SDS-PAGE migration of membrane proteins. *Proceedings of the National Academy of Sciences of the United States of America*, *106*(6), 1760–5. https://doi.org/10.1073/pnas.0813167106

Rechsteiner, M., & Hill, C. P. (2005). Mobilizing the proteolytic machine: Cell biological roles of proteasome activators and inhibitors. *Trends in Cell Biology*. https://doi.org/10.1016/j.tcb.2004.11.003

Reits, E. A. J., Benham, A. M., Plougastel, B., Neefjes, J., & Trowsdale, J. (1997). Dynamics of proteasome distribution in living cells. *EMBO Journal*, *16*(20), 6087–6094. https://doi.org/10.1093/emboj/16.20.6087

Renee Yew, P. (2001). Ubiquitin-mediated proteolysis of vertebrate G1- and S-phase regulators. *Journal of Cellular Physiology*. https://doi.org/10.1002/1097-4652(2001)9999:9999<1::AID-JCP1049>3.0.CO;2-O

Reverte, C. G., Ahearn, M. D., & Hake, L. E. (2001). CPEB degradation during Xenopus oocyte maturation requires a PEST domain and the 26S proteasome.

Developmental Biology, *231*(2), 447–58. https://doi.org/10.1006/dbio.2001.0153

Richardson, P. G., Barlogie, B., Berenson, J., Singhal, S., Jagannath, S., Irwin, D., … Anderson, K. C. (2003). A Phase 2 Study of Bortezomib in Relapsed, Refractory Myeloma. *New England Journal of Medicine*, *348*(26), 2609–2617. https://doi.org/10.1056/NEJMoa030288

Rivett, a. J., Palmer, a., & Knecht, E. (1992). Electron microscopic localization of the multicatalytic proteinase complex in rat liver and in cultured cells. *Journal of Histochemistry & Cytochemistry*, *40*(8), 1165–1172. https://doi.org/10.1177/40.8.1619280

Russell, A., Thompson, M. A., Hendley, J., Trute, L., Armes, J., & Germain, D. (1999). Cyclin D1 and D3 associate with the SCF complex and are coordinately elevated in breast cancer. *Oncogene*, *18*(11), 1983–91. https://doi.org/10.1038/sj.onc.1202511

Saeki, Y., Isono, E., & Toh-E, A. (2005). Preparation of ubiquitinated substrates by the PY motif-insertion method for monitoring 26S proteasome activity. *Methods in Enzymology*, *399*, 215–227. https://doi.org/10.1016/S0076-6879(05)99014-9

Sakata, E., Bohn, S., Mihalache, O., Kiss, P., Beck, F., Nagy, I., … Baumeister, W. (2012). Localization of the proteasomal ubiquitin receptors Rpn10 and Rpn13 by electron cryomicroscopy. *Proceedings of the National Academy of Sciences*, *109*(5), 1479–1484. https://doi.org/10.1073/pnas.1119394109

Satoh, K., Sasajima, H., Nyoumura, K. I., Yokosawa, H., & Sawada, H. (2001). Assembly of the 26S proteasome is regulated by phosphorylation of the p45/Rpt6 ATPase subunit. *Biochemistry*, *40*(2), 314–319. https://doi.org/10.1021/bi001815n

Sawyer, J. R., Lukacs, J. L., Munshi, N., Desikan, K. R., Singhal, S., Mehta, J., … Barlogie, B. (1998). Identification of new nonrandom translocations in multiple myeloma with multicolor spectral karyotyping. *Blood*, *92*(11), 4269–4278.

Schmid, H. P., Akhayat, O., Martins De Sa, C., Puvion, F., Koehler, K., & Scherrer, K. (1984). The prosome: an ubiquitous morphologically distinct RNP particle associated with repressed mRNPs and containing specific ScRNA and a characteristic set of proteins. *The EMBO Journal*, *3*(1), 29–34.

Schulman, B. A., & Wade Harper, J. (2009). Ubiquitin-like protein activation by E1

enzymes: the apex for downstream signalling pathways. *Nature Reviews Molecular Cell Biology*, *10*(5), 319–331. https://doi.org/10.1038/nrm2673

Scruggs, S. B., Zong, N. C., Wang, D., Stefani, E., & Ping, P. (2012). Post-translational modification of cardiac proteasomes: functional delineation enabled by proteomics. *AJP: Heart and Circulatory Physiology*, *303*(1), H9–H18. https://doi.org/10.1152/ajpheart.00189.2012

Selcuk Unal, E., Zhao, R., Qiu, A., & Goldman, I. D. (2008). N-linked glycosylation and its impact on the electrophoretic mobility and function of the human proton-coupled folate transporter (HsPCFT). *Biochimica et Biophysica Acta - Biomembranes*, *1778*(6), 1407–1414. https://doi.org/10.1016/j.bbamem.2008.03.009

Shaughnessy, J. (2005). Amplification and overexpression of CKS1B at chromosome band 1q21 is associated with reduced levels of p27Kip1 and an aggressive clinical course in multiple myeloma. *Hematology*, *10*, 117–126. https://doi.org/10.1080/10245330512331390140

Sheaff, R. J., Singer, J. D., Swanger, J., Smitherman, M., Roberts, J. M., & Clurman, B. E. (2000). Proteasomal turnover of p21Cip1 does not require p21Cip1 ubiquitination. *Molecular Cell*, *5*(2), 403–410. https://doi.org/10.1016/S1097-2765(00)80435-9

Shimura, H., Hattori, N., Kubo, S. I., Mizuno, Y., Asakawa, S., Minoshima, S., … Suzuki, T. (2000). Familial Parkinson disease gene product, parkin, is a ubiquitin-protein ligase. *Nature Genetics*, *25*(3), 302–305. https://doi.org/10.1038/77060

Shirane, M., Harumiya, Y., Ishida, N., Hirai, A., Miyamoto, C., Hatakeyama, S., … Kitagawa, M. (1999). Down-regulation of p27(Kip1) by two mechanisms, ubiquitin-mediated degradation and proteolytic processing. *Journal of Biological Chemistry*, *274*(20), 13886–18893. https://doi.org/10.1074/jbc.274.20.13886

Silvestris, F., Cafforio, P., Tucci, M., & Dammacco, F. (2002). Negative regulation of erythroblast maturation by Fas-L+/TRAIL+ highly malignant plasma cells: A major pathogenetic mechanism of anemia in multiple myeloma. *Blood*, *99*(4), 1305–1313. https://doi.org/10.1182/blood.V99.4.1305

Simpson, R. J. (2010). CTAB-PAGE. *Cold Spring Harbor Protocols*, *2010*(4),

pdb.prot5412.

Singer, J. D., Gurian-West, M., Clurman, B., & Roberts, J. M. (1999). Cullin-3 targets cyclin E for ubiquitination and controls S phase in mammalian cells. *Genes and Development*, *13*(18), 2375–2387. https://doi.org/10.1101/gad.13.18.2375

Singhal, S., Mehta, J., Desikan, R., Ayers, D., Roberson, P., Eddlemon, P., … Barlogie, B. (1999). Antitumor activity of thalidomide in refractory multiple myeloma. *N Engl J Med*, *341*(21), 1565–1571. https://doi.org/10.1056/NEJM199911183412102

Smadja, N. V., Bastard, C., Brigaudeau, C., Leroux, D., & Fruchart, C. (2001). Hypodiploidy is a major prognostic factor in multiple myeloma. *Blood*, *98*(7), 2229–2238. https://doi.org/10.1182/blood.V98.7.2229

Standal, T., Seidel, C., Hjertner, O., Plesner, T., Sanderson, R. D., Waage, A., … Sundan, A. (2002). Osteoprotegerin is bound, internalized, and degraded by multiple myeloma cells. *Blood*, *100*(8), 3002–3007. https://doi.org/10.1182/blood-2002-04-1190

Staub, O. (2004). Ubiquitylation and isgylation: overlapping enzymatic cascades do the job. *Science's STKE : Signal Transduction Knowledge Environment*, *2004*(245), pe43. https://doi.org/10.1126/stke.2452004pe43

Stephen, A. G., Trausch-Azar, J. S., Handley-Gearhart, P. M., Ciechanover, A., & Schwartz, A. L. (1997). Identification of a region within the ubiquitin-activating enzyme required for nuclear targeting and phosphorylation. *Journal of Biological Chemistry*, *272*(16), 10895–10903. https://doi.org/10.1074/jbc.272.16.10895

Sun, X.-M., Butterworth, M., MacFarlane, M., Dubiel, W., Ciechanover, A., & Cohen, G. M. (2004). Caspase activation inhibits proteasome function during apoptosis. *Molecular Cell*, *14*(1), 81–93. Retrieved from http://www.ncbi.nlm.nih.gov/pubmed/15068805

Tanaka, K., Kumatori, A., Ii, K., & Ichihara, A. (1989). Direct evidence for nuclear and cytoplasmic colocalization of proteasomes (Multiprotease complexes) in liver. *Journal of Cellular Physiology*, *139*(1), 34–41. https://doi.org/10.1002/jcp.1041390107

Teras, L. R., Kitahara, C. M., Birmann, B. M., Hartge, P. A., Wang, S. S., Robien, K., … Purdue, M. P. (2014). Body size and multiple myeloma mortality: A pooled

analysis of 20 prospective studies. *British Journal of Haematology*, *166*(5), 667–676. https://doi.org/10.1111/bjh.12935

The Royal Swedish Academy of Sciences. (2004). Ubiquitin-mediated proteolysis (Nobel Prize Chemistry 2004). *The Royal Swedish Academy of Sciences*, (October), 12.

Thullberg, M., Bartek, J., & Lukas, J. (2000). Ubiquitin/proteasome-mediated degradation of p19INK4d determines its periodic expression during the cell cycle. *Oncogene*, *19*(24), 2870–2876. https://doi.org/10.1038/sj.onc.1203579

Tian, E., Zhan, F., Walker, R., Rasmussen, E., Ma, Y., Barlogie, B., & Shaughnessy, J. D. (2003). The Role of the Wnt-Signaling Antagonist DKK1 in the Development of Osteolytic Lesions in Multiple Myeloma. *New England Journal of Medicine*, *349*(26), 2483–2494. https://doi.org/10.1056/NEJMoa030847

Tiedemann, R. E., Gonzalez-Paz, N., Kyle, R. A., Santana-Davila, R., Price-Troska, T., Van Wier, S. A., … Fonseca, R. (2008). Genetic aberrations and survival in plasma cell leukemia. *Leukemia*, *22*(5), 1044–52. https://doi.org/10.1038/leu.2008.4

Tomko, R. J., Funakoshi, M., Schneider, K., Wang, J., & Hochstrasser, M. (2010). Heterohexameric Ring Arrangement of the Eukaryotic Proteasomal ATPases: Implications for Proteasome Structure and Assembly. *Molecular Cell*, *38*(3), 393–403. https://doi.org/10.1016/j.molcel.2010.02.035

Turk, V., Stoka, V., Vasiljeva, O., Renko, M., Sun, T., Turk, B., & Turk, D. (2012). Cysteine cathepsins: From structure, function and regulation to new frontiers. *Biochimica et Biophysica Acta (BBA) - Proteins and Proteomics*, *1824*(1), 68–88. https://doi.org/10.1016/j.bbapap.2011.10.002

Ullrich, O., Reinheckel, T., Sitte, N., Hass, R., Grune, T., & Davies, K. J. (1999). Poly-ADP ribose polymerase activates nuclear proteasome to degrade oxidatively damaged histones. *Proceedings of the National Academy of Sciences of the United States of America*, *96*(11), 6223–6228. https://doi.org/10.1073/pnas.96.11.6223

Ustrell, V., Hoffman, L., Pratt, G., & Rechsteiner, M. (2002). Pa200, a nuclear proteasome activator involved in DNA repair. *EMBO Journal*, *21*(13), 3516–3525. https://doi.org/10.1093/emboj/cdf333

Vachon, C. M., Kyle, R. A., Therneau, T. M., Foreman, B. J., Larson, D. R., Colby, C. L., … Rajkumar, S. V. (2009). Increased risk of monoclonal gammopathy in first-degree relatives of patients with multiple myeloma or monoclonal gammopathy of undetermined significance. *Blood*, *114*(4), 785–790. https://doi.org/10.1182/blood-2008-12-192575

Van De Donk, N. W. C. J., Mutis, T., Poddighe, P. J., Lokhorst, H. M., Zweegman, S., & Van De Donk, N. W. C. J. (2016). Diagnosis, risk stratification and management of monoclonal gammopathy of undetermined significance and smoldering multiple myeloma. *Int. Jnl. Lab. Hem*, *38*, 110–122. https://doi.org/10.1111/ijlh.12504

van Wijk, S. J. L., & Timmers, H. T. M. (2010). The family of ubiquitin-conjugating enzymes (E2s): deciding between life and death of proteins. *FASEB Journal*, *24*(4), 981–93. https://doi.org/10.1096/fj.09-136259

Verma, R., Aravind, L., Oania, R., McDonald, W. H., Yates, J. R., Koonin, E. V, & Deshaies, R. J. (2002). Role of Rpn11 metalloprotease in deubiquitination and degradation by the 26S proteasome. *Science*, *298*(5593), 611–615. https://doi.org/10.1126/science.1075898

Verzijl, N., DeGroot, J., Thorpe, S. R., Bank, R. A., Shaw, J. N., Lyons, T. J., … TeKoppele, J. M. (2000). Effect of collagen turnover on the accumulation of advanced glycation end products. *Journal of Biological Chemistry*, *275*(50), 39027–39031. https://doi.org/10.1074/jbc.M006700200

Walker, B. A., Leone, P. E., Chiecchio, L., Dickens, N. J., Jenner, M. W., Boyd, K. D., … Morgan, G. J. (2010). A compendium of myeloma-associated chromosomal copy number abnormalities and their prognostic value. *Blood*, *116*(15). https://doi.org/10.1182/blood-2010-04-279596

Wallin, A., & Larsson, S. C. (2011). Body mass index and risk of multiple myeloma: A meta-analysis of prospective studies. *European Journal of Cancer*, *47*(11), 1606–1615. https://doi.org/10.1016/j.ejca.2011.01.020

Walters, K. J., Kleijnen, M. F., Goh, A. M., Wagner, G., & Howley, P. M. (2002). Structural studies of the interaction between ubiquitin family proteins and proteasome subunit S5a. *Biochemistry*, *41*(6), 1767–1777. https://doi.org/bi011892y [pii]

Wang, H. R., Kania, M., Baumeister, W., & Nederlof, P. M. (1997). Import of human and Thermoplasma 20S proteasomes into nuclei of HeLa cells requires functional NLS sequences. *Eur J Cell Biol*, *73*(2), 105–113.

Wang, J. X., Boice Jr., J. D., Li, B. X., Zhang, J. Y., & Fraumeni Jr., J. F. (1988). Cancer among medical diagnostic x-ray workers in China. *J Natl Cancer Inst*, *80*(5), 344–350.

Wang, X., Chen, C. F., Baker, P. R., Chen, P. L., Kaiser, P., & Huang, L. (2007). Mass spectrometric characterization of the affinity-purified human 26S proteasome complex. *Biochemistry*, *46*(11), 3553–3565. https://doi.org/10.1021/bi061994u

Waxman, A. J., Mink, P. J., Devesa, S. S., Anderson, W. F., Weiss, B. M., Kristinsson, S. Y., … Landgren, O. (2010). Racial disparities in incidence and outcome in multiple myeloma: A population-based study. *Blood*, *116*(25), 5501–5506. https://doi.org/10.1182/blood-2010-07-298760

Weinhold, N., Johnson, D. C., Rawstron, A. C., Försti, A., Doughty, C., Vijayakrishnan, J., … Houlston, R. S. (2014). Inherited genetic susceptibility to monoclonal gammopathy of unknown significance. *Blood*, *123*(16), 2513–2517. https://doi.org/10.1182/blood-2013-10-532283

Yeung, Y.-G., & Stanley, E. R. (2009). A solution for stripping antibodies from polyvinylidene fluoride immunoblots for multiple reprobing. *Analytical Biochemistry*, *389*(1), 89–91.

Zhan, F., Huang, Y., Colla, S., Stewart, J. P., Hanamura, I., Gupta, S., … Shaughnessy, J. D. (2006). The molecular classification of multiple myeloma. *Blood*, *108*(6), 2020–2028. https://doi.org/10.1182/blood-2005-11-013458

Zhang, F., Su, K., Yang, X., Bowe, D. B., Paterson, A. J., & Kudlow, J. E. (2003). O-GlcNAc modification is an endogenous inhibitor of the proteasome. *Cell*, *115*(6), 715–725. https://doi.org/10.1016/S0092-8674(03)00974-7

Zheng, N., Wang, P., Jeffrey, P. D., & Pavletich, N. P. (2000). Structure of a c-Cbl–UbcH7 Complex: RING Domain Function in Ubiquitin-Protein Ligases. *Cell*, *102*(4), 533–539. https://doi.org/10.1016/S0092-8674(00)00057-X